

# Connecting Ca<sup>2+</sup> Stores and Parkinson Disease

Bethan Susan Kilpatrick

A thesis submitted for the degree of Doctor of Philosophy

Department of Cell & Developmental Biology

University College London

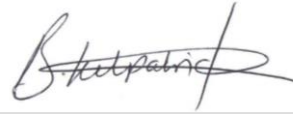
**November 2014**

# Declaration

---

I, Bethan Kilpatrick, confirm that the work presented in this thesis is my own. Where information has been derived from other sources, I confirm that this has been indicated in the thesis.

February, 2015



---

Bethan S. Kilpatrick

# Acknowledgements

---

Firstly, I would like sincerely to thank Professor Sandip Patel for his tremendous support, patience and wisdom. He has been an outstanding supervisor. I also express my gratitude to my other supervisor Professor Anthony Schapira for his guidance and enthusiasm. The work presented in this thesis was funded by Parkinson's UK. I hope that this work is of at least some benefit to sufferers of this disease. I also thank UCL for the IMPACT studentship.

I owe recognition to past and present members of the Patel laboratory. Drs Dev Churamani and Robert Hooper for their patience and teaching me most of the techniques I use in the lab. Also Leanne Hockey, Chris Penny, Lizzie Yates, Manuela Melchionda and honorary members of the Patel laboratory, Alice Roycroft and Sophie McLachlan, for the laughs (which can be heard down the corridor) and, of course, the biscuits. You have all given me many fond memories and made this PhD truly enjoyable.

I extend my thanks to members of the Schapira laboratory, Drs Joana Magalhaes, Mike Cleeter, Kai-Yin Chau and Mark Cooper for the dopaminergic cell models and to Drs Michelle Beavan, Alisdair McNeill, Jan-Willem Taanman and Tatiana Papkovskaia for establishing the fibroblast cultures. I am also very grateful to the individuals who have donated their skin cells.

Another laboratory that I must thank is that of Professor Michael Duchen and members of his team, particularly Drs Laura Osellame and Zhi Yao, for their advice, stimulating discussions and technical assistance. Thanks must also go to Dr Grant Churchill for providing the cell permeable mobilising messengers as well as Professor Clare Futter and Dr Emily Eden for their expertise and electron microscopy work.

I would like to express a special heartfelt thanks to my parents and my sisters for their love and encouragement. It was my Dad who inspired me to become a scientist. Last, I thank my partner Richard for his endless support and making the best cups of tea. Without him I would not have had the strength to complete this PhD.

# Abstract

---

Accumulating evidence implicates lysosomes as mobilisable stores of  $\text{Ca}^{2+}$ , but their relationship to the better-characterised endoplasmic reticulum (ER)  $\text{Ca}^{2+}$  store and significance for disease remains unclear.

Here I show that the rapid osmotic permeabilisation of lysosomes evokes prolonged, spatiotemporally complex  $\text{Ca}^{2+}$  signals in primary cultured human fibroblasts. These  $\text{Ca}^{2+}$  signals comprised an initial response that correlated with lysosomal disruption and secondary long-lasting spatially heterogeneous  $\text{Ca}^{2+}$  oscillations that required ER-localised inositol trisphosphate receptors. Pharmacological and molecular inhibition of the trafficking protein Rab7 suppressed lysosome induced  $\text{Ca}^{2+}$  oscillations. A synthetic agonist, of the endolysosomal ion channel TRPML, also evoked ER-dependent complex  $\text{Ca}^{2+}$  signals. Thus, like the  $\text{Ca}^{2+}$  messenger NAADP, direct mobilisation of lysosomal  $\text{Ca}^{2+}$  stores is sufficient to evoke ER-dependent  $\text{Ca}^{2+}$  signals through a mechanism that maybe Rab7-dependent.

I also identify  $\text{Ca}^{2+}$  defects in fibroblasts from Gaucher disease (GD) and Parkinson disease (PD) patients with mutations in the gene (*GBA1*) encoding the lysosomal enzyme glucocerebrosidase. ER  $\text{Ca}^{2+}$  levels were increased in younger (but not older) patients and associated with enhanced responses to the ryanodine receptor modulator, cyclic ADP-ribose. ER  $\text{Ca}^{2+}$  signalling was unaffected by molecular or chemical inhibition of glucocerebrosidase, implicating mis-folded enzyme in pathology. Conversely, lysosomal  $\text{Ca}^{2+}$  signals were reduced in GD and PD and associated with disrupted lysosome morphology. Therefore, remodelling of ER-lysosomal  $\text{Ca}^{2+}$  stores by pathogenic *GBA1* might predispose to PD.

Finally, I identify lysosomal morphology defects in fibroblasts from PD patients with a common mutation in the enzyme *LRRK2*. These defects were reversed by silencing the endolysosomal ion channel, TPC2. Lysosomal pathology was recapitulated in SH-SY5Y cells overexpressing mutant *LRRK2* and by an environmental toxin linked to PD.  $\text{Ca}^{2+}$  dependent regulation of lysosomal morphology may thus contribute in PD pathology.

In summary,  $\text{Ca}^{2+}$  stores are functionally *connected* and their compromised homeostasis might *connect* to PD pathology.

# Publications

---

Some of the figures and ideas presented in this thesis have been published in the following reports:

1. **Kilpatrick BS**, Eden ER, Schapira AH, Futter CE and Patel S (2013) Direct mobilisation of lysosomal  $\text{Ca}^{2+}$  triggers complex  $\text{Ca}^{2+}$  signals. *J Cell Sci.* 126, 60–66.
2. Penny CJ, **Kilpatrick BS**, Han S, Sneyd J, Patel S (2014) A computational model of lysosome-ER  $\text{Ca}^{2+}$  microdomains. *J Cell Sci.* 127, 2934-2943.
3. Penny CJ, **Kilpatrick BS**, Han S, Sneyd J, Patel S (2014) A ‘mix-and-match’ approach to designing  $\text{Ca}^{2+}$  microdomains at membrane-contact sites. *Commun Integr Biol.* 7, e29586.
4. Hockey LN, **Kilpatrick BS**, Eden ER, Lin-Moshier Y, Brailoiu GC, Brailoiu E, Futter CE, Schapira AH, Marchant JS and Patel S (2014) Dysregulation of lysosomal morphology by pathogenic LRRK2 is corrected by two-pore channel 2 inhibition. *J Cell Sci.* 128, 232-238.

# Table of Contents

---

|  |    |
|--|----|
| Declaration.....   | 2  |
| Acknowledgements.....  | 3  |
| Abstract.....  | 4  |
| Publications.....  | 5  |
| Abbreviations.....   | 11 |
| Chapter 1, Introduction .....  | 14 |
| Ca <sup>2+</sup> signalling.....   | 16 |
| ER Ca <sup>2+</sup> signalling.....  | 18 |
| Mitochondrial Ca <sup>2+</sup> signalling .....  | 21 |
| Lysosomal Ca <sup>2+</sup> signalling .....  | 22 |
| <i>Connecting</i> Ca <sup>2+</sup> stores.....   | 27 |
| ER-plasma membrane.....  | 27 |
| ER-mitochondria .....  | 30 |
| ER-lysosomes .....   | 32 |
| Parkinson disease and related disorders.....   | 34 |
| Parkinson disease.....   | 34 |
| Lysosomal storage disorders.....   | 37 |
| <i>Connecting</i> Ca <sup>2+</sup> with PD .....   | 40 |
| Aims .....   | 45 |
| Chapter 2, Direct Mobilisation of Lysosomal Ca <sup>2+</sup> Triggers Complex Ca <sup>2+</sup> Signals |    |
| Introduction .....   | 46 |
| Methods.....   | 46 |
| Results.....   | 49 |
| GPN evokes complex Ca <sup>2+</sup> signals .....  | 49 |
| GPN rapidly permeabilises lysosomes .....  | 51 |
| GPN evokes spatiotemporally complex Ca <sup>2+</sup> signals.....                                      | 51 |
| GPN-evoked Ca <sup>2+</sup> responses are concentration-dependent.....                                 | 51 |
| Complex GPN-evoked Ca <sup>2+</sup> responses are cell-type specific.....                              | 52 |
| GPN-evoked Ca <sup>2+</sup> responses are dependent upon acidic organelles.....                        | 53 |
| GPN-evoked Ca <sup>2+</sup> responses are dependent upon ER-localised IP <sub>3</sub> R.....           | 56 |

|   |    |
|---|----|
| GPN permeabilises lysosomes to small molecular weight solutes .....   | 56 |
| ER-evoked Ca <sup>2+</sup> responses are unaffected by lysosome disruption.....   | 56 |
| Discussion.....   | 59 |
| Chapter 3, On the Mechanism of Lysosome-ER Ca <sup>2+</sup> Coupling  |    |
| Introduction .....  | 64 |
| Methods.....  | 65 |
| Results.....  | 66 |
| GPN-evoked complex Ca <sup>2+</sup> responses are Rab7-dependent.....   | 66 |
| GPN-evoked complex Ca <sup>2+</sup> responses are VAP-independent .....   | 67 |
| ML-SA1 evokes complex Ca <sup>2+</sup> signals .....  | 69 |
| ML-SA1-evoked Ca <sup>2+</sup> responses are dependent upon acidic organelles and ER-Ca <sup>2+</sup> ....              | 70 |
| Discussion.....   | 72 |
| Chapter 4, Defective Calcium Signalling in Parkinson Disease: Clues from a Lysosomal Storage Disorder                   |    |
| Introduction .....  | 77 |
| Methods.....  | 78 |
| Results.....  | 79 |
| Establishing fibroblast cultures from individuals carrying the N370S mutation in <i>GBA1</i> .....                      | 79 |
| ER Ca <sup>2+</sup> content is increased in <i>young</i> GD and <i>GBA1</i> -PD fibroblasts .....                       | 80 |
| Messenger-evoked ER Ca <sup>2+</sup> release is increased in <i>young</i> GD and <i>GBA1</i> -PD fibroblasts .....      | 80 |
| ER Ca <sup>2+</sup> homeostasis is unaffected in <i>young</i> asymptomatic <i>GBA1</i> <sup>+/-</sup> fibroblasts ..... | 81 |
| ER Ca <sup>2+</sup> content is unaffected in <i>aged</i> <i>GBA1</i> -PD fibroblasts .....                              | 82 |
| ER Ca <sup>2+</sup> content increases in an age-dependent manner .....  | 82 |
| Inhibition of GCase does not affect ER Ca <sup>2+</sup> homeostasis.....  | 84 |
| Overexpression of mutant <i>GBA1</i> partially impairs ER Ca <sup>2+</sup> homeostasis.....                             | 85 |
| Mitochondrial Ca <sup>2+</sup> content is increased in <i>young</i> <i>GBA1</i> -PD fibroblasts .....                   | 88 |
| Lysosomal Ca <sup>2+</sup> content is decreased in <i>young</i> GD and <i>GBA1</i> -PD fibroblasts .....                | 88 |
| Lysosome morphology is disrupted in GD and <i>GBA1</i> -PD fibroblasts.....   | 89 |
| Agonist-evoked Ca <sup>2+</sup> release is not altered in <i>young</i> GD and <i>GBA1</i> -PD fibroblasts.....          | 92 |
| Spontaneous Ca <sup>2+</sup> signalling is increased <i>young</i> GD and <i>GBA1</i> -PD fibroblasts.....               | 93 |
| Discussion.....   | 94 |
| ER Dysfunction .....  | 94 |
| Mitochondrial Dysfunction .....   | 97 |

|   |     |
|---|-----|
| Lysosome Dysfunction .....  | 99  |
| Physiological Ca <sup>2+</sup> signalling .....   | 102 |
| Therapy .....   | 102 |
| Summary .....   | 103 |
| Chapter 5, Lysosome Dysfunction - a Common Feature of Parkinson Disease?                            |     |
| Introduction .....  | 104 |
| Methods .....   | 105 |
| Results .....   | 106 |
| Lysosome morphology is disrupted in <i>LRRK2</i> -PD models .....                                   | 106 |
| Late, but not early, endosome morphology is disrupted in <i>LRRK2</i> -PD patient fibroblasts ..... | 107 |
| Disrupted <i>LRRK2</i> -PD lysosome morphology is reversed by silencing TPC2 .....                  | 109 |
| Lysosome morphology is disrupted in fibroblasts treated with a PD inducing toxin ..                 | 110 |
| Discussion.....   | 111 |
| Chapter 6, Conclusions and Future Directions .....  | 115 |
| Appendix .....  | 119 |
| References .....  | 136 |



# List of Figures

| Figure | Title  | Page |
|--------|--|------|
| 1.1    | The Ca <sup>2+</sup> signalling network  | 17   |
| 1.2    | Lysosomes  | 23   |
| 1.3    | The diversity of ER membrane contact sites   | 28   |
| 1.4    | Ca <sup>2+</sup> signalling and PD   | 41   |
| 2.1    | GPN evokes complex Ca <sup>2+</sup> signals  | 50   |
| 2.2    | GPN rapidly permeabilises lysosomes  | 52   |
| 2.3    | ER-evoked Ca <sup>2+</sup> responses are unaffected by lysosome disruption   | 53   |
| 2.4    | GPN-evoked Ca <sup>2+</sup> responses are concentration-dependent  | 54   |
| 2.5    | Complex GPN-evoked Ca <sup>2+</sup> responses are cell-type specific   | 55   |
| 2.6    | GPN-evoked Ca <sup>2+</sup> responses are dependent upon acidic organelles   | 55   |
| 2.7    | GPN-evoked Ca <sup>2+</sup> responses are dependent upon ER-localised IP <sub>3</sub> R  | 57   |
| 2.8    | GPN permeabilises lysosomes to small molecular weight solutes  | 58   |
| 2.9    | ER-evoked Ca <sup>2+</sup> responses are unaffected by lysosome disruption   | 59   |
| 3.1    | GPN-evoked complex Ca <sup>2+</sup> responses are Rab7-dependent   | 67   |
| 3.2    | GPN-evoked complex Ca <sup>2+</sup> responses are Rab7-dependent   | 68   |
| 3.3    | GPN-evoked Ca <sup>2+</sup> signals and permeabilisation are cholesterol-dependent   | 69   |
| 3.4    | GPN-evoked complex Ca <sup>2+</sup> responses are VAP-independent  | 70   |
| 3.5    | ML-SA1 evokes complex Ca <sup>2+</sup> signals   | 71   |
| 3.6    | ML-SA1-evoked Ca <sup>2+</sup> responses are dependent upon acidic organelles and ER-Ca <sup>2+</sup>                          | 72   |
| 4.1    | ER Ca <sup>2+</sup> content is increased in <i>young</i> GD and <i>GBA1</i> -PD fibroblasts                                    | 80   |
| 4.2    | Messenger-evoked ER Ca <sup>2+</sup> release is increased in <i>young</i> GD and <i>GBA1</i> -PD fibroblasts                   | 81   |
| 4.3    | ER Ca <sup>2+</sup> homeostasis is unaffected in <i>young</i> asymptomatic <i>GBA1</i> <sup>+/-</sup> fibroblasts              | 82   |
| 4.4    | Messenger-evoked ER Ca <sup>2+</sup> release is unaffected in <i>young</i> asymptomatic <i>GBA1</i> <sup>+/-</sup> fibroblasts | 83   |
| 4.5    | ER Ca <sup>2+</sup> content is unaffected in <i>aged</i> <i>GBA1</i> -PD fibroblasts   | 83   |
| 4.6    | ER Ca <sup>2+</sup> content increases in an age-dependent manner   | 84   |
| 4.7    | Inhibition of GCCase does not affect ER Ca <sup>2+</sup> homeostasis in fibroblasts  | 85   |
| 4.8    | Inhibition of GCCase does not affect ER Ca <sup>2+</sup> homeostasis in dopaminergic SH-SY5Y cells                             | 86   |
| 4.9    | Inhibition of GCCase does not affect ER Ca <sup>2+</sup> homeostasis in neuronal cultures                                      | 87   |
| 4.10   | Overexpression of mutant <i>GBA1</i> partially impairs ER Ca <sup>2+</sup> homeostasis   | 87   |
| 4.11   | Mitochondrial Ca <sup>2+</sup> content is increased in <i>young</i> <i>GBA1</i> -PD fibroblasts                                | 88   |
| 4.12   | Lysosomal Ca <sup>2+</sup> content is decreased in <i>young</i> GD and <i>GBA1</i> -PD fibroblasts                             | 90   |
| 4.13   | Lysosome morphology is disrupted in <i>young</i> GD and <i>GBA1</i> -PD fibroblasts  | 91   |
| 4.14   | Lysosome morphology is disrupted in <i>aged</i> <i>GBA1</i> -PD fibroblasts  | 92   |
| 4.15   | Agonist-evoked Ca <sup>2+</sup> release is not altered in <i>young</i> GD and <i>GBA1</i> -PD fibroblasts                      | 93   |
| 4.16   | Spontaneous Ca <sup>2+</sup> signalling is increased <i>young</i> GD and <i>GBA1</i> -PD fibroblasts                           | 93   |
| 5.1    | Lysosome morphology is disrupted in <i>LRRK2</i> -PD fibroblasts   | 107  |
| 5.2    | Lysosome morphology is disrupted in dopaminergic SH-SY5Y cells overexpressing mutant <i>LRRK2</i>                              | 108  |

|     |   |     |
|-----|---|-----|
| 5.3 | Late, but not early, endosome morphology is disrupted in <i>LRRK2</i> -PD patient fibroblasts | 109 |
| 5.4 | Disrupted <i>LRRK2</i> -PD lysosome morphology is reversed by silencing TPC2                  | 110 |
| 5.5 | Lysosome morphology is disrupted in fibroblasts treated with a PD inducing toxin              | 111 |
| 6.1 | Connecting Ca <sup>2+</sup> stores and Parkinson Disease                                      | 116 |

## List of Tables

---

| <b>Table</b> | <b>Title</b>                                     | <b>Page</b> |
|--------------|--|-------------|
| 1.1          | Summary of GPN-evoked Ca <sup>2+</sup> responses | 24          |
| 4.1          | Details of patient-derived fibroblast cultures   | 79          |
| 5.1          | Details of patient-derived fibroblast cultures   | 105         |

# Abbreviations

---

|                   |   |
|-------------------|---|
| 2-APB             | 2-Aminoethoxydiphenyl borate                              |
| ADP               | Adenosine diphosphate                                     |
| AM                | Acetoxymethyl   |
| ANOVA             | Analysis of Variance                                      |
| ARL8B             | ADP-ribosylation factor-like 8B                           |
| ATP               | Adenosine triphosphate                                    |
| ATP1A1            | Na <sup>+</sup> /K <sup>+</sup> ATPase alpha-1 subunit    |
| Bcl-2             | B-cell lymphoma 2   |
| BiP               | Binding immunoglobulin protein                            |
| BK                | Bradykinin  |
| BSA               | Bovine serum albumin                                      |
| cADPR             | cyclic ADP-ribose   |
| CI-1              | Cathepsin-inhibitor 1                                     |
| CICR              | Ca <sup>2+</sup> -induced Ca <sup>2+</sup> release        |
| CREB              | cAMP response element-binding protein                     |
| CBE               | Conduritol B Epoxide                                      |
| DABCO             | 1,4-diazabicyclo[2,2,2]octane                             |
| DAG               | Diacylglycerol  |
| DAPI              | 4',6-diamidino-2-phenylindole                             |
| DMEM              | Dulbecco's modified eagle medium                          |
| DMSO              | Dimethyl sulfoxide  |
| EEA1              | Early endosome antigen 1                                  |
| EGFR              | Epidermal growth factor receptors                         |
| EGTA              | Ethylene glycol tetraacetic acid                          |
| ER                | Endoplasmic reticulum                                     |
| ERAD              | ER-associated degradation                                 |
| ERMES             | ER-mitochondria encounter structure                       |
| ERT               | Enzyme replacement therapy                                |
| E-syts            | Extended-synaptotagmins                                   |
| FBS               | Fetal bovine serum  |
| FCCP              | Carbonylcyanide-p-(trifluoromethoxy)-phenylhydrazone      |
| FDA               | Food and drug administration                              |
| <i>GBA1</i> -PD   | <i>GBA1</i> -associated Parkinson Disease                 |
| GCase             | Glucocerebrosidase  |
| GD                | Gaucher Disease   |
| GPCR              | G-protein coupled receptors                               |
| GPN               | Glycyl-l-phenylalanine 2-naphthylamide                    |
| Grp75             | Glucose-regulated protein 75                              |
| GTP               | Guanosine triphosphate                                    |
| HBS               | HEPES-buffered saline                                     |
| HEK               | Human embryonic kidney 293 cells                          |
| HVA               | High voltage activated                                    |
| IMM               | Inner mitochondrial membranes                             |
| IP <sub>3</sub>   | Inositol-1,4,5-trisphosphate                              |
| IP <sub>3</sub> R | Inositol-1,4,5-trisphosphate receptors                    |
| IPSc              | Induced pluripotent stem cells                            |
| LAMP1             | Lysosome associated membrane protein 1                    |
| LC3               | Light chain 3   |
| Letm1             | Leucine zipper-EF hand containing transmembrane protein 1 |
| LIMP2             | Lysosomal integral membrane protein type 2                |
| LRRK2             | Leucine-rich repeat kinase 2                              |
| <i>LRRK2</i> -PD  | <i>LRRK2</i> -associated Parkinson Disease                |
| LSD               | Lysosomal Storage Disorder                                |

|                       |   |
|-----------------------|---|
| LVA                   | Low voltage activated   |
| MAM                   | Mitochondria-associated membranes   |
| MBCD                  | Methyl- $\beta$ -cyclodextrin   |
| MCS                   | Membrane contact site   |
| MCU                   | Mitochondrial calcium uniporter   |
| Mfn1                  | Mitofusin 1   |
| Mfn2                  | Mitofusin 2   |
| MICU1                 | Mitochondrial Ca <sup>2+</sup> uptake 1 protein                                       |
| MLIV                  | Mucopolipidosis IV  |
| ML-SA1                | Mucolipin synthetic agonist 1   |
| MPTP                  | 1-methyl-4-phenyl-1,2,3,6-tetrahydropyridine  |
| mTORC2                | Mammalian target of rapamycin complex 2   |
| MYH9                  | Myosin heavy chain 9  |
| NAADP                 | Nicotinic acid adenine dinucleotide phosphate   |
| NAD                   | Nicotinamide adenine dinucleotide   |
| NCX                   | Na <sup>+</sup> /Ca <sup>2+</sup> exchanger   |
| NMDA                  | N-Methyl-D-Aspartate  |
| NPC                   | Niemann-Pick type C disease   |
| NVJ1                  | Nucleus-vacuolar junction protein 1   |
| OMM                   | Outer mitochondrial membranes   |
| ORP                   | Oxysterol-binding protein (OSBP)-related proteins                                     |
| paraquat              | 1,1-dimethyl-4,4-bipyridinium dichloride  |
| PBS                   | Phosphate buffered saline   |
| PC                    | Phosphatidylcholine   |
| PD                    | Parkinson Disease   |
| PE                    | Phosphatidylethanolamine  |
| PI(3,5)P <sub>2</sub> | Phosphatidylinositol 3,5-bisphosphate   |
| PINK1                 | PTEN-induced kinase 1   |
| PIP <sub>2</sub>      | Phosphatidylinositol bisphosphate   |
| PLC                   | Phospholipase C   |
| PM                    | Plasma membrane   |
| PMCA                  | Plasma membrane Ca <sup>2+</sup> ATPases  |
| PS                    | Phosphatidylserine  |
| PTP                   | Permeability transition pore  |
| PTP1B                 | Protein tyrosine phosphatase 1B   |
| PTPIP51               | Protein tyrosine phosphatase interacting protein 51                                   |
| RILP                  | Rab-interacting lysosomal protein   |
| ROS                   | Reactive oxygen species   |
| RyR                   | Ryanodine receptor  |
| SDS                   | Sodium dodecyl sulphate   |
| SERCA                 | Sarco- and endoplasmic-reticulum Ca <sup>2+</sup> -ATPases                            |
| siRNA                 | Small interfering RNA   |
| SNc                   | Substantia Nigra Pars Compacta  |
| SOCE                  | Store operated Ca <sup>2+</sup> entry   |
| SR                    | Sacroplasmic reticulum  |
| STARD3                | StAR [steroidogenic acute regulatory protein] related lipid transfer (START) domain-3 |
| STARD3NL              | STARD3 N-terminal like  |
| STIM1                 | Stromal interacting molecule  |
| TCA                   | Tricarboxylic acid cycle  |
| TFEB                  | Transcription factor EB   |
| Tg                    | Thapsigargin  |
| TIRF                  | Total internal reflection fluorescence  |
| TPC                   | Two Pore Channels   |
| TRP                   | Transient receptor potential  |
| TRPC                  | TRP Canonical   |
| TRPML                 | Transient receptor potential mucolipin  |
| UPR                   | Unfolded protein response   |

|                    |  |
|--------------------|--|
| Vac8               | Vacuolar protein 8   |
| VAP                | Vesicle associated membrane protein (VAMP)-associated proteins |
| VDAC               | Voltage-dependent anion channels                               |
| VGCC               | Voltage gated Ca <sup>2+</sup> channels                        |
| VPS35              | Vacuolar protein sorting 35                                    |
| VTA                | Ventral tegmental area   |
| α-syn              | Alpha-synuclein  |
| Δ Ca <sup>2+</sup> | Magnitude of Fura-2 response                                   |

# Chapter 1

---

## Introduction

Various cellular processes are regulated by changes in cytosolic  $\text{Ca}^{2+}$  (Berridge et al., 2000).  $\text{Ca}^{2+}$  signals originate from both the extracellular environment and intracellular  $\text{Ca}^{2+}$  stores. By far the best researched  $\text{Ca}^{2+}$  store is the endoplasmic reticulum (Berridge, 2002). Here,  $\text{Ca}^{2+}$ -permeable ion channels, like ryanodine receptors, mediate  $\text{Ca}^{2+}$  release. These channels are gated by  $\text{Ca}^{2+}$  mobilising messengers and  $\text{Ca}^{2+}$  itself.  $\text{Ca}^{2+}$  buffers, pumps and exchangers regulate and maintain cytosolic  $\text{Ca}^{2+}$  levels.  $\text{Ca}^{2+}$  release from the ER can be rapidly sequestered by the mitochondria, through the mitochondrial uniporter (De Stefani et al., 2011). This uptake is necessary for mitochondrial function. Increasing evidence identifies acidic organelles, such as lysosomes, as  $\text{Ca}^{2+}$  stores (Patel & Docampo, 2010). Lysosomes are known to trigger cytosolic  $\text{Ca}^{2+}$  signals. Indeed, the  $\text{Ca}^{2+}$  mobilising messenger NAADP (Nicotinic Acid Adenine Dinucleotide Phosphate), which targets lysosomes, evokes localised  $\text{Ca}^{2+}$  signals that become amplified by the ER (Cancela et al., 1999).

The ER, mitochondria and lysosomes form a delicately balanced, functionally connected  $\text{Ca}^{2+}$  network within the cell. Physical connections (membrane contact sites) between  $\text{Ca}^{2+}$  stores are known to facilitate this  $\text{Ca}^{2+}$  coupling (Prinz, 2014). For instance, the ER forms tight junctions with the mitochondria for ER  $\text{Ca}^{2+}$  release to regulate ATP synthesis (Csordás et al., 2006). Compartments of the endo-lysosomal system have also been shown to associate with the ER (Eden et al., 2010). The trafficking GTPase Rab7 regulates these contacts (Rocha et al., 2009). It has been suggested that similar components underpin NAADP signalling (Patel & Brailoiu, 2012).

The  $\text{Ca}^{2+}$  signalling “toolkit” generates, propagates and terminates  $\text{Ca}^{2+}$  signals. Any defect in this system make coping with a large increase in  $\text{Ca}^{2+}$  or persistent signals difficult to manage, resulting in stress to the cell (Berridge, 2012). This is a recurring problem in numerous diseases, including Parkinson disease (PD). PD is a common neurodegenerative movement disorder, characterised by the loss of dopaminergic neurons in the substantia nigra (Braak et al., 2004). The cause of this progressive disease is unknown, however genes (such as *LRRK2*) and environmental toxins (including paraquat) are increasingly implicated with disease development. Recently, mutations in *GBA1*, which encodes a lysosomal hydrolase, were identified as the most frequent genetic risk factor for PD (Sidransky et al., 2009). A single

mutation (like N370S) in *GBA1* can enhance the risk of PD development (up to 20-fold in certain populations). Recessive mutations cause the common lysosomal storage disorder (LSD) Gaucher disease (GD). However, the cellular mechanisms that link these two disorders are unknown.

Research has established that  $\text{Ca}^{2+}$  dysfunction contributes to both PD and GD pathology. Namely, substantia nigra neurons possess a unique pacemaking phenotype that is sustained by voltage gated  $\text{Ca}^{2+}$  channels (VGCC) (Chan et al., 2007). This constant  $\text{Ca}^{2+}$  influx has been shown to evoke mitochondrial stress and is thought to be the reason why these neurons selectively degenerate in PD (Guzman et al., 2010). The role of  $\text{Ca}^{2+}$  stores in PD has been largely neglected. However, irregular ER  $\text{Ca}^{2+}$  signalling has been implicated in GD (Korkotian et al., 1999; Lloyd-Evans et al., 2003; Pelled et al., 2005). Thus, dysfunctional  $\text{Ca}^{2+}$  signalling might *connect* GD and PD.

The genetic connection between GD and PD strongly implicates lysosomal dysfunction in PD. Mutations in the genes encoding several other lysosomal proteins (including the lysosomal ATPase, ATP13A2) have also been linked to PD (Ramirez et al., 2006). Another common genetic cause of PD, is a mutation in *LRRK2*, which encodes a multi-domain enzyme (Paisán-Ruíz et al., 2004). Although the function of LRRK2 is unknown, this protein can regulate autophagy (Plowey et al., 2008) and has been localised to the endolysosomal system (Biskup et al., 2006; Alegre-Abarategui et al., 2009; Higashi et al., 2009). Recent work has established that LRRK2 interacts with lysosomal ion channels (Gómez-Suaga et al., 2012). This interaction might disrupt lysosomal function and contribute to pathology.

In this thesis I examine if  $\text{Ca}^{2+}$  stores are functionally *connected* and whether their dysfunction *connects* GD and PD.

## Ca<sup>2+</sup> signalling

Ca<sup>2+</sup> is a ubiquitous, abundant and highly versatile signalling cation. It is capable of regulating a range of physiological events from fertilisation and mitosis to cell death (Berridge, et al., 2000). Variations in the frequency, location and amplitude of Ca<sup>2+</sup> signals (the “Ca<sup>2+</sup> signature”) provide the specificity needed to regulate Ca<sup>2+</sup>-dependent processes (Berridge, 1997). The Ca<sup>2+</sup> toolkit (figure 1.1), which includes Ca<sup>2+</sup> buffers, second messengers, ion channels, pumps and exchangers, permit this versatility and regulate Ca<sup>2+</sup> responses with high fidelity (Berridge, et al., 2000).

Ca<sup>2+</sup> signals are generated by influx and/or the mobilisation of intracellular Ca<sup>2+</sup> stores. Various families of ion channels mediate Ca<sup>2+</sup> influx and they are defined by their activation mechanism. For instance, changes in membrane potential can activate voltage-gated Ca<sup>2+</sup> channels (VGCCs) in excitable cells. VGCCs can be classified by their biophysical properties into low voltage activated (LVA) and high voltage activated (HVA) channels (reviewed in Zamponi et al. 2010). Larger depolarisations open HVA and these channels can be further subdivided according to their pharmacological and functional characteristics. One example is the dihydropyridine-sensitive L-type VGCC. There are four different members (Ca<sub>v</sub>1.1 through Ca<sub>v</sub>1.4) of this ion channel family and they are prominently expressed in neurons and muscle cells (Striessnig et al., 2010). In these locations L-type VGCC mediate synaptic transmission (Augustine, 2001) and contraction (discussed in more detail below).

Ligand-gated ion channels also regulate Ca<sup>2+</sup> influx. In neurons, the excitatory neurotransmitter glutamate mediates Ca<sup>2+</sup> influx through NMDA (N-Methyl-D-Aspartate) receptors (Grienberger & Konnerth 2012). This NMDA receptor-mediated Ca<sup>2+</sup> signalling is necessary for memory formation and consolidation. In other cell types, transient receptor potential (TRP) channels facilitate Ca<sup>2+</sup> entry (Montell, 2005). Currently, 28 different TRP channels have been identified and they are activated by a variety of stimuli. Members of this large family of ion channels mostly, although not always, associate with the plasma membrane. Due to their heterogeneity, TRP channels are further categorised into subtypes. One of these is the TRP Canonical (TRPC) group, which can be found in high levels within the brain (Moran et al., 2004). The enzyme phospholipase C (PLC) has been shown to activate all isoforms of TRPCs. These channels were thought to propagate Ca<sup>2+</sup> signals by refilling Ca<sup>2+</sup> stores, but other candidates have since emerged and these are discussed in more detail below.



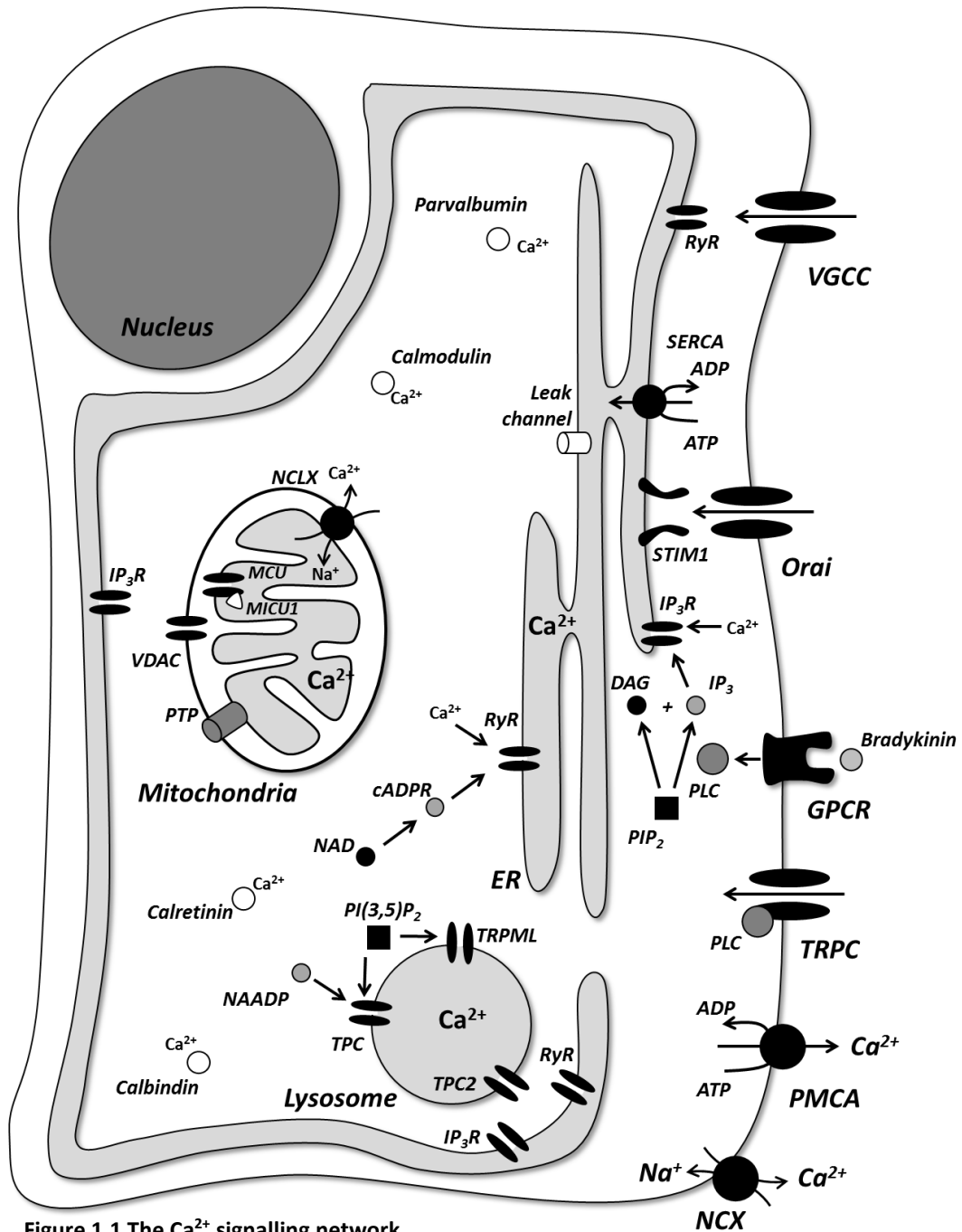


**Figure 1.1 The  $\text{Ca}^{2+}$  signalling network**

$\text{Ca}^{2+}$  signals are generated from  $\text{Ca}^{2+}$  influx (through VGCC, store operated  $\text{Ca}^{2+}$  Channels [Orai] and TRP channels) and the mobilisation of intracellular  $\text{Ca}^{2+}$  stores (the ER, mitochondria and lysosomes). On these  $\text{Ca}^{2+}$  stores, ion channels (including  $\text{IP}_3\text{R}$ , RyR, TPC and TRPML channels) are gated by  $\text{Ca}^{2+}$  mobilising messengers ( $\text{IP}_3$ , cADPR and NAADP) some of which can be activated by GPCR such as bradykinin receptors. The phosphoinositide  $\text{PI}(3,5)\text{P}_2$  is also known to activate lysosomal ion channels. Molecularly uncharacterised leak channels also mediate  $\text{Ca}^{2+}$  release from the ER.  $\text{Ca}^{2+}$  uptake into the mitochondria is regulated by channels (VDAC and MCU) on the outer and inner mitochondrial membranes respectively. The opening of PTP releases mitochondria  $\text{Ca}^{2+}$  into the cytosol. Intracellular  $\text{Ca}^{2+}$  homeostasis is maintained by  $\text{Ca}^{2+}$  binding proteins (calbindin, calmodulin, calretinin and parvalbumin),  $\text{Ca}^{2+}$  pumps (SERCA and PMCA) and  $\text{Ca}^{2+}$  exchangers (NCX and NCLX).

At rest, the cytosolic  $\text{Ca}^{2+}$  concentration of a cell is typically 100 nM, approximately 10,000 times lower than that in the extracellular space (Berridge, et al., 2000). Maintaining cytosolic  $\text{Ca}^{2+}$  is necessary to provide resolution to the  $\text{Ca}^{2+}$  signature and prevent the initiation of unwanted (e.g. apoptotic) pathways. Buffers, exchangers and pumps maintain intracellular  $\text{Ca}^{2+}$  homeostasis and fine-tune the spatial and temporal features of the  $\text{Ca}^{2+}$  signal. These mechanisms are so effective at regulating intracellular levels of  $\text{Ca}^{2+}$  that a free  $\text{Ca}^{2+}$  ion cannot diffuse more than 0.5  $\mu\text{m}$  before being sequestered (Clapham, 1995). This generates localised  $\text{Ca}^{2+}$  signals (Berridge, 1997).

Cytosolic buffers, such as calbindin D-28 and calretinin rapidly bind  $\text{Ca}^{2+}$  (Berridge et al., 2003). Although, some (i.e. parvalbumin) are slower acting (Arif, 2009), all buffers bind  $\text{Ca}^{2+}$  with high affinity. As well as buffering  $\text{Ca}^{2+}$ ,  $\text{Ca}^{2+}$ -binding proteins are capable of translating signals into cellular processes. For instance, calmodulin, which binds  $\text{Ca}^{2+}$  through EF-hands, interacts with many proteins to coordinate signal transduction. Calmodulin has also been shown to regulate  $\text{Ca}^{2+}$  channels (Parekh, 2011) and in neurons, it dissociates from activated L-type  $\text{Ca}^{2+}$  channels to initiate transcription via CREB (cAMP response element-binding protein; Wheeler et al. 2012). Many compounds have been specifically developed to bind  $\text{Ca}^{2+}$  (i.e. EGTA) and derivatives of these with fluorophores attached create  $\text{Ca}^{2+}$  dyes such as Fura-2 (Grienberger & Konnerth, 2012).

Other  $\text{Ca}^{2+}$  clearance mechanisms occur at the plasma membrane. Plasma membrane  $\text{Ca}^{2+}$  ATPases (PMCA) utilise ATP to extrude  $\text{Ca}^{2+}$  from the cell. More specifically, for each ATP molecule hydrolysed, 1  $\text{Ca}^{2+}$  ion is extruded (Brini & Carafoli, 2009). Notably, calmodulin can regulate PMCA activity (James et al., 1988). The  $\text{Na}^+/\text{Ca}^{2+}$  exchanger, named NCX, also controls the efflux of  $\text{Ca}^{2+}$ . NCX exchanges 3  $\text{Na}^+$  with 1  $\text{Ca}^{2+}$  ion and can function bi-directionally according to membrane potential (Liao et al., 2012).

Intracellular stores also sequester  $\text{Ca}^{2+}$  and these mechanisms are discussed in more detail below.

### ER $\text{Ca}^{2+}$ signalling

The endoplasmic reticulum (ER; sarcoplasmic reticulum in muscle cells) is an excitable, dynamic organelle that forms a continuous network throughout the cell (Park et al., 2000). Aside from its role in coordinating protein synthesis and folding, the ER is a prominent store of intracellular  $\text{Ca}^{2+}$  (reviewed in Berridge 2002). ER  $\text{Ca}^{2+}$  regulates many cellular processes including autophagy and apoptosis (Stutzmann & Mattson, 2011).

Upon cell stimulation,  $\text{Ca}^{2+}$  is released from the ER by various ion channels. Inositol-1,4,5-trisphosphate receptors ( $\text{IP}_3\text{R}$ ) are the most abundantly expressed ER  $\text{Ca}^{2+}$  channel (reviewed in Kiviluoto et al. 2013). These channels are encoded by three genes (*ITPR1-3*) and have an overlapping expression pattern in most tissues. Neurons, however, typically only express *ITPR1*. At the ER level, instead of being evenly distributed throughout the ER,  $\text{IP}_3\text{Rs}$  are clustered together (Rahman & Taylor, 2009). Seo et al. (2012) recently described the structure of these channels. It is noteworthy that the Golgi apparatus also express  $\text{IP}_3\text{R}$  and contribute to  $\text{Ca}^{2+}$  signalling (Pinton et al., 1998).  $\text{IP}_3\text{Rs}$  are regulated by various molecules, including the  $\text{Ca}^{2+}$  mobilising messenger Inositol-1,4,5-trisphosphate ( $\text{IP}_3$ ). Plasma membrane-localised G-protein coupled receptors (GPCR; such as Bradykinin receptors) activate phospholipase C to generate  $\text{IP}_3$  and diacylglycerol (DAG) from phosphatidylinositol bisphosphate ( $\text{PIP}_2$ ).

Another well characterised ER  $\text{Ca}^{2+}$  channel is the ryanodine receptor (RyR), named after the plant alkaloid ryanodine, which, at high concentrations, is a potent inhibitor of these channels (reviewed in Mackrill 2010). RyRs are non-selective cation channels, but upon stimulation release approximately 20 times more  $\text{Ca}^{2+}$  into the cytosol than  $\text{IP}_3\text{Rs}$  (Kiviluoto et al., 2013). RyRs are encoded by three different genes (*RYR1-3*). *RYR1* and 2 are predominantly expressed in muscle and cardiac cells, whereas *RYR3* is more ubiquitously expressed (Mackrill et al., 1997a). Mutations in *RYR* are associated with diseases like malignant hyperthermia and catecholaminergic polymorphic ventricular tachycardia (reviewed in Betzenhauser & Marks 2010). RyRs can be regulated by both  $\text{Ca}^{2+}$  (discussed below) and cyclic ADP-ribose (cADPR). cADPR is synthesised from NAD (Nicotinamide adenine dinucleotide) through a cyclisation reaction catalysed by ADP-ribosyl cyclases (Lee & Aarhus, 1991). cADPR sensitises RyRs to  $\text{Ca}^{2+}$  (Lee, 1993) and the action of cADPR on these channels requires additional proteins like calmodulin (Lee et al., 1994).

$\text{Ca}^{2+}$  mobilising messengers are hydrophilic and thus impermeable to the plasma membrane. Therefore, measuring physiological  $\text{Ca}^{2+}$  responses from ER channels is difficult. The traditional method for delivering messengers to the cells is through microinjection (Morgan et al., 2005). However, this requires considerable skill and is time consuming. Recently, through the addition of an acetoxymethyl (AM) group, cell permeable analogues have been developed (Parkesh et al., 2008; Rosen et al., 2012). Once inside the cell, esterases cleave the AM group and reveal the active  $\text{Ca}^{2+}$  mobilising messenger.

Both IP<sub>3</sub>R and RyR evoke complex Ca<sup>2+</sup> responses that are often spatio-temporally diverse (Berridge et al., 2000). In addition to IP<sub>3</sub> and cADPR, both these channels can be regulated by Ca<sup>2+</sup> itself. This Ca<sup>2+</sup> regulation is biphasic, where low Ca<sup>2+</sup> concentrations activate the channels (also known as Ca<sup>2+</sup>-Induced Ca<sup>2+</sup> Release [CICR]) and higher concentrations are inhibitory (Bezprozvanny et al., 1991). Such complex regulation can generate Ca<sup>2+</sup> oscillations (Berridge, 2007). It is important to note that, Ca<sup>2+</sup> is an allosteric modulator of IP<sub>3</sub>R but an activator of RyRs.

Many other molecules can inhibit ER Ca<sup>2+</sup> channel activity. For instance, the anti-apoptotic, ER-localised Bcl-2 (B-cell lymphoma 2) protein can inhibit IP<sub>3</sub>R Ca<sup>2+</sup> release and the initiation of Ca<sup>2+</sup>-mediated apoptosis (Eckenrode et al., 2010; Monaco et al., 2013). IP<sub>3</sub>Rs can also be pharmacologically inhibited with 2-Aminoethoxydiphenyl borate (2-APB) and Xestospongine C. Indeed, 2-APB identified the importance of IP<sub>3</sub>Rs in the generation and propagation of cytosolic Ca<sup>2+</sup> oscillations in sensory neurons (Zeng et al., 2008).

Ca<sup>2+</sup> can also passively leak from the ER through aqueous pores (Camello, et al., 2002). However, the molecular identity of the leak channel has been contested. Several putative channels have been proposed. These include Bcl-2, translocon and presenilins (reviewed in Kiviluoto et al. 2013). Notably mutations in presenilins have been associated with the neurodegenerative disorder Alzheimer disease (Tu et al., 2006).

The ER Ca<sup>2+</sup> leak is counterbalanced by high affinity ATP-dependent pumps called sarco- and endoplasmic-reticulum Ca<sup>2+</sup>-ATPases (SERCA) which transport cytosolic Ca<sup>2+</sup> into the ER lumen (reviewed in Michelangeli & East 2011). There are a variety of SERCA isoforms, but SERCA2b is most universally expressed. For each hydrolysed ATP, SERCA transports 2 Ca<sup>2+</sup> ions into the ER. Brody's disease is associated with mutations in the *ATP2A1* gene, which encodes the SERCA1 isoform. These mutations impair SERCA activity and elevate cytosolic Ca<sup>2+</sup> levels in muscle cells which prevents muscle relaxation. These pumps can be regulated by ER-localised proteins and the inhibitor thapsigargin. Thapsigargin is commonly used to assess ER Ca<sup>2+</sup> content by unmasking the leak pathway (reviewed in Michelangeli & East 2011).

Luminal Ca<sup>2+</sup> content of the ER ranges from 100-500 μM and is maintained by several high-affinity Ca<sup>2+</sup> buffers (Berridge, 2002). Many of these Ca<sup>2+</sup> binding proteins, such as calreticulin, BiP (Binding immunoglobulin protein) and calnexin, are also chaperones (Michalak et al., 2009). The binding of Ca<sup>2+</sup> to these chaperones can regulate protein folding. Changes in ER Ca<sup>2+</sup> can disrupt this process and trigger the unfolded protein response (UPR)

(Mekahli et al., 2011). In order to maintain appropriate luminal  $\text{Ca}^{2+}$  levels the ER refills by stimulating a  $\text{Ca}^{2+}$  current across the plasma membrane (Smyth, et al., 2010). This phenomenon is known as store operated  $\text{Ca}^{2+}$  entry (SOCE). SOCE is mediated through interactions between the proteins stromal interacting molecule (STIM1) and Orai. STIM1 is a  $\text{Ca}^{2+}$  binding protein localised to the ER membrane that senses luminal  $\text{Ca}^{2+}$  through EF-hands. At low ER  $\text{Ca}^{2+}$  levels, STIM1 re-locates to the plasma membrane and oligomerises. Here STIM1 opens the  $\text{Ca}^{2+}$ -selective channel Orai to replenish ER  $\text{Ca}^{2+}$  (Penna et al., 2008). The close apposition of the ER to the plasma membrane facilitates SOCE (this is discussed further below).

### **Mitochondrial $\text{Ca}^{2+}$ signalling**

It is well-known that the mitochondria synthesize ATP. Additionally, mitochondria can regulate cell death, differentiation and  $\text{Ca}^{2+}$  signalling. Indeed, mitochondria were the first organelles to be linked with  $\text{Ca}^{2+}$  signalling (reviewed in Carafoli 2012). Unlike cytosolic buffers, the mitochondria have a high capacity for  $\text{Ca}^{2+}$  and can therefore sequester large amounts of this signalling ion. For this reason, the mitochondria can significantly influence  $\text{Ca}^{2+}$  signalling. Indeed, these organelles can remain fixed in high  $\text{Ca}^{2+}$  environments to effectively buffer  $\text{Ca}^{2+}$  (Yi et al., 2004; Macaskill et al., 2009). This is particularly useful in neurons where mitochondria localise  $\text{Ca}^{2+}$  in the synaptic terminal (Rizzuto et al., 2012).

$\text{Ca}^{2+}$  must cross two membranes to enter the matrix, the outer and inner mitochondrial membranes (OMM and IMM respectively). Since the OMM is permeable to a variety of small molecules (including pyruvate and ATP/ADP)  $\text{Ca}^{2+}$  passes through this membrane easily. This permeability is attributed to the abundant presence of VDACs (voltage-dependent anion channels) which form diffusion pores on the OMM. Unlike the OMM, the IMM is impermeable and  $\text{Ca}^{2+}$  transport is regulated by the recently discovered mitochondrial  $\text{Ca}^{2+}$  uniporter (MCU or CCDC109A; De Stefani et al. 2011). MCU associates with various regulatory subunits such as MICU1 (mitochondrial  $\text{Ca}^{2+}$  uptake 1 protein). The knockdown of MICU1 increases mitochondrial  $\text{Ca}^{2+}$  content, thus it is likely that this EF-hand protein negatively regulates MCU (Mallilankaraman et al., 2012).  $\text{Ca}^{2+}$  is necessary for the appropriate functioning of these energetic organelles. Its presence in the matrix activates metabolic enzymes of the tricarboxylic acid cycle (TCA) to regulate energy production (reviewed in Rizzuto et al. 2012).

There is a temporal restriction to the  $\text{Ca}^{2+}$  buffering capacity of mitochondria; excessive, prolonged  $\text{Ca}^{2+}$  presence in the matrix opens the mitochondrial permeability transition pore

(PTP). The opening of the PTP releases  $\text{Ca}^{2+}$  into the cytosol (reviewed in Crompton 1999).  $\text{Ca}^{2+}$  can also escape the mitochondria through ion exchangers. The mitochondria-localised  $\text{Na}^+/\text{Ca}^{2+}$  exchanger NCLX regulates the exchange of  $\text{Ca}^{2+}$  with  $\text{Na}^+$  (Palty et al., 2010). Additionally, the  $\text{Ca}^{2+}/\text{H}^+$  antiporter Letm1 (leucine zipper-EF hand containing transmembrane protein 1) has also been proposed to mediate  $\text{Ca}^{2+}$  release (Jiang et al., 2009). Notably, deletions in the gene encoding Letm1 are associated with Wolf-Hirschhorn syndrome. This disorder is associated with seizures, congenital heart defects and mental retardation and identifies the importance in maintaining mitochondrial  $\text{Ca}^{2+}$  homeostasis (Jiang et al., 2013).

### Lysosomal $\text{Ca}^{2+}$ signalling

Lysosomes are acidic organelles that contain hydrolytic enzymes, such as Cathepsin C (figure 1.2). Acidic pH is generated by V-type ATPases. Lysosomal proteins (such as the lysosome associated membrane protein 1, LAMP1) are highly glycosylated to afford protection from lytic enzymes. Lysosomal hydrolases degrade unwanted macromolecules (lipids, proteins etc...) and organelles through the process of autophagy.

Against the long-standing view that lysosomes are simply passive degradative, organelles, evidence now suggests that these acidic organelles are also mobilisable  $\text{Ca}^{2+}$  stores (Patel & Docampo, 2010). Much of this evidence was based on studies using the lysosomotropic agent GPN (glycyl-L-phenylalanine 2-naphthylamide). GPN is freely diffusible, a di-peptide substrate for the lysosomal hydrolase Cathepsin C (Jadot et al., 1984). Once this compound is hydrolysed it permeabilises these organelles. Upon measuring cytosolic  $\text{Ca}^{2+}$ , Haller and colleagues (1996) were the first to demonstrate that GPN evokes  $\text{Ca}^{2+}$  responses in MDCK cells (Haller et al., 1996). This has since been confirmed in a variety of cell types including neurons and human fibroblasts (summarised in table 1.1). Acidic hydrolases and low luminal pH have made the direct measurements of lysosomal  $\text{Ca}^{2+}$  experimentally difficult. Nevertheless, Christensen and colleagues (2002) determined the concentration of luminal  $\text{Ca}^{2+}$  using dextran-based  $\text{Ca}^{2+}$  indicators (delivered the lysosomes through endocytosis). They established that luminal lysosomal  $\text{Ca}^{2+}$  concentration is approximately 500  $\mu\text{M}$  (Christensen et al., 2002). This value has since be confirmed in human fibroblasts (Lloyd-Evans et al., 2008) and is similar to the  $\text{Ca}^{2+}$  concentration reported within the ER (see above).

Lysosomes have an important role in regulating cytosolic  $\text{Ca}^{2+}$  signalling. Indeed, lysosomes have recently been shown to rapidly sequester cytosolic  $\text{Ca}^{2+}$  signals (López-Sanjurjo et al., 2013). However, the mechanism of lysosomal  $\text{Ca}^{2+}$  uptake remains elusive (Patel & Docampo,

2010). A proton gradient is likely important for lysosomal  $\text{Ca}^{2+}$  uptake since bafilomycin-A1 (a V-type ATPase inhibitor) reduces the  $\text{Ca}^{2+}$  content of these organelles (Christensen et al., 2002). It has been suggested that  $\text{Ca}^{2+}$ /hydrogen exchangers (such as those present in plant vacuoles) might regulate lysosomal  $\text{Ca}^{2+}$  uptake in mammalian cells (Patel & Docampo, 2010).

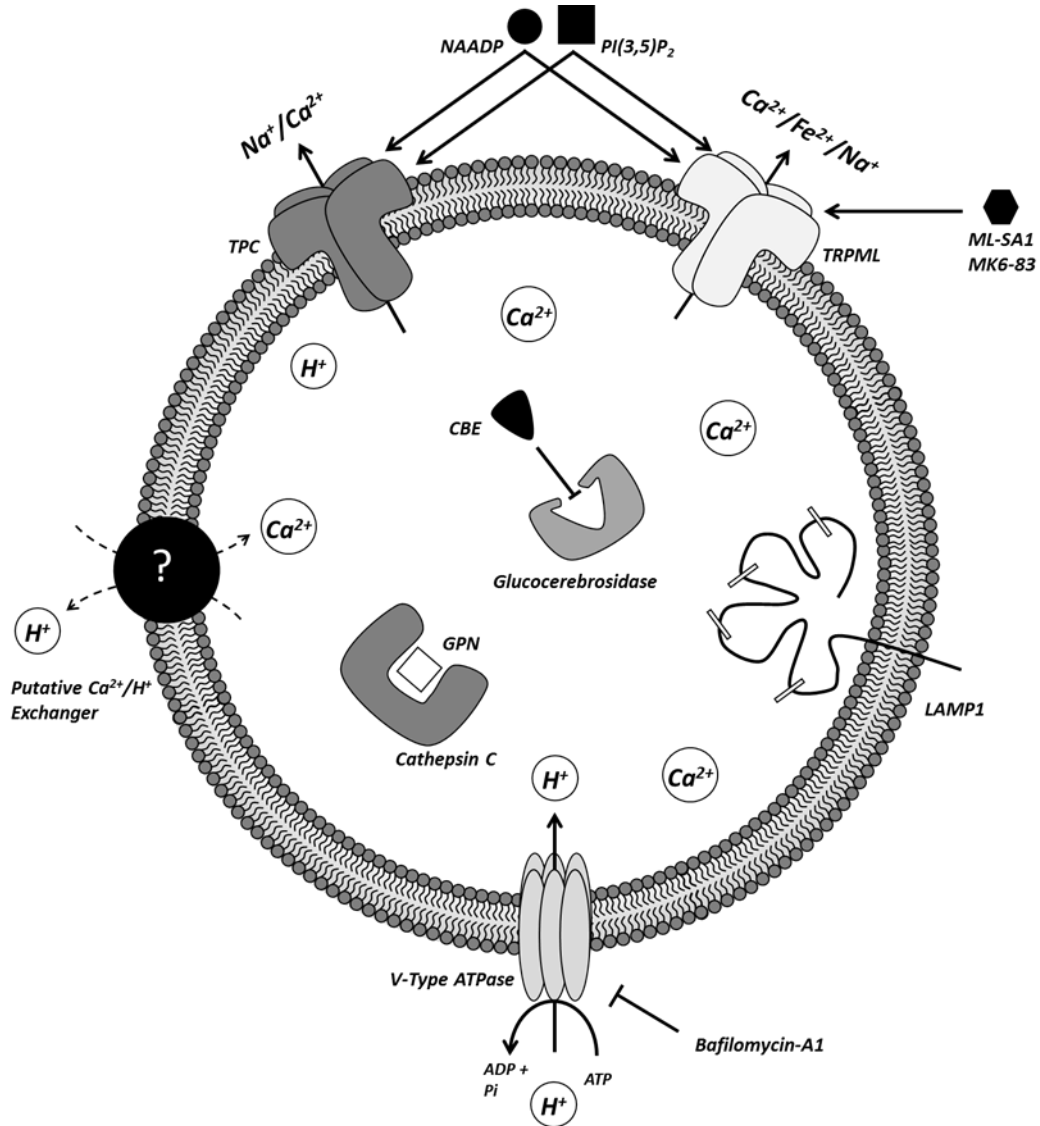


**Figure 1.2 Lysosomes**

Lysosomes are acidic, membrane bound organelles that maintain their pH by V-type ATPases. Lysosomes are filled with hydrolytic enzymes including cathepsin C and glucocerebrosidase. GPN is a substrate for cathepsin C that can be used to permeabilise lysosomes and Condurotol β epoxide (CBE) can inhibit glucocerebrosidase activity. Lysosomal membrane proteins (such as LAMP1) are highly glycosylated to afford protection from lytic enzymes. Lysosomes are also  $\text{Ca}^{2+}$  stores. TPC and TRPML channels mediate  $\text{Ca}^{2+}$  release. These receptors can be activated by NAADP ( $\text{Ca}^{2+}$  mobilising messenger) and PI(3,5)P<sub>2</sub> (a phosphoinositide). Additionally, the synthetic agonist ML-SA1 has been shown to activate TRPML channels. The mechanism of  $\text{Ca}^{2+}$  uptake into the lysosomes is unknown. It has been proposed that  $\text{Ca}^{2+}/\text{H}^+$  exchangers are involved.

**Table 1.1.** Summary of GPN-evoked Ca<sup>2+</sup> responses.

| <b>Cell type</b>                                 | <b>Characterisation of GPN-evoked Ca<sup>2+</sup> Response</b> | <b>[GPN] (μM)</b> | <b>Reference</b>                |
|--|--|-------------------|---------------------------------|
| <b>Pancreatic acinar cells</b>                   | Low magnitude, monotonic responses.                            | 50                | (Yamasaki et al., 2004)         |
|  | Oscillatory responses.   | 50                | (Gerasimenko et al., 2006)      |
|  | Transient response.  | 200               | (Menteyne et al., 2006)         |
| <b>Neuronal cultures</b>                         | Complex responses.   | 200               | (Tu et al., 2010)               |
|  | Large magnitude, complex responses.                            | 200               | (Pandey et al., 2009)           |
|  | Low magnitude, monotonic responses.                            | 500               | (Coen et al., 2012)             |
| <b>Human fibroblasts</b>                         | Low magnitude, monotonic responses.                            | 200               | (Visentin et al., 2013)         |
| <b>Mouse embryonic fibroblasts</b>               | Complex responses.   | 200               | (Coen et al., 2012)             |
| <b>T-lymphocytes</b>                             | Complex responses.   | 50                | (Steen et al., 2007)            |
| <b>B-lymphocytes</b>                             | Low magnitude, complex responses.                              | 50                | (Duman et al., 2006)            |
| <b>Human platelets</b>                           | Low magnitude, monotonic response.                             | 50                | (López et al., 2005)            |
| <b>Myometrial cells</b>                          | Low magnitude, monotonic response.                             | 50                | (Soares et al., 2007)           |
| <b>Cell lines</b>                                |  |                   |                                 |
| <b>HEK</b><br><i>Human embryonic kidney</i>      | Low magnitude, monotonic responses.                            | 200               | (Reeves et al., 2006)           |
| <b>MDCK</b><br><i>Madin Darby canine kidney</i>  | Transient, large magnitude responses.                          | 200               | (Haller et al., 1996)           |
| <b>THP-1</b><br><i>Human Monocytic</i>           | Monotonic responses.   | 200-400           | (Sivaramakrishnan et al., 2012) |
| <b>RBL-2H3</b><br><i>Rat basophilic leukemia</i> | No responses.  | 40                | (Moreno-Sanchez et al., 2012)   |
| <b>MEG01</b><br><i>Human megakaryoblastic</i>    | Low magnitude, monotonic responses.                            | 50                | (Dionisio et al., 2011)         |

Lysosomes have been identified as the targets of the most potent Ca<sup>2+</sup> mobilising messenger NAADP (Nicotinic Acid Adenine Dinucleotide Phosphate). This was first established by Churchill and colleagues (2002) when NAADP-evoked Ca<sup>2+</sup> responses were blocked with GPN and bafilomycin-A1. Thus, unlike IP<sub>3</sub> and cADPR, which release Ca<sup>2+</sup> through well-defined ER channels, NAADP is unique by activating acidic Ca<sup>2+</sup> stores. It is important to note that lysosomes are not the only acidic Ca<sup>2+</sup> stores. Endosomes, lysosome-related organelles (secretory lysosomes) and secretory granules also store and release Ca<sup>2+</sup> (reviewed in Patel & Docampo 2010; Morgan et al. 2011)

Several molecular targets for NAADP have been proposed, including RyR (Gerasimenko et al., 2003; Dammermann & Guse, 2005). However, in 2009 three independent laboratories identified Two Pore Channels (TPCs) as putative NAADP receptors (Brailoiu et al., 2009a; Calcraft et al., 2009; Zong et al., 2009). In these studies NAADP-evoked Ca<sup>2+</sup> responses were



i) inhibited in cells where TPC expression was silenced using RNA interference and ii) increased in cells overexpressing TPCs. TPCs contain two repeats of a 6 transmembrane domain that are bridged by a cytosolic loop (Ishibashi et al., 2000). It has been predicted that each form half of a functional channel and in order to mediate  $\text{Ca}^{2+}$  release TPCs dimerise (Churamani et al., 2012). Three TPC genes (*TPCN1*, *TPCN2* and *TPCN3*) have been identified, but *TPCN3* is absent in human genomes (Brailoiu et al., 2010a). TPCs are exclusively expressed in the endo-lysosomal system; TPC1 localises with endosomal compartments whereas TPC2 predominantly resides on lysosomal structures (Brailoiu et al., 2009a, 2010b). The localisation of TPC2 to the lysosomes is mediated by a dileucine targeting motif in the N-terminus (Brailoiu et al., 2010b).

Although many have established TPCs as the molecular targets of NAADP, Wang et al. (2012) recently challenged this view. By patch-clamping individual lysosomes, that had been enlarged with vacuolin-1, the authors showed that TPCs were gated by the lysosomal phosphoinositide  $\text{PI}(3,5)\text{P}_2$  (phosphatidylinositol3,5-bisphosphate) not NAADP. What was particularly surprising was that NAADP-evoked  $\text{Ca}^{2+}$  responses persisted in TPC1 and TPC2 double knockout mice. Furthermore, they identified that TPCs are predominantly  $\text{Na}^+$ -permeable. These findings contrasted with established electrophysiological analysis of TPC2 incorporated into lipid bilayers (Pitt et al., 2010), single lysosomes overexpressing TPC2 (Schieder et al., 2010) and plasma membrane targeted TPC2 (Brailoiu et al., 2010b) which demonstrated that TPCs are both  $\text{Ca}^{2+}$  permeable and NAADP-gated. Recent research by Jha and colleagues (2014), might resolve part of this conflict having shown that TPCs are regulated by both  $\text{PI}(3,5)\text{P}_2$  and NAADP (Jha et al., 2014). NAADP action is further complicated by the finding that this messenger binds with a low molecular weight accessory proteins (Lin-Moshier et al., 2012).

TRPML (transient receptor potential mucolipin) is another ion channel that has been shown to mediate lysosomal  $\text{Ca}^{2+}$  release. TRPML channels are members of the TRP family of non-selective cation channels. Originally named Mucolipins, TRPML channels are composed of 6 transmembrane domains and a pore region (reviewed in Cheng et al. 2010). Three TRPML isoforms (TRPML1-3) have been identified in mammals and they have been shown to associate with one another. Notably, mutations in the *MCOLN1* gene, which encodes TRPML1, are responsible for the autosomal recessive lysosomal storage disorder (LSD) Mucopolidosis IV (MLIV). MLIV is characterised by severe neurodegeneration and associated

with disrupted endo-lysosomal trafficking, substrate degradation and lysosomal biogenesis (reviewed in Lloyd-Evans & Platt 2011).

TRPML 1-3 have also been localised to the endo-lysosomal system. Overexpressed, fluorescently tagged TRPML1 co-localised with puncta labelled with the lysosomal marker LAMP1 (Kiselyov et al., 2005). Although, TRPML2 and 3 also localised with lysosomes they have been shown to additionally associated with late endosomes and the plasma membrane (Kim et al., 2009). The localisation of TRPML3 to the plasma membrane and the identification of point mutations that increase the open probability of TRPML3 permitted the characterisation of channel properties. Notably, in mice these mutations cause the varitint-waddler phenotype which is characterised by deafness, repetitive behaviour and pigmentation defects (Di Palma et al., 2002). By patch clamping the whole cell Kim and colleagues (2007) identified that TRPML3 is an inwardly-rectifying  $\text{Ca}^{2+}$  permeable channel (Kim et al., 2007). TRPML channels have since been shown to conduct a variety of cations. Indeed, Dong and colleagues (2008) identified that TRPML1 and TRPML2 (but not TRPML3) are also  $\text{Fe}^{2+}$  permeable. Given that TRPs are a family of non-selective cation channels, it is perhaps unsurprising that TRPML channels conduct a variety of cations. It is however notable that the channel properties of TRPML1 have been debated, where some have shown that this channel is actually outwardly rectifying and selectively permeable to monovalent cations (Kiselyov et al., 2005). Therefore, further characterisation of TRPML-mediated  $\text{Ca}^{2+}$  signalling is required.

We know very little about the gating of TRPML channels. Indeed, it has been proposed NAADP activates TRPML since NAADP-evoked  $\text{Ca}^{2+}$  responses are suppressed in human fibroblasts with the knockdown of TRPML1 (Zhang et al., 2011). However, these reports conflict with others, such as Yamaguchi et al. (2011), who have shown that pancreatic acinar cells from wild-type and TRPML knockout mice exhibit similar NAADP-evoked  $\text{Ca}^{2+}$  responses. It has also been shown that, like TPCs, TRPML channels are activated by  $\text{PI}(3,5)\text{P}_2$  (Dong et al., 2010). Recently, synthetic TRPML agonists ML-SA1 (Shen et al., 2012) and MK6-83 (Chen et al., 2014) were developed. One of these synthetic compounds has been used in chapter 3 to further characterise TRPML signalling.

TPCs and TRPML channels are important for various cellular functions, including autophagy. TRPML3 has been shown to associate with autophagic vacuoles and reducing the expression of this channel inhibits autophagy (Kim et al., 2009). Furthermore, the stimulation of astrocytes with the cell permeable NAADP analogue (NAADP-AM) increases levels of

autophagic markers (such as LC3, light chain 3; Pereira et al. 2011). Such increases were not seen in cells overexpressing TPC2<sup>L265P</sup> which has a mutation in the putative pore domain (Pereira et al., 2011). It is unknown how NAADP and TRPML mediate autophagy, although organelle fusion might be involved. The endo-lysosomal system is dynamic and the fusion of endocytic compartments is necessary for appropriate functioning. Pryor and colleagues (2000) showed that both lysosome reformation and the fusion of late endosomes with lysosomes are regulated by luminal Ca<sup>2+</sup> and local signalling (Pryor et al., 2000). Very recent, evidence has shown that TPCs might regulate lysosome fusion, morphology, and trafficking (Ruas et al., 2014; Lin-Moshier et al., 2014; Grimm et al., 2014). In *Xenopus* oocytes, TPC2 was shown to regulate lysosomal trafficking through interactions with Rab7; an established trafficking GTPase (Lin-Moshier et al., 2014). Moreover, Grimm and colleagues (2014) identified that TPC2 is necessary for cholesterol trafficking and regulating lysosome fusion. Deficiencies in TPC2 made mice susceptible to liver damage (Grimm et al., 2014). In chapter 5, I examine the role of TPC2 in Parkinson disease.

### *Connecting Ca<sup>2+</sup> stores*

Cells are compartmentalised to isolate specific cellular functions. However, this spatial separation poses certain difficulties for inter-organellar communication. Thus, cells have evolved several mechanisms to communicate including membrane contact sites (MCSs). MCSs form in regions where organelles are closely (<30 nm) associated (reviewed in Prinz 2014). The microdomains between organelles are highly specialised and are known to facilitate lipid exchange, organelle trafficking, cell death and Ca<sup>2+</sup> signalling.

The ER forms MCSs with several organelles and the plasma membrane (figure 1.3). These *connections* are known to regulate Ca<sup>2+</sup> homeostasis, signalling and storage. Here I will further discuss the components of ER MCSs and their role in Ca<sup>2+</sup> signalling.

#### **ER-plasma membrane**

The physical and functional interactions between the ER and plasma membrane (PM) are relatively well established (figure 1.3A). They play an important role in excitation-contraction coupling and SOCE.

In myocytes, contraction is stimulated by an influx of Ca<sup>2+</sup>. The increase in cytosolic Ca<sup>2+</sup> is a synchronised event and is derived from Ca<sub>v</sub>1.1 (L-type VGCC also known as dihydropyridine receptors) on the PM (sarcolemma) and RyR on the sarcoplasmic reticulum (SR) (reviewed in

Bers 2002; Endo 2009). Cav1.1 open after a change in membrane potential, this influx of  $Ca^{2+}$  activates RyR, through a process known as CICR (discussed above).

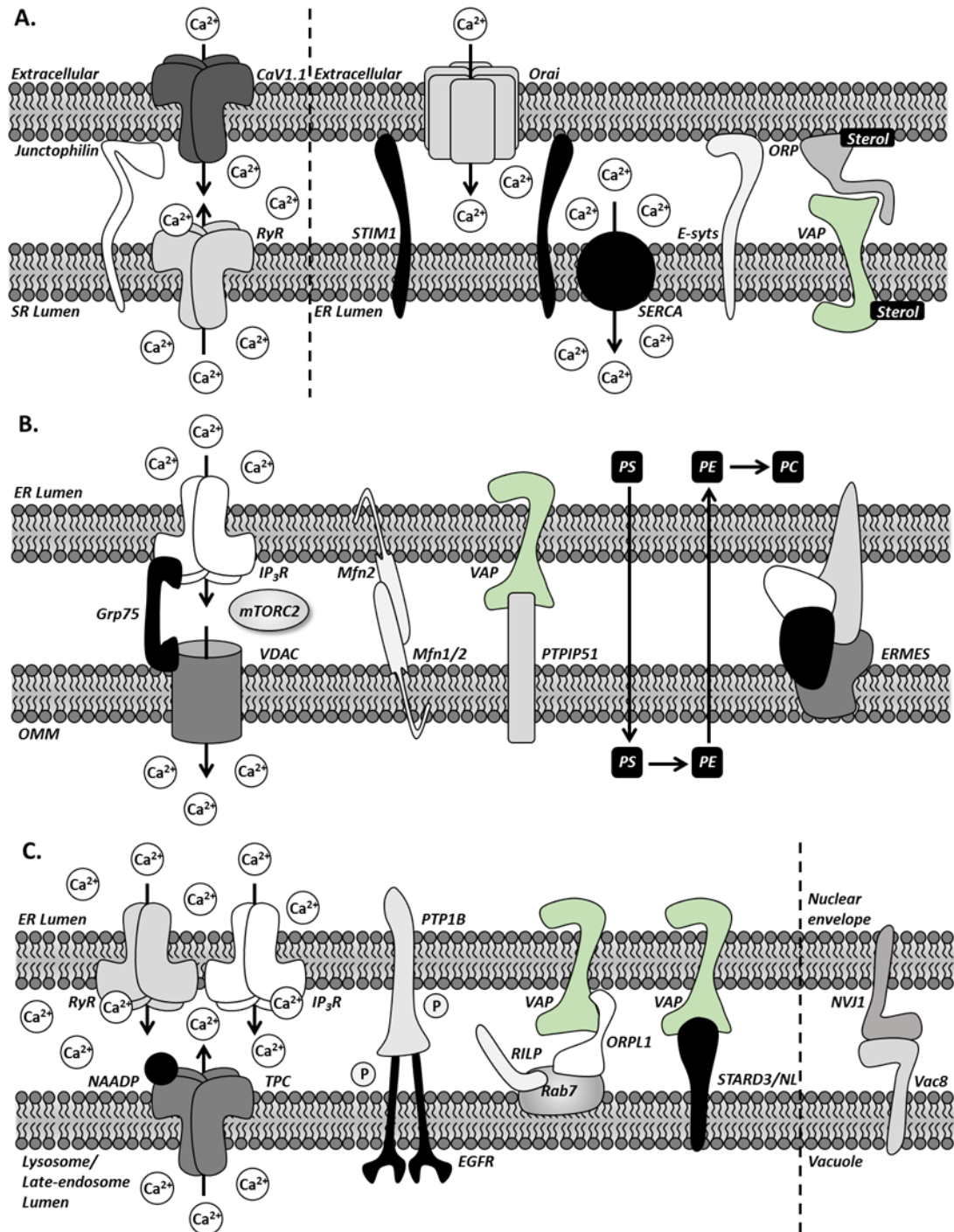


Figure 1.3 legend overleaf.

### Figure 1.3 The diversity of ER membrane contact sites

The ER/SR forms functional and physical connections with several components of the cell including the plasma membrane (A), mitochondria (B) and late-endosomes/lysosomes (C).

(A) In myocytes (left) the Ca<sub>v</sub>1.1 channels (L-type VGCC) on the plasma membrane (sarcolemma) associate with RyRs on the SR to mediate excitation contraction coupling. Some of these junctions are stabilised with junctophilins. In other cell types the ER and plasma membrane connect to regulate SOCE and lipid trafficking. During SOCE, STIM1 (on the ER) activates Orai channels which mediate Ca<sup>2+</sup> influx. In order to refill, the ER sequesters Ca<sup>2+</sup> using SERCA ATPases. Although not thought to regulate SOCE, E-syts are also present at ER-plasma membrane junctions. Sterol trafficking across these membrane contact sites are regulated VAP, which binds to ORP through its FFAT motif.

(B) ER-mitochondria junctions (MAMs) regulate Ca<sup>2+</sup> signalling and lipid synthesis. Ca<sup>2+</sup> release from the ER-IP<sub>3</sub>R is rapidly sequestered by the mitochondria. Physical associations between IP<sub>3</sub>Rs and VDAC enable this uptake. Grp75 and mTORC2 are important mediators of this junction. Mitofusins (which homo- and hetero-typically associate) and VAPs (which associate with PTPIP51) are also enriched in MAMs. Furthermore, MAMs facilitate the synthesis of phosphatidylcholine (PC) from phosphatidylserine (PS). The mechanism behind this lipid transfer is unknown in mammalian cells but in yeast the ERMES complex is important.

(C) The ER also associates with compartments of the endo-lysosomal system. These compartments are thought to potentiate NAADP signalling. Additionally, late-endosome ER contacts are important for the de-phosphorylation of endocytosed EGFR by PTP1B. VAP proteins can also regulate these junctions by associating with an ORP1L/RAB7/RILP complex and STARD3/STARD3NL. In yeast (right) the nuclear envelope and vacuole (the equivalents of ER and lysosomes) are tethered together by NVJ1 and Vac8.

The coordination of this Ca<sup>2+</sup> signalling is facilitated by MCSs between the SR and PM. The PM of myocytes is invaginated between sarcomeres and these invaginations are known as T-tubules. It is here that the t-tubules connect with the SR. These MCSs are found in both cardiac and skeletal myocytes and are known as dyads and triads respectively. Through electron microscopy, Brochet et al. (2005) identified that these MCSs are tight (<12 nm). Junctophilins have been shown to anchor the SR and PM together (Takeshima et al., 2000). Importantly, knocking down these tethering proteins reduced MCSs and perturbs Ca<sup>2+</sup> signalling and contraction (Takeshima et al., 2000). Thus, by apposing Cav1.1 and RyR with junctophilins, SR-PM MCSs enable excitation-contraction coupling.

MCSs between the ER and PM are also present in non-excitable cells. These contacts are essential for the process of SOCE. As discussed above, when STIM1 senses low levels of  $\text{Ca}^{2+}$  inside the ER, it clusters in ER regions that are closely apposed with the PM and activates the  $\text{Ca}^{2+}$  channel Orai. Using TIRF and electron microscopy, Wu et al. (2006) identified that STIM1 relocates to existing ER-PM MCSs. These MCSs are around 17 nm wide and, in an active confirmation, STIM1 extends across this distance to associate with Orai and plasma membrane phosphoinositides (Muik et al., 2011). However, the components that tether pre-existing ER-PM SOCE sites are unknown. Some have proposed that STIM1 itself mediates the formation of new MCSs (Orci et al., 2009). During SOCE,  $\text{Ca}^{2+}$  enters the ER through SERCA pumps, which are enriched at these contact sites (Manjarrés et al., 2010). Importantly, ER-PM MCS minimise the disturbance to cytosolic  $\text{Ca}^{2+}$  levels by localising  $\text{Ca}^{2+}$  entry.

It is notable that proteins not involved in SOCE also mediate ER-PM MCS. For instance, extended-synaptotagmins (E-syts) were recently shown to tether the ER with the PM (Giordano et al., 2013). The extent and distance between these E-syts-associated MCSs can be regulated by both  $\text{Ca}^{2+}$  and PI(4,5)P<sub>2</sub>.

MCSs are not only important for  $\text{Ca}^{2+}$  signalling but also lipid trafficking. The ER is the dominant site for lipid synthesis in the cell. Intracellular lipid transport relies heavily upon vesicle trafficking (Prinz, 2010). However, even when vesicle trafficking has been inhibited, lipids, such as cholesterol, still reach their appropriate destination in the PM (reviewed in Prinz 2010). MCSs are thought to mediate this trafficking. In yeast, ORPs (Oxysterol-binding protein (OSBP)-related proteins) are essential components of these contact sites (Schulz et al., 2009). These sterol binding proteins associate with the PM (Stefan et al., 2011) and have a motif (FFAT) that interacts with ER-localised VAPs (vesicle associated membrane protein-associated proteins) (Lehto et al., 2005). It is through this VAP-ORP complex that lipids can be trafficked towards the PM (reviewed in Stefan et al. 2013). It is important to note that, VAPs have been implicated in several MCSs and these are further discussed below.

#### **ER-mitochondria**

The mitochondria are known to effectively sequester ER  $\text{Ca}^{2+}$ , despite the low affinity of MCU (Rizzuto et al., 1993). Physical associations between these organelles facilitate this uptake by accumulating relatively high levels of  $\text{Ca}^{2+}$  (10  $\mu\text{M}$ ; Csordás et al. 2010). These localised increases in  $\text{Ca}^{2+}$  meet the low affinity of MCU and permit the entry of  $\text{Ca}^{2+}$  into the matrix (Rizzuto et al., 2012). The specialised ER-mitochondria MCSs are termed MAMs

(mitochondria-associated membranes; figure 1.3B) and they are important signalling platforms that occupy 5-20% of the mitochondrial surface (Rizzuto et al., 1998).

The transfer of  $\text{Ca}^{2+}$  from the ER and mitochondria is necessary for ATP synthesis. The ER is energetically expensive, both SERCA activity and protein folding rely on ATP. When the ER-localised ATP levels are reduced, the ER chaperone BiP (which hydrolyses ATP) is thought to stimulate  $\text{Ca}^{2+}$  release from the ER (Kaufman & Malhotra, 2014). Subsequently, this influx of  $\text{Ca}^{2+}$  into the mitochondrial matrix activates enzymes, such as pyruvate dehydrogenase, within the TCA cycle. Physical associations between the ER and mitochondria facilitate this cross-talk.

Protein contacts tether the ER and mitochondria signalling apparatus together. As mentioned above,  $\text{IP}_3\text{R}$  are known to cluster in specific regions. Many of these clusters are located within MAMs. Szabadkai and colleagues (2006) identified that VDAC (on the mitochondria) associates with  $\text{IP}_3\text{Rs}$ . Grp75 (Glucose-regulated protein 75; member of the heat shock protein family) stabilises  $\text{IP}_3\text{R}$ -VDAC junctions to mediate  $\text{Ca}^{2+}$  exchange (Szabadkai et al., 2006). The nutrient sensor mTORC2 (the mammalian target of rapamycin complex 2) has also been shown to interact with and regulate this junction (Betz et al., 2013).

Proteins that regulate mitochondrial fusion and fission are also enriched in MAMs. Mitofusin 1 and 2 (Mfn1 and Mfn2, respectively) are dynamin associated GTPases. Mitofusins associate hetero- and homo-typically within MAMs. de Brito and Scorrano (2008) have shown that the knockdown of Mfn2, in fibroblasts, reduces MAMs and impairs mitochondrial  $\text{Ca}^{2+}$  uptake.

An isoform of VAP (VAPb) has also been localised to MAMs (De Vos et al., 2012). Notably, mutations in VAPb are known to cause the neurodegenerative disorder amyotrophic lateral sclerosis (Nishimura et al., 2004). VAPb interacts with the OMM protein PTPIP51 (protein tyrosine phosphatase interacting protein 51) and regulates mitochondrial  $\text{Ca}^{2+}$  uptake (De Vos et al., 2012). Pathogenic mutations in VAPb were shown to increase PTPIP51 binding and disrupt mitochondrial  $\text{Ca}^{2+}$  uptake (De Vos et al., 2012).

MAMs are also important for the synthesis of lipids (reviewed in Osman et al. 2011). In order to synthesise phosphatidylcholine (PC) from phosphatidylserine (PS) lipids are exchanged between the ER and mitochondria. PS, which is produced in the ER, is decarboxylated by mitochondrial enzymes and the product, phosphatidylethanolamine (PE), is then methylated by ER proteins. This convoluted synthesis is thought to involve MAMs. In yeast, the ERMES (ER-mitochondria encounter structure) complex facilitates lipid trafficking across MAMs

(Kornmann et al., 2009). However, proteins associated with ERMES are not conserved in mammals and require further characterisation.

### ER-lysosomes

Functional connections between the lysosomes and ER have been widely reported. For instance, in mammalian (pancreatic acinar) cells, NAADP-evoked  $\text{Ca}^{2+}$  responses could be completely inhibited after blocking  $\text{IP}_3\text{R}$  and RyR receptors (Cancela et al., 1999). Yet, desensitising NAADP receptors, with high concentrations of NAADP, did not affect  $\text{IP}_3$  and cADPR signalling (Cancela et al., 1999). The authors concluded that NAADP might function upstream of  $\text{IP}_3\text{R}$  and RyR. Several others have also reported diminished NAADP responses after blocking  $\text{IP}_3\text{R}$  and RyR (Churchill & Galione, 2000; Brailoiu et al., 2005, 2009b; Kinnear et al., 2004). However, some have interpreted these findings as NAADP acting on ER receptors (Dammermann & Guse, 2005).

Since  $\text{IP}_3\text{R}$  and RyR can be activated by  $\text{Ca}^{2+}$ , local elevations in  $\text{Ca}^{2+}$  can stimulate signalling from these channels. It is generally believed that lysosomal  $\text{Ca}^{2+}$  release, in response to NAADP, triggers CICR (Figure 1.3C; reviewed in Patel & Brailoiu 2012). This can be seen when examining NAADP-evoked  $\text{Ca}^{2+}$  responses, which are biphasic. The first response is small (often termed the pacemaker) and thought to be lysosomal  $\text{Ca}^{2+}$  release. These initial responses are followed by a global  $\text{Ca}^{2+}$  signals that can be spatio-temporally diverse. It is these secondary responses that are sensitive to ER  $\text{Ca}^{2+}$  inhibitors. It is also notable that the functional coupling between lysosomes and the ER is bidirectional. Morgan and colleagues (2013) recently identified that  $\text{Ca}^{2+}$  release through  $\text{IP}_3\text{R}$  and RyR evoked  $\text{Ca}^{2+}$  signals from the lysosomes using lysosomal pH as an indicator of NAADP activity.

As discussed above, TPCs are the likely targets for NAADP. Part of this evidence came from redirecting TPCs to the PM (Brailoiu et al., 2010b). This was achieved by mutating the lysosomal targeting motif. However, when TPCs were re-directed to the plasma membrane NAADP-evoked  $\text{Ca}^{2+}$  responses became sluggish and were no longer sensitive to ER channel inhibitors (Brailoiu et al., 2010b). Additionally, NAADP-evoked  $\text{Ca}^{2+}$  responses in broken cell preparations are insensitive to ER channel blockade (Lee & Aarhus, 1995). Thus, the positioning of lysosomes close to the ER is necessary for “channel chatter” to occur. In 2004, Kinnear and colleagues identified that lysosomes and RyR co-localise in myocytes. We recently identified MCSs between ER-Lysosomes (Kilpatrick et al., 2013). Electron micrographs revealed that the majority of lysosomes (80%) form tight MCSs (20 nm) with the ER (Kilpatrick et al., 2013). However, the molecular identity of these junctions is unknown.



Yeast form stable MCSs between the acidic vacuoles and the nuclear envelope. The mammalian equivalents of these organelles are lysosomes and the ER, respectively. These junctions are anchored together through physical interactions between Vac8 (on the vacuole) and NVJ1 (on the nuclear envelope) (Pan et al., 2000). Overexpressing NVJ1 caused a marked proliferation of MCSs, whereas NVJ1 null yeast lost the majority of their vacuole-nuclear envelope MCSs (Pan et al., 2000). This junction is thought to facilitate the degradation of unwanted nuclear material. Further examination of these junctions and homologous mammalian proteins might reveal more about lysosome-ER MCSs.

In mammalian cells, MCSs between late-endosomes and the ER have been characterised (figure 1.3C). Eden and colleagues (2010) were the first to identify these junctions. These sites are necessary for the de-phosphorylation of endocytosed epidermal growth factor receptors (EGFR) by the protein tyrosine phosphatase PTP1B (Eden et al., 2010). Dephosphorylated EGFRs are then internalised into late-endosomes (multivesicular bodies) and degraded by lysosomes. This trafficking attenuates EGFR signalling, which has been associated with cellular migration, proliferation and survival (Eden et al., 2012). These MCSs might also facilitate  $\text{Ca}^{2+}$  exchange, especially since endosomes store  $\text{Ca}^{2+}$  (approximately 40  $\mu\text{M}$ ; Sherwood et al. 2007) and TPC1 has been localised to endosomal compartments (Brailoiu et al., 2009a).

These late-endosome-ER junctions have been molecularly characterised (Rocha et al., 2009; Alpy et al., 2013). Components that mediate MCSs also regulate late-endosome trafficking. Cytoskeletal motor proteins (dyneins and kinesins) determine the direction of endosomal trafficking (Korolchuk et al., 2011). These motor proteins are controlled by GTPases such as Rab and Arfs (Korolchuk et al., 2011). Rocha and colleagues (2009) identified that Rab7, localised to the late endosomes, can determine whether compartments remain fixed opposite the ER, or are trafficked along microtubules. When bound to GTP, Rab7 associates with RILP (Rab-interacting lysosomal protein) and the cholesterol sensor ORP1L. In cholesterol replete conditions RILP interacts with dynein through the adaptor protein p150<sup>Glued</sup> to be transported along microtubules. However, when cholesterol levels are low ORP1L attaches to VAPa on the ER through its FFAT motif. Under these low cholesterol conditions MCSs are formed. A recent study, using real-time imaging, revealed that lysosomes move along ER tubules (López-Sanjurjo et al., 2013). Thus, lysosomal trafficking might also occur whilst physically connected to the ER.

Alpy and colleague (2013) recently identified another late-endosome-ER bridging complex. They show that STARD3 (StAR [steroidogenic acute regulatory protein] related lipid transfer (START) domain-3) and STARD3NL (STARD3 N-terminal like) have FFAT motifs that interact with VAP proteins on the ER (Alpy et al., 2013). These junctions might regulate cholesterol transport. Thus cholesterol, can influence late-endosome-ER MCSs. This has important implications for diseases, such as atherosclerosis, where cholesterol accumulates.

## Parkinson disease and related disorders

### Parkinson disease

Parkinson disease (PD) is a disabling and common neurodegenerative movement disorder. Over 1% of individuals at 65 years of age develop PD and prevalence increases to 5% by the age of 85 (Shulman et al., 2011). PD is clinically characterised by postural instability, rigidity, bradykinesia and a resting tremor (Schapira, 2009). Motor impairment has been attributed to the degeneration of dopaminergic neurons within the substantia nigra pars compacta (SNc) and subsequent dysfunction of the basal ganglia (Braak et al., 2004). The basal ganglia are a cluster of nuclei necessary for the coordination of movement. Dopaminergic neurons develop intraneuronal inclusions, called Lewy bodies, which are composed of alpha-synuclein ( $\alpha$ -syn) (Braak et al., 2004). By the time PD is clinically diagnosed, more than 60% of dopaminergic neurons have degenerated (Shulman et al., 2011).

As well as advanced age, several other epidemiological factors have been linked to PD onset. In the 1980s, a PD outbreak was reported among drug abusers. The accidental injection of MPTP (1-methyl-4-phenyl-1,2,3,6-tetrahydropyridine), a precursor of MPP<sup>+</sup>, rapidly induced PD symptoms (Langston et al., 1983). This stimulated research examining the links between environmental toxins and PD pathogenesis (Goldman, 2014). A recent meta-analysis, conducted by van der Mark et al. (2012), identified that pesticide exposure can nearly double the risk of developing PD. One of these PD inducing pesticides, paraquat (1,1-dimethyl-4,4-bipyridinium dichloride) is a structural analogue of MPP<sup>+</sup>. Many (including Liou et al. 1997; Kamel et al. 2007; Tanner et al. 2011), although not all (Hertzman et al., 1994; Firestone et al., 2010), have associated paraquat exposure with PD. Paraquat was one of the most widely used pesticides, but it has since been outlawed in many European countries. Like MPTP, paraquat can cross the blood brain barrier and enter dopaminergic neurons via the dopamine transporter (reviewed in Goldman 2014). Thus, paraquat can selectively accumulate in dopaminergic neurons. Many of the pathological hallmarks of PD, including  $\alpha$ -syn

aggregation (Manning-Bog et al., 2002), are recapitulated in paraquat exposed animal models (reviewed in Dinis-Oliveira et al. 2006).

Traditionally, PD has been viewed as a sporadic disorder that can be linked to environmental triggers. It was even referred to as the quintessential “non-genetic disease” (Hardy, 2003). However, recent research has transformed the genetic understanding of PD. Between 10-30% of PD patients have family history of the disease. To date, 12 genes have been undisputedly linked with PD (Trinh & Farrer, 2013) and a number of other susceptibility loci have been identified through genome-wide association studies (GWAS; Nalls et al. 2011). The first gene associated with PD was identified in 1997 (Polymeropoulos et al., 1997). This gene, *SNCA*, encodes  $\alpha$ -syn, the protein that aggregates in Lewy bodies. Both point mutations and increased gene dosage (duplication and triplication) have been reported in PD (Singleton et al., 2003).

Until recently, sporadic PD was seen as distinct from familial forms. Those lines are now blurring since many familial gene variants have been identified in sporadic cases. For instance, mutations in the leucine-rich repeat kinase 2 gene (*LRRK2*) have been reported in 10% of familial cases (Di Fonzo et al., 2006) and up to 4% of sporadic PD (Paisán-Ruíz et al., 2008). This gene encodes a large, multi-domain protein called LRRK2. LRRK2 is particularly unusual having two enzymatic sites; a kinase and a GTPase. Several mutations have been described in LRRK2, however the most common mutation, G2019S, resides in the kinase domain (Gilks et al., 2005; Corti et al., 2011). Mutations are believed to enhance kinase activity (West et al., 2005) and this is consistent with a toxic gain-of-function. Neurons (and neuronal precursors) overexpressing mutant LRRK2 are vulnerable to death (Smith et al., 2005) and exhibit abnormal morphology (MacLeod et al., 2006; Plowey et al., 2008). LRRK2 is known to auto-phosphorylate (Greggio et al., 2009) and many candidate substrates have been proposed (Smith et al., 2005; MacLeod et al., 2013). One of these is TPC2 and this interaction is thought to regulate autophagy (Gómez-Suaga et al., 2012). LRRK2 is also known to associate with several intracellular membranes (reviewed in Cookson 2010). However, the mechanism underlying LRRK2 toxicity is unknown.

Although genetics studies have advanced our understanding of PD, the mechanism underlying PD pathology is not as well established (Obeso et al., 2010). Much evidence converges on a central role of mitochondria in PD pathogenesis. Indeed, many of the toxins that recapitulate PD (including paraquat and MPTP) disturb the mitochondria by inhibiting Complex I (a respiratory chain enzyme; Schapira 2008). Consequently, large amounts of

reactive oxygen species (ROS) are generated (Castello et al., 2007) and apoptotic pathways initiated (Yang & Tiffany-Castiglioni, 2008). A direct link between mitochondria dysfunction and PD was identified through the post-mortem analysis of PD patient brains. Schapira and colleagues (1989) established that complex I activity is impaired in SNc cells. Furthermore, many of the genes linked to PD encode proteins that localise to the mitochondria and maintain its function (Schapira, 2012). For instance, the interaction of PINK1 (PTEN-induced kinase 1) and Parkin (both linked with recessive forms of PD) is essential for the turnover of dysfunctional mitochondria (Narendra et al., 2010). Additionally, homozygotic mutations in *DJ-1*, which encodes a mitochondrial antioxidant protein that has been suggested to regulate neuro-protective responses, are associated with PD development (Taira et al., 2004).

It is now emerging that lysosomes might also be involved in PD pathogenesis. Lysosomal deficiencies, determined using a variety of lysosomal markers like LAMP1, have been reported in sporadic PD patient brains and mice exposed to MPTP (Dehay et al., 2010). Notably, lysosome dysfunction, in these mice, preceded degeneration. As discussed above, lysosomes are hydrolytic organelles that mediate autophagy. The accumulation of  $\alpha$ -syn implicates autophagic dysfunction in PD (Cuervo et al., 2004). Notably, impaired autophagy has been frequently reported in LRRK2-mediated PD (Plowey et al., 2008; Alegre-Abarrategui et al., 2009; Manzoni et al., 2013a). Perhaps the association of LRRK2 with lysosomal membranes (Biskup et al., 2006; Alegre-Abarrategui et al., 2009) instigates this defect. In chapter 5, I further examine the link between LRRK2 and lysosome pathology.

Many lysosomal genes have been linked to PD. Namely, loss of function mutations in *ATP13A2* cause autosomal recessive forms of PD. This gene encodes a lysosomal protein that actively transports cations across membranes. *ATP13A2* has a neuroprotective role against several cell stressors including ROS (Covy et al., 2012) and heavy metals (Schmidt et al., 2009). Dehay and colleagues (2012) recently analysed lysosome morphology in patient-derived fibroblasts. Lysosomes appeared enlarged and clustered in *ATP13A2*-mediated PD. In addition to disrupted lysosome morphology, lysosome acidification, membrane stability and substrate degradation were impaired (Dehay et al., 2012). Furthermore, mutations in *VPS35* have recently been associated with PD (Vilariño-Güell et al., 2011). *VPS35* (vacuolar protein sorting 35) is a component of the retromer complex that traffics proteins (including hydrolase receptors) from endosomes back to the Golgi apparatus. Lysosome function depends on *VPS35*. Indeed, the depletion of *VPS35* in HeLa cells disrupts lysosome

morphology (Arighi et al., 2004). Additionally, GWAS have identified other lysosomal proteins (GAK and LAMP3) as PD-risk factors (Nalls et al., 2011).

Finally, and perhaps the most convincingly, mutations in *GBA1* represent the greatest genetic risk factor for PD. *GBA1* mutations are also known to cause the lysosomal storage disorder Gaucher disease, discussed below. On average, across 34 studies (summarised in Beavan & Schapira 2013), 7% of sporadic PD cases are linked to a *GBA1* mutation. Some of these reports are conflicting, for instance Aharon-Peretz et al. (2004) estimate a much higher penetrance (31%) than others like Hu et al. (2010) at 2%. These variations might reflect differences in ethnicity and size of the cohort examined. It is also important to acknowledge that many individuals with *GBA1* mutations do not exhibit PD symptoms (McNeill et al., 2012; Rana et al., 2013). The clinical manifestations of PD in patients with a *GBA1* mutation are indistinguishable from other cases with subtle difference such as an earlier age of onset (Sidransky et al., 2009) and greater cognitive decline (Neumann et al., 2009).

*GBA1* encodes the lysosomal hydrolase glucocerebrosidase (GCase) which is important in the metabolism of glucocerebroside into glucose and ceramide. Mutations in *GBA1* impair protein folding and trafficking towards the lysosomes (Ron & Horowitz, 2005), which causes a GCase deficiency. Consequently, undegraded substrate accumulates in the lysosomes and mis-folded protein aggregates on the ER. The protein responsible for GCase trafficking is the lysosomal integral membrane protein type 2 (LIMP2) (Reczek et al., 2007; Rothaug et al., 2014). The gene that encodes LIMP2 (*SCARB2*) was recently highlighted as another PD-risk loci in GWAS (Do et al., 2011). This reinforces the involvement *GBA1* in PD.

*GBA1* is located on chromosome 1q21 and spans 7.6kb sequence (Horowitz et al., 1989). Over 300 pathogenic mutations have been identified in *GBA1* including insertions, point mutations and deletions (Beavan & Schapira, 2013). The prevalence of each mutation varies across ethnicity. In Europe, N370S and L444P mutations are the most frequently reported (Hruska et al., 2008). A single mutation in *GBA1* can increase the risk of PD risk. Yet, homozygotic mutations are the cause of the lysosomal storage disorder, Gaucher disease (GD).

### Lysosomal storage disorders

Lysosomal storage disorders (LSD) are a group of diseases characterised by an impairment of lysosome homeostasis (Futerman & van Meer, 2004). As a consequence, undegraded macromolecules accumulate in both the lysosomes and endosomes (Futerman & van Meer, 2004). To date, over 50 LSDs have been described. Individually they are rare disorders but together LSDs occur 1 in every 7,700 live births (Meikle et al., 1999). These diseases are one

of the most frequent causes of neurodegeneration in children (Verity et al., 2010). Parkinsonian symptoms have also been reported in several LSDs including GD and Niemann-Pick type C disease (NPC).

GD is the most common LSD, affecting 1/40,000-60,000 live births in the general population (Siebert et al., 2014). In GD, the accumulation of glucocerebroside predominantly occurs in the cells of the reticulo-endothelial system (e.g. macrophages) (Sidransky & Lopez, 2012). Macrophages adopt an unusual cytoplasmic appearance akin to “wrinkled tissue paper” filled with defective lysosomes (Sidransky, 2004). These macrophages localise to the spleen, liver and bone marrow and these organs are enlarged in GD patients (Sidransky, 2004). Three types of GD have been characterised; type II and type III are severe, defined by neurological deficits and distinguished by age of onset (6 months and adolescence respectively) (Butters, 2007). On the other hand, type I affects the peripheral organs and was once believed to spare the nervous system (Butters, 2007). However, the view that type I GD is non-neurological is now outdated. Recent evidence has established that peripheral neuropathy (Biegstraaten et al., 2010), dementia (Sidransky et al., 2009) and parkinsonism (Tayebi et al., 2001) feature in type I GD. By the age of 80, type I GD patients have an 9-12% increased risk of developing PD (Rosenbloom et al., 2011).

Despite clear clinical and genetic associations between *GBA1* and PD, little is known regarding the cellular mechanisms that connect these two diseases. In PD, most autosomal dominant mutations (*SNCA* and *LRRK2*) are associated with a toxic gain-of-function. On the other hand, recessive mutations (like *PINK*, *Parkin* and *DJ-1*) can be attributed to loss-of-function. For *GBA1*, arguments have been put forward for both cases. In chapter 4, I further examine the effects of loss- and gain-of-function in *GBA1*-pathology.

Although null alleles (84dupG) have been reported (Sidransky et al., 2009), most mutations lead to a mis-folded enzyme. This favours the toxic gain-of-function hypothesis. Newly synthesised proteins undergo a strict quality control, where non-functional proteins are degraded through various mechanisms collectively termed ER-associated degradation (ERAD) (Mekahli et al., 2011). A persistent accumulation of mis-folded proteins activates the unfolded protein response (UPR) (Chakrabarti et al., 2011). The post-mortem analysis of *GBA1*-PD patient brains revealed that UPR markers (like BiP) are up-regulated compared to control samples (Gegg et al., 2012). Furthermore, UPR was also activated in transgenic drosophila expressing mutant *GBA1* (N370S and L444P; Maor et al. 2013). The prolonged activation of UPR initiates apoptotic pathways (Fribley et al., 2009) and could contribute to

neurodegeneration. However, primary neuronal cultures treated with pharmacological inhibitor of GCase (Conduritol B epoxide; CBE) and *GBA1* knockout mice did not show UPR activation (Farfel-Becker et al., 2009). This highlights the difficulty involved when selecting *GBA1*-disease models.

According to the loss-of-function hypothesis, reduced enzyme activity is linked to pathology. The accumulation of undegraded substrates could alter lysosome-dependent processes like autophagy. Cleeter and colleagues (2012) mimicked GCase deficiency in neuronal precursor cells (SH-SY5Y) by knocking down *GBA1* and using CBE. Mitochondrial function was impaired in both these models. More specifically the authors reported reduced ATP synthesis, loss of mitochondrial membrane potential and increased ROS production (Cleeter et al., 2012). Osellame et al. (2013) report a similar mitochondrial-dysfunction in a knockout mouse model of GD and attribute this dysfunction to impaired autophagy.

Disrupted lipid homeostasis could be particularly harmful to cells. Indeed, associations between the impaired metabolism of ceramide (the product of GCase) and PD have been discussed (Bras et al., 2008). Ceramide forms the back bone of sphingolipids, which have an important role in signal transduction and membrane composition (Platt, 2014). Notably, mutations in *PLA2G6*, which encodes an enzyme that is involved in generating ceramide, are known to cause PD (Paisan-Ruiz et al., 2009). Thus, loss of ceramide in *GBA1*-disease could be linked with pathology.

Recent studies, investigating the interaction between GCase and  $\alpha$ -syn, have shed light on the cellular mechanisms underlying *GBA1* pathology. GCase has been localised to Lewy bodies (Goker-Alpan et al., 2010) and this association could contribute to PD pathology through a self-propagating feedback loop. Firstly, the dysfunction of lysosomes, caused by an accumulation of glucocerebroside, might impair the degradation of  $\alpha$ -syn. In support of this, Mazzulli and colleagues (2011) show that 50% depletion of GCase (using shRNA-mediated knockdown), hinders general lysosomal turnover of proteins and increases the level of  $\alpha$ -syn in neurons. This model is further complicated by the finding that  $\alpha$ -syn has been shown to disrupt the trafficking of proteins towards the lysosomes (Thayanidhi et al., 2010b). Mazzulli et al. (2011) showed that this includes GCase, which becomes retained on the ER further exacerbating pathology. Notably, GCase activity is reduced in the brains of PD patients without *GBA1* mutations (Gegg et al., 2012). Thus  $\alpha$ -syn itself might reduce GCase activity. Indeed, GCase activity is decreased in neurons overexpressing  $\alpha$ -syn (Mazzulli et al., 2011). This affirms the importance of researching *GBA1* pathology for the wider PD population.

It is important to highlight that none of these studies have addressed why many individuals with a *GBA1* mutation do not develop PD. In chapter 4, I investigate whether other pathological mechanisms are involved.

### *Connecting Ca<sup>2+</sup> with PD*

Several aspects of neuronal function rely on Ca<sup>2+</sup> (Berridge, 1998). For instance, Ca<sup>2+</sup> regulates neuronal plasticity (Mattson et al., 2000) and an influx of Ca<sup>2+</sup> at the presynaptic terminal triggers the release of neurotransmitters (Augustine, 2001). Any impairment in Ca<sup>2+</sup> homeostasis is particularly damaging to neurons since they are post mitotic cells. It therefore may not be surprising that Ca<sup>2+</sup> has a prominent role in neurodegenerative diseases (Mattson, 2007). Indeed emerging evidence has linked defective Ca<sup>2+</sup> homeostasis in pathology of PD (figure 1.4).

Dopaminergic SNc neurons are autonomously active, they generate repetitive action potentials (2-4Hz) in the absence of synaptic input (Grace & Bunney, 1983). This pacemaking activity sustains the basal levels of dopamine in connected brain regions like the striatum (Surmeier & Schumacker, 2013). Whilst some neurons rely on Na<sup>+</sup> to maintain pacemaking, SNc neurons are driven to spike threshold by Ca<sup>2+</sup> entry through an uncommon L-type VGCC named Ca<sub>v</sub>1.3 (Chan et al., 2007). Although this channels is necessary for pacemaking, it subjects SNc neurons to a continual influx of Ca<sup>2+</sup>. Regions that surround the SNc, like the ventral tegmental area (VTA), also rely on pacemaking activity. However, VTA neurons do not exhibit Ca<sup>2+</sup> oscillations (Chan et al., 2007) and they express Ca<sub>v</sub>1.3 at low levels (Khaliq & Bean, 2010). These neurons are relatively resistant to death and are spared in PD (German et al., 1992).

The increased Ca<sup>2+</sup> influx coupled with the reduced expression of Ca<sup>2+</sup> buffers might also make SNc neurons selectively vulnerable to degeneration. Unlike the preserved VTA neurons, calbindin is not expressed in high levels within the SNc (Yamada et al., 1990). Furthermore, the post-mortem analysis of PD brains identified reduced levels of calmodulin and calretinin in the SNc (Hurley et al., 2013). Importantly, calmodulin regulates the feedback inhibition of Ca<sub>v</sub>1.3 (Huang et al., 2012). GWAS have identified several Ca<sup>2+</sup> binding proteins as PD-risk factors. For instance, an association between mutations in *Calbindin-1* gene and PD have been reported in a Japanese population (Mizuta et al., 2008).



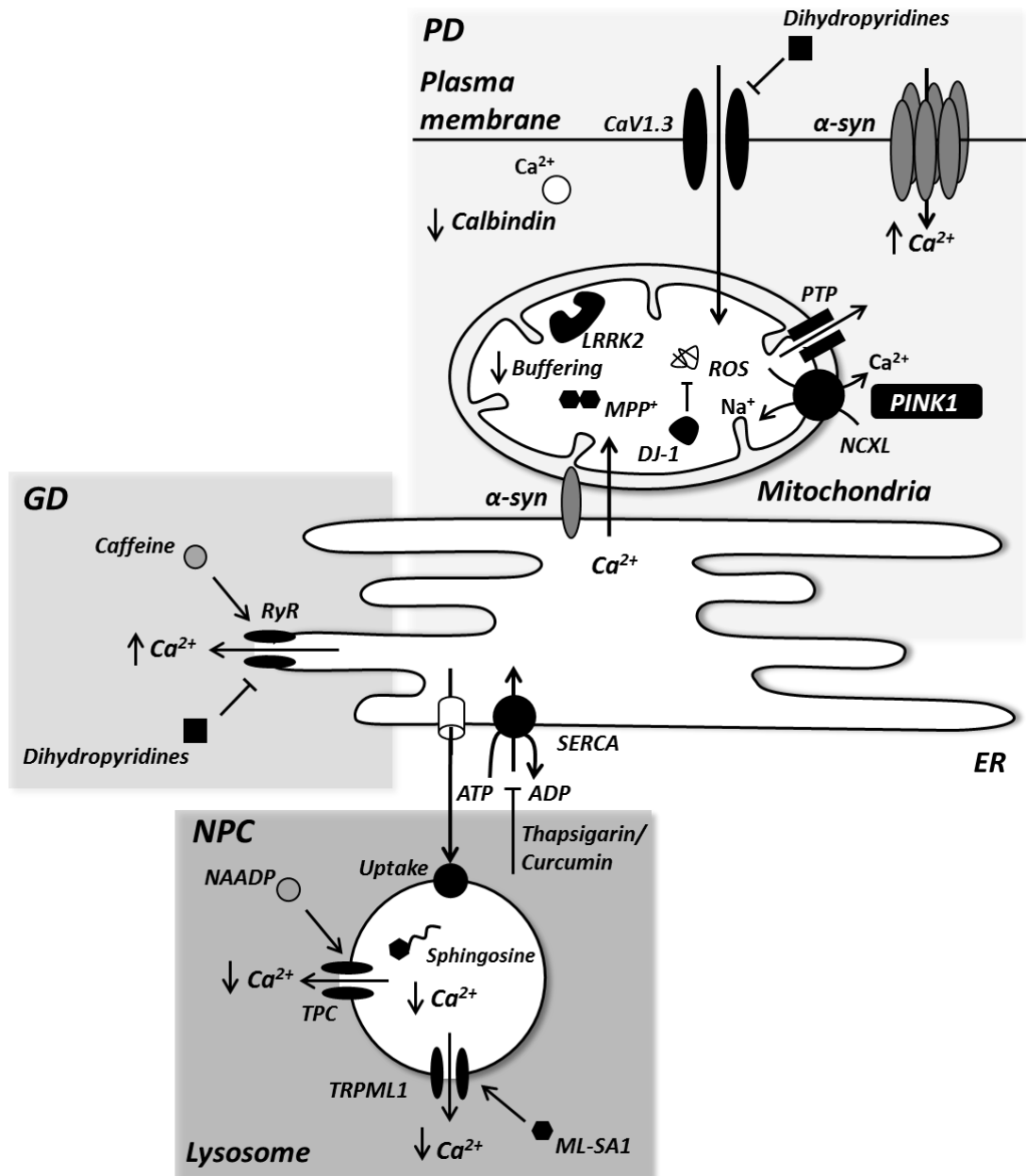


**Figure 1.4  $Ca^{2+}$  signalling and PD**

PD, GD and NPC are all associated with dysfunctional  $Ca^{2+}$  signalling. In PD, excess  $Ca^{2+}$  influx through  $Ca_v1.3$  can disrupt cause neurodegeneration by increasing the energetic demand of the mitochondria.  $DJ-1$ ,  $PINK1$  and  $LRRK2$  mutations can impair the ability of the mitochondria to combat this stress. The reduced presence of  $Ca^{2+}$  buffers and observation that  $\alpha$ -syn can form pores in the plasma membrane can further impair  $Ca^{2+}$  homeostasis in PD. Additionally,  $MPP^+$  and  $\alpha$ -syn have been shown to interfere with the transfer of  $Ca^{2+}$  from the ER to the mitochondria. In GD,  $RyR$  are known to be hypersensitive and dihydropyridines (traditional L-type VGCC antagonists) can improve GD pathology. In NPC lysosomal  $Ca^{2+}$  content is reduced and associated with impaired  $TPC$  and  $TRPML1$  signalling. These defects can be corrected by increasing  $Ca^{2+}$  uptake and reducing the accumulation of sphingosine.

Excess  $\text{Ca}^{2+}$  must also be pumped out of the cell. This is an energetically expensive process since ATP is needed to drive  $\text{Ca}^{2+}$  across a steep concentration gradient to the extracellular environment (Surmeier, et al., 2011). Surmeier and colleagues proposed that persistent and long-lasting increases in cytosolic  $\text{Ca}^{2+}$  impose significant stress on the mitochondria by elevating the metabolic demand. Guzman and colleagues (2010) used a redox-sensitive protein targeted to the mitochondria to assess the energetic impact of pacemaking on SNc neurons. Oxidative stress and the transient uncoupling of the mitochondria coincided with pacemaking- $\text{Ca}^{2+}$  influx. This stress was attenuated by DJ-1, another protein defective in PD that functions as a ROS scavenger and interacts with complex 1. Indeed, knockdown of DJ-1 exacerbated  $\text{Ca}_v1.3$ -mediated  $\text{Ca}^{2+}$  influx (Guzman et al., 2010).

Hurley and co-workers (2013) recently conducted a systematic examination of  $\text{Ca}_v1$  channels in the PD brain.  $\text{Ca}_v1.3$  levels increase in PD, often preceding pathology (Hurley et al., 2013). Therefore, this change in expression is an early event in PD and might influence disease progression. In further support of prominent role that L-type VGCC play in PD pathology, dihydropyridines (L-type VGCC antagonists) have been shown neuroprotective in animal models of PD (Ilijic et al., 2011). Furthermore, epidemiological studies have identified that these antagonists (FDA [Food and Drug Administration] approved for the treatment of hypertension) reduce the risk of PD development (Becker et al., 2008; Ritz et al., 2010; Pasternak et al., 2012).

$\alpha$ -syn, the primary component of Lewy bodies, can also modulate  $\text{Ca}^{2+}$  influx. Danzer et al. (2007) identified that the exogenous addition of  $\alpha$ -syn oligomers to neuronal cell lines (SH-SY5Y) increased the permeability of the plasma membrane. Over a 2-fold increase in cytosolic  $\text{Ca}^{2+}$  levels (250 nM) have been measured in cells overexpressing  $\alpha$ -syn (Furukawa et al., 2006). Since mutated  $\alpha$ -syn has an increased propensity to assemble as pores at the plasma membrane (Lashuel et al., 2002), it has been proposed that mutant  $\alpha$ -syn increases  $\text{Ca}^{2+}$  entry into the cell and evokes stress in PD.

Collectively these studies provide a mechanism for selective neuronal degeneration in PD. This process could affect us all as we age, since our reliance on SNc  $\text{Ca}^{2+}$  pacemaking increases with age (Chan et al., 2007). Any other disturbance in  $\text{Ca}^{2+}$  homeostasis is likely to advance the onset of PD. For instance, *PINK1* mutations might also make managing excess  $\text{Ca}_v1.3$ -mediated  $\text{Ca}^{2+}$  influx difficult. Gandhi and co-workers (2009) identified that mitochondrial  $\text{Ca}^{2+}$  release is impaired in *PINK1* deficient neurons. *PINK1* was shown to interact with NCLX and regulate efflux. A *PINK1* deficiency also reduced the threshold for PTP opening and made

the cells vulnerable to death (Gandhi et al., 2009). Others have shown that PINK can also regulate  $\text{Ca}^{2+}$  uptake into the mitochondria (Heeman et al., 2011).

Furthermore, *LRRK2* mutations have also been shown to damage mitochondrial  $\text{Ca}^{2+}$  homeostasis. Overexpressing G2019S-mutated *LRRK2* reduced the buffering capacity of mitochondria within neurons (Cherra et al., 2013). These effects were attenuated with  $\text{Ca}^{2+}$  chelators and L-type VGCC antagonists. This is reminiscent of studies conducted over 15 years ago where hybrid cells, containing mitochondria from PD patients, showed a delayed recovery from  $\text{IP}_3$  mediated  $\text{Ca}^{2+}$  signalling (Sheehan et al., 1997).

The role of  $\text{Ca}^{2+}$  stores in PD has been largely neglected. The PD toxin  $\text{MPP}^+$  (oxidised MPTP) has been shown to reduce ER  $\text{Ca}^{2+}$  levels (Arduíno et al. 2009). Concomitantly,  $\text{MPP}^+$  increased mitochondrial  $\text{Ca}^{2+}$  content. The authors demonstrated that  $\text{Ca}^{2+}$  is transferred from the ER to the mitochondria under stressful conditions. Moreover,  $\text{MPP}^+$ -induced cell death is dependent upon ER  $\text{Ca}^{2+}$  release since blocking RyR (with dantrolene) prevented the activation of mitochondrial caspases (Arduíno et al., 2009). Perhaps the passage of  $\text{Ca}^{2+}$  from the ER to mitochondria regulates  $\text{MPP}^+$ -mediated cell death. On a related note,  $\alpha$ -syn has been shown to enhance the transfer of ER  $\text{Ca}^{2+}$  to the mitochondria by increasing interaction sites (MAMs) between the organelles (Calì et al., 2012).

Those LSDs that have been linked to PD, also exhibit disrupted  $\text{Ca}^{2+}$  homeostasis (figure 1.4). Namely, GD is associated with abnormal ER  $\text{Ca}^{2+}$ . Korkotian and colleagues (1999) report that the pharmacological inhibition of GCase, in hippocampal neurons, perturbed ER morphology and increased  $\text{Ca}^{2+}$  release through RyR. This made cells vulnerable to glutamate-induced  $\text{Ca}^{2+}$  excitotoxicity. Pre-treatment with Ryanodine (which blocks RyR) protected neurons from glutamate, suggesting a close relationship between ER  $\text{Ca}^{2+}$  release and glutamate-mediated degeneration (Korkotian et al., 1999). Furthermore, microsome preparations (vesicle artefacts reformed from fragments of the ER) from rat brains treated with glucocerebroside (Lloyd-Evans et al., 2003) also exhibited increased RyR  $\text{Ca}^{2+}$  release. Pelled et al. (2005) extended these findings into clinical microsome preparations from GD patient brains. The authors identified that severe, neuronopathic forms of GD (type II) also exhibited increased ER  $\text{Ca}^{2+}$  release. These studies proposed that glucocerebroside affects the redox state of RyR (via its redox sensor; Feng et al. 2000), since the reducing agent DTT (dithiothreitol) abolished defects.

Dihydropyridines (e.g. diltiazem and verapamil) can, somewhat, recover the pathology of GD fibroblasts by significantly improving the translocation of GCase to the lysosomes and the enzyme activity (Mu et al., 2008; Ong et al., 2010). This effect on fibroblasts is surprising since they do not express VGCCs, however dihydropyridines were shown to block RyRs (Ong et al., 2010). It is perhaps significant that dihydropyridines have also been shown to block NAADP-mediated  $\text{Ca}^{2+}$  signalling (Genazzani et al., 1996). Despite being a well-known LSD, measurements of lysosomal  $\text{Ca}^{2+}$  signalling remain to be examined in GD.

Lysosomal  $\text{Ca}^{2+}$  has been shown to play a crucial role in the pathology of NPC. NPC is characterised by the degeneration of cerebellar purkinje neurons. This LSD is caused by mutations in either *NPC1* or *NPC2* which disrupt cholesterol trafficking. As briefly mentioned above, PD symptoms have been reported in NPC patients. Josephs et al. (2004) described parkinsonian tremor in an NPC individual and their relatives. Furthermore, the post mortem analysis of an NPC individual revealed significant  $\alpha$ -syn pathology in the SNc (Saito et al., 2004). Klunemann and co-workers (2013) recently associated several *NPC1* mutations with PD. Although another study also found *NPC1* and *NPC2* mutations associated with PD, the frequency of these mutations did not significantly differ from controls (Zech et al., 2013).

Dysfunctional lysosomal  $\text{Ca}^{2+}$  in NPC was first identified by Lloyd-Evans and colleagues (2008). Using cells (fibroblasts and lymphocytes) from NPC patients and neuronal cultures from an NPC mouse model the authors identified that mutant *NPC1* can rapidly reduce lysosomal  $\text{Ca}^{2+}$  content. Excess sphingosine (a lipid that accumulates in NPC) is believed to cause this reduction since the exogenous addition of sphingosine reduced lysosomal  $\text{Ca}^{2+}$ . Furthermore, a sphingosine synthesis inhibitor returned lysosomal  $\text{Ca}^{2+}$  levels to normal (Lloyd-Evans et al., 2008). The reduction of lysosomal  $\text{Ca}^{2+}$  hindered NAADP signalling (Lloyd-Evans et al., 2008). An important role of lysosomal  $\text{Ca}^{2+}$  is to regulate vesicular trafficking, recycling and fusion (Pryor et al., 2000). Disrupted endocytosis was also reported in NPC (Lloyd-Evans et al., 2008). Elevating cytosolic  $\text{Ca}^{2+}$ , by depleting stored ER  $\text{Ca}^{2+}$  with thapsigargin (a SERCA inhibitor), restored lysosomal  $\text{Ca}^{2+}$  levels and corrected endocytosis defects (Lloyd-Evans et al., 2008). Indeed, the NPC phenotype of a mouse model was improved after treatment with another, mild, SERCA inhibitor curcumin (Lloyd-Evans et al., 2008). Additional studies, conducted by Lee et al. (2010) and Visentin et al. (2013), also reported similar defects in cerebellar purkinje neurons from an NPC mouse model and patient fibroblasts. However, Shen and colleagues (2012) did not observe any differences in lysosomal  $\text{Ca}^{2+}$  content using similar models.

Although they do report defects in endocytosis and link this to the inhibitory action of sphingosine on TRPML1 channels (Shen et al., 2012).

## Aims

Ca<sup>2+</sup> is a highly versatile signalling cation that regulates many cellular functions. Ca<sup>2+</sup> signals can originate from both the extracellular environment and intracellular Ca<sup>2+</sup> stores. The intracellular Ca<sup>2+</sup> network is closely associated, where lysosomes can trigger Ca<sup>2+</sup> signals from the ER which can ultimately be transmitted to the mitochondria. Defects in any component of this pathway might impinge on Ca<sup>2+</sup> homeostasis and contribute to diseases like PD.

In this thesis, I examine the functional *connections* between Ca<sup>2+</sup> stores and if their dysfunction is *connected* to PD. My aims are described below:

1. Many have proposed that NAADP-responses are amplified by the ER. However, ambiguity surrounding the molecular target of NAADP has impeded the investigation of NAADP receptor-ER coupling. Using a lysosomal permeabilising agent I examine whether lysosomal Ca<sup>2+</sup> signalling is functionally *connected* to the ER.
2. The mechanism behind lysosome-ER Ca<sup>2+</sup> coupling is unknown. However, MCSs between late-endosomes and the ER have been molecularly characterised. Using molecular and pharmacological assays I determined if similar components *connect* and regulate lysosome-ER Ca<sup>2+</sup> coupling. I also examined whether TRPML channels trigger ER Ca<sup>2+</sup> signalling, using a recently developed synthetic agonist.
3. Emerging evidence shows that Ca<sup>2+</sup> defects are present in both PD and GD. Using clinical, pharmacological and molecular models I examined whether Ca<sup>2+</sup> might resolve the genetic *connection* between GD and PD.
4. Accumulating evidence implicates lysosomal dysfunction in PD. In the final chapter I examine if other genetic and environmental PD risk factors are *connected* by lysosomal dysfunction and corrected by targeting lysosomal ion channels.

# Chapter 2

---

## Direct Mobilisation of Lysosomal Ca<sup>2+</sup> Triggers Complex Ca<sup>2+</sup> Signals

### Introduction

Despite emerging evidence connecting lysosomal Ca<sup>2+</sup> dysfunction with disease (Lloyd-Evans et al., 2008; Coen et al., 2012; Shen et al., 2012), little is known regarding Ca<sup>2+</sup> signalling and uptake mechanism of these acidic stores. Furthermore, their relationship with the well-established ER Ca<sup>2+</sup> network is largely unknown. Previous research has proposed that lysosomal Ca<sup>2+</sup> release after NAADP stimulation “triggers” Ca<sup>2+</sup> signalling from the ER (Cancela et al., 1999). Notably, targeting overexpressed TPC2 to the plasma membrane, achieved through mutating the N-terminal lysosomal-targeting motif, uncoupled NAADP signalling (Brailoiu et al., 2010b). When at the plasma membrane, NAADP-evoked Ca<sup>2+</sup> signals were not potentiated by the ER and subsequently appeared “sluggish”. Intimate associations between lysosomes and the ER were therefore proposed important for NAADP signalling (Patel & Brailoiu, 2012).

However, the target of NAADP has been disputed. Instead of gating lysosomal ion channels, some have argued that this Ca<sup>2+</sup> mobilising messenger acts directly on RyR (Hohenegger et al., 2002; Gerasimenko et al., 2003; Dammermann et al., 2009). NAADP has been hypothesised to target several Ca<sup>2+</sup> stores by binding to promiscuous accessory proteins (Lin-Moshier et al., 2012; Marchant et al., 2012). The possibility that NAADP activates multiple receptors has hindered research examining the functional relationship between the ER and acidic Ca<sup>2+</sup> stores. Directly releasing lysosomal Ca<sup>2+</sup> might circumvent these difficulties. In this chapter I use a lysosomal permeabilising agent, to examine the functional *connections* between lysosomes and the ER.

### Methods

#### Cell culture

Human skin fibroblasts, established from healthy individuals, and HeLa cells were maintained in DMEM (Dulbecco's Modified Eagle Medium) supplemented with 10% (v/v) Fetal Bovine Serum (FBS), 100 µg/mL streptomycin and 100 units/mL penicillin (all from Invitrogen).

SH-SY5Y cells were cultured in a 1:1 mixture of DMEM and Ham's F12 media supplemented with 10% (v/v) FBS, 100 units/mL penicillin, 100 µg/mL streptomycin and 1% (v/v) non-essential amino acids (all from Invitrogen).

Mixed primary neuronal cultures were prepared from the brains of mouse pups at postnatal day 1 by Dr Laura Osellame (Department of Cell and Developmental Biology, UCL). Primary neuronal cultures were maintained in Neurobasal media (Invitrogen) supplemented with 2% (v/v) B-27, 2 mM L-glutamine (both sigma), 10% (v/v) FBS, 100 units/mL penicillin and 100 µg/mL streptomycin (Invitrogen). Neuronal cultures were analysed 8 days after isolation.

Fibroblasts, HeLa cells and neuronal cultures were fed fresh media every 5 days. Media of SH-SY5Y cells was changed every 2-3 days. Some fibroblast cultures were treated overnight with 100 nM, of the vacuolar-type H<sup>+</sup>-ATPase inhibitor, Bafilomycin-A1 (Sigma-Aldrich) prepared in DMSO (dimethyl sulfoxide). All cultures were kept at 37°C in a humidified atmosphere with 5% CO<sub>2</sub>. Before experimentation cells, were plated onto glass coverslips. For HeLa, SH-SY5Y and neuronal cells, glass coverslips were coated with 20 µg/mL poly-L-lysine.

### Live-cell imaging

#### *Ca<sup>2+</sup> imaging*

Cells were loaded with the ratiometric fluorescent Ca<sup>2+</sup> indicator Fura-2 after incubation with Fura-2 AM (2.5 µM) and 0.005% (v/v) pluronic acid (Invitrogen) for 1 hour at room temperature in HEPES-buffered saline (HBS) consisting of 10 mM HEPES, 2 mM MgSO<sub>4</sub>, 156 mM NaCl, 3 mM KCl, 2 mM CaCl<sub>2</sub>, 1.25 mM KH<sub>2</sub>PO<sub>4</sub> and 10 mM glucose (pH 7.4).

Following three washes in HBS, cells were stimulated with either GPN (20, 100 and 200 µM; glycyl-L-phenylalanine-naphthylamide; SantaCruz Biotech), NAADP-AM (150 nM; from Dr Grant Churchill, Department of Pharmacology, University of Oxford), FCCP (carbonylcyanide-p-(trifluoromethoxy)-phenylhydrazone; 1 µM; Sigma), bradykinin (0.1, 1 and 10 nM; Sigma), thapsigargin (1 µM; Merck), bafilomycin-A1 (1 µM; Sigma), 2-APB (2-aminoethoxydiphenyl borate; 100 µM; Sigma) or ryanodine (100 µM; Merck). Where indicated, extracellular Ca<sup>2+</sup> was removed using a modified HBS solution containing 1 mM EGTA (ethylene glycol tetraacetic acid) instead of CaCl<sub>2</sub>.

#### *Lysotracker imaging*

Fibroblasts were incubated with 100 nM Lysotracker red (Invitrogen) for 30 minutes in HBS. After loading, cells were washed three times in HBS and imaged after stimulation with GPN.

### *Dextran imaging*

Fibroblasts were loaded with either 0.2 mg/mL dextran-conjugated Rhodamine B (MW 10,000) or dextran-conjugated fluorescein (MW 10,000) (both from Invitrogen) overnight at 37°C in culture. Cells were subsequently chased for 3 hours in dextran-free culture medium to label lysosomes. Cells were then washed in HBS and imaged directly or in some cases further incubated with 100 nM LysoTracker red (Invitrogen) for 30 minutes.

### **Immunocytochemistry**

Cells were fixed for 10 minutes using 4% (w/v) paraformaldehyde in Phosphate buffered saline (PBS), washed three times with PBS and then permeabilised for 5 minutes with  $\beta$ -Escin (40  $\mu$ M in PBS). Cells were washed again (three times in PBS), and blocked for 1 hour with a PBS solution supplemented with 1% (w/v) bovine serum albumin (BSA) and 10% (v/v) FBS. Subsequently, cells were incubated for 1 hour at 37°C, with primary anti-LAMP1 (lysosomal associated membrane protein 1) antibody (H4A3 clone, mouse, Developmental Studies Hybridoma Bank) diluted (1:10-100) in blocking solution. Coverslips were washed three times in PBS containing 0.1% (v/v) tween (PBS-T) and incubated, for a further 1 hour at 37°C, in a secondary antibody conjugated to AlexaFluor 647 (mouse, 1:100 dilution; Invitrogen). Cells were washed again in PBS-T and incubated with 1  $\mu$ g/mL DAPI (4',6-diamidino-2-phenylindole) for 5 minutes to label the nuclei. Finally, coverslips were mounted onto microscope slides with DABCO (1,4-diazabicyclo[2,2,2]octane) and sealed.

### **Microscopy**

#### *Epifluorescence*

Epifluorescence images were captured every 3 seconds with a cooled coupled device camera (TILL photonics) attached to an Olympus IX71 inverted fluorescence microscope fitted with a 20x objective, and a monochromator light source. Fura-2 fluorescence (emission; 440 nm) was visualised after sequential excitation at 340 nm and 380 nm. LysoTracker red and Rhodamine dextran were excited at 568 nm and 570 nm respectively and emitted fluorescence was captured using a 590 nm filter.

#### *Confocal*

Confocal images were captured using an inverted Axiovert 200M microscope attached to a LSM510 confocal scanner (Zeiss) fitted with a 63x Plan Apochromat water-immersion objective. DAPI, fluorescein-dextran, LysoTracker and AlexaFluor 647 fluorescence was excited using wavelengths of 364 nm, 488 nm, 543 nm and 633 nm respectively. Emitted fluorescence was captured using either a long-pass 385 nm filter (DAPI) or band-pass filters set between 505-530 (fluorescein-dextran), 560-615 nm (LysoTracker) and 655-719 nm



(AlexaFluor 647). Zeiss LSM 510 software was used to acquire the images. For comparison of lysosome integrity (after treatment with GPN), images were captured using identical acquisition settings.

## Analysis

### *Ca<sup>2+</sup> imaging*

To quantify Fura-2 fluorescence, the background was subtracted from the images and the mean 340/380 nm ratio of cells (selected through user defined region-of-interest) was calculated at each time point during the experiment using TILLvisION software. Prior to stimulation, Fura-2 fluorescence was recorded for 60 seconds to ascertain a basal Fura-2 reading. The magnitude of Fura-2 response ( $\Delta \text{Ca}^{2+}$ ) was calculated by subtracting the basal ratio from the peak ratio. Spontaneous increases in Fura-2 fluorescence, defined by spikes in the basal recordings exceeding ratio values of 0.33, were excluded from  $\Delta \text{Ca}^{2+}$  analysis. Cells were classified oscillatory if more than 1 peak in Fura-2 fluorescence occurred during the time course of imaging. Fibroblasts were deemed responsive to stimuli if the Fura-2 fluorescence ratio, after stimulation, increased beyond the ratio value 0.4. This threshold value was selected because responses exceeding 0.4 could be clearly defined as a spike in Fura-2 fluorescence.

### *Lysotracker and dextran imaging*

After background subtraction Lysotracker and Dextran fluorescence was quantified within user defined regions-of-interest using TILLvisION software. For some measurements, fluorescence was normalised to basal values (recorded prior to stimulation).

### *Confocal*

Confocal images were analysed using Image J software. For LAMP1 intensity measurements, background was subtracted from the images and mean grey intensity per cell measured within user defined regions-of-interest (comprising the whole lysosome population).

### *Statistics*

Values are presented as mean  $\pm$  standard error. Statistical analysis was performed using Minitab 17. Two-sample *t*-test and ANOVA analysis (followed by a post-hoc Tukey test) were applied to test significance. Data of  $p < 0.05$  were classed statistically as significant.

## Results

### **GPN evokes complex Ca<sup>2+</sup> signals**

GPN is a freely diffusible substrate for the lysosomal enzyme Cathepsin C (Jadot et al., 1984) and when hydrolysed it osmotically permeabilises the lysosomes to Ca<sup>2+</sup> and other

constituents. GPN-evoked  $\text{Ca}^{2+}$  signals were examined in cultures of human fibroblasts loaded with the cytosolic ratiometric  $\text{Ca}^{2+}$  indicator Fura-2. GPN generated prolonged  $\text{Ca}^{2+}$  responses (Figure 2.1A) that persisted in the absence of extracellular  $\text{Ca}^{2+}$  (figure 2.1B). These  $\text{Ca}^{2+}$  signals resembled those induced by the agonist bradykinin (figure 2.1C) and a cell-permeable analogue of NAADP, called NAADP-AM (figure 2.1D). It is important to note that the majority of cells were unresponsive NAADP-AM (data not shown). Out of the 199 cells recorded only 10% responded to NAADP-AM and these cells are represented in figure 2.1D.

GPN-evoked  $\text{Ca}^{2+}$  signals were also compared to those induced by depleting mitochondrial  $\text{Ca}^{2+}$  with FCCP (figure 2.1E) and ER  $\text{Ca}^{2+}$  with thapsigargin (figure 2.1F). In contrast to GPN, both FCCP and thapsigargin evoked small, monotonic and transient  $\text{Ca}^{2+}$  responses.

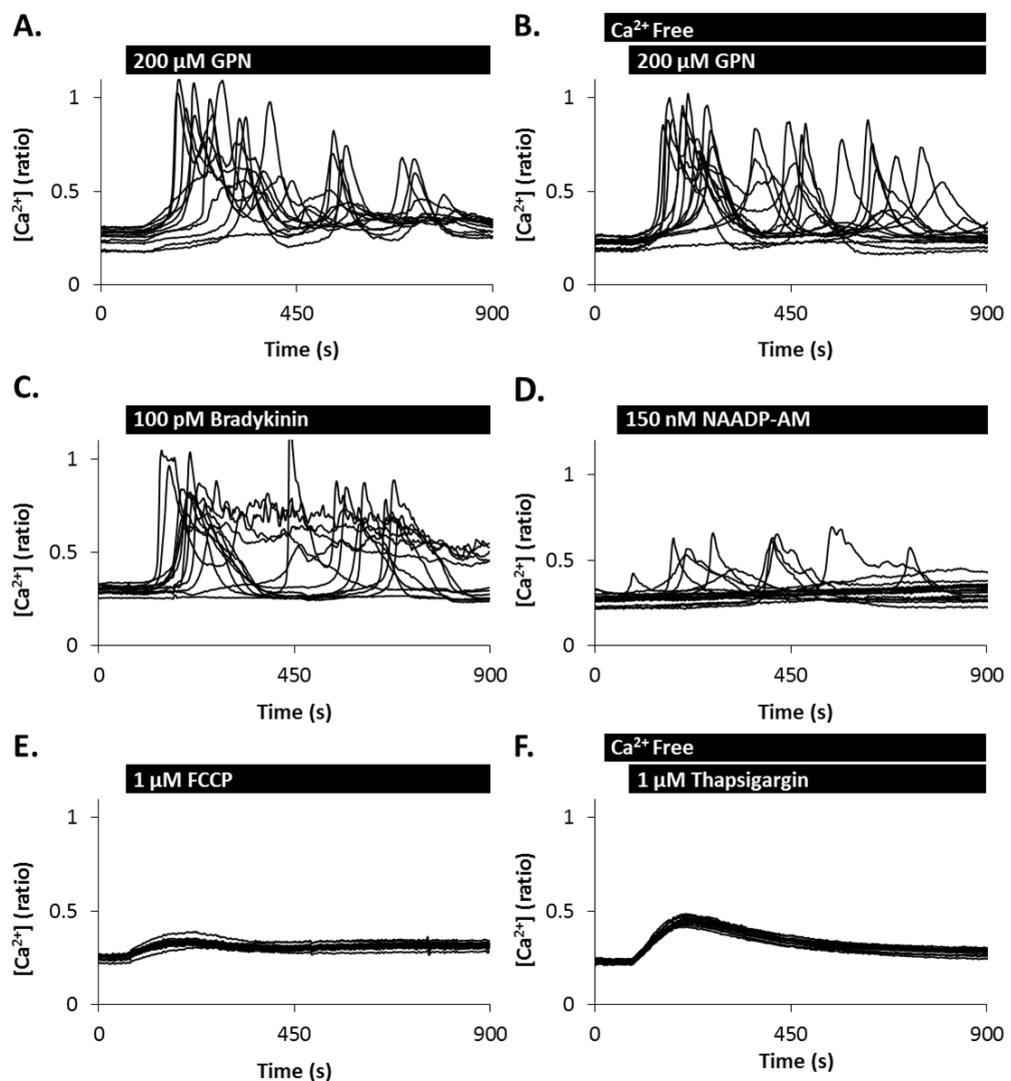


**Figure 2.1 GPN evokes complex  $\text{Ca}^{2+}$  signals**

(A-F) Cytosolic  $\text{Ca}^{2+}$  responses of individual fibroblasts stimulated with either GPN (200  $\mu\text{M}$ ; A-B), bradykinin (100 pM; C), NAADP-AM (150 nM; D; only responsive cells shown), FCCP (1  $\mu\text{M}$ ; E) or thapsigargin (1  $\mu\text{M}$ ; F). Extracellular  $\text{Ca}^{2+}$  was removed in (B and F). NAADP-AM-evoked  $\text{Ca}^{2+}$  responses have been pooled from 8 experiments.

### GPN rapidly permeabilises lysosomes

GPN evoked surprisingly long-lasting  $\text{Ca}^{2+}$  responses, so the rate of lysosome permeabilisation was investigated in fibroblasts using the acidotropic fluorescent indicator LysoTracker red (Figure 2.2A-B). LysoTracker accumulated in punctate structures, consistent with the labelling of lysosomes (figure 2.2A). As shown in confocal (figure 2.2A) and epifluorescence (figure 2.2B) imaging, GPN induced a rapid loss of LysoTracker fluorescence which occurred around 3 minutes after its addition.

GPN-evoked  $\text{Ca}^{2+}$  responses (figure 2.1A) therefore continue after the loss of LysoTracker fluorescence. This kinetic discrepancy was pursued by co-loading cells with Fura-2 and LysoTracker and simultaneously recording fluorescence emission (Figure 2.2C-E). In all cells examined, the loss of LysoTracker fluorescence correlated with a small increase in cytosolic  $\text{Ca}^{2+}$ . Once the LysoTracker signal was depleted, secondary  $\text{Ca}^{2+}$  responses were observed. These signals were categorised into three types. In most of the fibroblasts examined, a peak of large amplitude was either followed by a series of oscillations (Figure 2.2C;  $45\pm 3\%$ ,  $n=40$ ) or terminated after the initial  $\text{Ca}^{2+}$  spike (Figure 2.2D;  $36\pm 4\%$ ,  $n=40$ ). In other cells, a monotonic response that primarily peaked after the loss of LysoTracker was observed (Figure 2.2E;  $18\pm 3\%$ ,  $n=40$ ).

### GPN evokes spatiotemporally complex $\text{Ca}^{2+}$ signals

GPN-evoked oscillatory  $\text{Ca}^{2+}$  responses were further characterised by examining the spatial patterning of  $\text{Ca}^{2+}$  signals. Representative, pseudo-coloured, Fura-2 epifluorescence images are shown in figure 2.3. GPN-evoked  $\text{Ca}^{2+}$  signals either originated at one location (typically close to the plasma membrane) and spread throughout the cell in a wave-like fashion (figure 2.3A;  $67\pm 5\%$  cells,  $n=15$ ) or commenced around the cell periphery (figure 2.3B;  $33\pm 5\%$  cells,  $n=15$ ). For the latter of these responses, the  $\text{Ca}^{2+}$  wave advanced in a centripetal motion like the closing of an iris. In all 104 cells examined, repeated spikes originated from the same sub-cellular location.

### GPN-evoked $\text{Ca}^{2+}$ responses are concentration-dependent

The effect of GPN on LysoTracker fluorescence and cytosolic  $\text{Ca}^{2+}$  signalling was further characterised in fibroblasts using a range of GPN concentrations (figure 2.4). Reducing GPN concentration delayed the loss of LysoTracker fluorescence (figure 2.4A). This was quantified by calculating the time taken for fluorescence to decrease by 50% (figure 2.4E). As shown in figures 2.4B-D, GPN-evoked  $\text{Ca}^{2+}$  responses also varied according to GPN concentration. At 200  $\mu\text{M}$ , GPN-evoked  $\text{Ca}^{2+}$  signals similar to those seen in other figures. GPN also evoked complex  $\text{Ca}^{2+}$  signals at 100  $\mu\text{M}$ , but the responses were delayed (figure 2.4D and F).

Furthermore, 20  $\mu\text{M}$  GPN appeared at the threshold of  $\text{Ca}^{2+}$  signal generation since the magnitude of  $\text{Ca}^{2+}$  response (figure 2.4G) and percentage of responsive cells (figure 2.4H) were reduced at this concentration.

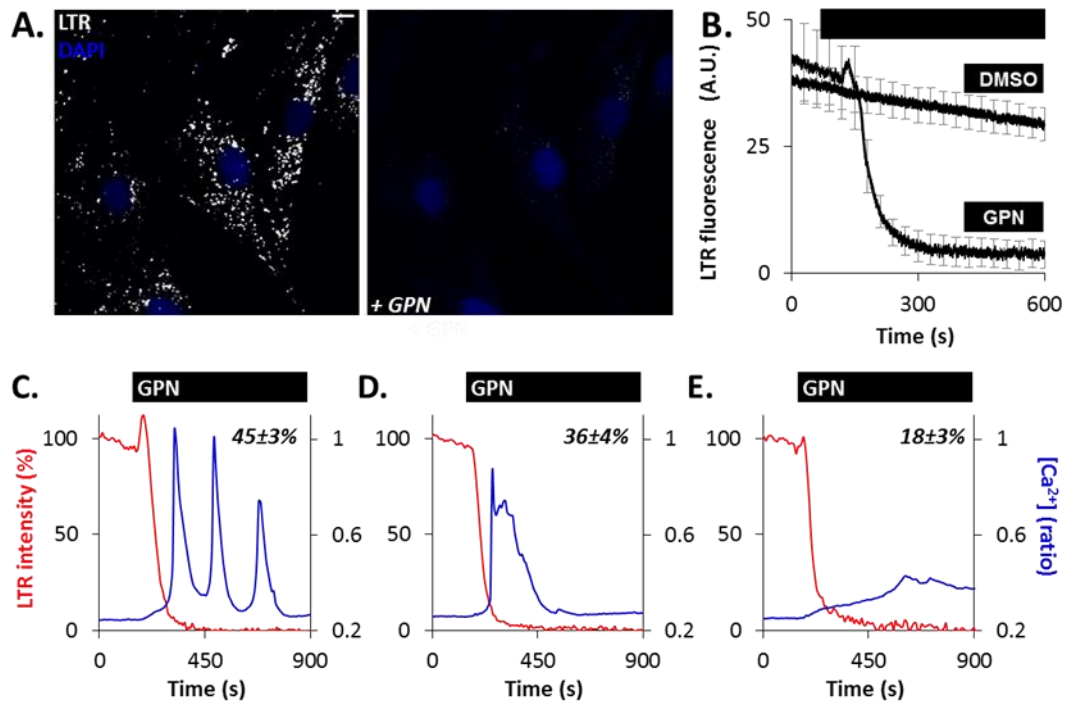


**Figure 2.2 GPN rapidly permeabilises lysosomes**

(A) Confocal images of fibroblasts labelled with Lysotracker (white) before and 216 seconds after the addition of GPN (200  $\mu\text{M}$ ). Scale bar; 10  $\mu\text{m}$ .

(B) Average epifluorescence responses of Lysotracker labelled cells after DMSO or GPN (200  $\mu\text{M}$ ) stimulation.

(C-E) Simultaneous measurements of Lysotracker Red (LTR; red line) and Fura-2 (blue line) fluorescence from individual fibroblasts stimulated with GPN (200  $\mu\text{M}$ ) in the absence of extracellular  $\text{Ca}^{2+}$ . Inset values indicate the number of cells categorised into each cell type across all 40 experiments ( $n$ ) analysing 557 cells.

#### Complex GPN-evoked $\text{Ca}^{2+}$ responses are cell-type specific

To further investigate GPN-evoked  $\text{Ca}^{2+}$  responses,  $\text{Ca}^{2+}$  signals were compared in multiple cell types. Similar to fibroblasts (figure 2.5A), GPN stimulated complex  $\text{Ca}^{2+}$  signals in cultures containing a mixed population of cortical cells (Figure 2.5B). However, in HeLa (figure 2.5C) and SH-SY5Y (Figure 2.5D) cells, responses were of low magnitude and monotonic.

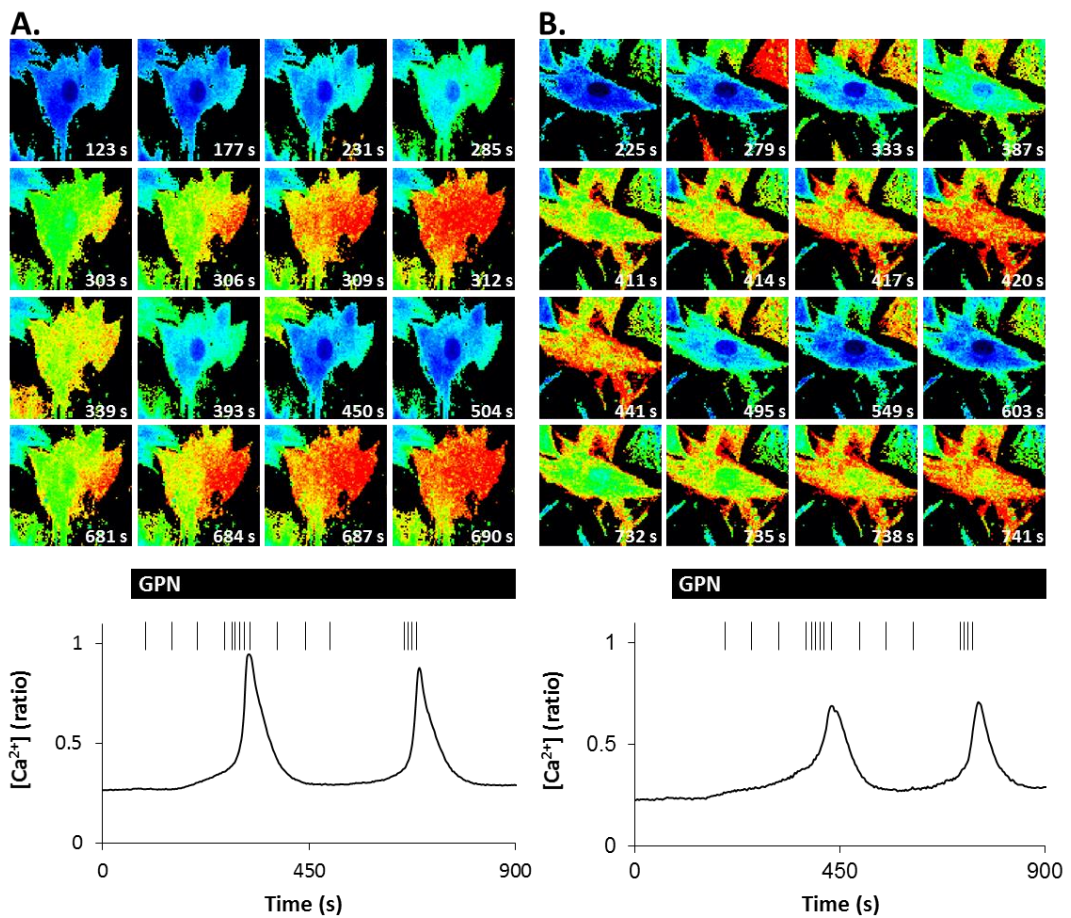


**Figure 2.3 GPN evokes spatiotemporally complex  $\text{Ca}^{2+}$  signals**

(A-B) Representative pseudo-coloured epifluorescence images of GPN-evoked  $\text{Ca}^{2+}$  signals that initiated in one location and spread throughout the cell (A) or propagated in a centripetal motion (B). The  $\text{Ca}^{2+}$  traces represent the temporal profiles of the spatial images. Each vertical line marks the time that each image was taken.

#### GPN-evoked $\text{Ca}^{2+}$ responses are dependent upon acidic organelles

To examine the contribution of acidic organelles to GPN-evoked  $\text{Ca}^{2+}$  responses, cells were treated with bafilomycin-A1. Bafilomycin-A1 is a V-type ATPase inhibitor that prevents the acidification of lysosomes. Maintenance of a low luminal pH is crucial for  $\text{Ca}^{2+}$  uptake (Christensen et al., 2002). As shown in figure 2.6B, complex GPN  $\text{Ca}^{2+}$  signalling was largely inhibited after an overnight exposure to 100 nM bafilomycin-A1. However, the acute addition of bafilomycin-A1 did not induce  $\text{Ca}^{2+}$  responses (figure 2.6C).

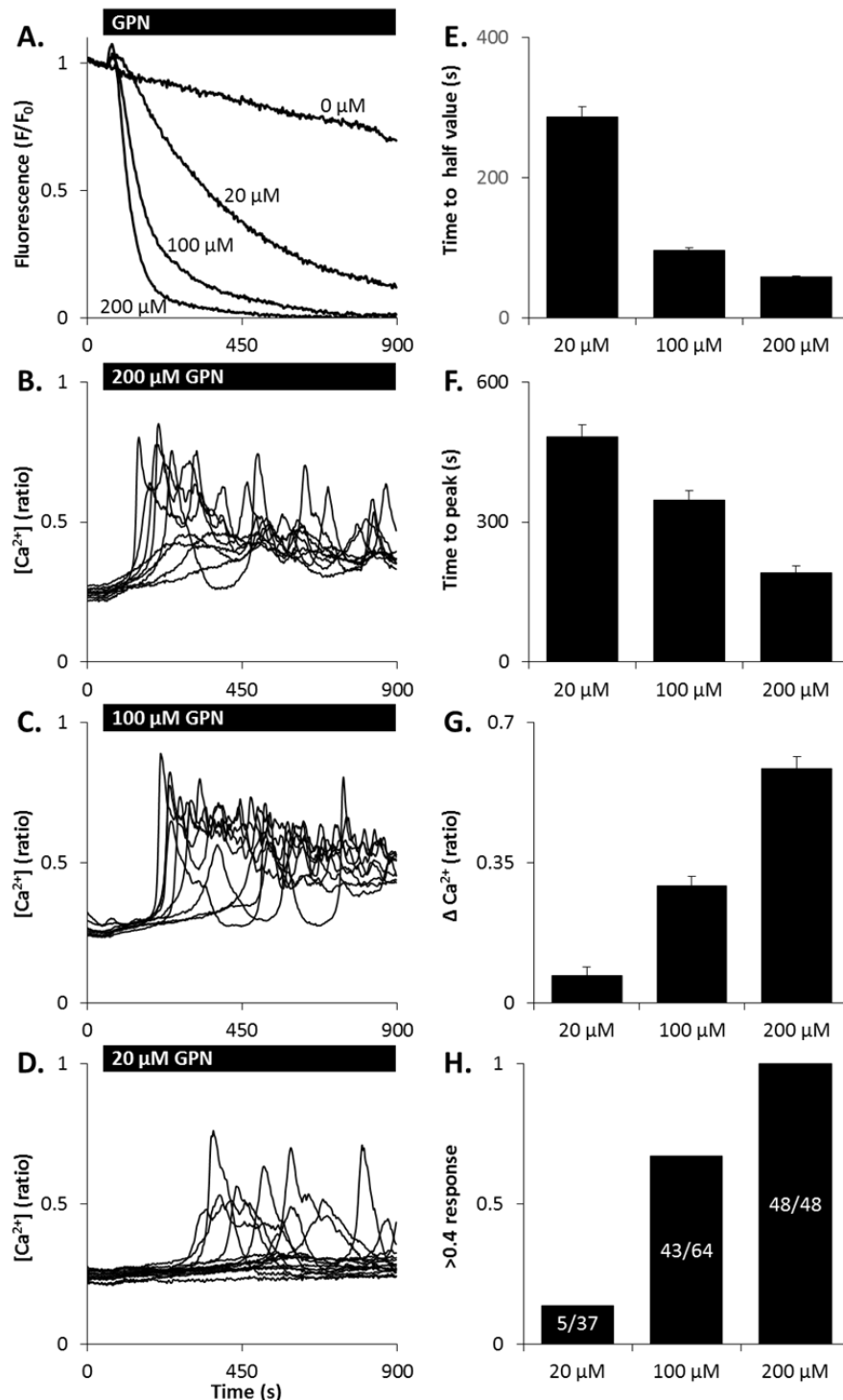


**Figure 2.4 GPN-evoked Ca<sup>2+</sup> responses are concentration-dependent**

(A-D) Lysotracker red fluorescence (A) and cytosolic Ca<sup>2+</sup> responses (B-D) of fibroblasts after stimulation with GPN (20, 100 and 200 μM). Lysotracker fluorescence values have been normalised to basal values.

(E-F) Summary data (mean ± S.E.M) quantifying the time to taken to reach a half-maximal loss of Lysotracker fluorescence (E) or maximal Ca<sup>2+</sup> responses (F).

(G-H) Pooled data (mean ± S.E.M) quantifying magnitude of Ca<sup>2+</sup> response (G) and percentage of responding cells (defined by >0.4 ratio value; H).

Ca<sup>2+</sup> results are from 37-64 (*n*) cells from 2-3 independent platings.

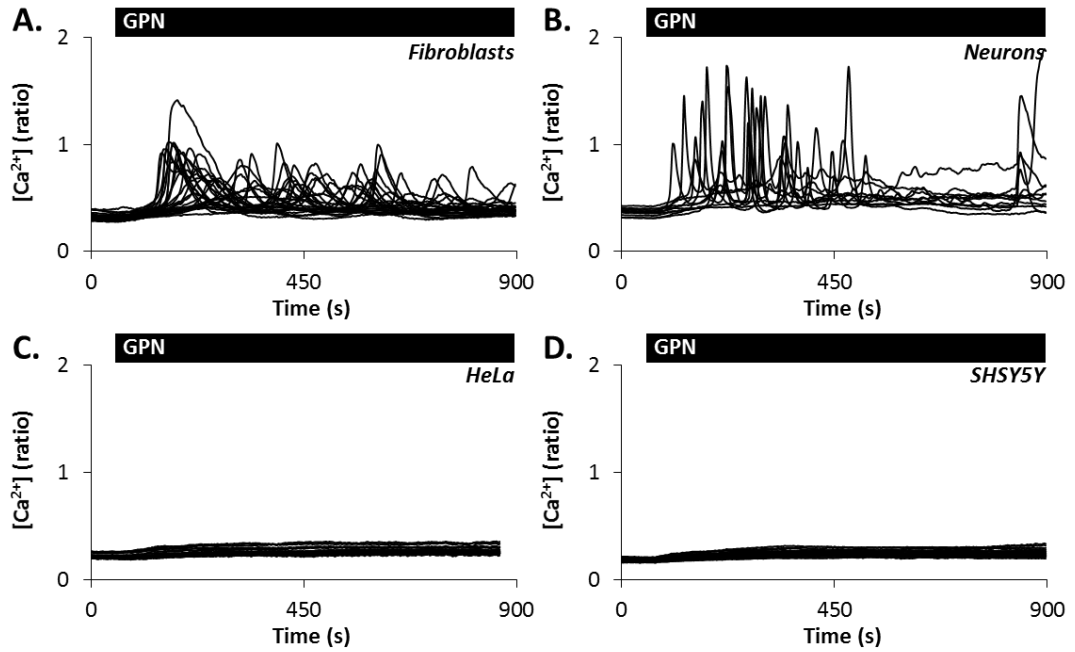


**Figure 2.5 Complex GPN-evoked  $\text{Ca}^{2+}$  responses are cell-type specific**

(A-D) Representative cytosolic  $\text{Ca}^{2+}$  responses of fibroblasts (A), mixed primary neuronal cultures (B), HeLa cells (C) and SH-SY5Y (D) cells after stimulation with GPN (200  $\mu\text{M}$ ).

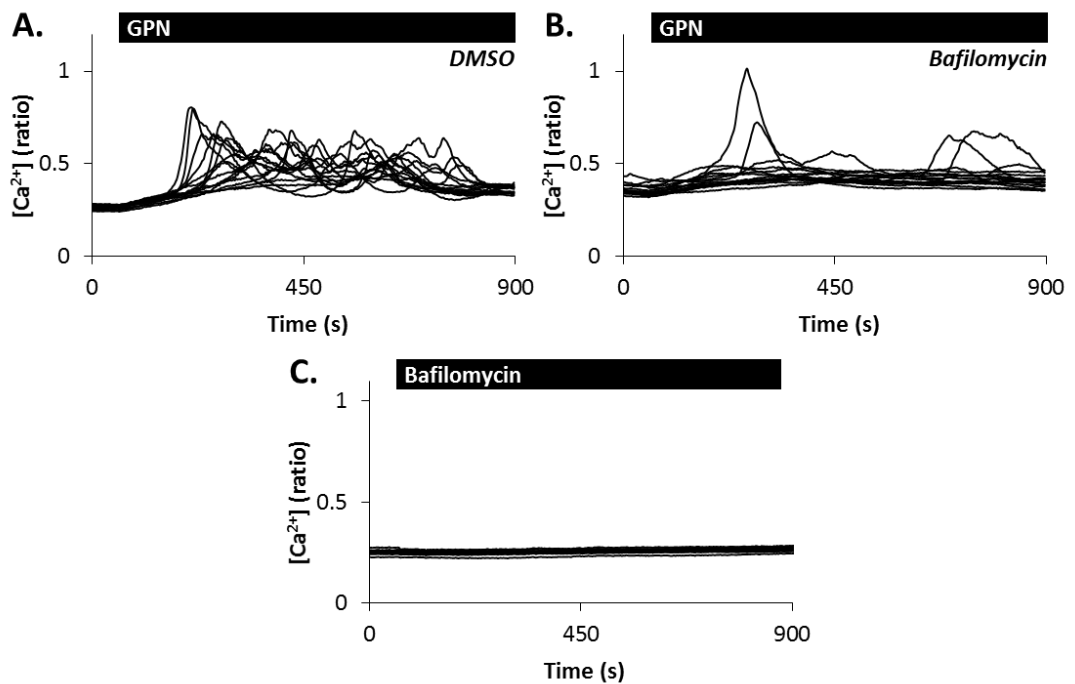


**Figure 2.6 GPN-evoked  $\text{Ca}^{2+}$  responses are dependent upon acidic organelles**

(A-B) Representative GPN-evoked  $\text{Ca}^{2+}$  responses of individual fibroblasts treated overnight with either DMSO (A) or bafilomycin-A1 (100 nM; B).

(C) Representative cytosolic  $\text{Ca}^{2+}$  responses of individual fibroblasts stimulated with bafilomycin-A1 (1  $\mu\text{M}$ ) in the absence of extracellular  $\text{Ca}^{2+}$ .

### **GPN-evoked Ca<sup>2+</sup> responses are dependent upon ER-localised IP<sub>3</sub>R**

To examine the contribution of ER Ca<sup>2+</sup> to GPN-evoked complex Ca<sup>2+</sup> responses, ER Ca<sup>2+</sup> was pharmacologically manipulated using thapsigargin, 2-APB and Ryanodine. The SERCA ATPase inhibitor thapsigargin, depleted ER Ca<sup>2+</sup> and eliminated GPN-induced oscillations, when compared to the DMSO control (figure 2.7A-B). Similarly the inhibition of IP<sub>3</sub>Rs with 2-APB significantly reduced secondary GPN responses (Figure 2.7C). However, GPN-evoked complex Ca<sup>2+</sup> signalling persisted after RyR inhibition (with ryanodine; Figure 2.7D). A concentration of the physiological agonist bradykinin which induces a large, transient Ca<sup>2+</sup> signal also largely inhibited oscillations (Figure 2.7E). Figure 2.7F summarises the inhibition of GPN-stimulated oscillations.

### **GPN permeabilises lysosomes to small molecular weight solutes**

Many have reported that GPN increases the osmolarity of lysosomes which subsequently *ruptures* these acidic organelles, however these experiments were conducted using isolated lysosome preparations (Berg et al., 1994; Jadot et al., 1984). This raises concerns that the complex Ca<sup>2+</sup> responses induced by GPN might be a consequence of released lysosomal hydrolases. To examine the effect of GPN on lysosome morphology, cells were fixed after stimulation and labelled with an antibody raised to the late endosome/lysosome marker LAMP1. The representative confocal images shown in Figure 2.8A, demonstrate that after treatment with GPN lysosomes appear intact but enlarged. These effects were associated with a 2-fold increase in LAMP1 intensity (figure 2.8B).

To further explore the effects of GPN on lysosome permeability, live cells were co-loaded with LysoTracker and a fluorescent dextran (fluorescein, MW 10,000) which was delivered through endocytosis. Figure 2.8C shows that LysoTracker co-localised with the fluorescein-dextran. Consistent with figure 2.2, GPN induced a prompt loss of LysoTracker fluorescence, however dextran fluorescence remained within punctate structures (Figure 2.8C). Epifluorescence imaging of rhodamine-dextran loaded cells revealed that instead of a reduction, a modest increase in fluorescence was observed upon stimulation with GPN (Figure 2.8D-E).

### **ER-evoked Ca<sup>2+</sup> responses are unaffected by lysosome disruption**

My results suggest that ER Ca<sup>2+</sup> is necessary for the generation of complex GPN-evoked Ca<sup>2+</sup> responses in fibroblasts. Recent research has identified that lysosomes sequester ER Ca<sup>2+</sup> and subsequently shape ER Ca<sup>2+</sup> signals (Morgan et al., 2013; López-Sanjurjo et al., 2013). ER Ca<sup>2+</sup> release, in response to thapsigargin, was compared in fibroblasts after overnight treatment with the vehicle control (DMSO, figure 2.9A) and bafilomycin-A1 (figure 2.9B). Pre-treatment



with bafilomycin-A1 did not affect the magnitude of thapsigargin  $\text{Ca}^{2+}$  response (figure 2.9C). However, it is noteworthy that bafilomycin-A1 significantly increased basal  $\text{Ca}^{2+}$  levels in fibroblasts (figure 2.9D).

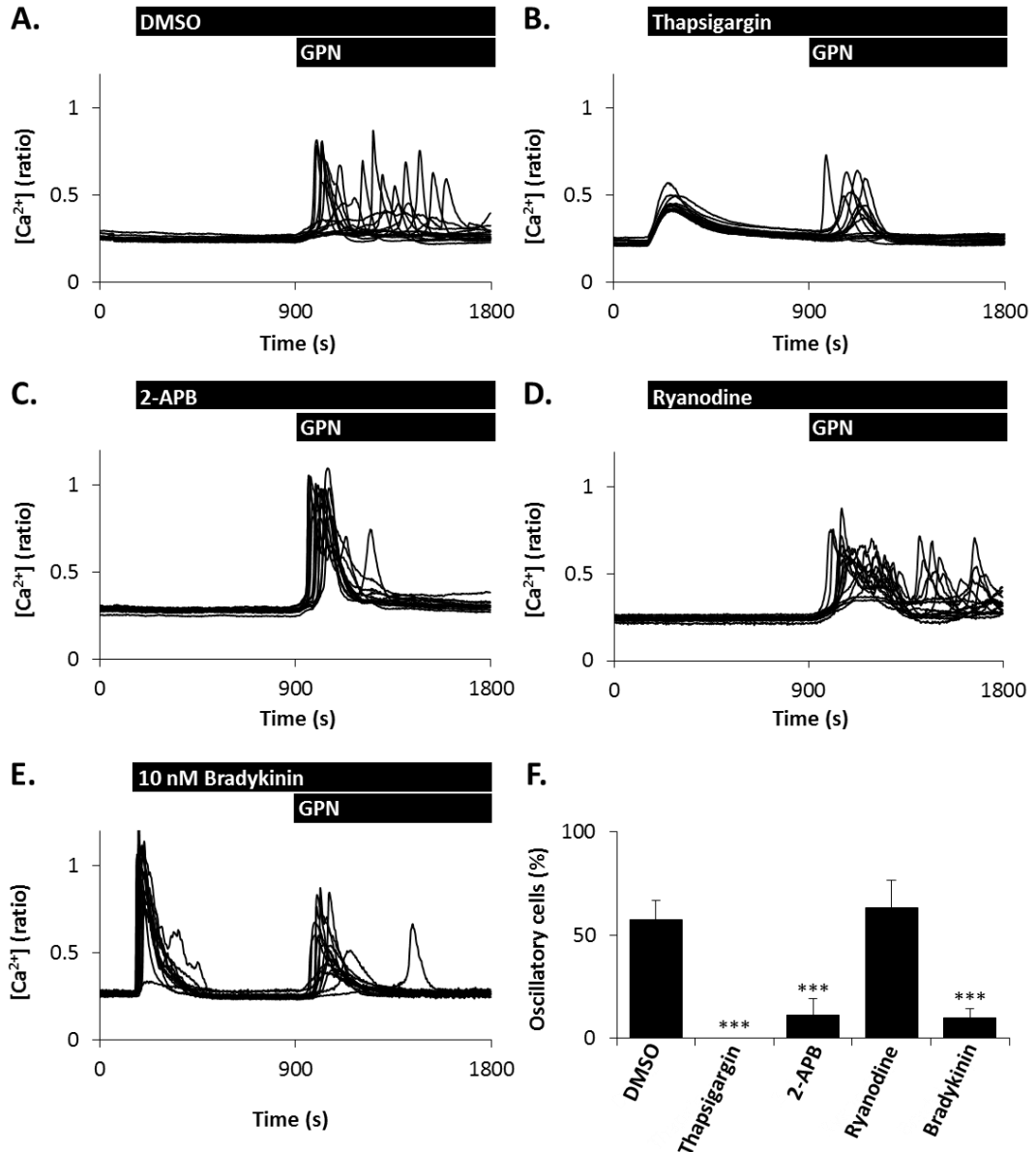


**Figure 2.7 GPN-evoked  $\text{Ca}^{2+}$  responses are dependent upon ER-localised  $\text{IP}_3\text{R}$**

(A-E) Cytosolic  $\text{Ca}^{2+}$  responses of individual fibroblasts stimulated with GPN (200  $\mu\text{M}$ ) after pre-treatment with either DMSO (A), thapsigargin (1  $\mu\text{M}$ ; B), 2-APB (100  $\mu\text{M}$ ; C), ryanodine (100  $\mu\text{M}$ ; D) or bradykinin (10 nM; E) in the absence of extracellular  $\text{Ca}^{2+}$ .

(F) Summary data (mean  $\pm$  S.E.M) quantifying the percentage of cells displaying oscillatory responses after GPN stimulation. Results are from 3-17 experiments ( $n$ ) analysing 45-279 cells. ANOVA analysis, followed by a post-hoc Tukey test, was applied to test significance against control.

\*\*\* $p < 0.001$ .

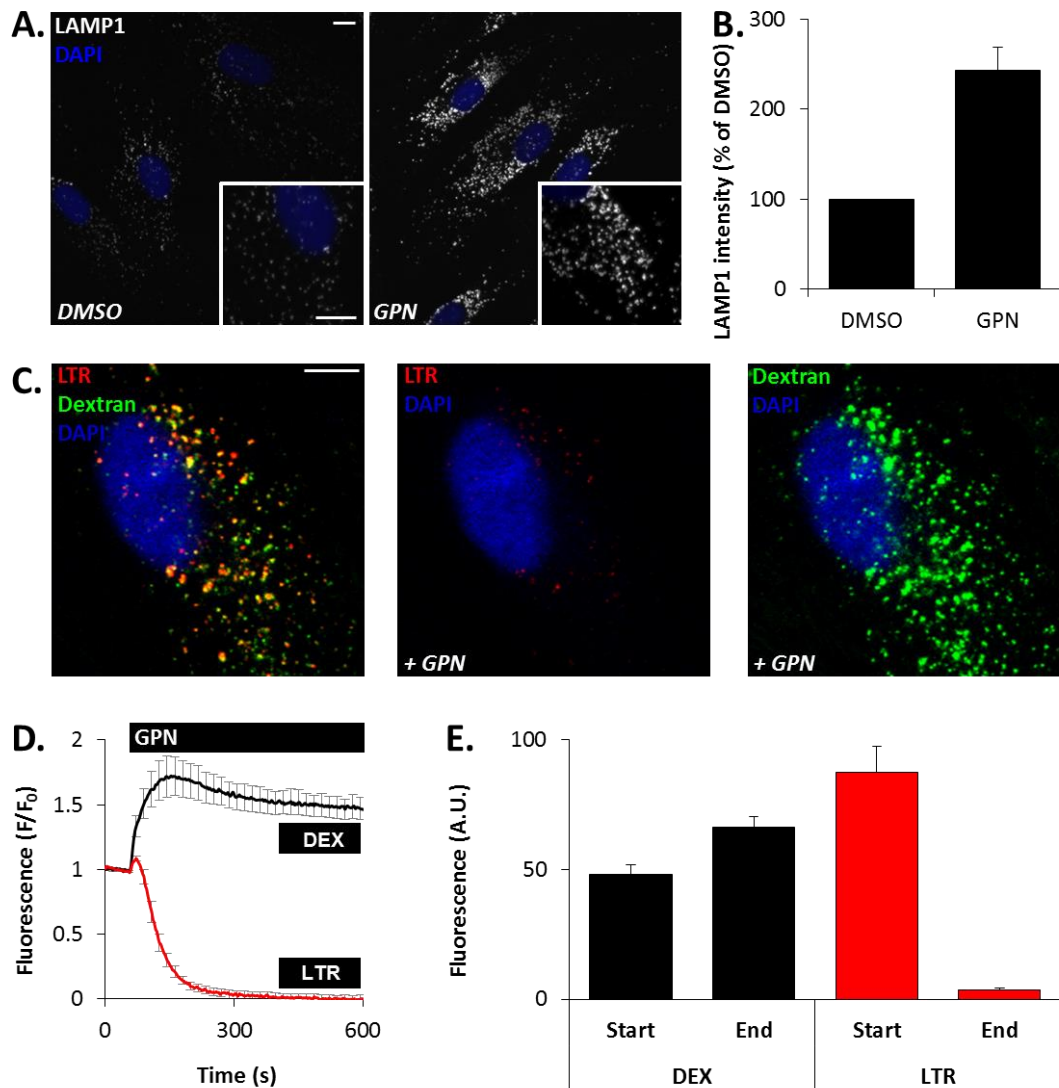


**Figure 2.8 GPN permeabilises lysosomes to small molecular weight solutes**

(A) Representative confocal images of LAMP1 (white) staining in fibroblasts fixed after 15 minutes treatment with either DMSO or GPN (200  $\mu$ M). Nuclei were stained using DAPI (blue). Insets are zoomed images. All Scale bar; 10  $\mu$ m.

(B) Summary data (mean  $\pm$  S.E.M) quantifying LAMP1 intensity as a percentage of DMSO CTRL. Results from 3 independent treatments ( $n$ ) analysing 84-94 cells.

(C) Representative confocal fluorescence images of a DAPI (blue), fluorescein-dextran (green) and lysotracker (red) labelled fibroblast before (left panel) and 152 seconds after (middle and right panels) stimulation with GPN (200  $\mu$ M). All Scale bar; 10  $\mu$ m.

(D) Average epifluorescence responses of lysotracker (LTR; red trace) and rhodamine-dextran (DEX; black trace) labelled cells after stimulation with GPN (200  $\mu$ M). Data has been normalised to basal fluorescence values.

(E) Summary data (mean  $\pm$  S.E.M) quantifying dextran and lysotracker intensity before (0-60 seconds) and after (540-600 seconds) GPN addition. Results are from 3-4 independent experiments analysing 54-43 cells ( $n$ ).

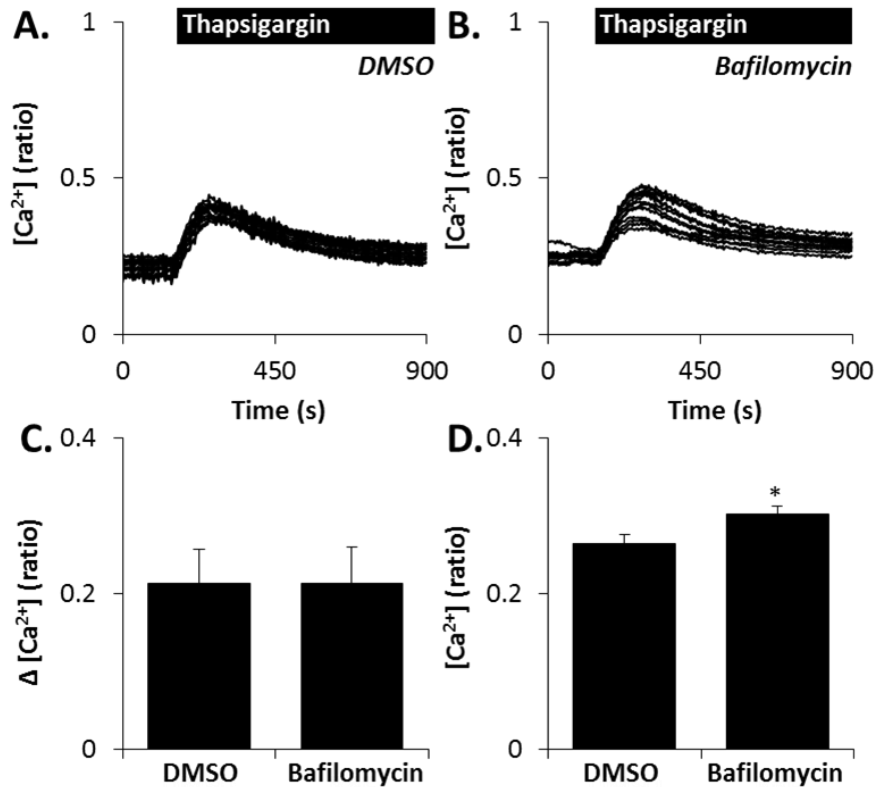


**Figure 2.9 ER-evoked  $Ca^{2+}$  responses are unaffected by lysosome disruption**

(A-B) Cytosolic  $Ca^{2+}$  responses of individual fibroblasts stimulated with thapsigargin ( $1 \mu M$ ) after an overnight treatment with either DMSO (A) or bafilomycin-A1 ( $100 \text{ nM}$ ; B).

(C-D) Summary data (mean  $\pm$  S.E.M) quantifying the magnitude of thapsigargin response (C) and basal  $Ca^{2+}$  ratios (D). Results are from 6 experiments ( $n$ ) of 3 independent treatments analysing 80-88 cells. A two-sample  $t$ -test was applied to test significance. \* $p < 0.05$ .

## Discussion

In this chapter I show that, in human fibroblasts, direct mobilisation of lysosomal  $Ca^{2+}$ , using GPN, evokes prolonged and complex  $Ca^{2+}$  signalling. These  $Ca^{2+}$  signals were insensitive to extracellular  $Ca^{2+}$  and similar to those evoked by agonists and NAADP. GPN-evoked  $Ca^{2+}$  responses were biphasic, consisting of an initial pacemaker signal, which coincides with lysosome disruption, followed by various secondary responses that were spatially heterogeneous. Like NAADP, secondary  $Ca^{2+}$  responses were dependent upon ER-localised  $IP_3R$ . Therefore, inducing a leak of small molecular weight solutes from the lysosomes with GPN, can be used as an effective tool to recapitulate NAADP signalling and probe the functional relationship between ER and acidic  $Ca^{2+}$  stores. Research presented in this chapter was published in Kilpatrick et al. (2013) and Penny et al. (2014) (both attached to the appendix).

The proposed TPC ligand NAADP, has previously been shown to induce complex  $\text{Ca}^{2+}$  responses. Evidence suggests that a localised release of lysosomal  $\text{Ca}^{2+}$  with NAADP, triggers global ER  $\text{Ca}^{2+}$  signalling. This was first reported by Cancela and co-workers (1999) where NAADP responses were suppressed in pancreatic acinar cells upon the blockade of  $\text{IP}_3\text{Rs}$  and  $\text{RyRs}$ . Notably, this NAADP-triggering phenomenon has been recapitulated in neuronal (Brailoiu et al., 2005; Heidemann et al., 2005; Brailoiu et al., 2009b) and immune (Berg et al., 2000; Steen et al., 2007) cells. In this chapter I demonstrate that GPN-induced  $\text{Ca}^{2+}$  responses resembled those evoked by NAADP-AM (Figure 2.1) and are also amplified by the ER (figure 2.7). Specifically, inhibiting ER  $\text{Ca}^{2+}$  release blocked GPN-evoked  $\text{Ca}^{2+}$  oscillations. These data agree with previous research where depleting ER  $\text{Ca}^{2+}$  with thapsigargin also reduced GPN responses (Haller et al., 1996; Sivaramakrishnan et al., 2012; Gerasimenko et al., 2006; Menteyne et al., 2006; Coen et al., 2012). However, thapsigargin has not always been shown to dampen GPN  $\text{Ca}^{2+}$  signalling (López et al., 2005; Visentin et al., 2013). Since secondary  $\text{Ca}^{2+}$  signals are inhibited with 2-APB (not ryanodine), GPN responses likely depend upon  $\text{IP}_3\text{Rs}$ . However, I cannot rule out the possibility that  $\text{IP}_3\text{Rs}$  on the Golgi apparatus are also involved in these complex GPN  $\text{Ca}^{2+}$  signals (Pinton et al., 1998).

A key feature of  $\text{IP}_3\text{Rs}$  and  $\text{RyRs}$  is that they are sensitive to  $\text{Ca}^{2+}$  (Bezprozvanny et al., 1991). It has therefore been proposed that NAADP responses are amplified by these ER channels through CICR (Cancela et al., 1999). Targeting overexpressed TPC2 to the plasma membrane, achieved through mutating the N-terminal lysosomal-targeting motif, altered NAADP signalling (Brailoiu et al., 2010b). When at the plasma membrane NAADP-evoked  $\text{Ca}^{2+}$  signals were sluggish and insensitive to the inhibition of ER  $\text{Ca}^{2+}$  release (Brailoiu et al., 2010b). Thus, for lysosome-ER “channel chatter” to occur it has been proposed that these  $\text{Ca}^{2+}$  stores must be closely associated.

The ER is known to form MCSs (membrane regions defined by a separation of less than 30 nm) with many organelles which are important for lipid transfer and  $\text{Ca}^{2+}$  signalling (reviewed in Prinz 2014). We have recently identified MCSs between lysosomes and the ER (report attached to the appendix, Kilpatrick et al. 2013). Dr Emily Eden and Professor Clare Futter report that more than 80% of lysosomes form contacts with the ER. Indeed, this is likely an underestimate since lysosomes are approximately 3-7 times larger than the sections used for electron microscopy, so further contacts may have been missed. Further examination of ER-Lysosomal MCSs, revealed that these  $\text{Ca}^{2+}$  stores appear tethered together. Much like those MCSs already reported between the ER and late-endosomes (Eden et al., 2010) as well as

mitochondria (Csordás et al., 2006). Despite extensive MCSs reported between the ER and mitochondria, release of mitochondrial  $\text{Ca}^{2+}$  using FCCP was not sufficient to induce complex  $\text{Ca}^{2+}$  signalling (Figure 2.1E). Therefore, to evoke complex  $\text{Ca}^{2+}$  responses the structure of lysosome-ER contact sites must be unique.

The physical coupling of these organelles likely facilitates lysosomal  $\text{Ca}^{2+}$  signalling by bringing the  $\text{Ca}^{2+}$  signalling apparatus together. An aggregation of  $\text{Ca}^{2+}$  and signalling proteins in such a confined space might form  $\text{Ca}^{2+}$  microdomains. In these microdomains accumulating  $\text{Ca}^{2+}$  could prime  $\text{IP}_3\text{Rs}$ . The concept that MCSs promote  $\text{Ca}^{2+}$  signalling is not novel. Mitochondria are known to form close (around 10 nm) junctions with the ER to promote  $\text{Ca}^{2+}$  uptake and subsequent ATP production (Csordás et al., 2006; Szabadkai et al., 2006; Tarasov et al., 2012). In addition, the sarcoplasmic reticulum connects with L-type  $\text{Ca}^{2+}$  channels on the plasma membrane for excitation-contraction coupling in muscle cells (Franzini-Armstrong et al., 1999).

The size of MCSs/microdomains obstructs their experimental characterisation. However, computational models can be developed to simulate these environments. With the help of collaborators in New Zealand, our laboratory constructed a model of ER-lysosomal  $\text{Ca}^{2+}$  microdomains (report attached to the appendix, Penny et al. (2014)). We used the loss of LysoTracker fluorescence in fibroblasts as a proxy to model lysosomal  $\text{Ca}^{2+}$  release. The computational model was capable of qualitatively reproducing GPN-induced  $\text{Ca}^{2+}$  signalling with the matched pharmacology. We then advanced the model to probe physiological NAADP signalling through TPCs. TPCs were modelled on established biophysical data (Pitt et al., 2010) and microdomains were shown to modulate NAADP-evoked  $\text{Ca}^{2+}$  signals. Furthermore, the frequency of NAADP-induced  $\text{Ca}^{2+}$  oscillations was dependent upon TPC density within the microdomain. Thus, similar to RyR clustering (important for driving excitation-contraction coupling), TPCs might accumulate in microdomains to drive NAADP signalling. Once appropriate antibodies have been developed, this should be examined using immunoelectron microscopy. An interesting, yet somewhat counter-intuitive, finding of this model was that a high concentration of  $\text{Ca}^{2+}$  in the microdomain was not necessary to initiate CICR. Although not claiming to be the physiological state, only nanomolar concentrations of  $\text{Ca}^{2+}$  are needed to prime  $\text{IP}_3\text{Rs}$  (Bezprozvanny et al., 1991).

GPN has been widely used to investigate lysosomal  $\text{Ca}^{2+}$  signalling (table 1.1, chapter 1). Much like the evidence presented in this chapter,  $\text{Ca}^{2+}$  responses to GPN can vary according to cell type (Figure 2.5). Similar to SHSY5Y and HeLa cells, GPN evokes low magnitude,

monotonic  $\text{Ca}^{2+}$  signals in MDCK (Haller et al., 1996) and HEK (Reeves et al., 2006) cells. Notably, GPN stimulates complex  $\text{Ca}^{2+}$  signalling in both fibroblasts and neuronal cultures. GPN has previously been shown to elicit robust, complex  $\text{Ca}^{2+}$  signals in neuronal cells (Pandey et al., 2009; Tu et al., 2010). The variations in  $\text{Ca}^{2+}$  responses might be a result of differences in Cathepsin C activity, lysosome number, volume and  $\text{Ca}^{2+}$  content. Furthermore, ER  $\text{Ca}^{2+}$  homeostasis, receptor levels and MCS composition might account for different GPN responses across cell types. Indeed, these differences require further characterisation.

GPN has also been used to examine lysosomal  $\text{Ca}^{2+}$  content (Lloyd-Evans et al., 2008; Dickinson et al., 2010; Shen et al., 2012; Coen et al., 2012). In order to effectively do this,  $\text{Ca}^{2+}$  stores must be uncoupled to get an accurate measure of acidic store content. Failure to prevent ER  $\text{Ca}^{2+}$  efflux might influence interpretations. A good example of this is whether lysosomal  $\text{Ca}^{2+}$  content is reduced in Niemann-Pick type C1 (NPC). Lloyd-Evans et al. (2008) report that lysosomal  $\text{Ca}^{2+}$  content is reduced in NPC, whereas Shen et al. (2012) do not see this disruption. These discrepancies could be attributed to the pre-treatment with (Lloyd-Evans et al., 2008), or without (Shen et al., 2012) thapsigargin. Perhaps a better approach for measuring lysosomal  $\text{Ca}^{2+}$  content is using 2-APB. Because, unlike thapsigargin, 2-APB would not cause a cytosolic  $\text{Ca}^{2+}$  response and the subsequent activation of buffering mechanisms (this approach has been used in chapter 4). It is notable that, GPN-evoked  $\text{Ca}^{2+}$  responses, following pre-stimulation with thapsigargin, differ from those evoked after 2-APB and bradykinin (Figure 2.7). Perhaps, the functional uncoupling from the ER is incomplete upon  $\text{IP}_3\text{R}$  inhibition/desensitisation. On the other hand, 2-APB has several non-specific effects on  $\text{Ca}^{2+}$  homeostasis (such as modifying store operated  $\text{Ca}^{2+}$  entry) which might also disturb GPN signalling.

Although lysosomal hydrolases are believed to be harmless at neutral pH, Gerisemenko and colleagues (2006) attribute GPN-induced complex  $\text{Ca}^{2+}$  signalling to a leak of enzymes from the lysosomes. Indeed, they show that the inhibition of papain and cathepsins B, L and S with the Cathepsin-inhibitor 1 (CI-1) reduced GPN-evoked complex  $\text{Ca}^{2+}$  signalling (Gerasimenko et al., 2006). However, others have shown that CI-1 has no effect on GPN stimulated  $\text{Ca}^{2+}$  responses (Menteyne et al., 2006; Steen et al., 2007). Data reported in this chapter shows that GPN causes a controlled, concentration-dependent leak of small molecular weight solutes (<10 kDa; Figure 2.8C-E). Therefore, hydrolases, most of which are larger than 35 kDa, likely remain within lysosomes upon exposure to GPN. This is consistent with previous reports showing the lysosomal retention of 10- (Steinberg et al., 2010) and 70- (Haller et al.,

1996) kDa dextrans after GPN treatment. To ensure hydrolases remain within the lysosomes, their localisation after GPN exposure requires further examination. Moreover, the effect of CI-1 on GPN induced  $\text{Ca}^{2+}$  responses in fibroblasts warrants investigation. I have also examined lysosomal morphology after exposure to GPN. Although the lysosomes appear intact, GPN appeared to enlarge these organelles (figure 2.8A). This might reflect the osmotic swelling. The increase in lysosome size could be significant since it might bring these acidic  $\text{Ca}^{2+}$  stores even closer to the ER. Notably, integrity and membrane contacts after exposure to GPN requires further examination using electron microscopy.

Evidence presented in this chapter suggests that lysosomes hold an essential position within the  $\text{Ca}^{2+}$  network since they are capable of triggering complex  $\text{Ca}^{2+}$  signalling. Indeed, some have reported that this functional coupling is bi-directional, where lysosomes also modify ER- $\text{Ca}^{2+}$  signalling (López-Sanjurjo et al., 2013; Morgan et al., 2013). Recent research, using sea urchin eggs, has identified that ER  $\text{Ca}^{2+}$  signalling stimulates lysosomal  $\text{Ca}^{2+}$  release (Morgan et al., 2013). This was established using an innovative technique whereby the alkalinisation of lysosomal pH was shown to be an indicator of NAADP activity (Morgan et al., 2013; Morgan & Galione, 2007). It is therefore possible that NAADP signalling is sustained by the bi-directional transfer of  $\text{Ca}^{2+}$  between lysosomal and ER stores. In addition, López-Sanjurjo and colleagues (2013) report that in HEK cells various lysosomal toxins, including bafilomycin, potentiate thapsigargin and  $\text{IP}_3$ -mediated  $\text{Ca}^{2+}$  signalling. Intimate physical associations between lysosomes and ER, identified using total internal reflection fluorescence microscopy, were also proposed to facilitate this lysosomal  $\text{Ca}^{2+}$  uptake. However, in fibroblasts bafilomycin did not affect thapsigargin  $\text{Ca}^{2+}$  signalling in fibroblasts (figure 2.9). Although, bafilomycin did increase cytosolic  $\text{Ca}^{2+}$  (as also reported in López-Sanjurjo et al., 2013), showing the importance of lysosomes in the maintenance  $\text{Ca}^{2+}$  homeostasis.

In conclusion, lysosomal  $\text{Ca}^{2+}$  is sufficient to trigger complex, ER-regulated  $\text{Ca}^{2+}$  signalling. Thus, GPN can be effectively used to examine  $\text{Ca}^{2+}$  signalling at the ER-lysosomal interface. This tool evades problems associated with the potential action of NAADP on ER  $\text{Ca}^{2+}$  channels. Recently described MCSs between the ER and lysosomes might facilitate the functional coupling between these  $\text{Ca}^{2+}$  stores. Indeed, *in silico* models suggest that MCSs promote lysosomal-ER  $\text{Ca}^{2+}$  signalling. However, further work characterising the composition of MCSs is warranted.

# Chapter 3

---

## On the Mechanism of Lysosome-ER Ca<sup>2+</sup> Coupling

### Introduction

In chapter 2, a functional relationship between lysosomes and ER Ca<sup>2+</sup> signalling was identified using a lysosomal permeabilising agent. The recently identified MCSs between these Ca<sup>2+</sup> stores might contribute to this Ca<sup>2+</sup> signalling partnership (Kilpatrick et al., 2013). Although our understanding of these connections is limited, we can draw parallels with research examining MCSs between late-endosomes and the ER (Eden et al., 2010; Rocha et al., 2009; Alpy et al., 2013). These studies identified the small trafficking GTPase Rab7 as an essential MCS component. Through interactions with RILP and ORP1L, Rab7 can regulate late-endosome trafficking and the formation of MCSs (Rocha et al., 2009; Johansson et al., 2007). Specifically, RILP interacts with cytoskeletal-components to regulate minus-end trafficking (Johansson et al., 2007) and ORP1L is recognised by ER-localised VAP (Rocha et al., 2009). VAP transmembrane proteins have an essential role in lipid transport (Peretti et al., 2008) and have been associated with plasma membrane- (reviewed in Prinz 2014) and mitochondria- (De Vos et al., 2012) ER MCSs. Similar proteins might also mediate lysosome-ER junctions and regulate Ca<sup>2+</sup> “chatter” between these organelles.

We have proposed that lysosome-ER MCSs facilitate signalling by NAADP (Kilpatrick et al., 2013; Penny et al., 2014), which, for over a decade, has been established as a “trigger” for IP<sub>3</sub> and ryanodine receptor activation (Cancela et al., 1999). At least two distinct ion channels reside on lysosomes, TPC2 and TRPMLs. Although much evidence indicates that TRPMLs are Ca<sup>2+</sup>-permeable, little is known regarding their role in Ca<sup>2+</sup> signalling.

Using knowledge derived from late-endosome-ER *connections*, this chapter examines if similar components affect lysosome-ER Ca<sup>2+</sup> signalling. Additionally I investigate the role of TRPML channels in Ca<sup>2+</sup> signalling and whether, like TPCs, they are functionally *connected* with the ER.



## Methods

### Cell culture

Primary human fibroblasts were cultured as described in chapter 2. In some experiments fibroblasts were treated overnight with the Rab7 GTPase inhibitor (CID 1067700; 100  $\mu$ M; EMD Millipore) prepared in DMSO.

### siRNA transfection

Fibroblasts were diluted  $1 \times 10^5$  cells/mL and transfected with siRNAs (small interfering RNA; 15 nM) using Lipofectamine RNAiMAX (Invitrogen) for 24 hours. Fibroblasts were transfected for a further 24 hours using fresh reagents and cultured for a final 24 hours in complete media without siRNA, before experimentation.

A control siRNA (Allstars Negative Control siRNA) and siRNAs targeting human Rab7a (5'-CACGTAGGCCTTCAACACAAT-3') were purchased from Qiagen. siRNAs targeting human VAPa and VAPb were a kind gift from Dr Emily Eden.

### Western blotting

Fibroblasts were harvested by scraping, washed in PBS and lysed in Ripa buffer (containing 150 mM NaCl, 50 mM Tris [pH 7.4], 0.5% [v/v] sodium deoxycholic acid, 0.1% [v/v] sodium dodecyl sulphate [SDS] and 1% [v/v] Triton X-100) in the presence of EDTA-free protease inhibitor cocktail (Roche) for 30 minutes on ice. Samples were centrifuged at 25,000 x g at 4°C and supernatant frozen until required for use. Protein concentration was determined using the bicinchoninic acid procedure.

NuPAGE LDS sample loading buffer (Invitrogen), supplemented with 100 mM dithiothreitol (Sigma) was added to the homogenate preparation prior to heating the sample for 10 minutes at 90°C. Samples were separated on NuPAGE 12% Bis-Tris gels (15 mm x 10 well, Invitrogen) with MOPS running buffer (Invitrogen) and protein transferred onto PVDF filters (Biorad) using buffer containing (48 mM Tris, 40 mM glycine, 0.04% [v/v] SDS, 20% [v/v] Methanol). Blots were washed with Tris-buffered saline (25 mM Tris, 137 mM NaCl and 2.7 mM KCl, pH 7.4) containing 0.1% (v/v) Tween (TBS-T) and blocked with 5% (w/v) dried skimmed milk in TBS-T for 1 hour at RT. Blots were sequentially incubated with primary and secondary antibodies (both for 1 hour at room temperature) diluted in TBS-T supplemented with 2.5% (w/v) non-fat milk. In between and after antibody incubations, blots were washed (3 x 30 minutes) with TBS-T. Blots were developed using the ECL Prime Western Blot Detection System (G.E. Healthcare) and densitometry performed using Image J software.

The primary antibodies used were anti-Rab7a (rabbit, Sigma; 1/500), anti-VAPa (mouse, R&D systems, 1/250), anti-VAPb (mouse, R&D systems, 1/500) and anti-actin (goat, Invitrogen, 1/500). The secondary antibodies used were anti-mouse (Santa Cruz Biotechnology), anti-rabbit (Bio-Rad) or anti-goat (Santa Cruz) all diluted 1/2000.

### Recurrent methods

Ca<sup>2+</sup> imaging was carried out as described in chapter 2. In some experiments, fibroblasts were stimulated with MBCD (Methyl- $\beta$ -cyclodextrin; 10 mM; Sigma), ML-SA1 (Mucolipin Synthetic Agonist 1; 10-200  $\mu$ M; Merck) and NH<sub>4</sub>Cl (100 mM; Sigma).

Lysotracker imaging, LAMP1 immunocytochemistry, microscopy and analysis were also performed as described in chapter 2.

## Results

### GPN-evoked complex Ca<sup>2+</sup> responses are Rab7-dependent

In chapter 2, I identified GPN as a useful tool to examine Ca<sup>2+</sup> “chatter” between lysosomes and the ER. We have speculated that MCSs promote ER-Lysosome Ca<sup>2+</sup> coupling, however the molecular identity of these junctions is unknown. To probe the role of Rab7 in regulating lysosome-ER Ca<sup>2+</sup> signalling, GPN-evoked Ca<sup>2+</sup> responses were compared after exposure to a Rab7 inhibitor (Agola et al., 2012). Overnight treatment with the Rab7 inhibitor suppressed GPN evoked oscillations (by 80%,  $n = 5$ , from 3 independent treatments, analysing 114 fibroblasts) and instead generated transient Ca<sup>2+</sup> responses (figure 3.1A-B). Notably, the Rab7 inhibitor did not affect GPN-induced lysosome permeabilisation as quantified using Lysotracker red (figure 3.1C-D).

These findings were extended into a molecular model of Rab7 inhibition, where expression of this GTPase was suppressed using siRNAs. As shown in figure 3.2, GPN evoked complex Ca<sup>2+</sup> signals in cells transfected with the control siRNA. However, Rab7 siRNA reduced oscillatory GPN responses by 87% ( $n = 7$ , from 3 independent treatments, analysing 139 fibroblasts). Like the pharmacological approach, lysosome permeabilisation was not affected by Rab7 siRNAs (figure 3.2C-D). siRNA efficacy was assessed through Western blotting and using a Rab7 antibody. As shown in figure 3.2E the Rab7 siRNA was highly effective at reducing Rab7 protein levels when compared to the control siRNA. Lysosome morphology, size and positioning appeared unaffected by Rab7 siRNA (figure 3.2F).

Rab7 interacts with cholesterol binding proteins which have also been localised to late-endosome-ER MCSs (Rocha et al., 2009). Thus, cholesterol homeostasis might be essential to

lysosome-ER junctions and impact the functional coupling between these  $\text{Ca}^{2+}$  stores. To examine the effect of cholesterol on GPN-evoked  $\text{Ca}^{2+}$  signalling, cholesterol was depleted using methyl- $\beta$ -cyclodextrin (MBCD). When compared to the vehicle control (figure 3.3A), MBCD inhibits complex  $\text{Ca}^{2+}$  responses induced by GPN (figure 3.3B). However, MBCD also delays the rate of GPN-induced lysosome permeabilisation as shown using LysoTracker (figure 3.3C-D).

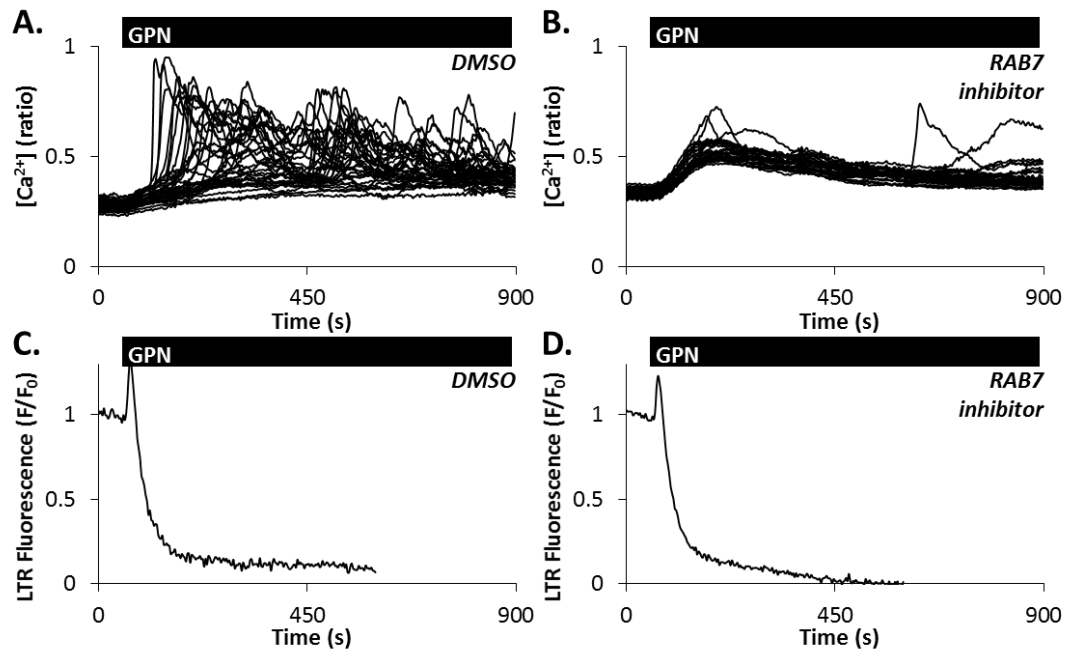


**Figure 3.1 GPN-evoked complex  $\text{Ca}^{2+}$  responses are Rab7-dependent**

(A-D) Individual cytosolic  $\text{Ca}^{2+}$  responses (A-B) and average LysoTracker fluorescence responses (C-D) of fibroblasts stimulated with GPN (200  $\mu\text{M}$ ) after overnight treatment with DMSO (A and C) or Rab7 inhibitor (100  $\mu\text{M}$ ; B and D). LysoTracker fluorescence values have been normalised to basal values.

#### GPN-evoked complex $\text{Ca}^{2+}$ responses are VAP-independent

Through interactions with intermediate proteins, VAP is known to associate with Rab7 (Rocha et al., 2009). Furthermore, VAP proteins have been shown to anchor various organelles with the ER. To examine whether VAPs impair GPN-evoked  $\text{Ca}^{2+}$  signalling, siRNAs were used to silence both isoforms of VAP. Complex GPN-evoked  $\text{Ca}^{2+}$  signals were maintained upon VAP silencing (figures 3.4A-D) despite an 80% reduction in VAP protein levels (figure 3.4E).

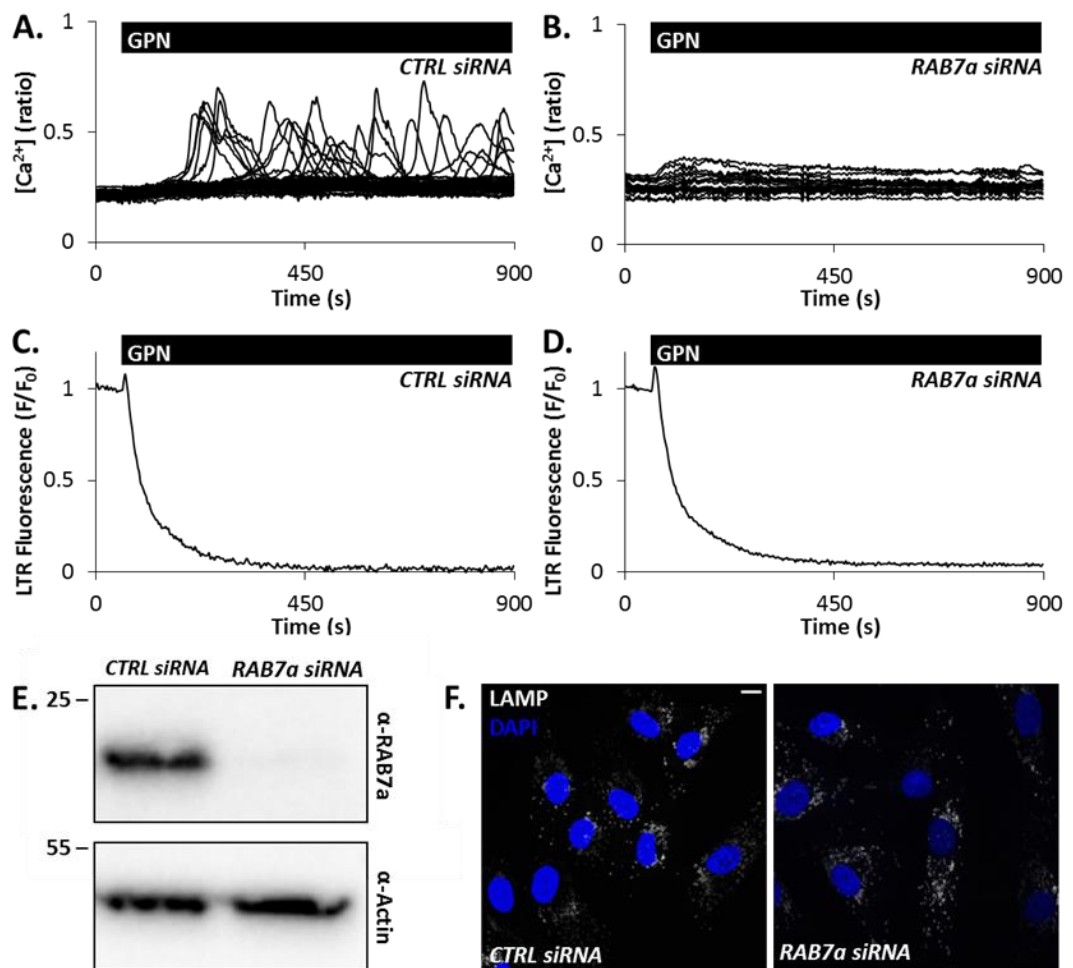


**Figure 3.2 GPN-evoked complex  $\text{Ca}^{2+}$  responses are Rab7-dependent**

(A-D) Individual cytosolic  $\text{Ca}^{2+}$  responses (A-B) and average Lysotracker fluorescence responses (C-D) of fibroblasts stimulated with GPN (200  $\mu\text{M}$ ) after treatment with CTRL siRNA (A and C) or RAB7a siRNA (B and D). Lysotracker fluorescence values have been normalised to basal values.

(E) Western blot using antibodies to RAB7a (top) or actin (bottom) and homogenates (14  $\mu\text{g}$ ) from fibroblasts treated with the indicated siRNA.

(F) Representative confocal images of LAMP1 (white) staining in fibroblasts fixed after treatment with CTRL siRNA or RAB7a siRNA. Nuclei were stained using DAPI (blue). Scale bar, 10  $\mu\text{m}$ .

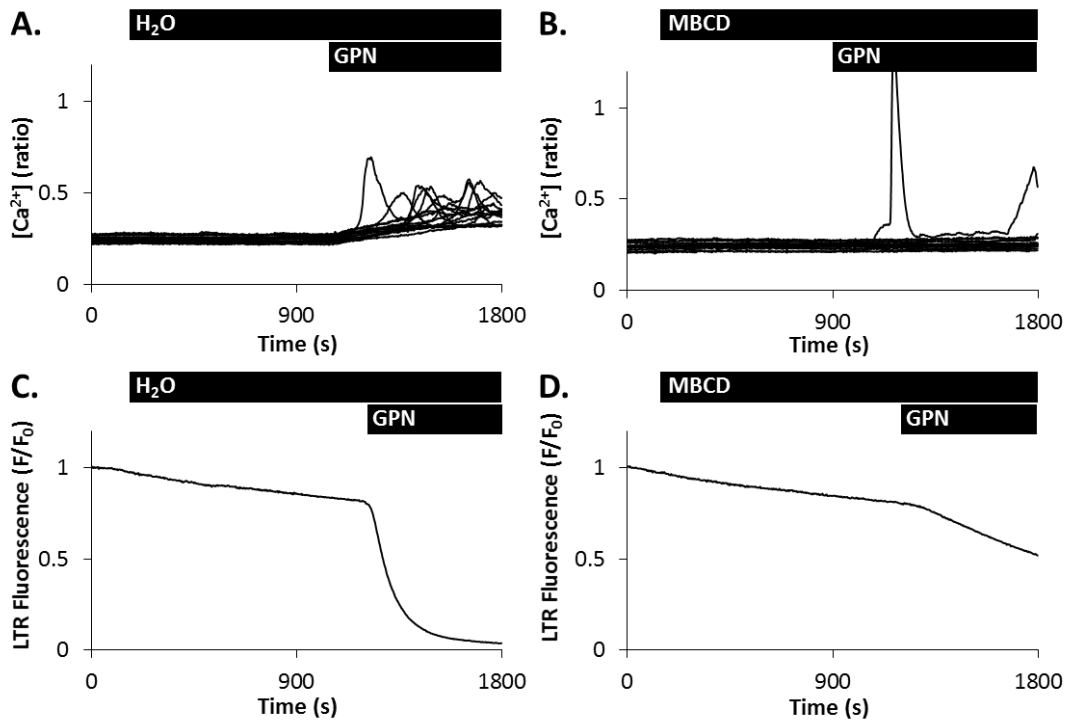


**Figure 3.3 GPN-evoked  $\text{Ca}^{2+}$  signals and permeabilisation are cholesterol-dependent**

(A-D) Individual cytosolic  $\text{Ca}^{2+}$  responses (A-B) and average Lysotracker fluorescence responses (C-D) of fibroblasts stimulated with GPN (200  $\mu\text{M}$ ) after pre-treatment with either  $\text{H}_2\text{O}$  (A and C) or MBCD (10 mM; B and D). Lysotracker fluorescence values have been normalised to basal values.

#### ML-SA1 evokes complex $\text{Ca}^{2+}$ signals

Although established as a  $\text{Ca}^{2+}$  permeable ion channel, little is known regarding TRPML  $\text{Ca}^{2+}$  signalling. I took advantage of a recently developed synthetic agonist of TRPML called ML-SA1 (Shen et al., 2012) to examine  $\text{Ca}^{2+}$  responses in fibroblasts. As shown in figure 3.5, ML-SA1 evoked robust, complex  $\text{Ca}^{2+}$  responses. Furthermore, ML-SA1 responses were concentration dependent. The magnitude, area under the curve and percentage of responsive cells are quantified in figures 3.5E-G. At 200  $\mu\text{M}$  (figure 3.5D), ML-SA1 stimulated oscillatory  $\text{Ca}^{2+}$  responses. Among the 72 cells analysed,  $45 \pm 4\%$  ( $n = 4$ ) displayed oscillatory  $\text{Ca}^{2+}$  signals.

Lysosome integrity after ML-SA1 stimulation was examined using Lysotracker red. The addition of ML-SA1 did not decrease Lysotracker fluorescence (figure 3.5H). As expected, GPN induced a prompt loss of Lysotracker red fluorescence (figure 3.5H).

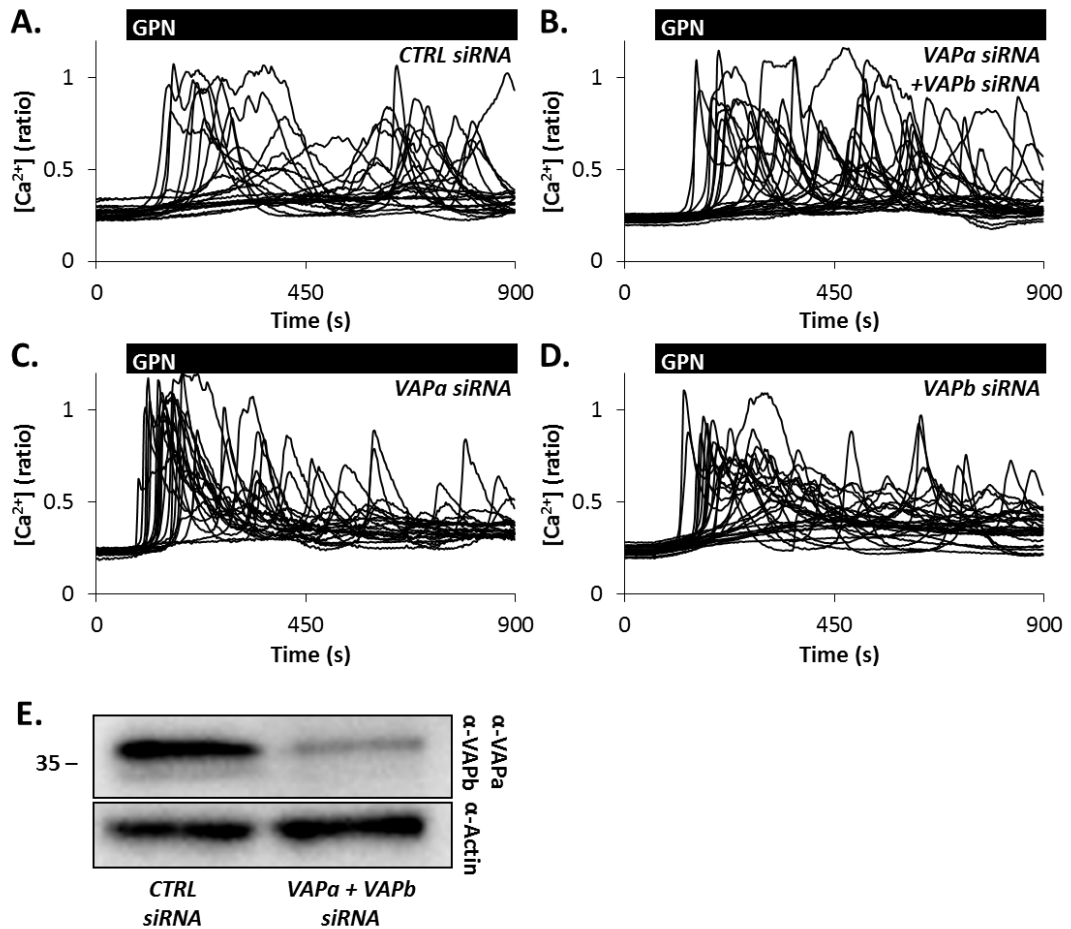


**Figure 3.4 GPN-evoked complex  $Ca^{2+}$  responses are VAP-independent**

(A-D) Representative cytosolic  $Ca^{2+}$  responses of individual fibroblasts stimulated with GPN (200  $\mu$ M) after treatment with CTRL (A), VAPa and VAPb siRNA (B), VAPa (C) or VAPb (D).

(E) Western blot using antibodies to VAPa and VAPb (top) or actin (bottom) and homogenates (30  $\mu$ g) from fibroblasts treated with the indicated siRNA.

#### ML-SA1-evoked $Ca^{2+}$ responses are dependent upon acidic organelles and ER- $Ca^{2+}$

The role of lysosomes in ML-SA1-evoked  $Ca^{2+}$  responses was examined by pre-stimulating cells with ammonium chloride ( $NH_4Cl$ ).  $NH_4Cl$  dissipates the lysosomal proton gradient and causes significant dysfunction to these acidic organelles (de Duve et al., 1974).  $NH_4Cl$  itself induced transient  $Ca^{2+}$  signal and  $NH_4Cl$  inhibited ML-SA1 signalling (figure 3.6A-B).

To further investigate the complex nature of ML-SA1-induced  $Ca^{2+}$  responses, the contribution of ER  $Ca^{2+}$  to these signals was examined. Fibroblasts were incubated with thapsigargin as well as  $IP_3R$  and RyR antagonists prior to ML-SA1 stimulation. As shown in figure 3.6, ML-SA1 evoked  $Ca^{2+}$  responses were completely inhibited in the presence of thapsigargin and 2-APB (which inhibits  $IP_3R$ ). Although ML-SA1-induced  $Ca^{2+}$  signals persisted upon treatment with Ryanodine (a RyR inhibitor),  $Ca^{2+}$  responses appeared delayed (figure

3.6F). Notably, these experiments were conducted in the absence of extracellular  $\text{Ca}^{2+}$  demonstrating ML-SA1 responses do not rely upon  $\text{Ca}^{2+}$  influx.

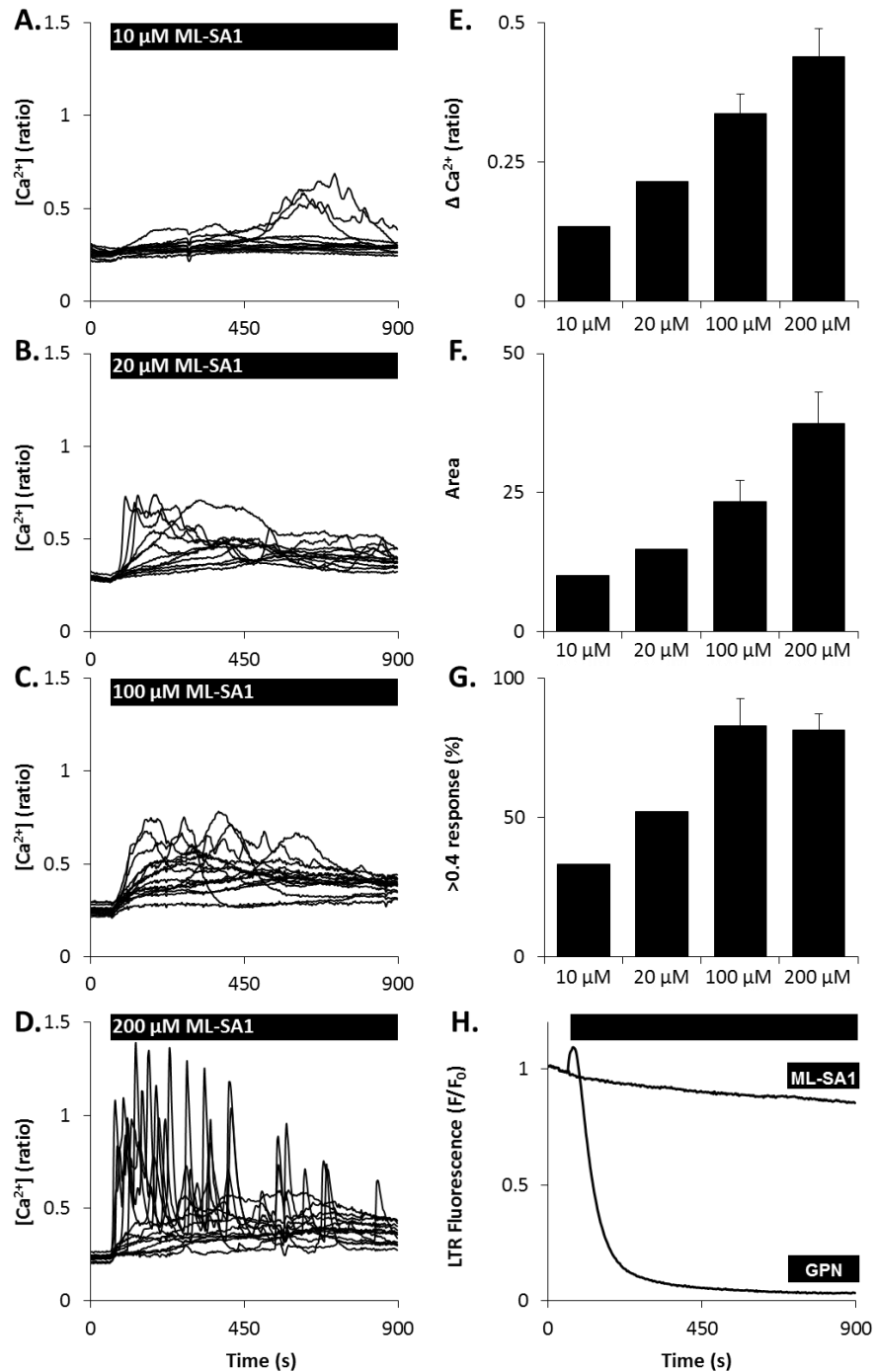


**Figure 3.5 ML-SA1 evokes complex  $\text{Ca}^{2+}$  signals**

(A-E) Cytosolic  $\text{Ca}^{2+}$  responses of fibroblasts after stimulation with ML-SA1 (10, 20, 100 and 200  $\mu\text{M}$ ).

(E-G) Summary data (mean  $\pm$  S.E.M) quantifying magnitude of  $\text{Ca}^{2+}$  response (E), area under the  $\text{Ca}^{2+}$  curve (F) and percentage of responding cells (defined by  $>0.4$  ratio value; G) after ML-SA1 stimulation. Results are from 2-4 independent platings ( $n$ ) analysing 30-72 cells.

(H) Average Lysotracker fluorescence responses (C-D) of fibroblasts stimulated GPN (200  $\mu\text{M}$ ) and ML-SA1 (100  $\mu\text{M}$ ). Fluorescence values have been normalised to basal values.

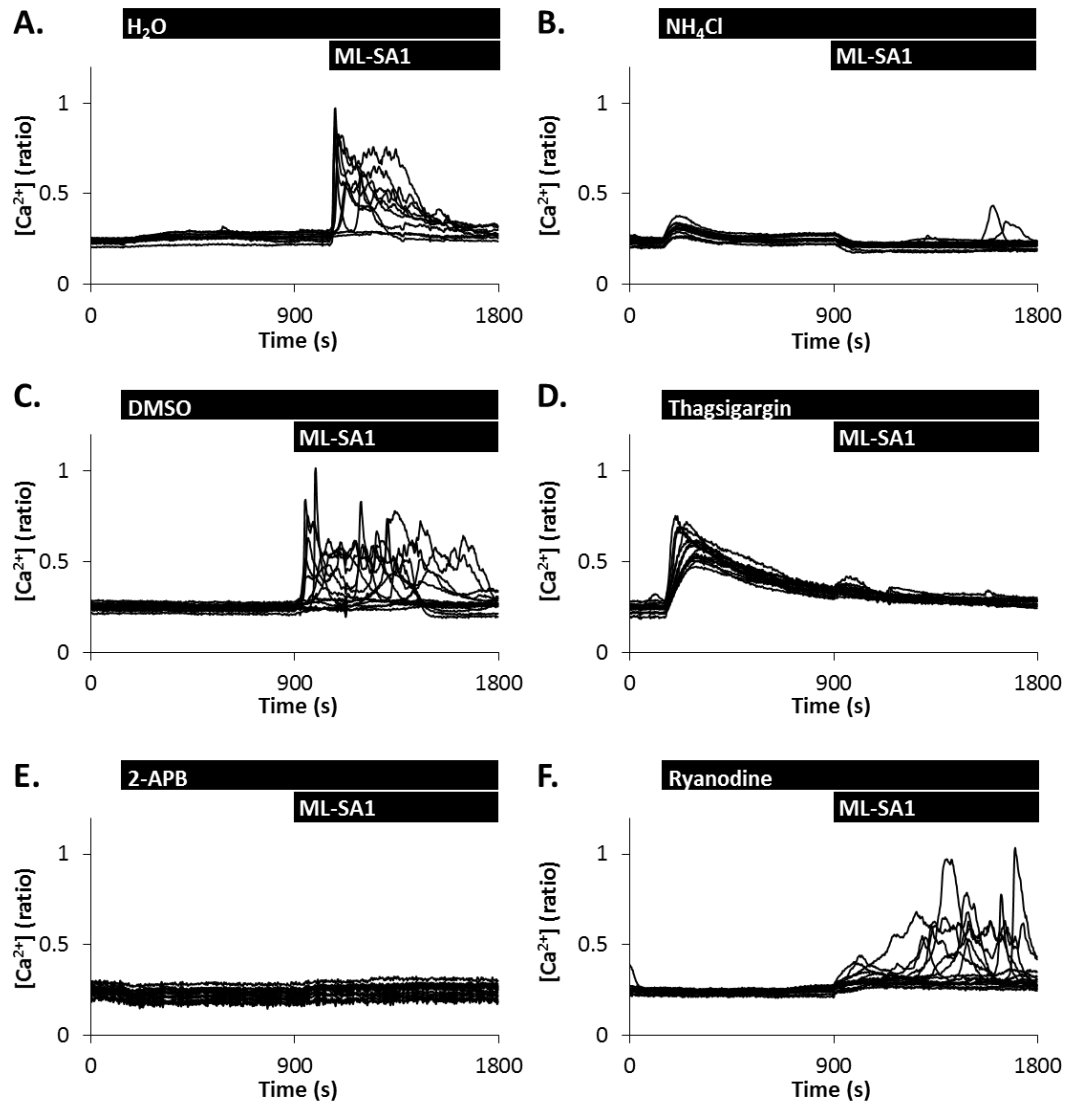


**Figure 3.6 ML-SA1-evoked  $\text{Ca}^{2+}$  responses are dependent upon acidic organelles and ER- $\text{Ca}^{2+}$**   
 (A-F) Cytosolic  $\text{Ca}^{2+}$  responses of individual fibroblasts stimulated with ML-SA1 (200  $\mu\text{M}$ ) after pre-treatment with either  $\text{H}_2\text{O}$  (A),  $\text{NH}_4\text{Cl}$  (100 mM; B), DMSO (C), thapsigargin (1  $\mu\text{M}$ ; D), 2-APB (100  $\mu\text{M}$ ; E) or ryanodine (100  $\mu\text{M}$ ; F). C-F were conducted in the absence of extracellular  $\text{Ca}^{2+}$ .

## Discussion

I have already established that the direct permeabilisation of lysosomes, with GPN, evokes complex  $\text{Ca}^{2+}$  signals (chapter 2). In this chapter I demonstrate that Rab7, a known mediator of late-endosome-ER MCSs, disrupts GPN-evoked  $\text{Ca}^{2+}$  signals. Although Rab7 is known to interact with VAPs at late-endosome-ER MCSs, VAPs do not appear to mediate lysosome-ER  $\text{Ca}^{2+}$  coupling. Additionally, I show that the activation of TRPML channels, using a synthetic agonist, induces complex  $\text{Ca}^{2+}$  signals that require ER  $\text{Ca}^{2+}$  channels. These responses are similar to those induced by both NAADP (Brailoiu et al., 2009b) and GPN (chapter 2). Thus,



the Ca<sup>2+</sup> “chatter” between the ER and lysosomes can be recapitulated upon TRPML activation and might occur through a mechanism that is Rab7-dependent.

As well as co-ordinating transport of late-endosomes and lysosomes, Rab7 regulates neuronal migration, neurite outgrowth, apoptosis and autophagy (reviewed in Bucci & De Luca 2012). Through interactions with cholesterol sensing proteins, Rab7 associates with VAP to stabilise late endosomes with the ER (Rocha et al., 2009). It was hypothesised that similar components might also mediate lysosome-ER junctions and impact lysosomal Ca<sup>2+</sup> signalling. Indeed, results demonstrated that the chemical and molecular inhibition of Rab7 suppressed complex, GPN-evoked Ca<sup>2+</sup> responses and functionally uncoupled lysosome-ER signalling (Figure 3.1 and 3.2). However, transfection with VAP siRNA did not dampen GPN signalling (figure 3.4). Therefore, Rab7 might regulate ER-lysosome junctions but not through an interaction with VAP. The lack of VAP effect attests to the specificity of Rab7 inhibition. It is possible that since lysosomes are highly dynamic organelles, Rab7 might not be a component of MCSs but instead mediate the appropriate positioning of lysosomes to facilitate their Ca<sup>2+</sup> coupling. The examination of lysosome morphology (figure 3.2F) did not reveal any obvious changes in positioning. Nevertheless, MCSs after the pharmacological and molecular inhibition Rab7 require examination through electron microscopy.

It is notable that, mutations in Rab7 are associated with the neuropathic Charcot–Marie–Tooth type 2B disease (Bucci & De Luca, 2012). Furthermore, mutations in the gene encoding Rab7L (Rab7-like protein) are thought to increase the risk of PD (Tucci et al., 2010). Thus, the finding that Rab7 mediates functional Ca<sup>2+</sup>-connections between lysosomes and the ER could be pathologically relevant. The consequences for disease require further examination. Indeed, these neurodegenerative disorders could also be a valuable model to further investigate Rab7 regulated lysosome-ER Ca<sup>2+</sup> signalling.

We know little about the regulation lysosomal-ER MCSs, but this data shows that Rab7 might be involved. Identifying proteins that interact with Rab7 might reveal more regarding these MCSs. Notably, TPCs have recently been shown to associate with Rab7 (Lin-Moshier et al., 2014). Therefore, TPCs themselves might also form essential components of lysosome-ER junctions. GPN-evoked Ca<sup>2+</sup> signalling should be investigated in fibroblasts after exposure to Ned-19 (an NAADP antagonist; Naylor et al. 2009) and siRNAs that silence TPC expression. The recently published proteomic analysis of TPC interactors (Lin-Moshier et al., 2014) might identify other components of ER-lysosome contact sites. For instance, ATP1A1 (Na<sup>+</sup>/K<sup>+</sup> ATPase alpha-1 subunit) and MYH9 (myosin heavy chain 9) were found to associate with TPCs

(Lin-Moshier et al., 2014). These proteins also interact with IP<sub>3</sub>Rs (Zhang et al., 2006; Walker et al., 2002). So perhaps ATP1A1 and MYH9 associate with both TPCs and IP<sub>3</sub>Rs within lysosome-ER junctions.

We could also learn more about these MCSs using research established in model organisms (Kvam & Goldfarb, 2006). For instance, in yeast, the nuclear envelope and vacuole form stable contacts with one another. Respectively, these organelles are the yeast equivalents of ER and lysosomes. Vac8 and NVJ1p are important components of these junctions, which function to deliver substrates for autophagic degradation (Pan et al., 2000). Perhaps the further examination of these yeast contacts and analogous mammalian proteins might reveal more concerning lysosome-ER junctions.

MCSs not only facilitate Ca<sup>2+</sup> signalling, but also lipid trafficking between various organelles. The effects of cholesterol on GPN-evoked Ca<sup>2+</sup> signalling were difficult to investigate in fibroblasts because MBCD inhibited GPN-induced lysosome permeabilisation (Figure 3.3). This might be because Cathepsin C (among other hydrolases) are cholesterol sensitive. The enzyme activity of lysosomal hydrolases is dependent upon the cholesterol/lysobisphosphatidic acid ratio on lysosomal membranes (Kolter & Sandhoff, 2005). Thus, by sequestering cholesterol, MBCD might affect the hydrolytic activity of Cathepsin C and the capacity for GPN to permeabilise lysosomes. To avoid this problem and still examine the impact cholesterol has on Ca<sup>2+</sup> coupling, the effect MBCD has on ML-SA1 and NAADP signalling should be investigated.

Lysosome-ER junctions likely promote the coupling of lysosome-ER Ca<sup>2+</sup> stores. It has been well established that NAADP-selective Ca<sup>2+</sup> channels are functionally coupled to the ER. Although it has been 10 years since TRPMLs were proposed to be Ca<sup>2+</sup> channels (Piper & Luzio, 2004), we know relatively little about TRPML signalling. Even the Ca<sup>2+</sup> permeability of this channel has been questioned (Kiselyov et al., 2005). Using the recently developed synthetic agonist of TRPML named ML-SA1 (Shen et al., 2012), Ca<sup>2+</sup> signals were examined in fibroblasts (Figure 3.5). ML-SA1 evoked robust Ca<sup>2+</sup> responses that were concentration dependent and strikingly similar to those induced by GPN. Notably, after stimulation with ML-SA1 the percentage of cells displaying Ca<sup>2+</sup> oscillations was 45±4%, this is remarkably similar to signals evoked by GPN where 45±3% of fibroblasts were oscillatory (chapter 2). However, unlike GPN, ML-SA1 did not induce lysosome membrane permeabilisation.

ML-SA1-evoked  $\text{Ca}^{2+}$  responses are likely of lysosomal origin since they were blocked by alkalinisation of acidic organelles with  $\text{NH}_4\text{Cl}$  (Figure 3.6). However, inducing such a significant change in cytosolic pH is bound to have many off-target effects. Thus, examining ML-SA1 responses after exposure to bafilomycin is essential. Furthermore, since siRNA transfection has proven so effective in fibroblasts, knocking down TRPMLs is necessary to assess the specificity of ML-SA1.

Contrary to GPN-evoked  $\text{Ca}^{2+}$  responses, ML-SA1 signalling was completely inhibited in fibroblasts incubated with thapsigargin and 2-APB (Figure 3.6). Perhaps release of  $\text{Ca}^{2+}$  by ML-SA1 is smaller than can be detected with Fura-2. This is similar to the findings reported by Cancela and colleagues (1999) where NAADP signalling was completely blocked upon  $\text{IP}_3\text{R}$  and RyR inhibition. Although ML-SA1 responses persist after the inhibition of ryanodine receptors, signals are delayed. Thus, TRPML signalling requires ER- $\text{IP}_3$  (and to a lesser extent ryanodine) receptors. To the best of my knowledge, this is the first report showing the functional coupling of TRPML channels with the ER.

The development of ML-SA1 provides many opportunities to investigate  $\text{Ca}^{2+}$  signalling. Functional coupling between TRPML and ER calcium channels should be further characterised by adapting the research that established NAADP-ER “chatter”. Namely, uncoupling the channels by targeting overexpressed TRPML to the plasma membrane and analysing  $\text{Ca}^{2+}$  responses.

Further characterisation of TRPML-mediated  $\text{Ca}^{2+}$  signalling is of significant importance to disease. The lysosomal storage disorder MLIV (mucopolysaccharidosis IV) is associated with mutations in TRPML1, which renders the  $\text{Ca}^{2+}$  channel inactive. Indeed in electrophysiological assays, ML-SA1 cannot evoke a cation current in patch-clamped MLIV lysosomes (Shen et al., 2012). This validates the specificity of ML-SA1 and highlights the disrupted  $\text{Ca}^{2+}$  signalling present in this disease.

NPC (Neimann Pick Type C1; another LSD) has also been associated with reduced ML-SA1 signalling (Shen et al., 2012). NPC is clinically characterised by an accumulation of cholesterol and sphingosine. U-18666A, a compound which induces cholesterol accumulation and recapitulates NPC phenotypes (Lloyd-Evans et al., 2008), disrupts late endosome-ER junctions (Rocha et al., 2009). Rocha and colleagues (2009) have shown that, through interactions with ORP1L, silencing NPC1 induces late endosome clustering. Perhaps, NPC mutations disrupt lysosome-ER junctions which then impair NAADP- (Lloyd-Evans et al., 2008), ML-SA1- (Shen et

al., 2012) and GPN- (Lloyd-Evans et al., 2008; Visentin et al., 2013) evoked Ca<sup>2+</sup> signalling. Crucially, lysosome-ER MCSs require characterisation in NPC disease.

Rab7 might also associate with TRPML (like TPCs) to regulate signalling. Although direct association between TRPML and Rabs have yet to be identified. TRPML2 has been shown to associate with the another GTPase trafficking protein – Arf6 (Karacsonyi et al., 2007). Examining MLSA1-evoked Ca<sup>2+</sup> signalling after Rab7 inhibition is critical. TRPMLs and their endogenous ligand PI(3,5)P<sub>2</sub> are also involved in trafficking (Cheng et al., 2010). Therefore, similar to Rab7, TRPML signalling might regulate the positioning of acidic Ca<sup>2+</sup> stores with ER Ca<sup>2+</sup> channels. I could verify this hypothesis by inhibiting the synthesis of PI(3,5)P<sub>2</sub> with YM-201636 (Jefferies et al., 2008) or transfecting cells with siRNAs against TRPML

In summary, I have established that lysosomal Ca<sup>2+</sup> release triggers complex, ER-regulated Ca<sup>2+</sup> signalling. Although we still have an incomplete understanding of the mechanism that regulates lysosome-ER Ca<sup>2+</sup> coupling, the trafficking GTPase Rab7 is likely involved. Like late-endosomes, Rab7 might regulate the formation of MCSs and facilitate Ca<sup>2+</sup> exchange. Although, unlike many other MCSs, VAPs are not necessary for the functional coupling between lysosomes and the ER. Additionally, I have shown that this Ca<sup>2+</sup> coupling can be physiologically recapitulated upon the activation TPRML channels. These findings have wider significance for diseases including LSDs and neurodegenerative disorders.

# Chapter 4

---

## Defective Calcium Signalling in Parkinson Disease: Clues from a Lysosomal Storage Disorder

### Introduction

Mutations in *GBA1*, the gene which encodes the lysosomal enzyme glucocerebrosidase (GCase), that is impaired in GD, have been identified as the most frequent genetic risk factor for PD (Sidransky & Lopez, 2012; Sidransky et al., 2009). These mutations cause an accumulation of mis-folded enzyme on the ER (Ron & Horowitz, 2005), and subsequent build-up of substrate in the lysosomes. Despite a clear genetic association between GD and PD, less is known regarding the physiological mechanisms that connect these two diseases.

The co-ordination of intracellular  $\text{Ca}^{2+}$  stores is necessary for cellular  $\text{Ca}^{2+}$  signalling. Lysosomes have been shown to “trigger” complex  $\text{Ca}^{2+}$  signals that require neighbouring ER  $\text{Ca}^{2+}$  channels (Cancela et al. 1999; Kilpatrick et al. 2013; chapters 2 and 3). ER-derived  $\text{Ca}^{2+}$  signals are ultimately transmitted to the mitochondria (Rizzuto et al., 1998). Thus, stores operate as an inter-connected network and defects, in any component of this pathway, will impinge on  $\text{Ca}^{2+}$  homeostasis. Indeed, emerging evidence shows that dysfunctional  $\text{Ca}^{2+}$  signalling features in neurodegenerative diseases including PD and GD (Chan et al., 2007; Guzman et al., 2010; Korkotian et al., 1999; Lloyd-Evans et al., 2003; Pelled et al., 2005).

$\text{Ca}^{2+}$  has an important role in PD since the dopaminergic neurons of the SNc are dependent upon VGCC for pacemaking activity (Chan et al., 2007). This  $\text{Ca}^{2+}$  entry, is a unique feature of these neurons and imposes significant energetic stress, which might render them vulnerable to degeneration (Guzman et al., 2010). This highlights the possibility that any other disturbance in  $\text{Ca}^{2+}$  homeostasis is likely to advance the onset of PD. Notably, disturbed ER  $\text{Ca}^{2+}$  signalling has been identified in various models of GD. For instance, both neuronal cultures (Korkotian et al., 1999) and microsome preparations (Pelled et al., 2005; Lloyd-Evans et al., 2003) exposed to excess GCase substrate exhibit increased  $\text{Ca}^{2+}$  release through RyR.

The aim of this chapter is to examine whether intracellular  $\text{Ca}^{2+}$  storage dysregulation *connects* GD and PD using pharmacological, genetic and clinical cell models.

## Methods

### Cell details

Primary human fibroblasts (table 4.1), established from skin biopsies, were acquired by Dr Michelle Beavan, Dr Alisdair McNeill (Royal free hospital, UCL) and Dr Laura Osellame (Department of Cell and Developmental Biology, UCL).

Dopaminergic SH-SY5Y cells with the stable knock down of *GBA1* were created by Dr Michael Cleeter (Cleeter et al., 2012). Briefly, SH-SY5Ys were transfected with either a scrambled control or a “hush” *GBA1* knockdown plasmid and successfully transfected cells were selected for using puromycin.

Mixed primary neuronal cultures were prepared from the brains of a neuronopathic mouse model of GD at postnatal day 1 by Dr Laura Osellame (Department of Cell and Developmental Biology, UCL). In this mouse model (developed by Enquist et al., 2007) the insertion of a loxp-neo-loxp (Inl) cassette, under K14 (keratin) promoter (via cre recombinase), into the *GBA1* gene silenced expression in all locations except the skin. Pups were derived from heterozygote parents and kindly genotyped by Dr Laura Osellame (as described in Osellame et al. 2013). Neuronal cultures were isolated from wild-type (*GBA1*<sup>+/+</sup>) and *GBA1* knockout mice (*GBA1*<sup>-/-</sup>) and cultured for 8 days before analysis.

*GBA1*-overexpression was done by Dr Joana Magalhaes (Royal free hospital). Briefly, cDNA coding wild-type and mutant (N370S) *GBA1* were cloned into lentiviral transfer vectors. SH-SY5Y cells were seeded in 24 well plates (5x10<sup>4</sup> cells/well). The following day, cells were treated with polybrene (8 ug/mL, Millipore) for 2 hours then transduced with the *GBA1* lentivirus (Multiplicity of infection = 2). 24 hours after transduction, media was replaced with fresh complete media. Cells were incubated for a further 2 days before analysis.

### Cell culture

Fibroblast, SH-SY5Y and neuronal cultures were maintained as described in chapter 2.

In some experiments, fibroblasts and SH-SY5Y cells were incubated for 8-11 days with 10 μM of the irreversible GCCase inhibitor, Condurotol B Epoxide (CBE, Sigma-Aldrich) prepared in H<sub>2</sub>O. Fibroblasts were fed fresh media, containing CBE, every 5 days. SH-SY5Y media was replenished every 2-3 days also with CBE.

All cultures were analysed in parallel and fibroblast passages differed by no more than 2. Prior to experimentation, cells were plated onto glass coverslips (for Ca<sup>2+</sup> imaging and confocal microscopy) or directly into tissue culture flasks (for western blotting).

## Ca<sup>2+</sup> imaging

Ca<sup>2+</sup> imaging was performed as described in chapter 2. In some experiments cells were stimulated with thapsigargin (1  $\mu$ M; Merck) or 25  $\mu$ M cADPR-AM (from Dr Grant Churchill, Department of Pharmacology, University of Oxford). Where indicated, extracellular Ca<sup>2+</sup> was removed using a modified HBS solution containing 1 mM EGTA instead of Ca<sup>2+</sup>. For some SH-SY5Y cultures, cells were washed with EGTA-containing HBS and stimulated with thapsigargin using a perfusion system.

## Western Blotting

Western blotting was conducted as described in chapter 3. Blots were sequentially incubated with the primary anti-GBA1 (overnight at 4 °C, diluted 1:500, EMD Millipore) antibody and secondary anti-mouse (1 hour at room temperature, 1:2000, Santa Cruz Biotechnology) antibody.

## Recurrent methods

Lysotracker imaging, LAMP1 immunocytochemistry, analysis, epifluorescence and confocal microscopy were performed as described in chapter 2.

**Table 4.1.** Details of patient-derived fibroblast cultures.

| Category | Patient ID<br>(Genotype <sub>Age</sub> Phenotype) | Sex    | Age | Genotype            | Clinical features       |
|----------|---|--------|-----|---------------------|-------------------------|
| Young    | <i>GBA1</i> <sup>+/+</sup> <sub>55</sub>          | Female | 55  | WT/WT               | Apparently healthy      |
|          | <i>GBA1</i> <sup>-/-</sup> <sub>55</sub> GD       | Male   | 55  | N370S/<br>1263del55 | Type I Gaucher Disease  |
|          | <i>GBA1</i> <sup>+/-</sup> <sub>55</sub> PD       | Female | 55  | N370S/WT            | Parkinson Disease       |
|          | <i>GBA1</i> <sup>+/-</sup> <sub>58</sub> ASX      | Male   | 58  | N370S/WT            | Non-manifesting carrier |
|          | <i>GBA1</i> <sup>+/-</sup> <sub>59</sub> ASX      | Female | 59  | N370S/WT            | Non-manifesting carrier |
| Aged     | <i>GBA1</i> <sup>+/+</sup> <sub>70</sub>          | Female | 70  | WT/WT               | Apparently healthy      |
|          | <i>GBA1</i> <sup>+/+</sup> <sub>78</sub>          | Male   | 78  | WT/WT               | Apparently healthy      |
|          | <i>GBA1</i> <sup>+/-</sup> <sub>75</sub> PD       | Female | 75  | N370S/WT            | Parkinson Disease       |
|          | <i>GBA1</i> <sup>+/+</sup> <sub>82</sub>          | Female | 82  | WT/WT               | Apparently healthy      |
|          | <i>GBA1</i> <sup>+/-</sup> <sub>80</sub> ASX      | Female | 80  | N370S/WT            | Non-manifesting carrier |

## Results

### Establishing fibroblast cultures from individuals carrying the N370S mutation in *GBA1*

To examine whether GD and *GBA1*-PD pathology is associated with impaired Ca<sup>2+</sup> signalling, primary fibroblast cultures were generated from skin biopsies of patients suffering from GD and PD. Both carried the N370S allele, however the GD patient was a compound

heterozygote with an additional 1263del55 mutation. For simplicity, these genotypes will be referred to as  $GBA1^{-/-GD}$  and  $GBA1^{+/-PD}$ , respectively. Cultures were also established from asymptomatic (ASX), non-manifesting  $GBA1$  carriers ( $GBA1^{+/-ASX}$ ). For control purposes, fibroblasts were acquired from age-matched, apparently healthy individuals without mutations in  $GBA1$  ( $GBA1^{+/+}$ ). The fibroblast cultures were categorised according to age. The “young” fibroblasts were obtained from individuals under the age of 60 whereas the “aged” fibroblasts were derived from individuals over 70 years old. Additional details of the fibroblasts, including patient codes, are provided in table 4.1.

#### ER $Ca^{2+}$ content is increased in *young* GD and $GBA1$ -PD fibroblasts

Since previous research has reported increased ER  $Ca^{2+}$  release in GD models (Korkotian et al., 1999; Lloyd-Evans et al., 2003; Pelled et al., 2005) ER  $Ca^{2+}$  content was examined in patient fibroblast cultures by measuring cytosolic  $Ca^{2+}$  in responses to 1  $\mu$ M thapsigargin. Thapsigargin inhibits SERCA ATPase activity and depletes ER  $Ca^{2+}$ . This allows a good (although indirect) estimation of ER  $Ca^{2+}$  content to be obtained. Thapsigargin stimulated transient  $Ca^{2+}$  responses (Figure 4.1A), consistent with revealing the ER  $Ca^{2+}$  leak pathway. These thapsigargin-evoked  $Ca^{2+}$  responses were significantly elevated in  $GBA1^{-/-55GD}$  and in  $GBA1^{+/-55PD}$  when compared to fibroblasts from an age-matched healthy individual ( $GBA1^{+/+55}$ ; Figure 4.1B).

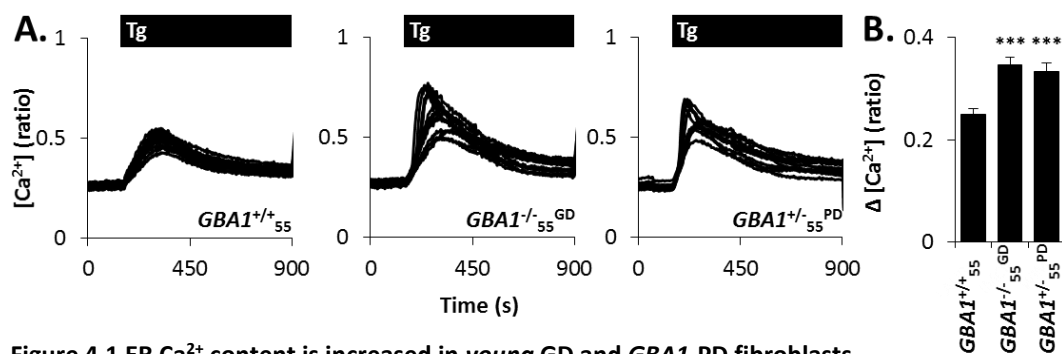


**Figure 4.1 ER  $Ca^{2+}$  content is increased in *young* GD and  $GBA1$ -PD fibroblasts**

(A) Cytosolic  $Ca^{2+}$  responses of individual fibroblasts stimulated with thapsigargin (Tg; 1  $\mu$ M) from a representative population of  $GBA1^{+/+55}$ ,  $GBA1^{-/-55GD}$  and  $GBA1^{+/-55PD}$  cells. All experiments were performed in the absence of extracellular  $Ca^{2+}$ .

(B) Summary data (mean  $\pm$  S.E.M) quantifying the magnitude of thapsigargin response. Results are from 11-26 experiments ( $n$ ) from 5-9 independent platings analysing 154-367 cells. ANOVA analysis, followed by a post-hoc Tukey test, was applied to test significance against  $GBA1^{+/+55}$ . \*\*\* $p < 0.001$ .

#### Messenger-evoked ER $Ca^{2+}$ release is increased in *young* GD and $GBA1$ -PD fibroblasts

To examine the consequences of disrupted ER  $Ca^{2+}$  content on physiological  $Ca^{2+}$  signalling, fibroblasts were stimulated with cADPR-AM (a cell-permeable derivative of the intracellular



Ca<sup>2+</sup>-mobilising messenger cyclic-ADP ribose; Rosen et al. 2012). The addition of 25 μM cADPR-AM evoked complex Ca<sup>2+</sup> responses in fibroblasts (Figure 4.2A). The magnitude of Ca<sup>2+</sup> response (Figure 4.2B), percentage of responsive cells (Figure 4.2C) and area under the curve (Figure 4.2C) were increased in *GBA1*<sup>+/-</sup><sub>55</sub><sup>PD</sup> fibroblasts compared to fibroblasts from an age-matched healthy individual. Modest, increases in cADPR-AM-evoked Ca<sup>2+</sup> responses were also apparent in *GBA1*<sup>-/-</sup><sub>55</sub><sup>GD</sup> cultures (Figure 4.2A-C) compared to *GBA1*<sup>+/-</sup><sub>55</sub> fibroblasts.

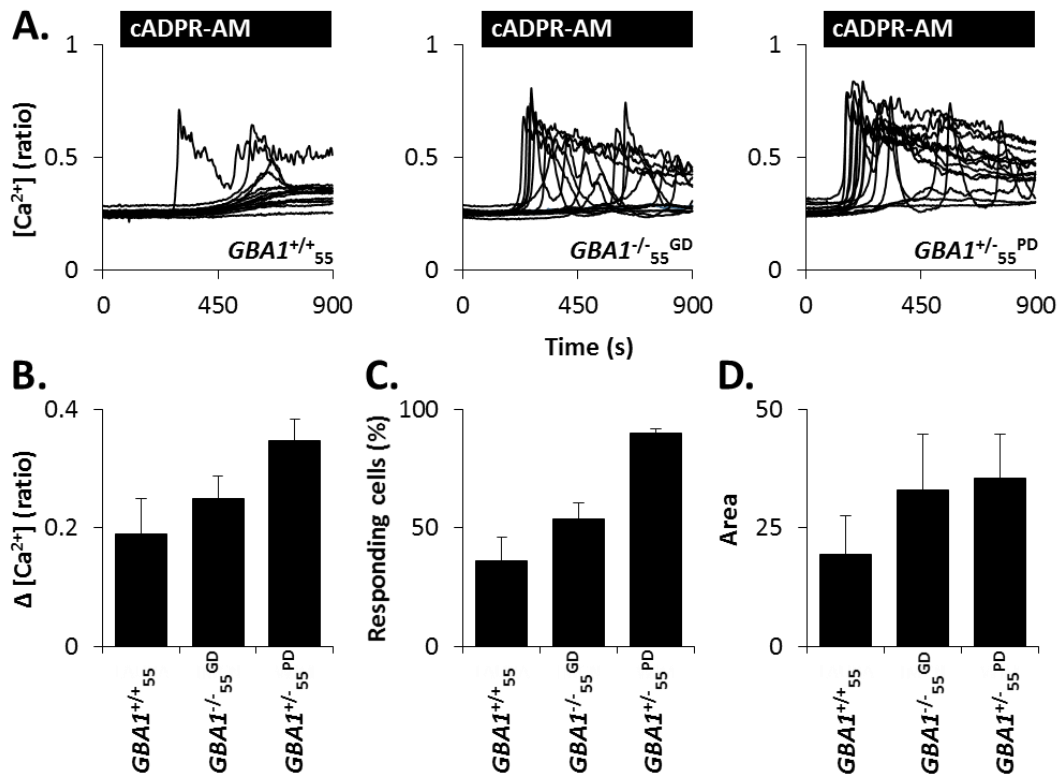


**Figure 4.2 Messenger-evoked ER Ca<sup>2+</sup> release is increased in young GD and *GBA1*-PD fibroblasts**

(A) Cytosolic Ca<sup>2+</sup> responses of individual fibroblasts stimulated with cADPR-AM (25 μM) from a representative population of *GBA1*<sup>+/-</sup><sub>55</sub>, *GBA1*<sup>-/-</sup><sub>55</sub><sup>GD</sup> and *GBA1*<sup>+/-</sup><sub>55</sub><sup>PD</sup> cells. All experiments were performed in the presence of extracellular Ca<sup>2+</sup>.

(B-D) Summary data (mean ± S.E.M) quantifying the magnitude of response (B), percentage of responsive cells (C) and area under the curve (D) after cADPR-AM stimulation. Results are from 3-5 experiments (*n*) from 2-3 independent platings analysing 39-75 cells.

#### ER Ca<sup>2+</sup> homeostasis is unaffected in young asymptomatic *GBA1*<sup>+/-</sup> fibroblasts

A significant proportion of individuals with mutations in *GBA1* never develop neurological conditions (Sidransky et al., 2009). I therefore examined ER Ca<sup>2+</sup> content in fibroblast cultures established from an asymptomatic individual with a heterozygotic mutation in *GBA1* (*GBA1*<sup>+/-</sup><sub>58</sub><sup>ASX</sup>). Although thapsigargin-evoked Ca<sup>2+</sup> responses appeared more heterogeneous in *GBA1*<sup>+/-</sup><sub>58</sub><sup>ASX</sup> fibroblasts when compared with control *GBA1*<sup>+/-</sup><sub>55</sub> fibroblasts (Figure 4.3A), the magnitude of Ca<sup>2+</sup> response (Figure 4.2B) did not differ between these cultures. Consistent

with data presented in figure 4.1, thapsigargin-evoked  $\text{Ca}^{2+}$  responses were significantly elevated in  $\text{GBA1}^{+/-55PD}$  fibroblasts compared to the controls.

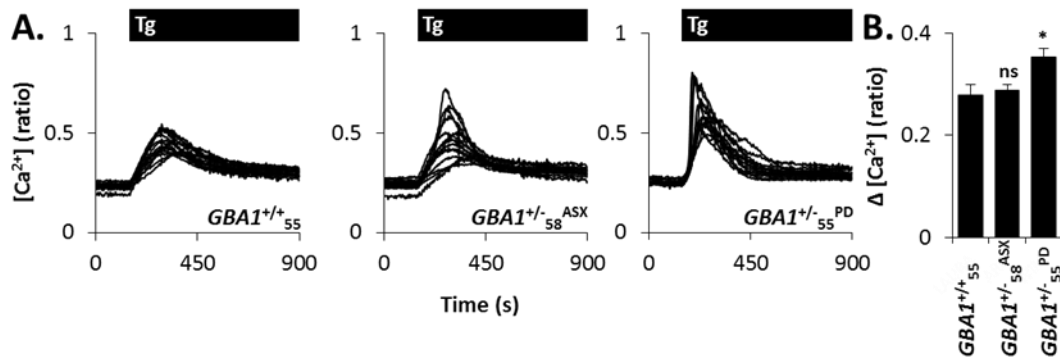


**Figure 4.3 ER  $\text{Ca}^{2+}$  homeostasis is unaffected in young asymptomatic  $\text{GBA1}^{+/-}$  fibroblasts**

(A) Cytosolic  $\text{Ca}^{2+}$  responses of individual fibroblasts stimulated with thapsigargin (Tg; 1  $\mu\text{M}$ ) from a representative population of  $\text{GBA1}^{+/+55}$ ,  $\text{GBA1}^{+/-58ASX}$  and  $\text{GBA1}^{+/-55PD}$  cells. All experiments were performed in the absence of extracellular  $\text{Ca}^{2+}$ .

(B) Summary data (mean  $\pm$  S.E.M) quantifying the magnitude of thapsigargin response. Results are from 3-4 experiments ( $n$ ) from 3-4 independent platings analysing 88-127 cells. ANOVA analysis, followed by a post-hoc Tukey test, was applied to test significance against  $\text{GBA1}^{+/+55}$ . \* $p < 0.05$ .

Similarly, as shown in figure 4.4, cADPR-AM-evoked  $\text{Ca}^{2+}$  responses in  $\text{GBA1}^{+/-58ASX}$  fibroblasts were not different from control  $\text{GBA1}^{+/+55}$  fibroblasts and lower than  $\text{GBA1}^{+/-55PD}$ .

#### ER $\text{Ca}^{2+}$ content is unaffected in aged $\text{GBA1}$ -PD fibroblasts

ER  $\text{Ca}^{2+}$  content in  $\text{GBA1}^{+/-PD}$  was further examined using fibroblasts from the aged cohort. Unlike the young  $\text{GBA1}^{+/-PD}$  fibroblasts, thapsigargin-evoked  $\text{Ca}^{2+}$  responses in  $\text{GBA1}^{+/-75PD}$  fibroblasts were similar to fibroblasts from the age-matched healthy control ( $\text{GBA1}^{+/+78}$ ) (Figure 4.5A-B). It is notable that thapsigargin responses in fibroblasts from both  $\text{GBA1}^{+/+78}$  and  $\text{GBA1}^{+/-75PD}$  were kinetically irregular and larger than signals evoked in fibroblasts from younger controls (Figure 4.1A and 4.3A).

#### ER $\text{Ca}^{2+}$ content increases in an age-dependent manner

I further investigated the effect of ageing on ER  $\text{Ca}^{2+}$  content using fibroblasts from healthy individuals of increasing age. As shown in figure 4.6, thapsigargin responses increased in an age-dependent manner in fibroblasts from  $\text{GBA1}^{+/+}$  individuals (Figure 4.6A-C). Thapsigargin signals in the oldest fibroblasts examined ( $\text{GBA1}^{+/+82}$ ) were kinetically distinct from responses evoked in the youngest control (Figure 4.6A). Thapsigargin-evoked  $\text{Ca}^{2+}$  responses in the oldest  $\text{GBA1}^{+/+}$  fibroblasts resembled those evoked in fibroblasts from young  $\text{GBA1}^{-/-GD}$  and  $\text{GBA1}^{+/-PD}$  individuals (Figure 4.6C).

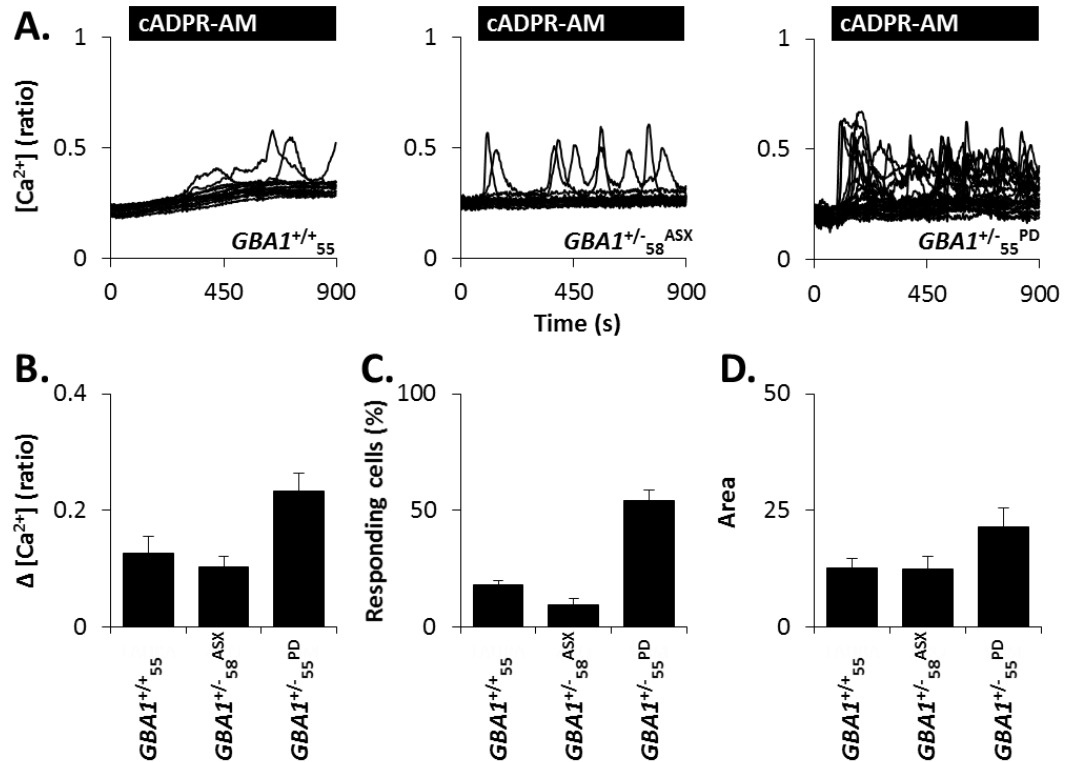


**Figure 4.4 Messenger-evoked ER Ca<sup>2+</sup> release is unaffected in *young* asymptomatic *GBA1*<sup>+/-</sup> fibroblasts**

(A) Cytosolic Ca<sup>2+</sup> responses of individual fibroblasts stimulated with cADPR-AM (25 μM) from a representative population of *GBA1*<sup>+/+</sup><sub>55</sub>, *GBA1*<sup>+/-</sup><sub>58</sub><sup>ASX</sup> and *GBA1*<sup>+/-</sup><sub>55</sub><sup>PD</sup> cells. All experiments were performed in the presence of extracellular Ca<sup>2+</sup>.

(B-D) Summary data (mean ± S.E.M) quantifying the magnitude of response (B) percentage of responsive cells (C) and area under the curve (D) after cADPR-AM stimulation. Results are from 4-13 experiments (*n*) from 3-6 independent platings analysing 73-257 cells.

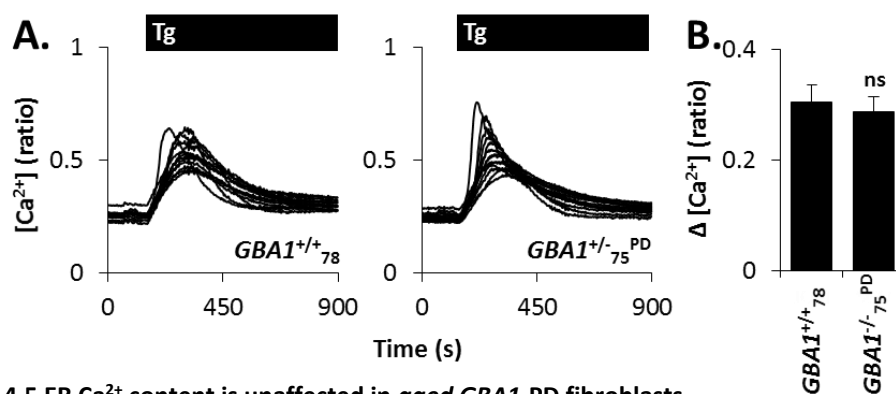


**Figure 4.5 ER Ca<sup>2+</sup> content is unaffected in *aged* *GBA1*-PD fibroblasts**

(A) Cytosolic Ca<sup>2+</sup> responses of individual fibroblasts stimulated with thapsigargin (Tg; 1 μM) from a representative population of *GBA1*<sup>+/+</sup><sub>78</sub>, *GBA1*<sup>+/-</sup><sub>75</sub><sup>PD</sup> cells. All experiments were performed in the absence of extracellular Ca<sup>2+</sup>.

(B) Summary data (mean ± S.E.M) quantifying the magnitude of thapsigargin response. Results are from 8 experiments (*n*) from 3 independent platings analysing cells 112-117 cells. A two-sample *t*-test was applied to test significance. ns, not significant.

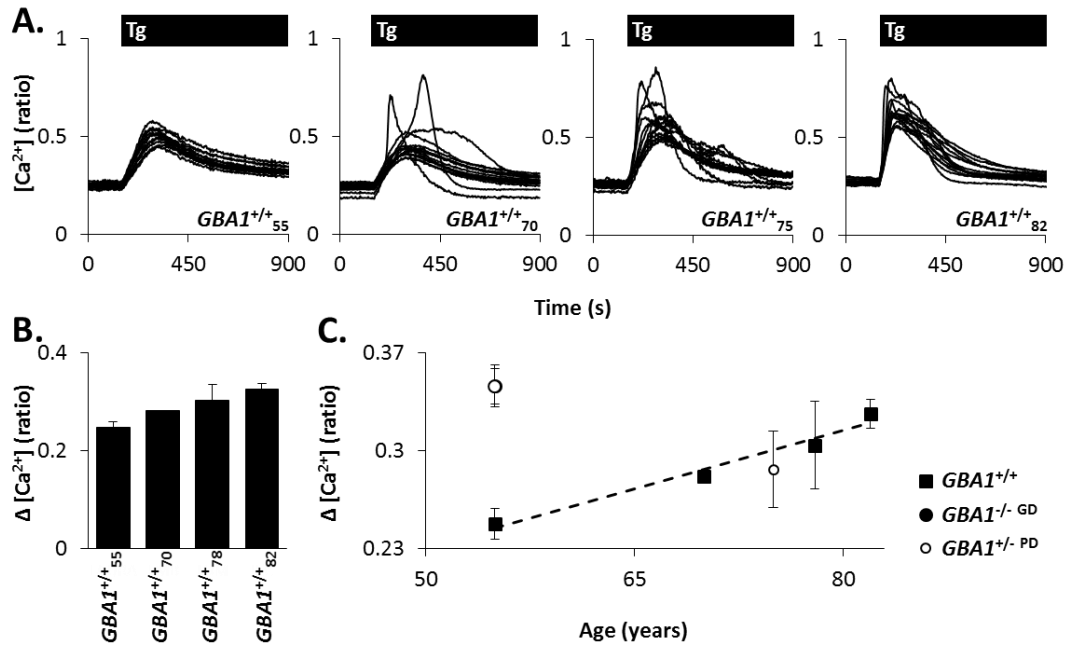


**Figure 4.6 ER  $Ca^{2+}$  content increases in an age-dependent manner**

(A) Cytosolic  $Ca^{2+}$  responses of individual fibroblasts stimulated with thapsigargin (Tg; 1  $\mu$ M) from a representative population of  $GBA1^{+/+}$  fibroblasts with increasing age (55, 70, 78 and 82 years). All experiments were performed in the absence of extracellular  $Ca^{2+}$ .

(B) Summary data (mean  $\pm$  S.E.M) quantifying the magnitude of thapsigargin response.

(C) Summary data (mean  $\pm$  S.E.M) plotting magnitude of thapsigargin response against age. The fitted line is  $y = 0.002786 + 0.09284 \chi$  ( $F = 15$ , d.f. = 1,47,  $p < 0.001$ ).

Results are from 2-30 experiments ( $n$ ) from 1-14 independent platings analysing 30-483 cells.

#### Inhibition of GCCase does not affect ER $Ca^{2+}$ homeostasis

Data thus far has identified an ER  $Ca^{2+}$  content defect in young patient fibroblasts carrying a *GBA1* mutation. However, the mechanism underlying this defect remains unknown. Since accumulating GCCase substrate might affect ER  $Ca^{2+}$  signalling (Lloyd-Evans et al., 2003), ER  $Ca^{2+}$  content was examined after reducing the activity of GCCase using pharmacological (Figure 4.7-4.8) and genetic (Figure 4.8-4.9) methods. Fibroblasts were chronically treated with a selective inhibitor of GCCase called Condurotol B epoxide (CBE; 10  $\mu$ M). Thapsigargin-induced  $Ca^{2+}$  responses after exposure to CBE were similar to the control (Figure 4.7A-B). The inhibition of GCCase was extended into a more neurologically-relevant model using a human dopaminergic SH-SY5Y cell line. Similar to the fibroblasts, treatment with CBE did not affect thapsigargin responses in SH-SY5Y cells (Figure 4.8A-C). Notably, thapsigargin-evoked  $Ca^{2+}$  responses are smaller in SH-SY5Y cells (Figure 4.8) compared to fibroblasts (Figure 4.7) making comparisons difficult. I therefore normalised thapsigargin responses, on a given day,

to the vehicle control. No increase in the percentage of thapsigargin response was observed between CBE and vehicle exposed SH-SY5Y cells (Figure 4.8C).

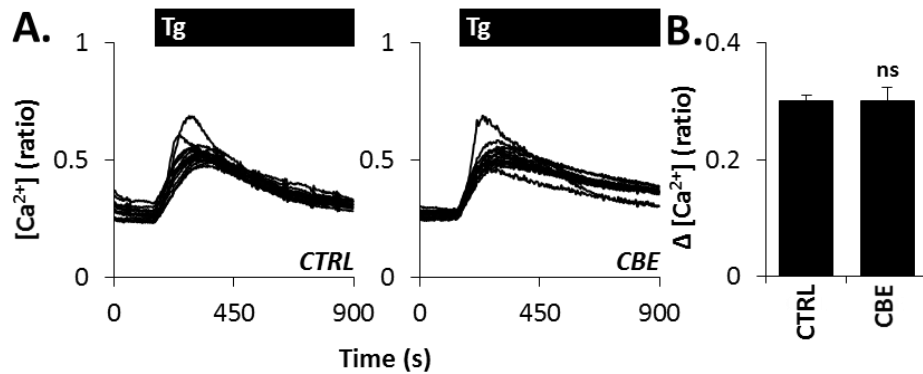


**Figure 4.7 Inhibition of GCase does not affect ER Ca<sup>2+</sup> homeostasis in fibroblasts**

(A) Cytosolic Ca<sup>2+</sup> responses of individual fibroblasts stimulated with thapsigargin (Tg; 1 μM) from a representative population of cells treated with 10 μM CBE for 8 days. All experiments were performed in the absence of extracellular Ca<sup>2+</sup>.

(H) Summary data (mean ± S.E.M) quantifying the magnitude of thapsigargin response in CBE treated fibroblasts. Results are from 6 experiments (*n*) from 2 independent treatments analysing 87-90 cells. A two-sample *t*-test was applied to test significance. ns, not significant.

These findings were further extended into molecular models of GCase inhibition (Figure 4.8) using SH-SY5Y cells with the stable, shRNA-mediated, genetic knockdown of *GBA1*. As shown in figure 4.8D-F, thapsigargin-evoked Ca<sup>2+</sup> responses in *GBA1*<sup>-/-</sup> cells were similar to those evoked in the parental cell line stably overexpressing scrambled shRNA (*GBA1*<sup>+/+</sup>). Western blot analysis indicated that GCase protein level was reduced by 56% ± 7 (*n* = 4) in *GBA1*<sup>-/-</sup> SH-SY5Y cells when compared to scrambled (*GBA1*<sup>+/+</sup>) controls (inset Figure 4.8F).

Finally, I examined thapsigargin-evoked Ca<sup>2+</sup> responses in a transgenic mouse model with a neuronopathic GD phenotype (see methods). Ca<sup>2+</sup> responses were analysed in cultures containing a mixed population of cortical cells (Figure 4.9A). Once again, no difference in magnitude of thapsigargin response was seen between W/T (*GBA1*<sup>+/+</sup>) and *GBA1* knockdown (*GBA1*<sup>-/-</sup>) neuronal cells (Figure 4.9B).

#### Overexpression of mutant *GBA1* partially impairs ER Ca<sup>2+</sup> homeostasis

Figures 4.7-4.9 present strong evidence that ER Ca<sup>2+</sup> dysfunction is not a result of reduced GCase enzyme activity. Thus, the alternative explanation that the retention of mutant enzyme at the ER (Ron & Horowitz, 2005) could cause a direct ER Ca<sup>2+</sup> dysfunction was tested. SH-SY5Y cells were infected with lentiviral vectors encoding wild-type and N370S mutated

*GBA1* (*GBA1*<sup>WT</sup> and *GBA1*<sup>N370S</sup> respectively) and thapsigargin responses were compared between cultures (Figure 4.10). The overexpression of *GBA1*<sup>N370S</sup> caused a modest (10%) increase in thapsigargin responses when compared to *GBA1*<sup>WT</sup> (Figure 4.10B-C). However, the effects of *GBA1*<sup>N370S</sup> may have been underestimated since transduction efficiency was low (approximately 40%) and *GBA1*<sup>N370S</sup> was not fluorescently labelled. Thus, a frequency plot of thapsigargin responses was created (Figure 4.10D). When compared to *GBA1*<sup>WT</sup>, a rightward shift (\*) in the *GBA1*<sup>N370S</sup> thapsigargin responses were observed (Figure 4.10D).

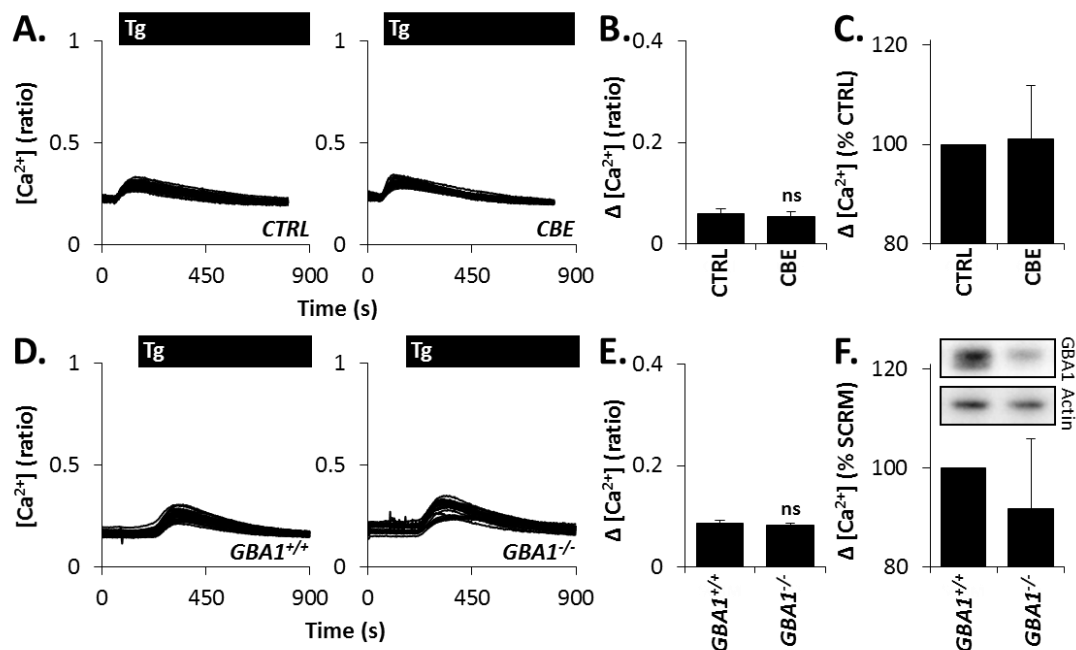


**Figure 4.8 Inhibition of GCase does not affect ER Ca<sup>2+</sup> homeostasis in dopaminergic SH-SY5Y cells**

(A) Cytosolic Ca<sup>2+</sup> responses of individual SH-SY5Y stimulated with thapsigargin (Tg; 1 μM) from a representative population of cells treated with 10 μM CBE for 10-11 days.

(B-C) Summary data (mean ± S.E.M) quantifying the magnitude of thapsigargin response in CBE treated SH-SY5Y cells (B) and as a percentage of CTRL (C). Results are from 8 experiments (*n*) from 3 independent treatments analysing 224-231 cells. A two-sample *t*-test was applied to test significance. ns, not significant.

(D) Cytosolic Ca<sup>2+</sup> responses of representative SH-SY5Y cells stimulated with thapsigargin following stable shRNA knockdown of *GBA1* (*GBA1*<sup>+/+</sup>) or expression of scrambled (*GBA1*<sup>+/+</sup>) shRNA.

(E-F) Summary data (mean ± S.E.M) quantifying the magnitude of thapsigargin response in the SH-SY5Y cells (E) and as a percentage of *GBA1*<sup>+/+</sup> (F). Inset is a Western blot using antibodies to GCase (top) or actin (bottom) and homogenates (14 μg) from SH-SY5Y cells treated with the indicated shRNA. Ca<sup>2+</sup> imaging results are from 5 experiments (*n*) from 3 independent platings analysing 143-150 cells. A two-sample *t*-test was applied to test significance. ns, not significant.

All Ca<sup>2+</sup> imaging experiments were performed in the absence of extracellular Ca<sup>2+</sup>.

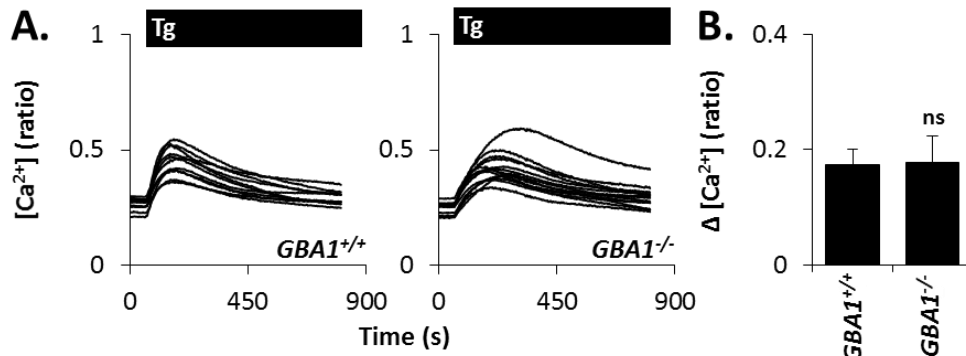


**Figure 4.9 Inhibition of GCase does not affect ER Ca<sup>2+</sup> homeostasis in neuronal cultures**

(A) Cytosolic Ca<sup>2+</sup> responses of mixed primary neuronal cultures from wild-type (*GBA1*<sup>+/+</sup>) and *GBA1* knockout (*GBA1*<sup>-/-</sup>) mice stimulated with thapsigargin (Tg; 1 μM). All experiments were performed in the absence of extracellular Ca<sup>2+</sup>.

(B) Summary data (mean ± S.E.M) quantifying the magnitude of thapsigargin response in neuronal cultures. Results are from 4-5 experiments (*n*) from 2 independent cultures analysing 53-69 cells. A two-sample *t*-test was applied to test significance. ns, not significant.

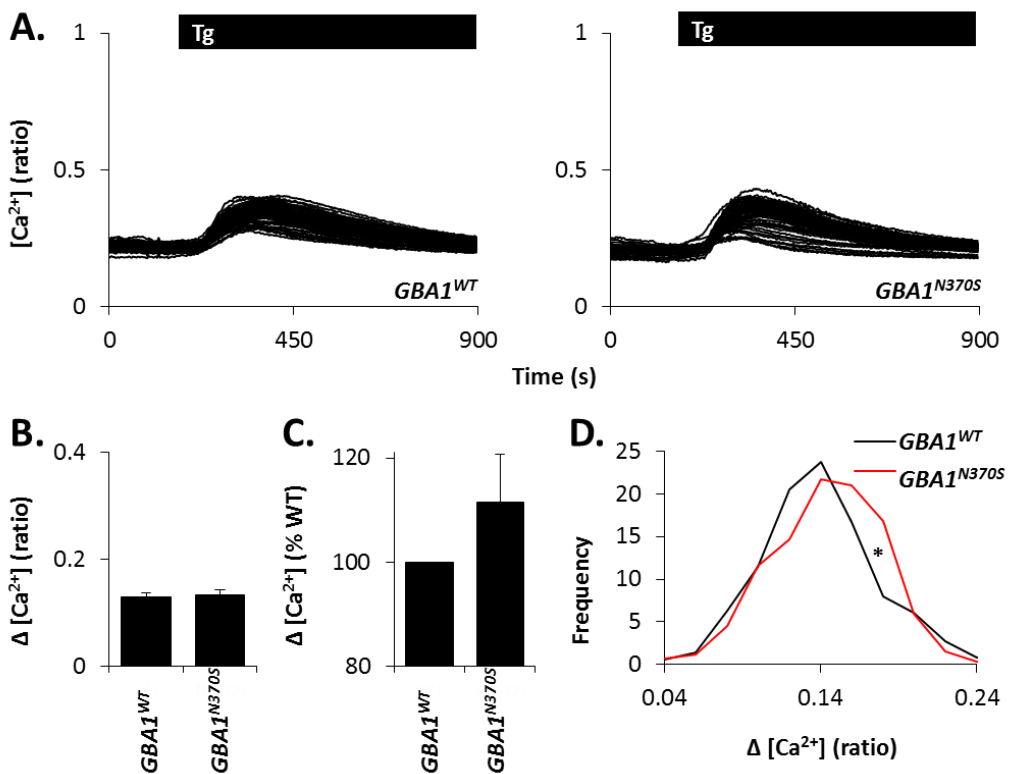


**Figure 4.10 Overexpression of mutant *GBA1* partially impairs ER Ca<sup>2+</sup> homeostasis**

(A) Cytosolic Ca<sup>2+</sup> responses of representative SH-SY5Y cells overexpressing WT or N370S mutated *GBA1* stimulated with thapsigargin (Tg; 1 μM).

(B-C) Summary data (mean ± S.E.M) quantifying the magnitude of thapsigargin response in the SH-SY5Y cells (B) and as a percentage of *GBA1*<sup>WT</sup> (C).

(D) Frequency plot of thapsigargin responses in all SH-SY5Y cells.

Results are from 4-5 experiments (*n*) from 3 independent transductions analysing 266-365 cells.

### Mitochondrial Ca<sup>2+</sup> content is increased in *young GBA1*-PD fibroblasts

It has been well established that the ER forms functional (Rizzuto et al., 1998) and physical connections (Csordás et al., 2006) with the mitochondria. Given that ER Ca<sup>2+</sup> disruption has been reported in young *GBA1*<sup>-/-GD</sup> and *GBA1*<sup>+/-PD</sup> fibroblasts, mitochondrial Ca<sup>2+</sup> content was indirectly examined in the fibroblast cultures using carbonylcyanide-p-(trifluoromethoxy)-phenylhydrazone (FCCP). FCCP is a protonophore that uncouples the mitochondrial membrane potential, releases mitochondrial Ca<sup>2+</sup> and permits the indirect measurement of mitochondrial Ca<sup>2+</sup> content. Stimulating fibroblasts with 1 μM FCCP evoked small and transient Ca<sup>2+</sup> signals (Figure 4.11A). FCCP-evoked Ca<sup>2+</sup> responses were larger in *GBA1*<sup>+/-55PD</sup> fibroblast cultures when compared to fibroblasts from an age-matched healthy individual (*GBA1*<sup>+/+55</sup>; Figure 4.11B). However, *GBA1*<sup>-/-55GD</sup> fibroblasts did not show increases in FCCP Ca<sup>2+</sup> response (Figure 4.11B). It is important to note that because FCCP-evoked Ca<sup>2+</sup> responses were modest, I again compared FCCP signals by quantifying the percentage change in Δ[Ca<sup>2+</sup>].

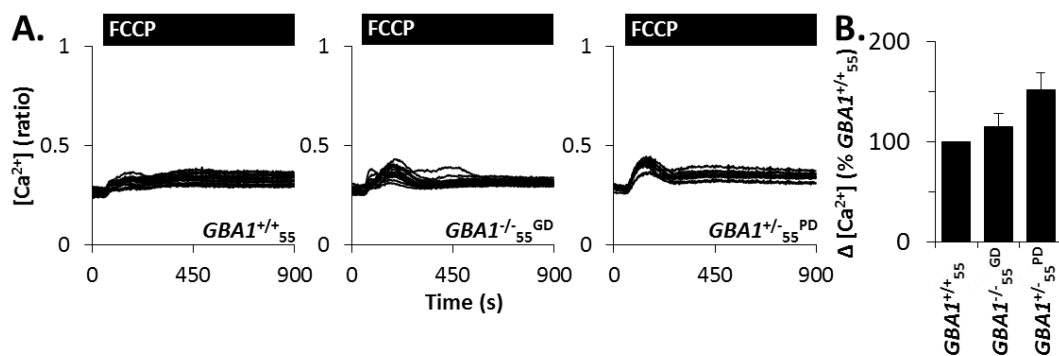


**Figure 4.11 Mitochondrial Ca<sup>2+</sup> content is increased in *young GBA1*-PD fibroblasts**

(A) Cytosolic Ca<sup>2+</sup> responses of individual fibroblasts stimulated with FCCP (1 μM) from a representative population of *GBA1*<sup>+/+55</sup>, *GBA1*<sup>-/-55GD</sup> and *GBA1*<sup>+/-55PD</sup> cells. All experiments were performed in the presence of extracellular Ca<sup>2+</sup>.

(B) Summary data (mean ± S.E.M) quantifying the magnitude of FCCP response as a percentage of *GBA1*<sup>+/+55</sup> control. Results are from 13-18 experiments (*n*) from 5-8 independent platings analysing 184-265 cells.

### Lysosomal Ca<sup>2+</sup> content is decreased in *young GD* and *GBA1*-PD fibroblasts

We recently showed that the ER forms functional and physical connections with acidic Ca<sup>2+</sup> stores (Kilpatrick et al., 2013). Since ER Ca<sup>2+</sup> is disrupted in young *GBA1*<sup>-/-GD</sup> and *GBA1*<sup>+/-PD</sup> fibroblasts, I examined lysosomal Ca<sup>2+</sup> content in these cultures. Measurements of lysosomal Ca<sup>2+</sup> content were estimated using GPN (200 μM). GPN stimulated the typical complex Ca<sup>2+</sup>



responses reported in chapter 2. These GPN-evoked complex  $\text{Ca}^{2+}$  responses, appeared similar across the  $\text{GBA1}^{+/+}_{55}$ ,  $\text{GBA1}^{-/-}_{55}^{\text{GD}}$  and  $\text{GBA1}^{+/-}_{55}^{\text{PD}}$  fibroblast cultures (Figure 4.12A). The proportion of cells that oscillate in response to GPN did not significantly differ between the fibroblast cultures (Figure 4.12D).

GPN-evoked  $\text{Ca}^{2+}$  oscillations are dependent upon ER localised  $\text{IP}_3\text{R}$ . So to isolate lysosomal  $\text{Ca}^{2+}$  release, I took advantage of the antagonistic effects that 2-APB has on GPN-evoked  $\text{Ca}^{2+}$  oscillations (chapter 2). As shown in figure 4.12B, GPN-evoked  $\text{Ca}^{2+}$  responses become largely monotonic after pre-treatment with 100  $\mu\text{M}$  2-APB. When compared to fibroblasts from an age-matched healthy individual ( $\text{GBA1}^{+/+}_{55}$ ), GPN-evoked  $\text{Ca}^{2+}$  responses (after exposure to 2-APB) were reduced in  $\text{GBA1}^{-/-}_{55}^{\text{GD}}$ ,  $\text{GBA1}^{+/-}_{55}^{\text{PD}}$  (Figure 4.12E).

The rate of GPN-induced lysosome membrane permeabilisation was compared in the fibroblast cultures using LysoTracker red. The decrease in LysoTracker fluorescence, did not differ between fibroblasts cultures (Figure 4.12C). This was quantified by calculating the time taken for fluorescence to decrease by 50% (Figure 4.12F).

#### Lysosome morphology is disrupted in GD and *GBA1*-PD fibroblasts

Lysosome dysfunction is often associated with changes in lysosome morphology. Using an antibody raised to the late-endosome/lysosome marker LAMP1, lysosome morphology was compared in the fibroblasts established from the young and aged individuals. Representative confocal images are shown in figures 4.13 and 4.14, data were quantified using LAMP1 fluorescence intensity. When compared to age-matched control fibroblasts ( $\text{GBA1}^{+/+}_{55}$ ; Figure 4.13A), increased lysosome structures were observed in both  $\text{GBA1}^{-/-}_{55}^{\text{GD}}$  (Figure 4.13B) and  $\text{GBA1}^{+/-}_{55}^{\text{PD}}$  (Figure 4.13C) fibroblasts. Furthermore, the lysosomes appeared enlarged and clustered in  $\text{GBA1}^{-/-}_{55}^{\text{GD}}$  and  $\text{GBA1}^{+/-}_{55}^{\text{PD}}$  cells. To a lesser extent, young and asymptomatic *GBA1* carriers ( $\text{GBA1}^{+/-}_{58}^{\text{ASX}}$  and  $\text{GBA1}^{+/-}_{59}^{\text{ASX}}$ ) also exhibited pathological morphology when compared to  $\text{GBA1}^{+/+}_{55}$  (Figure 4.13D-E).

Similar to  $\text{GBA1}^{+/-}_{55}^{\text{PD}}$  fibroblasts, lysosome morphology was also disrupted in the  $\text{GBA1}^{+/-}_{75}^{\text{PD}}$  fibroblasts (Figure 4.14A-B). However, these defects were modest and only associated with a 30% increase in LAMP1 intensity (Figure 4.14E). Furthermore, fibroblasts established from  $\text{GBA1}^{+/-}_{80}^{\text{ASX}}$  did not exhibit disrupted lysosome morphology when compared to  $\text{GBA1}^{+/+}_{82}$  (Figure 4.14C-E).

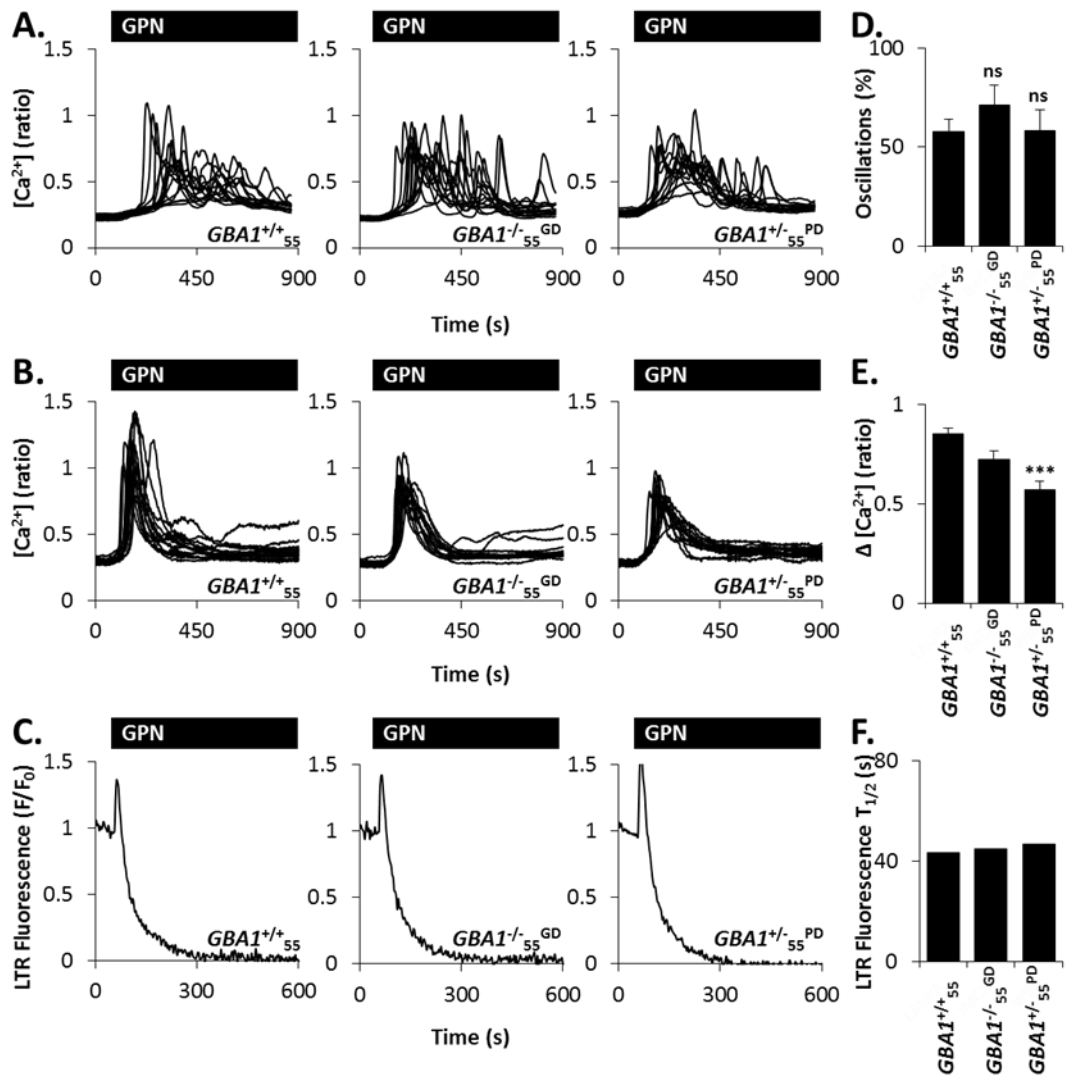


**Figure 4.12 Lysosomal  $Ca^{2+}$  content is decreased in *young* GD and *GBA1*-PD fibroblasts**

(A-B) Cytosolic  $Ca^{2+}$  responses of individual fibroblasts stimulated with GPN (200  $\mu$ M) from a representative population of  $GBA1^{+/+}_{55}$ ,  $GBA1^{-/-}_{55}^{GD}$  and  $GBA1^{+/-}_{55}^{PD}$  cells. With (B) or without (A) a 12.5 minute pre-treatment with 2APB (100  $\mu$ M).

(C) Average Lysotracker red responses of fibroblasts stimulated with GPN (200  $\mu$ M) from  $GBA1^{+/+}_{55}$ ,  $GBA1^{-/-}_{55}^{GD}$  and  $GBA1^{+/-}_{55}^{PD}$  cultures.

(D-F) Summary data (mean  $\pm$  S.E.M) quantifying the percentage of cells that oscillate after GPN stimulation (D; 7 experiments ( $n$ ) from 2 independent platings analysing 118-120 cells), the magnitude of GPN response (after pre-incubation with 2-APB; E; 6 experiments ( $n$ ) from 2 independent platings analysing 72-88 cells) and the time to taken to reach a half-maximal loss of lysotracker red fluorescence (F; 2 experiments ( $n$ ) from 1 independent plating analysing 25-34 cells). ANOVA analysis, followed by a post-hoc Tukey test, was applied to test significance against  $GBA1^{+/+}_{55}$ . ns, not significant. \*\*\* $p < 0.001$ . All experiments were performed in the presence of extracellular  $Ca^{2+}$ .

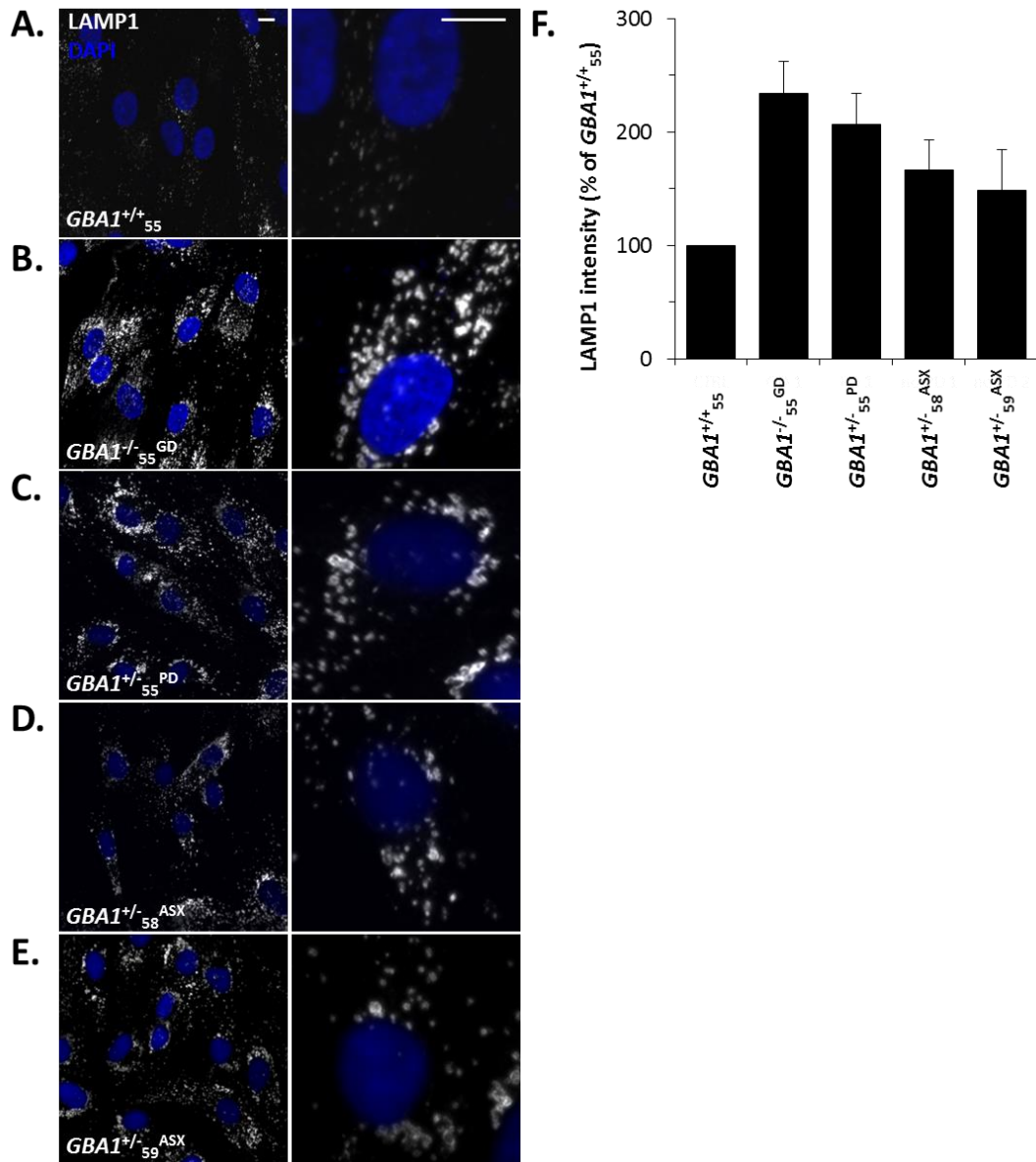


**Figure 4.13 Lysosome morphology is disrupted in *young* GD and *GBA1*-PD fibroblasts**

(A-E) Representative confocal fluorescence images of LAMP1 (white) staining in  $GBA1^{+/+}_{55}$ ,  $GBA1^{-/-}_{55}^{GD}$ ,  $GBA1^{+/-}_{55}^{PD}$ ,  $GBA1^{+/-}_{58}^{ASX}$  and  $GBA1^{+/-}_{59}^{ASX}$  fibroblasts. Zoomed images are displayed in the right panels. Nuclei were stained using DAPI (blue). Scale bars, 10  $\mu$ m.

(F) Summary data (mean  $\pm$  S.E.M) quantifying LAMP1 intensity as a percentage of  $GBA1^{+/+}_{55}$ . Results are from 3-17 independent platings ( $n$ ) analysing 130-654 cells.

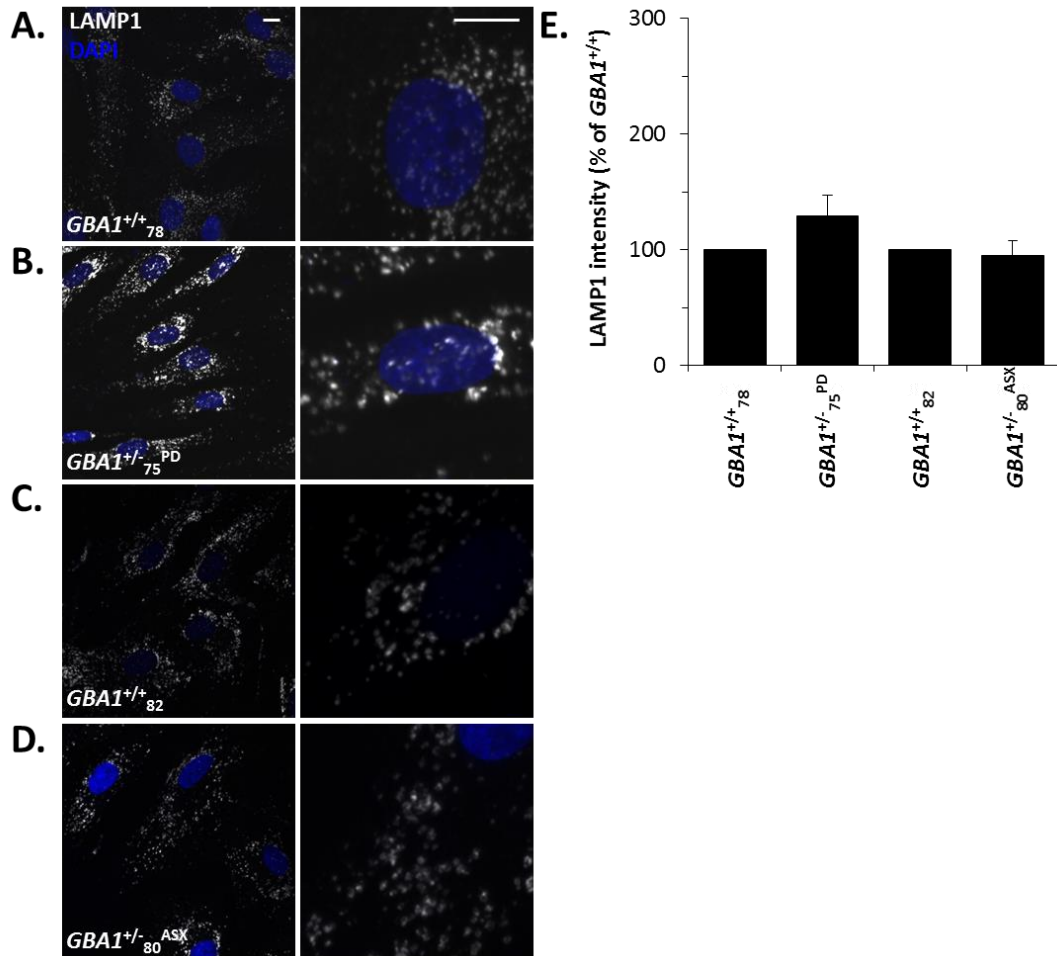


**Figure 4.14 Lysosome morphology is disrupted in aged *GBA1*-PD fibroblasts**

(A-E) Representative confocal fluorescence images of LAMP1 (white) staining in *GBA1*<sup>+/+</sup><sub>78</sub>, *GBA1*<sup>+/-</sup><sub>75</sub><sup>PD</sup>, *GBA1*<sup>+/+</sup><sub>82</sub> and *GBA1*<sup>+/-</sup><sub>80</sub><sup>ASX</sup> fibroblasts. Nuclei were stained using DAPI (blue). Scale bars, 10  $\mu$ m.

(F) Summary data (mean  $\pm$  S.E.M) quantifying LAMP1 intensity as a percentage of each age matched *GBA1*<sup>+/+</sup>. Fibroblast results are from 3 independent platings (*n*) analysing 82-190 cells.

#### Agonist-evoked Ca<sup>2+</sup> release is not altered in young GD and *GBA1*-PD fibroblasts

Intracellular Ca<sup>2+</sup> stores are delicately balanced to ensure appropriate physiological signalling. Since defective Ca<sup>2+</sup> storage and signalling has been identified in both *GBA1*<sup>-/-</sup><sub>55</sub><sup>GD</sup> and *GBA1*<sup>+/-</sup><sub>55</sub><sup>PD</sup> fibroblasts, Ca<sup>2+</sup> responses evoked by a physiological agonist were measured. Bradykinin is the principle ligand that activates the G protein-coupled bradykinin receptor (Hall, 1992). Fibroblasts are highly responsive to bradykinin (chapter 2, Figure 2.7E), thus a low concentration (1 nM) was applied to *GBA1*<sup>+/+</sup><sub>55</sub>, *GBA1*<sup>-/-</sup><sub>55</sub><sup>GD</sup> and *GBA1*<sup>+/-</sup><sub>55</sub><sup>PD</sup> cultures. Bradykinin stimulated robust and complex Ca<sup>2+</sup> signals (Figure 4.15A). Ca<sup>2+</sup> responses evoked by bradykinin were similar in the *GBA1*<sup>+/+</sup><sub>55</sub>, *GBA1*<sup>-/-</sup><sub>55</sub><sup>GD</sup> and *GBA1*<sup>+/-</sup><sub>55</sub><sup>PD</sup> fibroblasts (Figure 4.15A). The magnitude of bradykinin response was not significantly different between *GBA1*<sup>+/+</sup><sub>55</sub>, *GBA1*<sup>-/-</sup><sub>55</sub><sup>GD</sup> and *GBA1*<sup>+/-</sup><sub>55</sub><sup>PD</sup> cultures (Figure 4.15B).

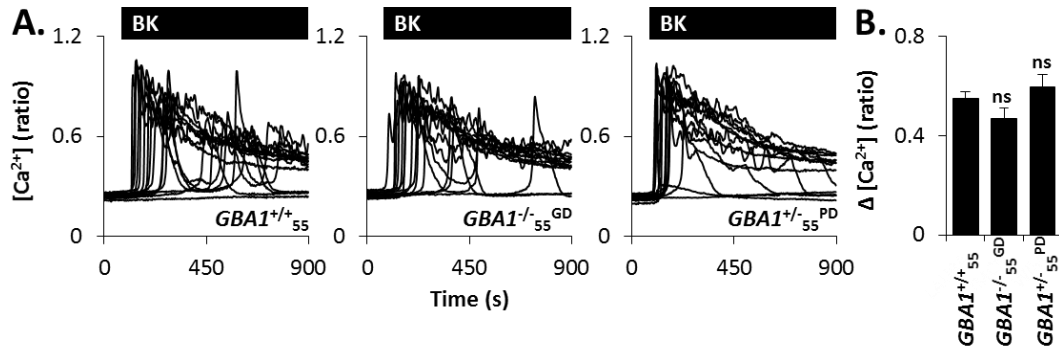


**Figure 4.15 Agonist-evoked  $Ca^{2+}$  release is not altered in *young* GD and *GBA1*-PD fibroblasts**

(A) Cytosolic  $Ca^{2+}$  responses of individual fibroblasts stimulated with bradykinin (BK; 1 nM) from a representative population of  $GBA1^{+/+}_{55}$ ,  $GBA1^{-/-}_{55}^{GD}$  and  $GBA1^{+/-}_{55}^{PD}$  cells. All experiments were performed in the presence of extracellular  $Ca^{2+}$ .

(B) Summary data (mean  $\pm$  S.E.M) quantifying the magnitude of bradykinin response. Results are from 6-14 experiments ( $n$ ) from 3-6 independent platings analysing 89-210 cells. ANOVA analysis, followed by a post-hoc Tukey test, was applied to test significance against  $GBA1^{+/+}_{55}$ . ns, not significant.

#### Spontaneous $Ca^{2+}$ signalling is increased *young* GD and *GBA1*-PD fibroblasts

To further probe the physiological impact of impaired  $Ca^{2+}$  storage, basal  $Ca^{2+}$  signalling was examined in the fibroblast cultures. Basal  $Ca^{2+}$  levels were similar across  $GBA1^{+/+}_{55}$ ,  $GBA1^{-/-}_{55}^{GD}$  and  $GBA1^{+/-}_{55}^{PD}$  fibroblast cultures (Figure 4.16A). However, spontaneous  $Ca^{2+}$  spikes were sometimes observed in the basal recordings of  $GBA1^{-/-}_{55}^{GD}$  and  $GBA1^{+/-}_{55}^{PD}$  fibroblasts (Figure 4.16). Over a 3 year data-collection period, the percentage of cells displaying spontaneous  $Ca^{2+}$  spikes in  $GBA1^{+/-}_{55}^{PD}$  were significantly increased when compared to  $GBA1^{+/+}_{55}$  (Figure 4.16B). It is important to note that only cells with stable basal  $Ca^{2+}$  levels were selected for quantifying thapsigargin, cADPR-AM, GPN, FCCP and bradykinin responses.

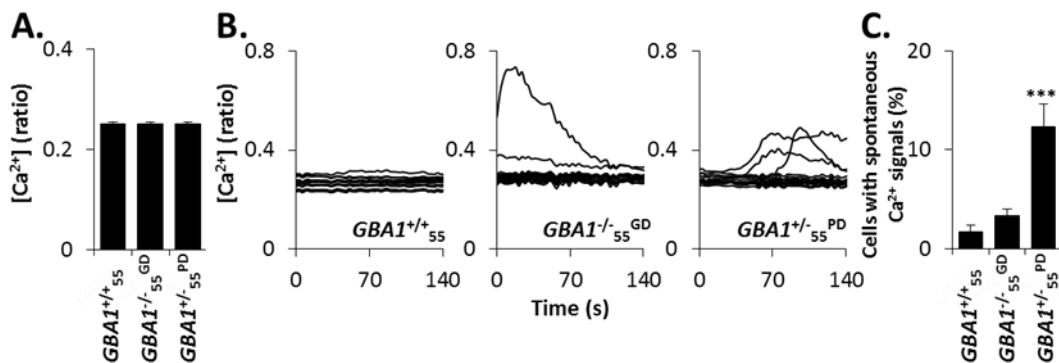


**Figure 4.16 Spontaneous  $Ca^{2+}$  signalling is increased *young* GD and *GBA1*-PD fibroblasts**

(A) Summary data (mean  $\pm$  S.E.M) quantifying basal  $Ca^{2+}$  ratios.

(B) Cytosolic  $Ca^{2+}$  signalling from a representative population of  $GBA1^{+/+}_{55}$ ,  $GBA1^{-/-}_{55}^{GD}$  and  $GBA1^{+/-}_{55}^{PD}$  cells. Cells were maintained in the presence of extracellular  $Ca^{2+}$ .

(C) Summary data (mean  $\pm$  S.E.M) quantifying the percentage cells displaying spontaneous spikes. Results are from 44-75 experiments ( $n$ ) from 20-32 independent platings analysing 721-1196 cells.

## Discussion

Here I show that ER  $\text{Ca}^{2+}$  content was increased in primary fibroblasts established from younger GD and *GBA1*-PD patients relative to aged-matched control fibroblasts. Enhanced ER  $\text{Ca}^{2+}$  content was associated with increased responses to the RyR activator, cyclic ADP-ribose. Dysfunctional ER  $\text{Ca}^{2+}$  signalling was shown to be a unique feature of disease since asymptomatic *GBA1* carriers did not show disrupted ER  $\text{Ca}^{2+}$  homeostasis. Furthermore, ER  $\text{Ca}^{2+}$  content, in the fibroblasts established from healthy individuals, was increased in an age dependent manner. ER  $\text{Ca}^{2+}$  signalling was unaffected by molecular or chemical inhibition of GCase. However, the overexpression of mutant *GBA1* in dopaminergic SH-SY5Y cells modestly recapitulated defective ER  $\text{Ca}^{2+}$  responses, implicating mis-folded GCase in the pathology of PD. Other  $\text{Ca}^{2+}$  stores *connected* with the ER were also dysfunctional in GD and *GBA1*-PD. Mitochondrial  $\text{Ca}^{2+}$  content was increased in *GBA1*-PD fibroblasts, whereas lysosomal  $\text{Ca}^{2+}$  content was reduced and associated with disrupted lysosome morphology. Impaired  $\text{Ca}^{2+}$  storage and signalling in *GBA1*-PD fibroblasts disrupted basal  $\text{Ca}^{2+}$  homeostasis but not agonist-evoked  $\text{Ca}^{2+}$  signals. Thus, accelerated remodelling of  $\text{Ca}^{2+}$  stores by pathogenic *GBA1* may predispose individuals to PD.

### ER Dysfunction

$\text{Ca}^{2+}$  dysfunction is intimately associated with disease (reviewed in Berridge 2012) and this research suggests that GD and *GBA1*-PD are no exception. Indeed,  $\text{Ca}^{2+}$  signalling from RyR has previously been shown increased in GD microsome preparations (Pelled et al., 2005) and a neuropathic mouse model (Korkotian et al., 1999). Based on this foundation, I examined ER  $\text{Ca}^{2+}$  signalling in *GBA1*-associated diseases. Results demonstrate increased  $\text{Ca}^{2+}$  signalling in response to thapsigargin (used as an indirect measure to determine ER  $\text{Ca}^{2+}$  content) and the RyR agonist cADPR-AM in young diseased fibroblasts (figure 4.1-4.2). This suggests that ER  $\text{Ca}^{2+}$  content is increased in disease and associated with disrupted physiological ER  $\text{Ca}^{2+}$  signalling.

This data contrasts with previous reports which speculate that excessive RyR flux actually lowers luminal ER  $[\text{Ca}^{2+}]$  (Wang et al., 2011a). However, measurements of ER  $\text{Ca}^{2+}$  content have not been previously examined in GD. Furthermore, previous research did not report significant differences in ER  $\text{Ca}^{2+}$  release from type I GD microsomes. Instead only severe neuropathic GD models presented with defects (Pelled et al., 2005). Thus, to the best of my knowledge, this is the first account of increased ER  $\text{Ca}^{2+}$  content and release in type I GD.

A recent study has shown enhanced RyR-mediated Ca<sup>2+</sup> signalling in iPSC-derived neurons from GD and *GBA1*-PD patients (Schöndorf et al., 2014). This complements data reported in this chapter. However, PD has not always been associated with increased ER Ca<sup>2+</sup> signalling. For instance, Arduino and colleagues (2009) have reported reduced ER Ca<sup>2+</sup> content in an MPP<sup>+</sup> model of PD (Arduíno et al., 2009).

Although thapsigargin, which inhibits SERCA and exposes the ER Ca<sup>2+</sup> leak pathway, has frequently been used as an indirect measure of ER Ca<sup>2+</sup> content (reviewed in Michelangeli & East 2011). This inhibitor might also be providing insight into ER Ca<sup>2+</sup> leak itself. Therefore, elevated Ca<sup>2+</sup> responses, after the addition of thapsigargin, might not just indicate increased ER Ca<sup>2+</sup> content but also increased ER Ca<sup>2+</sup> leak. Perhaps, the diseased fibroblasts express more leak channels. However, this hypothesis would be difficult to test since the molecular identity of these leak channels remains elusive (Kiviluoto et al., 2013). To conclusively examine ER Ca<sup>2+</sup> content, more direct approaches, like using the genetically encoded Ca<sup>2+</sup> sensor D1-ER (Palmer et al., 2004), should be employed.

Compromised ER Ca<sup>2+</sup> signalling might result from the accumulation of glucocerebroside (GCcase substrate). This substrate not only aggregates within the lysosomes but also on the ER and the Golgi complex (Martin & Pagano, 1994). At the ER, glucocerebroside can be metabolised to other, high order, sphingolipids (Schnaar et al., 2009). Here, the substrate could directly impact Ca<sup>2+</sup> homeostasis. Indeed lyso-sphingo lipids have been shown to modulate Ca<sup>2+</sup> mobilisation (Furuya et al., 1996). Lloyd-Evans and colleagues (2003) concluded that glucocerebroside can adjust the redox potential of the RyR, through its interaction with the redox sensor, and modulate Ca<sup>2+</sup> release.

However, the data presented in this chapter suggests that an accumulation of substrate is not sufficient to induce ER Ca<sup>2+</sup> dysfunction in either fibroblasts, SH-SY5Y cells or neurons. Pharmacologically inhibiting GCcase did not induce ER dysfunction (Figures 4.7-4.8). Likewise the genetic knockdown of *GBA1* did not affect ER Ca<sup>2+</sup> signals (figures 4.8-4.9). Intriguingly fibroblasts are known to accumulate relatively low levels of substrate (Vitner et al., 2010). Thus the identification of ER Ca<sup>2+</sup> dysfunction in these fibroblasts further suggests other mechanisms must be involved in ER pathogenesis.

The retention of mis-folded GCcase on the ER could destabilise the organelle and perturb homeostasis. Newly synthesised proteins undergo a strict quality control, where non-functional proteins are degraded through various mechanisms collectively termed ERAD.

Many have shown that ERAD pathways are activated in GD (Mu et al., 2008; Wei et al., 2008) and that the severity of GD symptoms has been associated with the degree of GCase accumulation at the ER (Ron & Horowitz, 2005; Bendikov-Bar et al., 2011). Using lentiviral infection, marginally increased thapsigargin responses were seen cells in overexpressing mutant (N370S) *GBA1* (Figure 4.10). However, these effects were modest and impeded by low transduction efficiency. Further work optimising this protocol is essential.

Unfortunately, it is not possible to examine physiological ER  $\text{Ca}^{2+}$  signalling in SH-SY5Y cells since they are unresponsive to RyR agonists such as cADPR-AM and caffeine (data not shown), despite the expression of RyR (Mackrill et al., 1997a). Thus, further work is required to uncover the mechanism behind disrupted ER  $\text{Ca}^{2+}$  signalling.

Currently it is unknown why 85-90% (McNeill et al., 2012) of individuals with a *GBA1* mutation never develop PD (Sidransky et al., 2009). Very few studies have compared the pathology of *GBA1*-PD against asymptomatic carriers. When these comparisons have been made, similar defects are reported between asymptomatic *GBA1* carriers and *GBA1*-PD patients. For instance, GCase activity and accumulation of GCase on the ER were not different in fibroblast cultures (McNeill et al., 2014). Here I report that non-manifesting *GBA1* heterozygotes do not show increased  $\text{Ca}^{2+}$  signalling in response to thapsigargin and cADPR-AM when compared to PD patient cells (figures 4.3-4.4). Thus, ER  $\text{Ca}^{2+}$  homeostasis might be the defining feature of PD development in *GBA1* carriers and can be exploited as a biomarker for disease. However, further work with increased patient numbers is required to validate the efficacy of this biomarker. Furthermore, the question remains why these *GBA1* carriers not have increase ER  $\text{Ca}^{2+}$  despite similar biochemical characteristics to PD. It is important to also note that because risk of developing PD in *GBA1* carriers is age related (McNeill et al., 2012; Rana et al., 2013), these carriers might still develop PD.

Intriguingly, ageing is associated with increased ER  $\text{Ca}^{2+}$  content (Figure 4.6). Thapsigargin-evoked  $\text{Ca}^{2+}$  signals in the fibroblasts established from aged individuals resembled  $\text{Ca}^{2+}$  responses evoked in young diseased cells. Previous reports have shown that ageing increases ER  $\text{Ca}^{2+}$  signalling in neurons (Gant et al., 2006; Puzianowska-Kuznicka & Kuznicki, 2009). Thus, in this respect, fibroblasts behave like neurons. However, this increased ER  $\text{Ca}^{2+}$  content perturbed the examination of older *GBA1*-PD fibroblasts as they were no different from their respective age matched controls. Perhaps *GBA1*-PD ER pathology is associated with accelerating ageing phenotypes and this effect becomes masked later in life. Notably, reliance upon  $\text{Ca}^{2+}$  influx for pacemaking activity in SNc neurons increases with age (Chan et



al., 2007) and imposes metabolic stress (Guzman et al., 2010). These studies provide a mechanism for selective neuronal degeneration in PD that will likely affect us all as we age. Conceivably, age-related increased ER Ca<sup>2+</sup> signalling could exacerbate Ca<sup>2+</sup> stress and contribute to PD development.

An examination of basal Ca<sup>2+</sup> in these cultures revealed that *GBA1*-PD is associated with increased spontaneous Ca<sup>2+</sup> fluxes (Figure 4.16). Notably, spontaneous ER Ca<sup>2+</sup> release has been reported in type II GD microsomes (Pelled et al., 2005). It is possible that increased ER Ca<sup>2+</sup> contributes to these spikes. Indeed, these spontaneous fluxes might impose further stress on SNc neurons.

The ER has a finite Ca<sup>2+</sup> capacity (Berridge, 2002) and the potential increased ER Ca<sup>2+</sup> content present in GD, *GBA1*-PD and aged individuals could impose significant stress upon the cell. Indeed, enhanced ER Ca<sup>2+</sup>-mobilisation has been shown to heighten neuronal sensitivity to glutamate (Korkotian et al., 1999). Apoptosis is often triggered by ER Ca<sup>2+</sup> (Pinton et al., 2008), thus an increased ER Ca<sup>2+</sup> pool present might increase the propensity for the induction of cell death.

The ER is a specialised organelle, aside from its role in the regulation and storage of Ca<sup>2+</sup>, it is critically involved in the synthesis of proteins and lipids. Aberrant ER Ca<sup>2+</sup> can interfere with these processes (reviewed in Paschen & Mengesdorf (2005)). Several ER chaperones are Ca<sup>2+</sup> binding proteins, sensitive to any variation in Ca<sup>2+</sup> (Michalak et al., 2009). Of importance, manipulating ER Ca<sup>2+</sup> has been shown to recover protein folding in GD models (Sun et al., 2009; Ong et al., 2010). Preventing the leak (by blocking RyR release; Mu et al. (2008)) or increasing the uptake (by overexpressing SERCA; Ong et al. (2010)) of ER Ca<sup>2+</sup> can improve GCase folding. The Ca<sup>2+</sup>-dependent ER chaperone calnexin is believed to regulate GCase protein homeostasis. Ong and colleagues (2010) demonstrate that increasing ER Ca<sup>2+</sup> enhances the ability for calnexin to fold dysfunctional GCase. Perhaps the raised ER Ca<sup>2+</sup> levels present in GD and *GBA1*-PD acts as a compensatory mechanism to rescue GCase folding via calnexin. Indeed McNeill et al. (2014) have already demonstrated that calnexin levels are increased in these GD and *GBA1*-PD fibroblast cultures.

#### Mitochondrial Dysfunction

The ER forms functional and physical connections with acidic Ca<sup>2+</sup> stores (Kilpatrick et al., 2013) and the mitochondria (Csordás et al., 2006). Pathological ER Ca<sup>2+</sup> signalling could damage these associated organelles and impact upon their Ca<sup>2+</sup> homeostasis.

Much evidence converges on a central role of mitochondria in PD pathogenesis. Many of the genes linked to PD encode mitochondrial proteins (Schapira, 2012). Recent evidence has identified mitochondrial dysfunction in numerous *GBA1* disease models. Several markers for mitochondrial dysfunction (such as fragmentation, reduced membrane potential and increased in ROS production) are present in SH-SY5Y cells after GCase activity has been impaired with CBE and silencing *GBA1* (Cleeter et al., 2012). Similar mitochondrial phenotypes have also been reported in primary neuronal cultures from the same GD mouse model used in this report (Osellame et al., 2013). Furthermore, these cultures exhibit an impaired recruitment of Parkin (a PD-linked gene) to mitochondrial membranes and impaired mitophagy.

Since the mitochondria are impaired in *GBA1* disease models, I examined mitochondrial  $\text{Ca}^{2+}$  in the fibroblast cultures. Responses to FCCP were increased in *GBA1*-PD cells indicating increased mitochondrial  $\text{Ca}^{2+}$  content (figure 4.11). However, GD mitochondrial  $\text{Ca}^{2+}$  levels were unchanged.  $\text{Ca}^{2+}$  defects in PD have been previously reported. For instance, cells deficient in the mitochondrial PD protein PINK1, exhibit a substantial delay in the efflux of  $\text{Ca}^{2+}$  from mitochondria (Gandhi et al., 2009) and defective  $\text{Ca}^{2+}$  uptake into the mitochondria (Heeman et al., 2011). Furthermore, previous research has shown mitochondrial fragmentation and defective  $\text{Ca}^{2+}$  uptake in the LSD Mucopolipidosis IV (Jennings et al., 2006). However, uptake and efflux of mitochondrial  $\text{Ca}^{2+}$  requires further examination in GD and *GBA1*-PD.

In addition, although widely employed, this method for measuring mitochondrial  $\text{Ca}^{2+}$  is indirect. Notably this is an issue that can also be applied to the measurements of ER and lysosomal  $\text{Ca}^{2+}$ . Future work requires the use of  $\text{Ca}^{2+}$  indicators targeted to each of these organelles to obtain a better estimation of luminal  $\text{Ca}^{2+}$  content.

The ER and mitochondria are also physically coupled to one another through mitochondria-associated membrane (MAM) proteins (reviewed in Hayashi et al. (2009)).  $\text{Ca}^{2+}$  release from the ER is sequestered by the mitochondria (Rizzuto et al., 1993) and therefore mitochondrial  $\text{Ca}^{2+}$  dysfunction in *GBA1*-PD might be a consequence of impaired ER  $\text{Ca}^{2+}$ . It is notable that, this excessive transfer of  $\text{Ca}^{2+}$  could initiate apoptotic pathways. Alternatively, dysfunctional lysosomes (further discussed below) might impair mitophagy (already reported in *GBA1*-diseased models (Osellame et al., 2013; Cleeter et al., 2012) and cause an excessive build-up of troubled mitochondria. These hypotheses require further examination.

Ca<sup>2+</sup> is essential for mitochondrial function, its presence in the matrix activates metabolic enzymes of the tricarboxylic acid cycle to regulate energy production (Rizzuto et al., 2012). An imbalance of Ca<sup>2+</sup> could affect ATP synthesis in *GBA1*-PD. Moreover, the prolonged presence of Ca<sup>2+</sup> in the mitochondria opens the permeability transition pore (PTP) initiating apoptosis (Crompton, 1999). Thus, the increased mitochondrial Ca<sup>2+</sup> present in *GBA1*-PD could promote neurodegeneration. The increased Ca<sup>2+</sup> influx into dopaminergic SNc neurons is energetically expensive to temper and thus imposes mitochondrial stress (Guzman et al., 2010). As the mitochondria are dysfunctional in *GBA1*-PD this will likely only further provoke degeneration. However, further examination mitochondrial function is required in these fibroblast cultures.

#### Lysosome Dysfunction

Lysosomal dysfunction has been reported in multiple LSDs (Meikle et al., 1997). For instance, studies have reported increased levels of lysosome membrane proteins (primarily LAMP-1) in GD (Meikle et al., 1997; Whitfield et al., 2002; Zimmer et al., 1999). In this report, *GBA1* mutations were associated with aberrant lysosome morphology in young fibroblasts (Figure 4.13). These acidic organelles appeared proliferated, enlarged and aggregated. Furthermore, unlike ER Ca<sup>2+</sup> signalling, lysosome morphology was also disrupted in the fibroblasts established from young asymptomatic *GBA1* heterozygotes. However, with increasing age *GBA1*-PD lysosome dysfunction is not as severe (Figure 4.14). Increased lysosome structures have recently been quantified in NPC patients and this assay has been identified as a useful biomarker (te Vrugte et al., 2014). It is notable that, with increasing age NPC lysosome dysfunction is also less severe (te Vrugte et al., 2014).

Emerging evidence implicates lysosome dysfunction in neurodegenerative diseases (Zhang et al., 2009). For instance, lysosome disruption has been identified as an early pathological event in axon degeneration (Zheng et al., 2010). Furthermore, in familial Alzheimer Disease aberrant lysosome turnover is linked to mutations in presenilin-1 (Lee et al., 2010c). Thus the pathological lysosome morphology identified in GD and *GBA1*-PD agrees with other neurodegenerative disorders.

Lysosome dysfunction has also been reported in PD. However, the pathology observed can vary between PD model examined. For instance, a recent study showed robust reductions in lysosomal markers within the SNc neurons of sporadic PD patients (Chu et al., 2009). Moreover, significant lysosome depletion has also been reported in an MPTP murine model of PD (Dehay et al., 2010). In contrast, fibroblasts with mutations in ATP13A2 (Dehay et al.,

2012) and neurons overexpressing LRRK2 (MacLeod et al., 2006) are associated with increased lysosome structures. The recent study by Schondoroff and colleagues (2014) also show a proliferation and enlargement lysosome in *GBA1*-PD patient derived iPSC neurons. A more extensive analysis of lysosome morphology is required in my fibroblast cultures. For example, electron microscopy is necessary to better examine the ultra-structure of the lysosome.

An increased need to sequester excess glucocerebroside in *GBA1* mutant fibroblasts is a possible cause of these abnormal lysosomes. Further analysis in SH-SY5Y cells with the stable knock-down of *GBA1* or overexpressing mutant *GBA1* is necessary to determine the mechanism underlying lysosome dysfunction.

The transcription factor EB (TFEB) coordinates lysosomal biogenesis (Sardiello et al., 2009). TFEB is dephosphorylated and translocated to the nucleus upon lysosome dysfunction (Settembre et al., 2012). Notably, TFEB is currently the only established transcription factor for *GBA1* (Blech-Hermoni et al., 2010). Indeed recent research has identified Ambroxol hydrochloride as an activator of TFEB, which increases the expression of lysosomal genes including *GBA1* (McNeill et al., 2014). Perhaps TFEB is activated in GD and *GBA1*-PD to stimulate *GBA1* expression. As a consequence lysosomes become proliferated. However, TFEB activation requires further investigation in these fibroblasts.

The degradation of  $\alpha$ -syn is dependent upon chaperone mediated autophagy (Cuervo et al., 2004). Many have reported an accumulation of  $\alpha$ -syn in *GBA1*-disease models (Cullen et al., 2011; Osellame et al., 2013; Manning-Boğ et al., 2009). Perhaps aberrant lysosome morphology impairs the degradation of  $\alpha$ -syn. Indeed,  $\alpha$ -syn itself has been shown to inhibit the trafficking of proteins from the ER to the Golgi apparatus (Thayanidhi et al., 2010a), including GCase (Mazzulli et al., 2011). Therefore in *GBA1*-PD, an increase in  $\alpha$ -syn (likely caused by lysosome dysfunction) could further impact ER  $\text{Ca}^{2+}$  homeostasis by impairing GCase trafficking.

Lysosomes are also known as “suicide bags” and have a key role in the induction of apoptosis (reviewed in Aits & Jäättelä 2013). A leak of cathepsin D and B (lysosomal hydrolases) into the cytosol promotes the release of cytochrome C from the mitochondria initiating cell death (Guicciardi et al., 2000). The increased lysosome presence observed in GD and *GBA1*-PD could functionally impair the cell increasing the probability of apoptosis and neurodegeneration. However, this hypothesis requires testing.

Lysosomes also function as significant  $\text{Ca}^{2+}$  stores. As described in chapters 2 and 3, the lysosomal permeabilising agent GPN induces prolonged complex  $\text{Ca}^{2+}$  signalling. These GPN-evoked oscillatory signals were similar in the diseased fibroblast cultures. To ascertain a better estimation of lysosomal  $\text{Ca}^{2+}$  content, ER  $\text{IP}_3\text{R}$  must be inhibited (discussed in chapter 2). Under ER blockade GD and *GBA1*-PD fibroblasts exhibited reduced responses to GPN (despite similar permeabilisation rates), indicative of lowered lysosomal  $\text{Ca}^{2+}$  content (Figure 4.12). This is consistent with the phenotypes observed in the other LSD NPC (Lloyd-Evans et al., 2008) and also Alzheimer Disease (Coen et al., 2012). This reduction in lysosomal  $\text{Ca}^{2+}$  content requires further characterisation. Crucially, direct measurements of luminal  $\text{Ca}^{2+}$  content must be obtained.

The reduced lysosomal  $\text{Ca}^{2+}$  content in GD and *GBA1*-PD could impact physiological  $\text{Ca}^{2+}$  signalling. Indeed reduced content has been shown to diminish NAADP signalling in NPC (Lloyd-Evans et al., 2008). Unfortunately, NAADP-AM responses have not been examined in these fibroblast cultures due to the unresponsive nature of recent batches (chapter 2). However, since GPN-evoked  $\text{Ca}^{2+}$  oscillatory signals are no different between cultures (figure 4.12C) NAADP-AM responses may not differ. This could be because the increased ER  $\text{Ca}^{2+}$  balances the loss of lysosomal  $\text{Ca}^{2+}$ .

Lysosomal  $\text{Ca}^{2+}$  is required for the induction of macroautophagy (Pereira et al., 2011). The disruption to lysosome morphology and  $\text{Ca}^{2+}$  homeostasis in GD and *GBA1*-PD could cause the aggregation of  $\alpha$ -syn and effete mitochondria, both of which are autophagic substrates. Notably, many have reported autophagic dysfunction in *GBA1*-PD (Cleeter et al., 2012; Osellame et al., 2013). Thus, examining how lysosome morphology and  $\text{Ca}^{2+}$  homeostasis impacts autophagy in these fibroblast cultures would be of interest.

It is interesting that despite an increase in lysosome structures, lysosomal  $\text{Ca}^{2+}$  content is reduced. This contrasts with previous data presented by Dickinson and colleagues (2010) who report increased GPN responses after pharmacologically imposing lysosome proliferation, using the cathepsin B and L inhibitor Z-Phe-Ala-diazomethylketone (Dickinson et al., 2010). Perhaps in GD and *GBA1*-PD these dysfunctional acidic organelles are “leaky” or have defective  $\text{Ca}^{2+}$  uptake. Indeed, since the mechanism of lysosomal  $\text{Ca}^{2+}$  uptake is unknown the latter would be difficult to investigate.

Alternatively, the reduced lysosomal  $\text{Ca}^{2+}$  content could be a compensation mechanism for the increased ER  $\text{Ca}^{2+}$  signalling (or *vice versa*). Lloyd-Evans and co-workers (2008) report that

depleting ER  $\text{Ca}^{2+}$  using SERCA ATPase inhibitors can reverse NPC pathology. Notably, NPC is associated with reduced lysosomal  $\text{Ca}^{2+}$  content and signalling. The authors demonstrate that SERCA ATPase inhibitors elevate cytosolic  $\text{Ca}^{2+}$  and compensate for lysosomal dysfunction. This reciprocal redistribution of  $\text{Ca}^{2+}$  in GD and *GBA1*-PD might be crucial to maintain  $\text{Ca}^{2+}$  homeostasis and could be facilitated by MCSs.

#### Physiological $\text{Ca}^{2+}$ signalling

Although *GBA1*-PD was associated with disrupted basal  $\text{Ca}^{2+}$  homeostasis (Figure 4.16), responses to bradykinin were unchanged in the diseased fibroblast cultures (Figure 4.15). Bradykinin has previously been shown to stimulate  $\text{IP}_3$ -mediated  $\text{Ca}^{2+}$  signalling in fibroblasts (Tao et al., 1988). Thus a lack of bradykinin effect could indicate that  $\text{IP}_3$ -mediated signalling is not affected in *GBA1*-disease. However, Madin-Darby Canine Kidney Cells treated with CBE exhibited reduced  $\text{IP}_3$  formation after bradykinin stimulation (Mahdiyoun et al., 1992). Further examination of  $\text{IP}_3$  signalling in these cultures is necessary. Alternatively, agonist responses might be similar because the  $\text{Ca}^{2+}$  network, which has been remodelled, can still function appropriately as a whole.

#### Therapy

Current FDA approved treatment of GD focusses on reducing substrate accumulation through enzyme replacement therapy (ERT) (Tekoah et al., 2013). However, this treatment is inadequate at alleviating neuronopathic symptoms since recombinant enzymes are unable to permeate the blood brain barrier (Erikson, 2001). Therefore, neuro-pathology cannot be targeted by ERT. Alternative approaches for reducing substrate accumulation include inhibiting the synthesis of glucocerebroside with Miglustat (Cox, 2005). Yet, research presented in this chapter suggests that substrate accumulation does not impair  $\text{Ca}^{2+}$  homeostasis. Instead, mis-folded GCCase contributes to the pathology of GD and *GBA1*-PD. Indeed, many of the mis-folded enzymes retain catalytic activity provided they can reach the lysosomes (Lieberman et al., 2009; Bendikov-Bar et al., 2013). Thus, pharmacological chaperones, which enable the correct folding of GCCase and subsequent trafficking to the lysosomes, might prove therapeutically beneficial.

I show that the remodelling of  $\text{Ca}^{2+}$  stores by pathogenic *GBA1* might predispose to individuals to PD. Therefore,  $\text{Ca}^{2+}$  signalling proteins could represent new therapeutic targets for both GD and PD. Notably, inhibiting excessive RyR flux through the antagonism of these channels, using either siRNA, dantrolene, ryanodine or VGCC antagonists (Mu et al., 2008; Ong et al., 2010; Sun et al., 2009; Wang et al., 2011a, 2011b; Rigat & Mahuran, 2009) have

been shown to improve GD pathology. Moreover, these RyR antagonists are known to protect neurons from excitotoxicity (Korkotian et al., 1999). However, since these antagonists have been shown to increase ER Ca<sup>2+</sup> content (Ong et al., 2010), they might prove even more harmful in PD. Nevertheless, the effects of these compounds on Ca<sup>2+</sup> homeostasis requires further examination.

### Summary

Ca<sup>2+</sup> is an important signalling ion and its dysfunction has a prominent role in the onset of disease. Lysosomes trigger Ca<sup>2+</sup> signals which are amplified by the ER and ultimately received by the mitochondria. These Ca<sup>2+</sup> stores are delicately balanced to ensure appropriate physiological signalling. In this chapter, defects in ER, lysosomal and mitochondrial Ca<sup>2+</sup> homeostasis were identified in *GBA1* associated disease. Previous evidence has shown that a unique Ca<sup>2+</sup> stress is imposed upon SNc neurons (Chan et al., 2007). Thus the pathological Ca<sup>2+</sup> homeostasis, associated with *GBA1* mutations, might further disrupt SNc neurons and cause neurodegeneration. Aberrant Ca<sup>2+</sup> might also influence protein folding, autophagy, ATP production and apoptotic pathways to initiate PD onset. Targeting Ca<sup>2+</sup> signalling might therefore represent new therapeutic strategy for both GD and *GBA1*-PD.

# Chapter 5

---

## Lysosome Dysfunction - a Common Feature of Parkinson Disease?

### Introduction

Lysosomes are acidic structures that have an important role in regulating  $\text{Ca}^{2+}$  signalling and autophagy. Typically lysosomes adopt a spherical form with a diameter of ~500 nm. These acidic structures can be found throughout the cell and their movement along microtubules requires the trafficking GTPases Rab7 (Bucci & De Luca, 2012) and ARL8B (ADP-ribosylation factor-like 8B; Korolchuk et al. 2011). In fibroblasts, lysosomes occupy >0.5% percent of the cell volume (Lüllmann-rauch, 2005). Dysfunction of these acidic organelles is increasingly implicated in the pathology of PD. For instance, mutations in the genes encoding lysosomal proteins, such as GCase and ATP13A2, are known to cause PD and lysosome dysfunction (chapter 4, Dehay et al. 2012).

One of the most common, single genetic causes of familial PD is a mutation in *LRRK2*, which encodes the multi-domain enzyme LRRK2. The prevalent mutation, G2019S, targets the kinase domain of LRRK2 and increases catalytic activity (West et al., 2005). Downstream consequences of this gain-of-function are largely unknown. However, some reports have shown defects in the lysosomal-autophagic pathway. For instance, *LRRK2* kinase mutations have been shown to activate autophagy (Plowey et al., 2008). A recent study suggested that this activation involves the NAADP-sensitive  $\text{Ca}^{2+}$  channels (TPCs) which interact with LRRK2 (Gómez-Suaga et al., 2012). Furthermore, many have localised LRRK2 to structures of the endolysosomal system (Biskup et al., 2006; Alegre-Abarrategui et al., 2009; Higashi et al., 2009; Papkovskaia et al., 2012). Thus, like *GBA1*-mediated PD, lysosome dysfunction might feature in *LRRK2*-PD.

The onset of PD in the majority of patients is unknown. However, sporadic PD has been linked to variations in *LRRK2* (Di Fonzo et al., 2006) and exposure to environmental toxins (reviewed in Goldman 2014). One of these toxins, paraquat, is known to impair mitochondrial function and cause oxidative stress (Cochemé & Murphy, 2008). Like *LRRK2*, paraquat has also been shown to activate autophagy (Kiffin et al., 2004; González-Polo et al., 2007). Mak et al. (2010) established that the expression of a lysosomal membrane protein (LAMP type 2A), which



regulates autophagy, is increased in the dopaminergic neurons of paraquat exposed mice. Therefore, paraquat might also disrupt lysosome function.

In this chapter I will explore whether lysosomal defects *connect* genetic and environmental PD.

## Methods

### Cell details

Primary human fibroblasts, established from skin biopsies, were generated by Dr Jan-Willem Taanman and Dr Tatiana Papkovskaia (Royal free hospital, UCL). PD patients carried the G2019S mutation in *LRRK2*. For comparison, fibroblasts were also acquired from age-matched, apparently healthy individuals without mutations in *LRRK2*. Additional details of the fibroblasts are included in table 5.1.

Table 5.1. Details of patient-derived fibroblast cultures.

| Patient code                  | Sex    | Age | Genotype  | Clinical features  |
|-------------------------------|--------|-----|-----------|--------------------|
| CTRL <sub>1</sub>             | Female | 50  | WT/WT     | Apparently healthy |
| CTRL <sub>2</sub>             | Female | 52  | WT/WT     | Apparently healthy |
| <i>LRRK2</i> -PD <sub>1</sub> | Female | 48  | G2019S/WT | Parkinson disease  |
| <i>LRRK2</i> -PD <sub>2</sub> | Female | 52  | G2019S/WT | Parkinson disease  |

SH-SY5Y cell lines with the stable expression of wild-type and G2019S mutated *LRRK2* (Papkovskaia et al., 2012) were developed by Drs Kai-Yin Chau and Mark Cooper (Royal free hospital, UCL).

Fibroblast and SH-SY5Y cultures were maintained as described in chapter 2. In some cases, fibroblasts were treated overnight in culture with 500  $\mu$ M Paraquat (dissolved in H<sub>2</sub>O).

### Immunocytochemistry

LAMP1 immunocytochemistry was conducted as described in chapter 2. Fibroblasts were also incubated for 1 hour at 37°C with anti-EEA1 (Early Endosome Antigen 1; diluted 1:100; SantaCruz Biotechnology) and anti-CD63 (H5C6 clone; diluted 1:10; Developmental Studies Hybridoma Bank) antibodies. Respectively, the secondary antibodies used were conjugated to Alexafluor 488 (goat) and Alexafluor 647 (mouse) (both diluted 1:100, Invitrogen).

### Microscopy

Confocal microscopy was performed as described in chapter 2. Alexafluor 488 and AlexaFluor 647 fluorescence was excited using wavelengths of 488 nm and 633 nm and emitted

fluorescence was captured using either 505-530 nm or 655-719 nm band-pass filters respectively.

#### siRNA

siRNA transfection was performed as described in chapter 3 using siRNA duplexes targeting TPC1 (5'-CGAGCTGTATTTTCATCATGAA-3') and TPC2 (5'-CAGGTGGGACCTCTGCATTGA-3') (both Qiagen).

#### Western blotting

Western blotting was conducted as described in chapter 3, except homogenates were denatured for 1 hour at room temperature and run on NuPage 4-12% Bis-Tris gels (Invitrogen). Blots were sequentially incubated with the primary anti-TPC1 (1 hour at RT, diluted 1:200, Abcam) antibody and secondary anti-rabbit (1 hour at room temperature, 1:2000, Biorad) antibody.

#### Recurrent methods

Lysotracker imaging and image analysis were performed as described in chapter 2.

## Results

#### Lysosome morphology is disrupted in *LRRK2*-PD models

Since lysosome dysfunction is often associated with changes in lysosome morphology, I examined lysosome form in *LRRK2*-PD patient fibroblasts by immunocytochemistry using an antibody raised against LAMP1. Representative confocal images are shown in figure 5.1A-B. When compared to age-matched controls, the lysosomes in *LRRK2*-PD fibroblasts appeared enlarged and clustered together. *LRRK2*-PD lysosome pathology was associated with increased LAMP1 fluorescence intensity (Figure 5.1C). Lysosome morphology was also examined in live cells using the acidotropic fluorescent indicator LysoTracker red (Figure 5.1D-E). Again, lysosome form was disrupted in *LRRK2*-PD fibroblasts (Figure 5.1F) and associated with increased LysoTracker fluorescence intensity.

To examine lysosome morphology in a more neuronal context, dopaminergic SH-SY5Y cells, which stably express wild-type and G2019S mutated *LRRK2*, were analysed (Figure 5.2). Similar to the diseased fibroblasts, lysosomes appeared enlarged and clustered the G2019S expressing SH-SY5Y cells when compared to the parental (control) and wild-type *LRRK2* expressing lines (Figure 5.2A-C). These defects were associated with a 70% increase in LAMP1 fluorescence intensity.

Late, but not early, endosome morphology is disrupted in *LRRK2*-PD patient fibroblasts  
 Since *LRRK2*-PD has been associated with disrupted lysosomal morphology, other compartments of the endo-lysosomal system were examined. Endosome morphology in the fibroblasts was assessed using antibodies raised to either EEA1 or CD63 which are markers for early and late endosomes, respectively. Early-endosome morphology in *LRRK2*-PD fibroblasts was similar to age matched controls, as shown by representative confocal images and EEA1 fluorescence intensity (Figure 5.3 A-B and E). In contrast, late-endosomes appeared enlarged and proliferated in *LRRK2*-PD cultures, much like the lysosomes seen in figure 5.1. Late endosome defects were associated with a 2-fold increase in CD63 fluorescence intensity (Figure 5.3F).

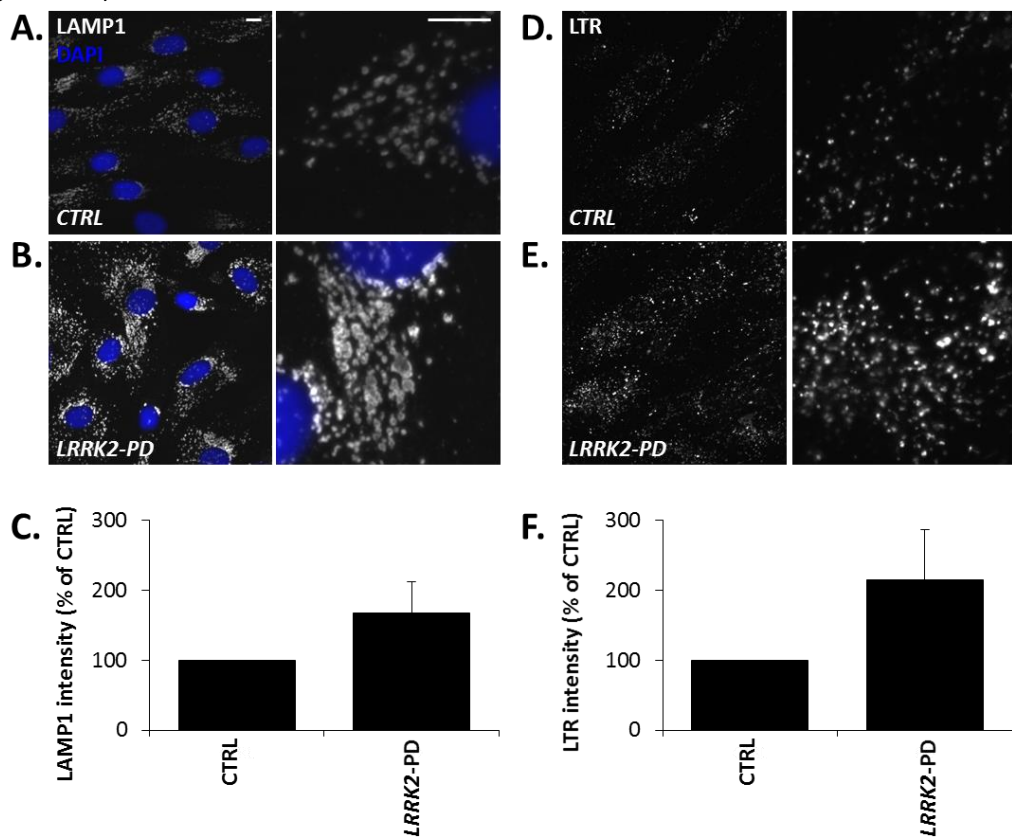


**Figure 5.1 Lysosome morphology is disrupted in *LRRK2*-PD fibroblasts**

(A-B) Representative confocal fluorescence images of LAMP1 (white) staining in CTRL (A) and *LRRK2*-PD (B) fibroblasts. Zoomed images are displayed in the right panels. Nuclei were stained using DAPI (blue). Scale bars, 10  $\mu$ m.

(C) Summary data (mean  $\pm$  S.E.M) quantifying LAMP1 intensity as a percentage of CTRL. Results are from 4 independent experiments analysing 94-153 cells in 2 patient and paired control fibroblast lines.

(D-E) Representative confocal fluorescence images of CTRL (D) and *LRRK2*-PD (E) fibroblasts labelled with Lysotracker (White). Zoomed images are displayed in the right panels.

(F) Summary data (mean  $\pm$  S.E.M) quantifying Lysotracker intensity as a percentage of CTRL. Results are from 3 independent platings (*n*) analysing 108-109 cells in 2 patient and paired control fibroblast lines.

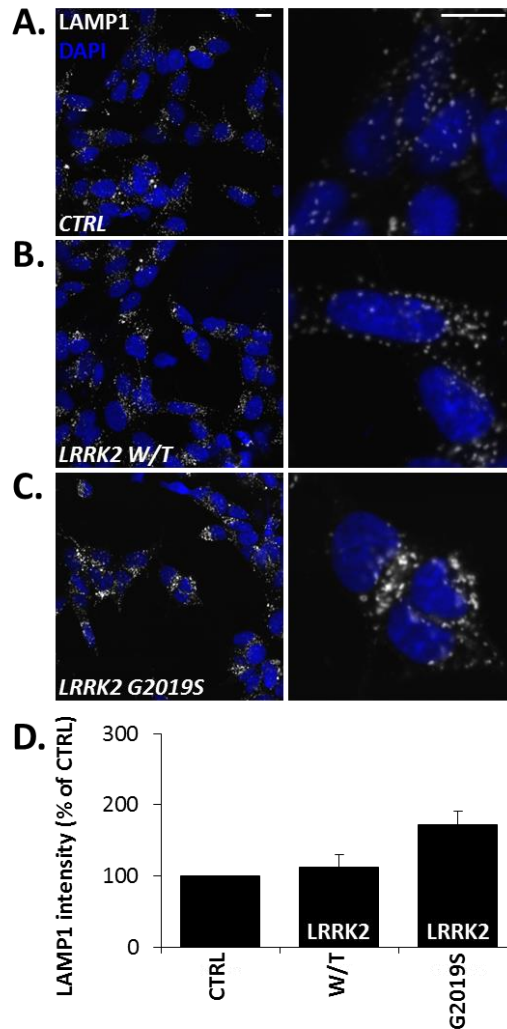


**Figure 5.2 Lysosome morphology is disrupted in dopaminergic SH-SY5Y cells overexpressing mutant *LRRK2***

(A-B) Representative confocal fluorescence images of LAMP1 (white) staining in CTRL dopaminergic SH-SY5Y cells (A) or SH-SY5Y cells overexpressing wild-type *LRRK2* (B) and G2019S mutated *LRRK2* (C). Zoomed images are displayed in the right panels. Nuclei were stained using DAPI (blue). Scale bars, 10  $\mu$ m.

(D) Summary data (mean  $\pm$  S.E.M) quantifying LAMP1 intensity as a percentage of CTRL. Results from 3 independent platings ( $n$ ) analysing 254-340 cells.

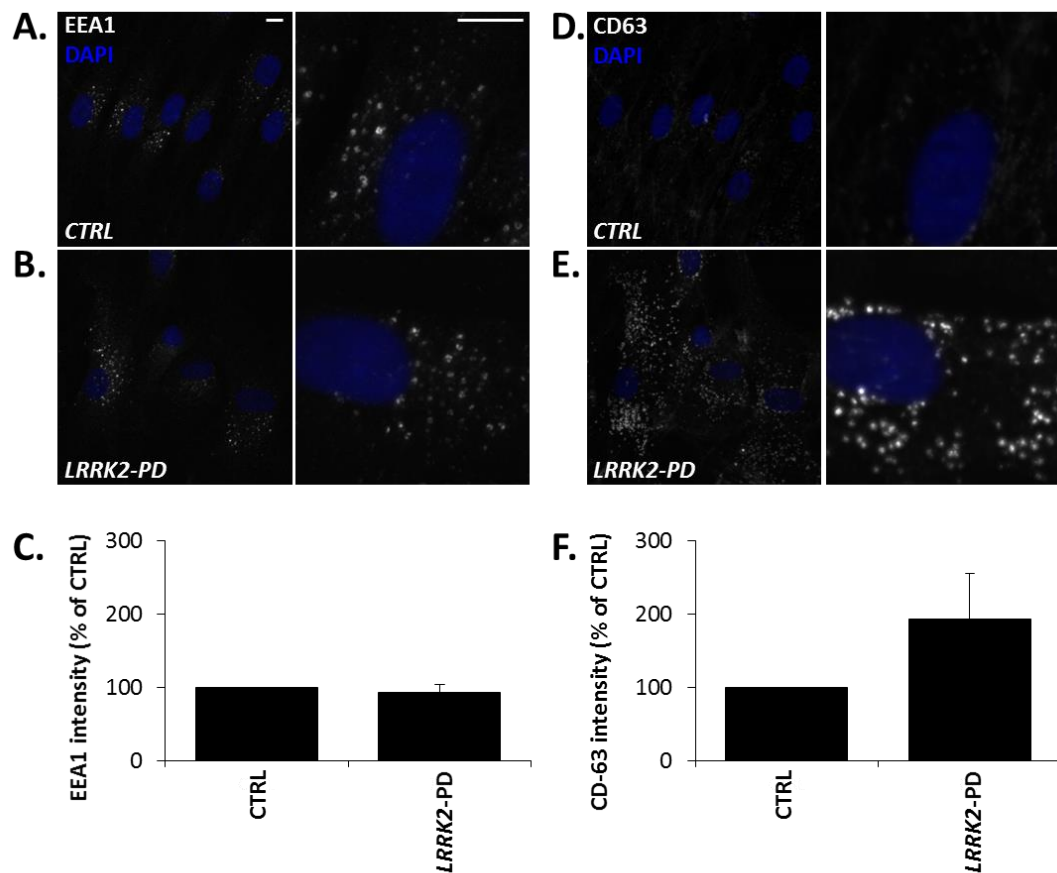


**Figure 5.3 Late, but not early, endosome morphology is disrupted in *LRRK2*-PD patient fibroblasts**

(A-B) Representative confocal fluorescence images of EEA1 (white) staining in CTRL (A) and *LRRK2*-PD (B) fibroblasts. Zoomed images are displayed in the right panels. Nuclei were stained using DAPI (blue). Scale bars, 10  $\mu$ m.

(C) Summary data (mean  $\pm$  S.E.M) quantifying EEA1 intensity as a percentage of CTRL. Results are from 5 experiments of 3 independent platings analysing 155-134 cells in 2 patient and paired control fibroblast lines.

(D-E) Representative confocal fluorescence images of CD63 (white) staining in CTRL (D) and *LRRK2*-PD (E) fibroblasts. Zoomed images are displayed in the right panels. Nuclei were stained using DAPI (blue).

(F) Summary data (mean  $\pm$  S.E.M) quantifying CD63 intensity as a percentage of CTRL. Results are from 3 independent experiments (*n*) analysing 65-66 cells in 2 patient and paired control fibroblast line.

#### Disrupted *LRRK2*-PD lysosome morphology is reversed by silencing TPC2

Previous research has reported interactions between TPCs and *LRRK2* (Gómez-Suaga et al., 2012). To probe the role of these lysosomal ion channels in *LRRK2*-PD pathology, siRNAs targeting TPCs were used. The impaired lysosome morphology seen in *LRRK2* PD (Figures 5.4

A-B) was reversed upon TPC2 siRNA treatment (figure 5.4D and E). Notably, this reversal was isoform-specific since TPC1 siRNA (Figure 5.4C) did not affect lysosome morphology despite a 90% knockdown of TPC1 protein levels in *LRRK2*-PD fibroblasts (shown in the inset of 5.4E).

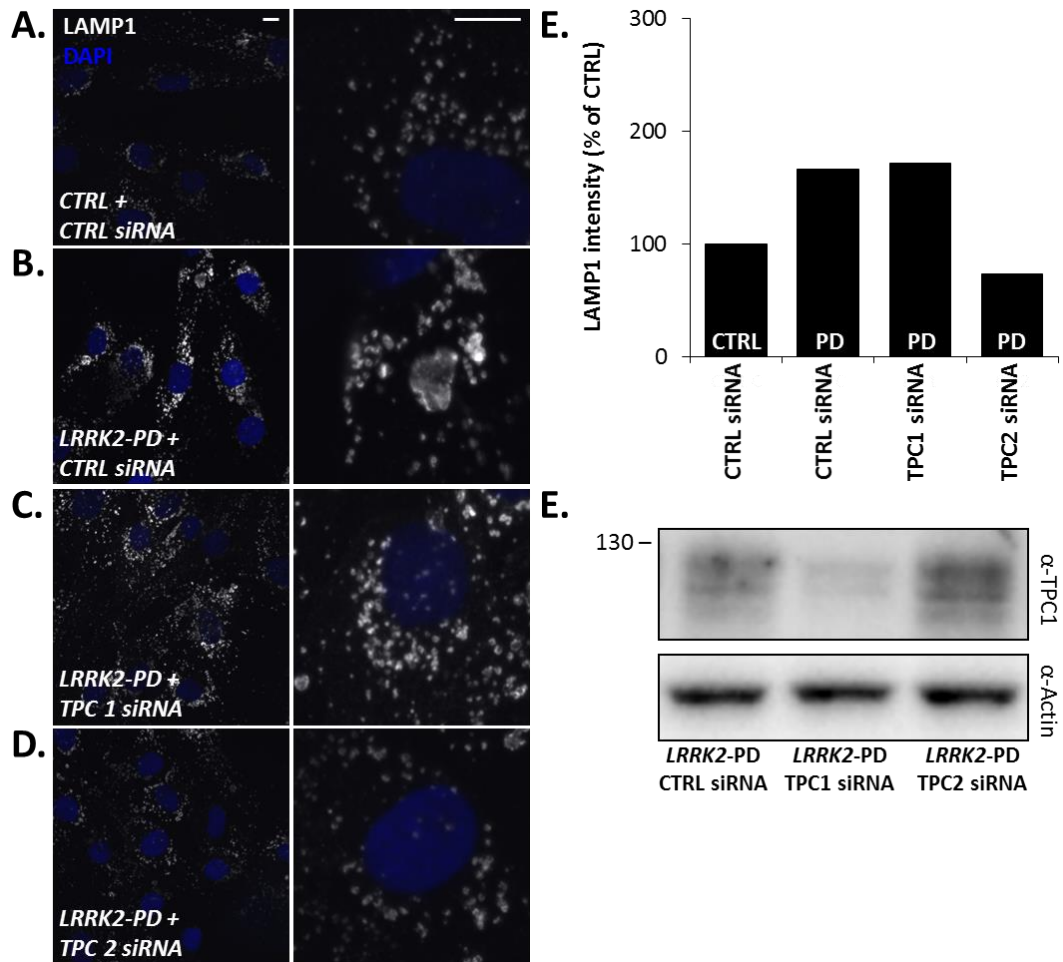


**Figure 5.4 Disrupted *LRRK2*-PD lysosome morphology is reversed by silencing TPC2**

(A-B) Representative confocal fluorescence images of LAMP1 (white) staining in CTRL (A) and *LRRK2*-PD (B-D) fibroblasts treated with CTRL siRNA (A-B), TPC1 siRNA (C) and TPC2 siRNA (D). Zoomed images are displayed in the right panels. Nuclei were stained using DAPI (blue). Scale bars, 10  $\mu$ m.

(E) Summary data (mean) quantifying LAMP1 intensity as a percentage of CTRL. Results are from 2 independent knockdowns (*n*) analysing 63-76 cells.

(F) Western blot using antibodies to TPC1 (top) or actin (bottom) and homogenates (17  $\mu$ g) from *LRRK2*-PD fibroblasts treated with the indicated siRNA.

#### Lysosome morphology is disrupted in fibroblasts treated with a PD inducing toxin

Data reported in this thesis demonstrates that mutations in two of the most common PD-associated genes (*GBA1* and *LRRK2*) disrupt lysosome morphology. However, the cause of PD

in a significant portion patients is unknown. Environmental toxins, such as paraquat (Liou et al., 1997; Tanner et al., 2011), have been linked to the onset of PD. To examine whether lysosome pathology extends into environmental models of PD, the morphology of lysosomes was assessed in fibroblasts exposed to paraquat. As shown in figure 5.5, lysosomes appeared enlarged in paraquat-treated fibroblasts relative to the control cells (figure 5.5A-B). These defects were associated with a 2-fold increase in LAMP1 intensity (figure 5.5C).

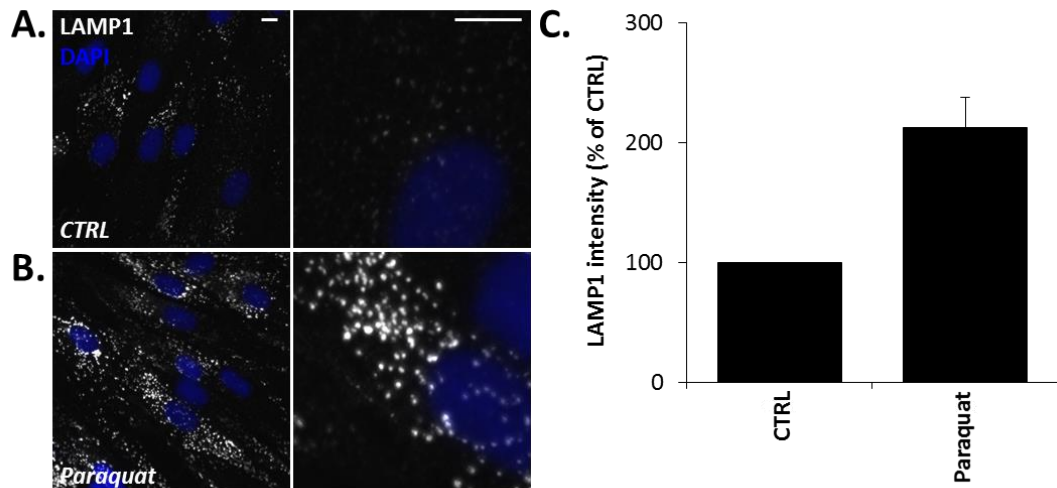


**Figure 5.5 Lysosome morphology is disrupted in fibroblasts treated with a PD inducing toxin**

(A-B) Representative confocal fluorescence images of LAMP1 (white) staining in CTRL fibroblasts (A) and fibroblasts treated with Paraquat (500  $\mu$ M) overnight (B). Zoomed images are displayed in the right panels. Nuclei were stained using DAPI (blue). Scale bars, 10  $\mu$ m.

(C) Summary data (mean  $\pm$  S.E.M) quantifying LAMP intensity as a percentage of CTRL. Results are from 6 treatments ( $n$ ) from 4 independent platings analysing 110-157 cells.

## Discussion

In this chapter I have identified pronounced endo-lysosomal morphology defects, in genetic and environmental models of PD. These defects can be corrected by silencing TPC2, which establishes these ion channels as potential therapeutic targets in PD.

Emerging evidence has connected LRRK2 pathology with lysosomal dysfunction. As discussed above, LRRK2 has been localised to membranes of the endo-lysosomal system (Biskup et al., 2006; Alegre-Abarategui et al., 2009; Higashi et al., 2009; Papkovskaia et al., 2012). In Lewy body pathology, LRRK2-associated vesicular structures are swollen (Higashi et al., 2009). Additionally, MacLeod et al. (2006) report that mutant (G2019S) LRRK2 expression in neuronal cultures cause spheroid inclusions made up of enlarged lysosomes. Therefore, endo-lysosomal dysfunction in patient fibroblasts (Figure 5.1) and mutant LRRK2 expressing dopaminergic cells (figure 5.2) agrees with established research. However, it is notable that,

some have reported reduced LysoTracker fluorescence in HEK cells overexpressing LRRK2 (Gómez-Suaga et al., 2012). The authors proposed that this is a consequence of increased luminal pH. This contrasts with the data presented herein. Thus, further investigation into lysosomal pH in *LRRK2*-PD is warranted.

Changes in lysosomal morphology can impact a number of functions. For instance, lysosome proliferation, stimulated by activating the lysosomal transcription factor TFEB, can affect protein clearance (Sardiello et al., 2009). Lysosome proliferation is also known to impair lysosomal  $\text{Ca}^{2+}$  signalling (Dickinson et al., 2010). Furthermore, lysosome positioning can influence recovery from nutrient deprivation as well as autophagy (Korolchuk et al., 2011). Thus, *LRRK2*-dependent defects in lysosomal morphology likely affect many lysosomal functions.

LRRK2 is known to regulate intracellular membrane trafficking. LRRK2 can exert effects on endocytosis (Gómez-Suaga et al., 2014; Shin et al., 2008), synaptic vesicle trafficking (Piccoli et al., 2011) and retromer trafficking from late endosomes to Golgi (MacLeod et al., 2013). The association between LRRK2 and Rab trafficking proteins is thought to be essential in mediating these events (Shin et al., 2008; Dodson et al., 2012; MacLeod et al., 2013; Gómez-Suaga et al., 2014). Indeed, I noted a propensity for lysosomes to cluster together in *LRRK2*-PD fibroblasts. This suggests lysosomal trafficking is impaired in *LRRK2*-PD. The effects of inhibiting Rab GTPase activity on lysosomal morphology and distribution should be examined. The recent discoveries that TPCs interact with both Rab7 (Lin-Moshier et al., 2014) and LRRK2 (Gómez-Suaga et al., 2012) are perhaps significant to LRRK2 pathology because these proteins might associate in a ternary complex to regulate vesicular trafficking.

Although late-endosome and lysosomal morphology is disrupted in *LRRK2*-PD, early endosome morphology is spared (Figure 5.3). Perhaps LRRK2 exerts effects on the later stages of the endocytic pathway. Indeed, both Gómez-Suaga et al. (2014) and MacLeod et al. (2013) report that only late-endosome trafficking is impaired in *LRRK2*-PD.

It is also well established that LRRK2 regulates autophagy (Tong et al., 2010, 2012; Plowey et al., 2008; Gómez-Suaga et al., 2012; Manzoni et al., 2013b). Perhaps, the lysosome dysfunction present in *LRRK2*-PD impairs autophagic balance. Of importance, antagonising NAADP signalling with Ned-19 and expressing TPC2 dominant negative pore mutants have been shown to restore autophagy in *LRRK2*-G2019S expressing cells (Gómez-Suaga et al.,



2012). This is reminiscent of data presented in this chapter, where TPC2 silencing reverses lysosomal morphology defects (Figure 5.4).

It is intriguing that silencing TPC2, but not TPC1, corrected morphology defects. Perhaps this selectivity is because LRRK2 interacts with TPC2 (Gómez-Suaga et al., 2012). LRRK2 might over-activate TPC2 and cause lysosomal dysfunction. In support of this statement, Lin-Moshier et al. (2014) have recently shown that overexpressing TPC2, yet not TPC1, recapitulated lysosome dysfunction in *Xenopus* oocytes. Increased TPC2 activity might promote lysosomal fusion, which is known to be Ca<sup>2+</sup> dependent process (Pryor et al., 2000). Buffering cytosolic Ca<sup>2+</sup> and measuring TPC-mediated Ca<sup>2+</sup> signalling in *LRRK2*-PD is necessary to test this hypothesis.

It is necessary to further examine the therapeutic benefits of targeting TPCs in *LRRK2*-PD. Antagonising NAADP action, with Ned-19 (Naylor et al., 2009), might also reverse lysosomal defects. Furthermore, since PI(3,5)P<sub>2</sub> has recently been identified as an activator of TPCs (Jha et al., 2014), the effects of depleting this phosphoinositide should be determined. This could be achieved by inhibiting its synthesis with YM-201636 (Jefferies et al., 2008). The therapeutic benefits of targeting TPC2 could be assessed in neuronal models. It has been well-established that LRRK2 affects the complexity and length of neurites (MacLeod et al., 2006; Plowey et al., 2008). Accordingly, neurite morphology serves as a sensitive measure of LRRK2 pathogenic activity. Neurite complexity has already been used to test the efficacy of LRRK2 kinase inhibitors (Lee et al., 2010a; Ramsden et al., 2011) and could now be applied to examine the benefits of targeting TPC2.

To the best of my knowledge, this is the first report of lysosome pathology following exposure to paraquat (Figure 5.5). However, the mechanism behind this dysfunction requires further examination. Perhaps the reactive oxygen species (ROS) that paraquat generates causes lysosome dysfunction. It has already been well-established that ROS target lysosomes (reviewed in Kiffin et al. 2006). Indeed paraquat-evoked oxidative stress was recently shown to increase the expression of lysosomal membrane proteins (Mak et al., 2010). However, it is noteworthy that MPTP, a structurally similar analogue, has actually been shown to reduce the number of lysosomes by inducing lysosomal membrane permeabilisation (Dehay et al., 2010).

Recent work has established that cells overexpressing the lysosomal ATPase *ATP13A2* (associated with PD) are more vulnerable to paraquat toxicity (Pinto et al., 2012). This

suggests more direct role of paraquat on lysosomes. Since paraquat is an amine perhaps it accumulates within lysosomes (Kaufmann & Krise, 2007) and causes dysfunction. It has been estimated that paraquat has a  $pK_a$  between 9-9.5 (Milman, 2003). Consistent with this hypothesis, a weak base with  $pK_a$  value of 9 was shown to accumulate at very high levels in the lysosomes (Duvvuri et al., 2005). Further work is required to uncover the mechanism behind paraquat-evoked lysosomal defects.

In summary, data identifies extensive endo-lysosomal morphology defects in genetic and environmental forms of PD. These defects likely to impair many cellular processes. The striking lysosome pathology present in PD identifies lysosomes as important markers of disease. Indeed lysosome morphology has already been used to track disease progression in LSDs (te Vrugte et al., 2014). Since this lysosome impairment can be corrected by TPC2, efforts should focus on therapeutic viability of targeting TPCs in PD.

# Chapter 6

---

## Conclusions and Future Directions

Ca<sup>2+</sup> is a ubiquitous signalling ion that controls a plethora of cellular functions. Many Ca<sup>2+</sup> signals originate from intracellular Ca<sup>2+</sup> stores. These Ca<sup>2+</sup> stores are delicately balanced within the cell and defects in the Ca<sup>2+</sup> network are increasingly implicated in disease. In this thesis I set out to examine the *connections* between Ca<sup>2+</sup> stores and determine whether their dysfunction is *connected* to Parkinson disease.

In chapter 2, I established that the lysosomes and ER are functionally coupled (Figure 6.1). It had already been known that NAADP can trigger Ca<sup>2+</sup> release from ER channels (Cancela et al., 1999). However, the uncertainty surrounding NAADP action (Gerasimenko et al., 2003; Dammermann et al., 2009) had led some to doubt these findings. So I examined the functional coupling between these stores using a more direct approach. Much like NAADP, I found that the direct mobilisation of lysosomal Ca<sup>2+</sup>, with GPN, was sufficient to induce complex, IP<sub>3</sub>R-mediated Ca<sup>2+</sup> signalling. Physical *connections* (MCSs) between lysosomes and the ER (Kilpatrick et al., 2013) could facilitate this Ca<sup>2+</sup> coupling. Indeed, computational models confirmed that these close contacts regulate Ca<sup>2+</sup> signalling (Penny et al., 2014).

In chapter 3, I further examined the mechanism behind lysosomal-ER Ca<sup>2+</sup> coupling. Previous research established that endosome-ER MCSs are regulated by Rab7 and VAP proteins (Rocha et al., 2009). So I questioned whether similar components also mediate lysosome-ER Ca<sup>2+</sup> signalling. Both the molecular and chemical inhibition of Rab7, but not VAP, blocked the Ca<sup>2+</sup> coupling between these stores. These findings suggest that Rab7 regulates lysosome-ER *connections*. However, our understanding of these junctions is still limited. Perhaps examining MCSs between other organelles and working on model organisms would advance this research. Additionally, using a novel synthetic activator of TRPML (Shen et al., 2012), I established that like TPCs, TRPML channels are capable of “chatter” with the ER. Further characterisation of this Ca<sup>2+</sup> coupling is of pathological relevance since LSDs have been linked to dysfunctional TRPML-mediated Ca<sup>2+</sup> signalling.

In the subsequent chapters I identified that Ca<sup>2+</sup> stores are disrupted in PD (Figure 6.1). Specifically in *GBA1*-PD, both ER and mitochondrial Ca<sup>2+</sup> levels were increased, whereas lysosomal Ca<sup>2+</sup> was reduced. These defects were shown to be age-dependent and associated disrupted physiological Ca<sup>2+</sup> signalling. It was very interesting that ER Ca<sup>2+</sup> was not

compromised asymptomatic *GBA1* carriers. Thus,  $\text{Ca}^{2+}$  homeostasis might represent a useful diagnostic marker for PD.

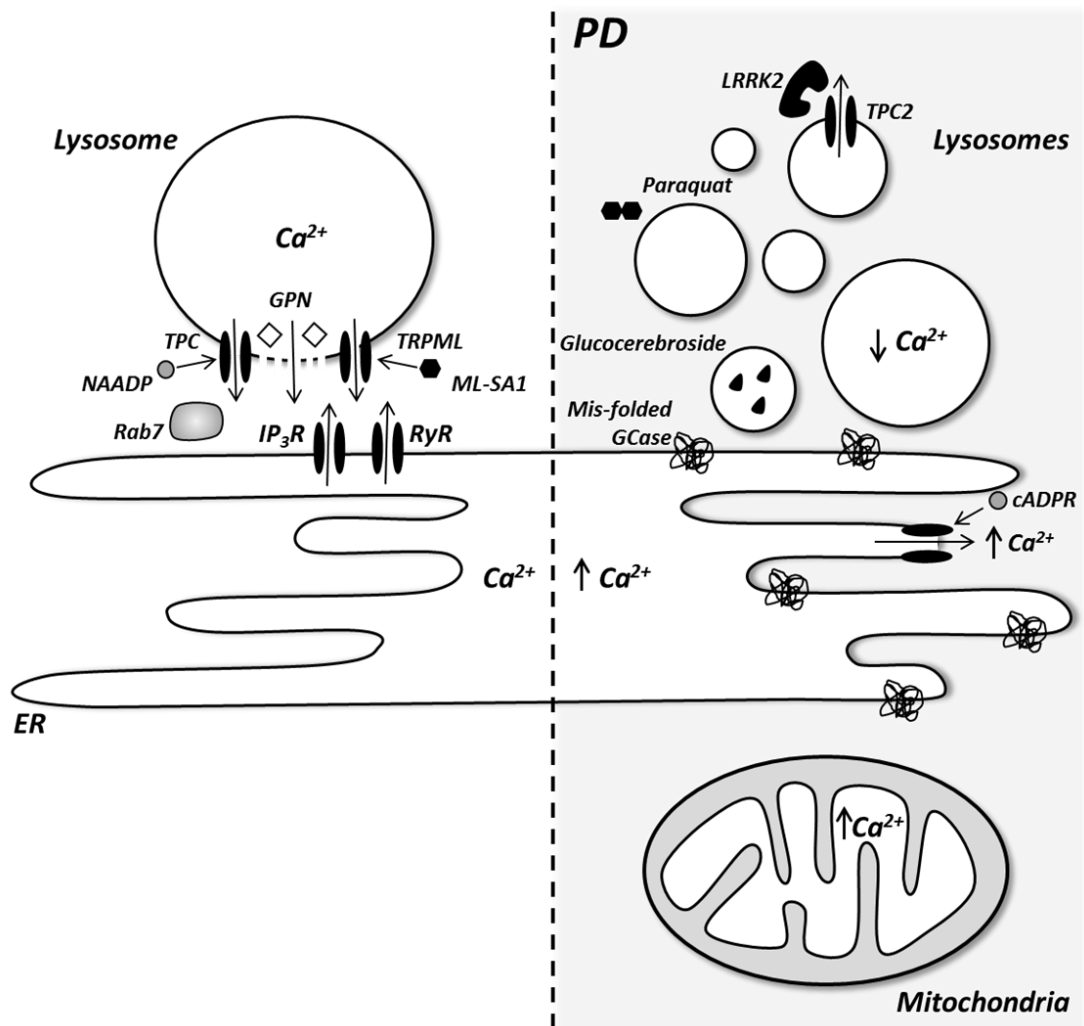


**Figure 6.1. Connecting  $\text{Ca}^{2+}$  stores and Parkinson Disease**

In healthy fibroblasts, the direct mobilisation of lysosomal  $\text{Ca}^{2+}$ , with GPN, can stimulate complex,  $\text{IP}_3\text{R}$ -dependent  $\text{Ca}^{2+}$  signalling. Both NAADP and ML-SA1, which activate TPCs and TRPMLs, can also evoke complex  $\text{Ca}^{2+}$  signals. ML-SA1-evoked  $\text{Ca}^{2+}$  responses required ER- $\text{Ca}^{2+}$  channels. Membrane contact sites and the trafficking GTPase Rab7 likely facilitate lysosome-ER  $\text{Ca}^{2+}$  coupling.

In Parkinson disease (PD)  $\text{Ca}^{2+}$  stores are disrupted. In *GBA1*-PD patient fibroblasts the  $\text{Ca}^{2+}$  content the mitochondria and ER was increased. Enhanced ER  $\text{Ca}^{2+}$  content was associated with increased responses to the RyR activator, cADPR. Mis-folded enzyme (GCase), but not an accumulations of substrate (glucocerebroside), was shown to disrupt ER  $\text{Ca}^{2+}$  homeostasis. Conversely, lysosomal  $\text{Ca}^{2+}$  content was reduced in *GBA1*-PD and associated with disrupted lysosome morphology. Lysosome pathology was also identified in *LRRK2*-PD patient fibroblasts and paraquat exposed fibroblasts. In *LRRK2*-PD, lysosomal defects might be associated with aberrant TPC2 activity since silencing TPC2 corrected the phenotype.

The functional coupling between  $\text{Ca}^{2+}$  stores might explain the redistribution of  $\text{Ca}^{2+}$ . At the ER-lysosomal level, the reciprocal changes in  $\text{Ca}^{2+}$  content could be attributed to compensation. For instance, an accumulation of mis-folded enzyme on the ER could increase ER  $\text{Ca}^{2+}$  and to balance the  $\text{Ca}^{2+}$  network, lysosomal content reduces. On the other hand, lysosomal dysfunction might impair the capacity of lysosomes to temper  $\text{Ca}^{2+}$  and to compensate the ER has to sequester the excess  $\text{Ca}^{2+}$ . In any scenario, the increased ER  $\text{Ca}^{2+}$  could be transmitted to the mitochondria, via MAMs.

Since many cellular functions rely on a delicately balanced intracellular  $\text{Ca}^{2+}$  network, altered  $\text{Ca}^{2+}$  signalling might contribute to PD pathology, particularly in SNc neurons. It is already known that the unusual pace-making activity of SNc neurons, which relies on  $\text{Ca}^{2+}$  influx through VGCCs (Chan et al., 2007), imposes a unique stress on these cells (Guzman et al., 2010). Thus, the disrupted intracellular  $\text{Ca}^{2+}$  signalling in ageing and *GBA1*-disease, could further impair SNc neurons and increase the risk of neurodegeneration.

$\text{Ca}^{2+}$  signalling proteins and antagonists might therefore represent viable therapeutic targets in PD. Already, dihydropyridines have been shown neuroprotective in animal models of PD (Ilijic et al., 2011) and these antagonists, which are FDA approved for the treatment of hypertension, reduce the risk of PD development (Becker et al., 2008; Ritz et al., 2010; Pasternak et al., 2012). Other strategies might involve reducing ER  $\text{Ca}^{2+}$  content or increasing  $\text{Ca}^{2+}$  uptake into lysosomes. However, since we do not know the mechanism of lysosomal  $\text{Ca}^{2+}$  uptake this hypothesis is difficult to test. Uncovering the molecular identity of this exchanger is pathologically relevant. Instead, we could reduce ER  $\text{Ca}^{2+}$  content by targeting SERCA with thapsigargin and curcumin (an antioxidant that also functions as mild SERCA inhibitor). Indeed, these compounds have been effectively used in NPC (Lloyd-Evans et al., 2008).

In addition to impaired  $\text{Ca}^{2+}$  signalling I also identified that both genetic (*GBA1* and *LRRK2*) and environmental (paraquat) forms of PD were associated with impaired lysosomal morphology. Perhaps these defects disrupt lysosome-dependent processes as well as the physical and functional coupling with the ER (Kilpatrick et al., 2013). It is important to examine whether similar defects feature in idiopathic PD. For *LRRK2*-PD, at least, lysosome pathology could be corrected by silencing TPC2. This identifies TPC2 as a potential therapeutic target in PD. Future work should examine whether targeting TPC2 can reverse *GBA1*- and paraquat-mediated defects.

Fibroblasts have been used extensively in this thesis to examine  $\text{Ca}^{2+}$  signalling and PD. The large size (120  $\mu\text{m}$ ) and flat nature of these cells facilitates their imaging. As human cells they are of significant physiological relevance and are frequently used to model PD (Papkovskaia et al., 2012; McNeill et al., 2014). However, using skin cells to study neurodegenerative disease has some drawbacks. Namely, fibroblasts do not display the same gene expression profile as neurons. For instance,  $\alpha$ -syn is only expressed in low levels in fibroblasts (Auburger et al., 2012). Furthermore, the control of receptors and ion channels in fibroblasts is not as complex as neurons. Therefore, the work presented here might not be representative of pathology in neurons. In an attempt to bridge this gap, I also used dopaminergic cell lines. Indeed, the pathology identified in fibroblasts could be recapitulated in these cell lines. However, a better, although technically demanding, approach would be reprogramming fibroblasts into adult IPS (induced pluripotent stem) cells and then differentiated them into dopaminergic neurons (Pfisterer et al., 2011; Caiazzo et al., 2011). Indeed, GD (Panicker et al., 2012), *GBA1*-PD (Schöndorf et al., 2014) and *LRRK2*-PD (Nguyen et al., 2011) patient fibroblasts have recently been converted to neurons. It is important that future research examines  $\text{Ca}^{2+}$  signalling and lysosomal morphology in these cells.

In summary, I identified that lysosomal and ER  $\text{Ca}^{2+}$  stores are functionally *connected* and that their dysfunction is *connected* to PD. While this research has advanced our understanding of lysosomal and pathological  $\text{Ca}^{2+}$  signalling, many questions remain. Future research should focus on characterising lysosome-ER junctions and identifying therapies for PD and associated LSDs. It is also important to establish whether similar dysfunction features in idiopathic PD. Finally, this research should be replicated in human iPSc-derived lines to validate findings in a more neuronal context.

# References

---

- Agola, J.O., Hong, L., Surviladze, Z., Ursu, O., Waller, A., Strouse, J.J., Simpson, D.S., Schroeder, C.E., Oprea, T.I., Golden, J.E., Aubé, J., Buranda, T., Sklar, L. a & Wandinger-Ness, A. (2012). A competitive nucleotide binding inhibitor: in vitro characterization of Rab7 GTPase inhibition. *ACS chemical biology*. 7 (6). p.pp. 1095–108.
- Aharon-Peretz, J., Rosenbaum, H. & Gershoni-Baruch, R. (2004). Mutations in the glucocerebrosidase gene and Parkinson's disease in Ashkenazi Jews. *The New England journal of medicine*. 351 (19). p.pp. 1972–7.
- Aits, S. & Jäättelä, M. (2013). Lysosomal cell death at a glance. *Journal of cell science*. 126 (Pt 9). p.pp. 1905–12.
- Alegre-Abarrategui, J., Christian, H., Lufino, M.M.P., Mutihac, R., Venda, L.L., Ansorge, O. & Wade-Martins, R. (2009). LRRK2 regulates autophagic activity and localizes to specific membrane microdomains in a novel human genomic reporter cellular model. *Human molecular genetics*. 18 (21). p.pp. 4022–34.
- Alpy, F., Rousseau, A., Schwab, Y., Legueux, F., Stoll, I., Wendling, C., Spiegelhalter, C., Kessler, P., Mathelin, C., Rio, M.-C., Levine, T.P. & Tomasetto, C. (2013). STARD3 or STARD3NL and VAP form a novel molecular tether between late endosomes and the ER. *Journal of cell science*. 126 (Pt 23). p.pp. 5500–12.
- Arduíno, D.M., Esteves, a R., Cardoso, S.M. & Oliveira, C.R. (2009). Endoplasmic reticulum and mitochondria interplay mediates apoptotic cell death: relevance to Parkinson's disease. *Neurochemistry international*. 55 (5). p.pp. 341–8.
- Arif, S.H. (2009). A Ca(2+)-binding protein with numerous roles and uses: parvalbumin in molecular biology and physiology. *BioEssays : news and reviews in molecular, cellular and developmental biology*. 31 (4). p.pp. 410–21.
- Arighi, C.N., Hartnell, L.M., Aguilar, R.C., Haft, C.R. & Bonifacino, J.S. (2004). Role of the mammalian retromer in sorting of the cation-independent mannose 6-phosphate receptor. *The Journal of cell biology*. 165 (1). p.pp. 123–33.
- Auburger, G., Klinkenberg, M., Drost, J., Marcus, K., Morales-Gordo, B., Kunz, W.S., Brandt, U., Broccoli, V., Reichmann, H., Gispert, S. & Jendrach, M. (2012). Primary skin fibroblasts as a model of Parkinson's disease. *Molecular neurobiology*. 46 (1). p.pp. 20–7.
- Augustine, G.J. (2001). How does calcium trigger neurotransmitter release? *Current Opinion in Neurobiology*. 11 (3). p.pp. 320–326.
- Beavan, M.S. & Schapira, A.H. V (2013). Glucocerebrosidase mutations and the pathogenesis of Parkinson disease. *Annals of medicine*. 45 (8). p.pp. 511–21.

- Becker, C., Jick, S.S. & Meier, C.R. (2008). Use of antihypertensives and the risk of Parkinson disease. *Neurology*. 70 (16 Pt 2). p.pp. 1438–44.
- Bendikov-Bar, I., Maor, G., Filocamo, M. & Horowitz, M. (2013). Ambroxol as a pharmacological chaperone for mutant glucocerebrosidase. *Blood cells, molecules & diseases*. 50 (2). p.pp. 141–5.
- Bendikov-Bar, I., Ron, I., Filocamo, M. & Horowitz, M. (2011). Characterization of the ERAD process of the L444P mutant glucocerebrosidase variant. *Blood cells, molecules & diseases*. 46 (1). p.pp. 4–10.
- Berg, I., Potter, B. V, Mayr, G.W. & Guse, a H. (2000). Nicotinic acid adenine dinucleotide phosphate (NAADP(+)) is an essential regulator of T-lymphocyte Ca(2+)-signaling. *The Journal of cell biology*. 150 (3). p.pp. 581–8.
- Berg, T.O., Strømhaug, E., Løvdaal, T., Seglen, O. & Berg, T. (1994). Use of glycyl-L-phenylalanine 2-naphthylamide, a lysosome-disrupting cathepsin C substrate, to distinguish between lysosomes and prelysosomal endocytic vacuoles. *The Biochemical journal*. 300 ( Pt 1. p.pp. 229–36.
- Berridge, M.J. (2012). Calcium signalling remodelling and disease. *Biochemical Society transactions*. 40 (2). p.pp. 297–309.
- Berridge, M.J. (1997). Elementary and global aspects of calcium signalling. *The Journal of physiology*. 499 ( Pt 2. p.pp. 291–306.
- Berridge, M.J. (2007). Inositol trisphosphate and calcium oscillations. *Biochemical Society symposium*. 265 (74). p.pp. 1–7.
- Berridge, M.J. (1998). Neuronal calcium signaling. *Neuron*. 21 (1). p.pp. 13–26.
- Berridge, M.J. (2002). The endoplasmic reticulum: a multifunctional signaling organelle. *Cell calcium*. 32 (5-6). p.pp. 235–49.
- Berridge, M.J., Bootman, M.D. & Roderick, H.L. (2003). Calcium signalling: dynamics, homeostasis and remodelling. *Nature reviews. Molecular cell biology*. 4 (7). p.pp. 517–29.
- Berridge, M.J., Lipp, P. & Bootman, M.D. (2000). The versatility and universality of calcium signalling. *Nature reviews. Molecular cell biology*. 1 (1). p.pp. 11–21.
- Bers, D.M. (2002). Cardiac excitation-contraction coupling. *Nature*. 415 (6868). p.pp. 198–205.
- Betz, C.A. mTOR complex 2-A. signaling at mitochondria-associated endoplasmic reticulum membranes (MAM) regulates mitochondrial physiology., Stracka, D., Prescianotto-Baschong, C., Frieden, M., Demaurex, N. & Hall, M.N. (2013). Feature Article: mTOR complex 2-Akt signaling at mitochondria-associated endoplasmic reticulum membranes (MAM) regulates mitochondrial physiology. *Proceedings of the National Academy of Sciences of the United States of America*. 110 (31). p.pp. 12526–34.



- Betzenhauser, M.J. & Marks, A.R. (2010). Ryanodine receptor channelopathies. *Pflügers Archiv : European journal of physiology*. 460 (2). p.pp. 467–80.
- Bezprozvanny, I., Watras, J. & Ehrlich, B.E. (1991). Bell-shaped calcium-response curves of Ins(1,4,5)P<sub>3</sub>- and calcium-gated channels from endoplasmic reticulum of cerebellum. *Nature*. 351 (6329). p.pp. 751–4.
- Biegstraaten, M., Mengel, E., Maródi, L., Petakov, M., Niederau, C., Giraldo, P., Hughes, D., Mrcic, M., Mehta, A., Hollak, C.E.M. & van Schaik, I.N. (2010). Peripheral neuropathy in adult type 1 Gaucher disease: a 2-year prospective observational study. *Brain : a journal of neurology*. 133 (10). p.pp. 2909–19.
- Biskup, S., Moore, D.J., Celsi, F., Higashi, S., West, A.B., Andrabi, S. a, Kurkinen, K., Yu, S.-W., Savitt, J.M., Waldvogel, H.J., Faull, R.L.M., Emson, P.C., Torp, R., Ottersen, O.P., Dawson, T.M. & Dawson, V.L. (2006). Localization of LRRK2 to membranous and vesicular structures in mammalian brain. *Annals of neurology*. 60 (5). p.pp. 557–69.
- Blech-Hermoni, Y.N., Ziegler, S.G., Hruska, K.S., Stubblefield, B.K., Lamarca, M.E., Portnoy, M.E., Green, E.D. & Sidransky, E. (2010). In silico and functional studies of the regulation of the glucocerebrosidase gene. *Molecular genetics and metabolism*. 99 (3). p.pp. 275–82.
- Braak, H., Ghebremedhin, E., Rüb, U., Bratzke, H. & Del Tredici, K. (2004). Stages in the development of Parkinson's disease-related pathology. *Cell and tissue research*. 318 (1). p.pp. 121–34.
- Brailoiu, E., Churamani, D., Cai, X., Schrlau, M.G., Brailoiu, G.C., Gao, X., Hooper, R., Boulware, M.J., Dun, N.J., Marchant, J.S. & Patel, S. (2009a). Essential requirement for two-pore channel 1 in NAADP-mediated calcium signaling. *The Journal of cell biology*. 186 (2). p.pp. 201–9.
- Brailoiu, E., Hoard, J.L., Filipeanu, C.M., Brailoiu, G.C., Dun, S.L., Patel, S. & Dun, N.J. (2005). Nicotinic acid adenine dinucleotide phosphate potentiates neurite outgrowth. *The Journal of biological chemistry*. 280 (7). p.pp. 5646–50.
- Brailoiu, E., Hooper, R., Cai, X., Brailoiu, G.C., Keebler, M. V, Dun, N.J., Marchant, J.S. & Patel, S. (2010a). An ancestral deuterostome family of two-pore channels mediates nicotinic acid adenine dinucleotide phosphate-dependent calcium release from acidic organelles. *The Journal of biological chemistry*. 285 (5). p.pp. 2897–901.
- Brailoiu, E., Rahman, T., Churamani, D., Prole, D.L., Brailoiu, G.C., Hooper, R., Taylor, C.W. & Patel, S. (2010b). An NAADP-gated two-pore channel targeted to the plasma membrane uncouples triggering from amplifying Ca<sup>2+</sup> signals. *The Journal of biological chemistry*. 285 (49). p.pp. 38511–6.
- Brailoiu, G.C., Brailoiu, E., Parkesh, R., Galione, A., Churchill, G.C., Patel, S. & Dun, N.J. (2009b). NAADP-mediated channel “chatter” in neurons of the rat medulla oblongata. *The Biochemical journal*. 419 (1). p.pp. 91–7, 2 p following 97.

- Bras, J., Singleton, A., Cookson, M.R. & Hardy, J. (2008). Emerging pathways in genetic Parkinson's disease: Potential role of ceramide metabolism in Lewy body disease. *The FEBS journal*. 275 (23). p.pp. 5767–73.
- Brini, M. & Carafoli, E. (2009). Calcium pumps in health and disease. *Physiological reviews*. 89 (4). p.pp. 1341–78.
- De Brito, O.M. & Scorrano, L. (2008). Mitofusin 2 tethers endoplasmic reticulum to mitochondria. *Nature*. 456 (7222). p.pp. 605–10.
- Brochet, D.X.P., Yang, D., Di Maio, A., Lederer, W.J., Franzini-Armstrong, C. & Cheng, H. (2005). Ca<sup>2+</sup> blinks: rapid nanoscopic store calcium signaling. *Proceedings of the National Academy of Sciences of the United States of America*. 102 (8). p.pp. 3099–104.
- Bucci, C. & De Luca, M. (2012). Molecular basis of Charcot-Marie-Tooth type 2B disease. *Biochemical Society transactions*. 40 (6). p.pp. 1368–72.
- Butters, T.D. (2007). Gaucher disease. *Current opinion in chemical biology*. 11 (4). p.pp. 412–8.
- Caiazzo, M., Dell'Anno, M.T., Dvoretzkova, E., Lazarevic, D., Taverna, S., Leo, D., Sotnikova, T.D., Menegon, A., Roncaglia, P., Colciago, G., Russo, G., Carninci, P., Pezzoli, G., Gainetdinov, R.R., Gustincich, S., Dityatev, A. & Broccoli, V. (2011). Direct generation of functional dopaminergic neurons from mouse and human fibroblasts. *Nature*. 476 (7359). p.pp. 224–7.
- Calcraft, P.J., Ruas, M., Pan, Z., Cheng, X., Arredouani, A., Hao, X., Tang, J., Rietdorf, K., Teboul, L., Chuang, K.-T., Lin, P., Xiao, R., Wang, C., Zhu, Y., Lin, Y., Wyatt, C.N., Parrington, J., Ma, J., Evans, a M., Galione, A. & Zhu, M.X. (2009). NAADP mobilizes calcium from acidic organelles through two-pore channels. *Nature*. 459 (7246). p.pp. 596–600.
- Cali, T., Ottolini, D., Negro, A. & Brini, M. (2012).  $\alpha$ -Synuclein controls mitochondrial calcium homeostasis by enhancing endoplasmic reticulum-mitochondria interactions. *The Journal of biological chemistry*. 287 (22). p.pp. 17914–29.
- Cancela, J.M., Churchill, G.C. & Galione, A. (1999). Coordination of agonist-induced Ca<sup>2+</sup>-signalling patterns by NAADP in pancreatic acinar cells. *Nature*. 398 (6722). p.pp. 74–6.
- Carafoli, E. (2012). The interplay of mitochondria with calcium: an historical appraisal. *Cell calcium*. 52 (1). p.pp. 1–8.
- Castello, P.R., Drechsel, D. a & Patel, M. (2007). Mitochondria are a major source of paraquat-induced reactive oxygen species production in the brain. *The Journal of biological chemistry*. 282 (19). p.pp. 14186–93.
- Chakrabarti, A., Chen, A.W. & Varner, J.D. (2011). A review of the mammalian unfolded protein response. *Biotechnology and bioengineering*. 108 (12). p.pp. 2777–93.

- Chan, C.S., Guzman, J.N., Ilijic, E., Mercer, J.N., Rick, C., Tkatch, T., Meredith, G.E. & Surmeier, D.J. (2007). "Rejuvenation" protects neurons in mouse models of Parkinson's disease. *Nature*. 447 (7148). p.pp. 1081–6.
- Chen, C.-C., Keller, M., Hess, M., Schiffmann, R., Urban, N., Wolfgardt, A., Schaefer, M., Bracher, F., Biel, M., Wahl-Schott, C. & Grimm, C. (2014). A small molecule restores function to TRPML1 mutant isoforms responsible for mucopolipidosis type IV. *Nature communications*. 5 (May). p.p. 4681.
- Cheng, X., Shen, D., Samie, M. & Xu, H. (2010). Mucolipins: Intracellular TRPML1-3 channels. *FEBS Letters*. 584 (10). p.pp. 2013–2021.
- Cherra, S.J., Steer, E., Gusdon, A.M., Kiselyov, K. & Chu, C.T. (2013). Mutant LRRK2 elicits calcium imbalance and depletion of dendritic mitochondria in neurons. *The American journal of pathology*. 182 (2). p.pp. 474–84.
- Christensen, K. a, Myers, J.T. & Swanson, J. a (2002). pH-dependent regulation of lysosomal calcium in macrophages. *Journal of cell science*. 115 (Pt 3). p.pp. 599–607.
- Chu, Y., Dodiya, H., Aebischer, P., Olanow, C.W. & Kordower, J.H. (2009). Alterations in lysosomal and proteasomal markers in Parkinson's disease: relationship to alpha-synuclein inclusions. *Neurobiology of disease*. 35 (3). p.pp. 385–98.
- Churamani, D., Hooper, R., Brailoiu, E. & Patel, S. (2012). Domain assembly of NAADP-gated two-pore channels. *The Biochemical journal*. 441 (1). p.pp. 317–23.
- Churchill, G.C. & Galione, a (2000). Spatial control of Ca<sup>2+</sup> signaling by nicotinic acid adenine dinucleotide phosphate diffusion and gradients. *The Journal of biological chemistry*. 275 (49). p.pp. 38687–92.
- Clapham, D.E. (1995). Calcium signaling. *Cell*. 80 (2). p.pp. 259–68.
- Cleeter, M.W.J., Chau, K.-Y., Gluck, C., Mehta, A., Hughes, D. a, Duchen, M., Wood, N.W., Hardy, J., Mark Cooper, J. & Schapira, A.H. (2012). Glucocerebrosidase Inhibition Causes Mitochondrial Dysfunction And Free Radical Damage. *Neurochemistry international*.
- Cochemé, H.M. & Murphy, M.P. (2008). Complex I is the major site of mitochondrial superoxide production by paraquat. *The Journal of biological chemistry*. 283 (4). p.pp. 1786–98.
- Coen, K., Flannagan, R.S., Baron, S., Carraro-Lacroix, L.R., Wang, D., Vermeire, W., Michiels, C., Munck, S., Baert, V., Sugita, S., Wuytack, F., Hiesinger, P.R., Grinstein, S. & Annaert, W. (2012). Lysosomal calcium homeostasis defects, not proton pump defects, cause endo-lysosomal dysfunction in PSEN-deficient cells. *The Journal of cell biology*. 198 (1). p.pp. 23–35.
- Cookson, M.R. (2010). The role of leucine-rich repeat kinase 2 (LRRK2) in Parkinson's disease. *Nature reviews. Neuroscience*. 11 (12). p.pp. 791–7.

- Corti, O., Lesage, S. & Brice, A. (2011). What genetics tells us about the causes and mechanisms of Parkinson's disease. *Physiological reviews*. 91 (4). p.pp. 1161–218.
- Covy, J.P., Waxman, E. a & Giasson, B.I. (2012). Characterization of cellular protective effects of ATP13A2/PARK9 expression and alterations resulting from pathogenic mutants. *Journal of neuroscience research*. 90 (12). p.pp. 2306–16.
- Cox, T.M. (2005). Substrate reduction therapy for lysosomal storage diseases. *Acta paediatrica (Oslo, Norway : 1992). Supplement*. 94 (447). p.pp. 69–75; discussion 57.
- Crompton, M. (1999). The mitochondrial permeability transition pore and its role in cell death. *The Biochemical journal*. 341 ( Pt 2. p.pp. 233–49.
- Csordás, G., Renken, C., Várnai, P., Walter, L., Weaver, D., Buttle, K.F., Balla, T., Mannella, C. a & Hajnóczky, G. (2006). Structural and functional features and significance of the physical linkage between ER and mitochondria. *The Journal of cell biology*. 174 (7). p.pp. 915–21.
- Csordás, G., Várnai, P., Golenár, T., Roy, S., Purkins, G., Schneider, T.G., Balla, T. & Hajnóczky, G. (2010). Imaging interorganelle contacts and local calcium dynamics at the ER-mitochondrial interface. *Molecular cell*. 39 (1). p.pp. 121–32.
- Cuervo, A.M., Stefanis, L., Fredenburg, R., Lansbury, P.T. & Sulzer, D. (2004). Impaired degradation of mutant alpha-synuclein by chaperone-mediated autophagy. *Science (New York, N.Y.)*. 305 (5688). p.pp. 1292–5.
- Cullen, V., Sardi, S.P., Ng, J., Xu, Y.-H., Sun, Y., Tomlinson, J.J., Kolodziej, P., Kahn, I., Saftig, P., Woulfe, J., Rochet, J.-C., Glicksman, M. a, Cheng, S.H., Grabowski, G. a, Shihabuddin, L.S. & Schlossmacher, M.G. (2011). Acid  $\beta$ -glucosidase mutants linked to Gaucher disease, Parkinson disease, and Lewy body dementia alter  $\alpha$ -synuclein processing. *Annals of neurology*. 69 (6). p.pp. 940–53.
- Dammermann, W. & Guse, A.H. (2005). Functional ryanodine receptor expression is required for NAADP-mediated local  $\text{Ca}^{2+}$  signaling in T-lymphocytes. *The Journal of biological chemistry*. 280 (22). p.pp. 21394–9.
- Dammermann, W., Zhang, B., Nebel, M., Cordiglieri, C., Odoardi, F., Kirchberger, T., Kawakami, N., Dowden, J., Schmid, F., Dornmair, K., Hohenegger, M., Flügel, A., Guse, A.H. & Potter, B.V.L. (2009). NAADP-mediated  $\text{Ca}^{2+}$  signaling via type 1 ryanodine receptor in T cells revealed by a synthetic NAADP antagonist. *Proceedings of the National Academy of Sciences of the United States of America*. 106 (26). p.pp. 10678–83.
- Danzer, K.M., Haasen, D., Karow, A.R., Moussaud, S., Habeck, M., Giese, A., Kretschmar, H., Hengerer, B. & Kostka, M. (2007). Different species of alpha-synuclein oligomers induce calcium influx and seeding. *The Journal of neuroscience : the official journal of the Society for Neuroscience*. 27 (34). p.pp. 9220–32.
- Dehay, B., Bové, J., Rodríguez-Muela, N., Perier, C., Recasens, A., Boya, P. & Vila, M. (2010). Pathogenic lysosomal depletion in Parkinson's disease. *The Journal of neuroscience : the official journal of the Society for Neuroscience*. 30 (37). p.pp. 12535–44.

- Dehay, B., Ramirez, A., Martinez-Vicente, M., Perier, C., Canron, M.-H., Doudnikoff, E., Vital, A., Vila, M., Klein, C. & Bezdard, E. (2012). Loss of P-type ATPase ATP13A2/PARK9 function induces general lysosomal deficiency and leads to Parkinson disease neurodegeneration. *Proceedings of the National Academy of Sciences of the United States of America*. 109 (24). p.pp. 9611–6.
- Dickinson, G.D., Churchill, G.C., Brailoiu, E. & Patel, S. (2010). Deviant nicotinic acid adenine dinucleotide phosphate (NAADP)-mediated Ca<sup>2+</sup> signaling upon lysosome proliferation. *The Journal of biological chemistry*. 285 (18). p.pp. 13321–5.
- Dinis-Oliveira, R.J., Remião, F., Carmo, H., Duarte, J. a, Navarro, a S., Bastos, M.L. & Carvalho, F. (2006). Paraquat exposure as an etiological factor of Parkinson's disease. *Neurotoxicology*. 27 (6). p.pp. 1110–22.
- Dionisio, N., Albarrán, L., López, J.J., Berna-Erro, A., Salido, G.M., Bobe, R. & Rosado, J. a (2011). Acidic NAADP-releasable Ca(2+) compartments in the megakaryoblastic cell line MEG01. *Biochimica et biophysica acta*. 1813 (8). p.pp. 1483–94.
- Do, C.B., Tung, J.Y., Dorfman, E., Kiefer, A.K., Drabant, E.M., Francke, U., Mountain, J.L., Goldman, S.M., Tanner, C.M., Langston, J.W., Wojcicki, A. & Eriksson, N. (2011). Web-based genome-wide association study identifies two novel loci and a substantial genetic component for Parkinson's disease. *PLoS genetics*. 7 (6). p.p. e1002141.
- Dodson, M.W., Zhang, T., Jiang, C., Chen, S. & Guo, M. (2012). Roles of the Drosophila LRRK2 homolog in Rab7-dependent lysosomal positioning. *Human molecular genetics*. 21 (6). p.pp. 1350–63.
- Dong, X., Shen, D., Wang, X., Dawson, T., Li, X., Zhang, Q., Cheng, X., Zhang, Y., Weisman, L.S., Delling, M. & Xu, H. (2010). PI(3,5)P(2) controls membrane trafficking by direct activation of mucolipin Ca(2+) release channels in the endolysosome. *Nature communications*. 1 (4). p.p. 38.
- Duman, J.G., Chen, L., Palmer, A.E. & Hille, B. (2006). Contributions of intracellular compartments to calcium dynamics: implicating an acidic store. *Traffic (Copenhagen, Denmark)*. 7 (7). p.pp. 859–72.
- De Duve, C., de Barse, T., Poole, B., Trouet, A., Tulkens, P. & Van Hoof, F. (1974). Commentary. Lysosomotropic agents. *Biochemical pharmacology*. 23 (18). p.pp. 2495–531.
- Duvvuri, M., Konkar, S., Funk, R.S., Krise, J.M. & Krise, J.P. (2005). A chemical strategy to manipulate the intracellular localization of drugs in resistant cancer cells. *Biochemistry*. 44 (48). p.pp. 15743–9.
- Eckenrode, E.F., Yang, J., Velmurugan, G. V, Foskett, J.K. & White, C. (2010). Apoptosis protection by Mcl-1 and Bcl-2 modulation of inositol 1,4,5-trisphosphate receptor-dependent Ca<sup>2+</sup> signaling. *The Journal of biological chemistry*. 285 (18). p.pp. 13678–84.

- Eden, E.R., Huang, F., Sorkin, A. & Futter, C.E. (2012). The role of EGF receptor ubiquitination in regulating its intracellular traffic. *Traffic (Copenhagen, Denmark)*. 13 (2). p.pp. 329–37.
- Eden, E.R., White, I.J., Tsapara, A. & Futter, C.E. (2010). Membrane contacts between endosomes and ER provide sites for PTP1B-epidermal growth factor receptor interaction. *Nature cell biology*. 12 (3). p.pp. 267–72.
- Endo, M. (2009). Calcium-induced calcium release in skeletal muscle. *Physiological reviews*. 89 (4). p.pp. 1153–76.
- Enquist, I.B., Lo Bianco, C., Ooka, A., Nilsson, E., Månsson, J., Ehinger, M., Richter, J., Brady, R.O., Kirik, D. & Karlsson, S. (2007). Murine models of acute neuronopathic Gaucher disease. *Proceedings of the National Academy of Sciences of the United States of America*. 104 (44). p.pp. 17483–8.
- Erikson, A. (2001). Remaining problems in the management of patients with Gaucher disease. *Journal of inherited metabolic disease*. 24 Suppl 2. p.pp. 122–6; discussion 87–8.
- Farfel-Becker, T., Vitner, E., Dekel, H., Leshem, N., Enquist, I.B., Karlsson, S. & Futerman, A.H. (2009). No evidence for activation of the unfolded protein response in neuronopathic models of Gaucher disease. *Human molecular genetics*. 18 (8). p.pp. 1482–8.
- Feng, W., Liu, G., Allen, P.D. & Pessah, I.N. (2000). Transmembrane redox sensor of ryanodine receptor complex. *The Journal of biological chemistry*. 275 (46). p.pp. 35902–7.
- Firestone, J. a, Lundin, J.I., Powers, K.M., Smith-Weller, T., Franklin, G.M., Swanson, P.D., Longstreth, W.T. & Checkoway, H. (2010). Occupational factors and risk of Parkinson's disease: A population-based case-control study. *American journal of industrial medicine*. 53 (3). p.pp. 217–23.
- Di Fonzo, A., Tassorelli, C., De Mari, M., Chien, H.F., Ferreira, J., Rohé, C.F., Riboldazzi, G., Antonini, A., Albani, G., Mauro, A., Marconi, R., Abbruzzese, G., Lopiano, L., Fincati, E., Guidi, M., Marini, P., Stocchi, F., Onofrj, M., Toni, V., Tinazzi, M., Fabbrini, G., Lamberti, P., Vanacore, N., Meco, G., Leitner, P., Uitti, R.J., Wszolek, Z.K., Gasser, T., Simons, E.J., Breedveld, G.J., Goldwurm, S., Pezzoli, G., Sampaio, C., Barbosa, E., Martignoni, E., Oostra, B. a & Bonifati, V. (2006). Comprehensive analysis of the LRRK2 gene in sixty families with Parkinson's disease. *European journal of human genetics : EJHG*. 14 (3). p.pp. 322–31.
- Franzini-Armstrong, C., Protasi, F. & Ramesh, V. (1999). Shape, size, and distribution of Ca(2+) release units and couplons in skeletal and cardiac muscles. *Biophysical journal*. 77 (3). p.pp. 1528–39.
- Fribley, A., Zhang, K. & Kaufman, R.J. (2009). Regulation of apoptosis by the unfolded protein response. P. Erhardt & A. Toth (eds.). *Methods in molecular biology (Clifton, N.J.)*. 559. p.pp. 191–204.

- Furukawa, K., Matsuzaki-Kobayashi, M., Hasegawa, T., Kikuchi, A., Sugeno, N., Itoyama, Y., Wang, Y., Yao, P.J., Bushlin, I. & Takeda, A. (2006). Plasma membrane ion permeability induced by mutant alpha-synuclein contributes to the degeneration of neural cells. *Journal of neurochemistry*. 97 (4). p.pp. 1071–7.
- Furuya, S., Kurono, S. & Hirabayashi, Y. (1996). Lysosphingomyelin-elicited Ca<sup>2+</sup> mobilization from rat brain microsomes. *Journal of lipid mediators and cell signalling*. 14 (1-3). p.pp. 303–11.
- Futerman, A.H. & van Meer, G. (2004). The cell biology of lysosomal storage disorders. *Nature reviews. Molecular cell biology*. 5 (7). p.pp. 554–65.
- Gandhi, S., Wood-Kaczmar, A., Yao, Z., Plun-Favreau, H., Deas, E., Klupsch, K., Downward, J., Latchman, D.S., Tabrizi, S.J., Wood, N.W., Duchen, M.R. & Abramov, A.Y. (2009). PINK1-associated Parkinson's disease is caused by neuronal vulnerability to calcium-induced cell death. *Molecular cell*. 33 (5). p.pp. 627–38.
- Gant, J.C., Sama, M.M., Landfield, P.W. & Thibault, O. (2006). Early and simultaneous emergence of multiple hippocampal biomarkers of aging is mediated by Ca<sup>2+</sup>-induced Ca<sup>2+</sup> release. *The Journal of neuroscience : the official journal of the Society for Neuroscience*. 26 (13). p.pp. 3482–90.
- Gegg, M.E., Burke, D., Heales, S.J.R., Cooper, J.M., Hardy, J., Wood, N.W. & Schapira, A.H. V (2012). Glucocerebrosidase deficiency in substantia nigra of parkinson disease brains. *Annals of neurology*. 72 (3). p.pp. 455–63.
- Genazzani, a. a., Empson, R.M. & Galione, A. (1996). Unique inactivation properties of NAADP-sensitive Ca<sup>2+</sup> release. *The Journal of biological chemistry*. 271 (20). p.pp. 11599–602.
- Gerasimenko, J. V, Maruyama, Y., Yano, K., Dolman, N.J., Tepikin, A. V, Petersen, O.H. & Gerasimenko, O. V (2003). NAADP mobilizes Ca<sup>2+</sup> from a thapsigargin-sensitive store in the nuclear envelope by activating ryanodine receptors. *The Journal of cell biology*. 163 (2). p.pp. 271–82.
- Gerasimenko, J. V, Sherwood, M., Tepikin, A. V, Petersen, O.H. & Gerasimenko, O. V (2006). NAADP, cADPR and IP<sub>3</sub> all release Ca<sup>2+</sup> from the endoplasmic reticulum and an acidic store in the secretory granule area. *Journal of cell science*. 119 (Pt 2). p.pp. 226–38.
- German, D.C., Manaye, K.F., Sonsalla, P.K. & Brooks, B.A. (1992). Midbrain dopaminergic cell loss in Parkinson's disease and MPTP-induced parkinsonism: sparing of calbindin-D28k-containing cells. *Annals of the New York Academy of Sciences*. 648. p.pp. 42–62.
- Gilks, W.P., Abou-Sleiman, P.M., Gandhi, S., Jain, S., Singleton, A., Lees, A.J., Shaw, K., Bhatia, K.P., Bonifati, V., Quinn, N.P., Lynch, J., Healy, D.G., Holton, J.L., Revesz, T. & Wood, N.W. (2005). A common LRRK2 mutation in idiopathic Parkinson's disease. *Lancet*. 365 (9457). p.pp. 415–6.
- Giordano, F., Saheki, Y., Idevall-Hagren, O., Colombo, S.F., Pirruccello, M., Milosevic, I., Gracheva, E.O., Bagriantsev, S.N., Borgese, N. & De Camilli, P. (2013). PI(4,5)P(2)-

dependent and Ca(2+)-regulated ER-PM interactions mediated by the extended synaptotagmins. *Cell*. 153 (7). p.pp. 1494–509.

Goker-Alpan, O., Stubblefield, B.K., Giasson, B.I. & Sidransky, E. (2010). Glucocerebrosidase is present in  $\alpha$ -synuclein inclusions in Lewy body disorders. *Acta neuropathologica*. 120 (5). p.pp. 641–9.

Goldman, S.M. (2014). Environmental toxins and Parkinson's disease. *Annual review of pharmacology and toxicology*. 54. p.pp. 141–64.

Gómez-Suaga, P., Luzón-Toro, B., Churamani, D., Zhang, L., Bloor-Young, D., Patel, S., Woodman, P.G., Churchill, G.C. & Hilfiker, S. (2012). Leucine-rich repeat kinase 2 regulates autophagy through a calcium-dependent pathway involving NAADP. *Human molecular genetics*. 21 (3). p.pp. 511–25.

Gómez-Suaga, P., Rivero-Ríos, P., Fdez, E., Ramírez, M.B., Ferrer, I., Aiastui, A., López de Munain, A. & Hilfiker, S. (2014). LRRK2 delays degradative receptor trafficking by impeding late endosomal budding through decreasing Rab7 activity. *Human molecular genetics*. p.pp. 1–52.

González-Polo, R. a, Niso-Santano, M., Ortíz-Ortíz, M. a, Gómez-Martín, A., Morán, J.M., García-Rubio, L., Francisco-Morcillo, J., Zaragoza, C., Soler, G. & Fuentes, J.M. (2007). Inhibition of paraquat-induced autophagy accelerates the apoptotic cell death in neuroblastoma SH-SY5Y cells. *Toxicological sciences : an official journal of the Society of Toxicology*. 97 (2). p.pp. 448–58.

Grace, A.A. & Bunney, B.S. (1983). Intracellular and extracellular electrophysiology of nigral dopaminergic neurons--1. Identification and characterization. *Neuroscience*. 10 (2). p.pp. 301–15.

Greggio, E., Taymans, J.-M., Zhen, E.Y., Ryder, J., Vancaenenbroeck, R., Beilina, A., Sun, P., Deng, J., Jaffe, H., Baekelandt, V., Merchant, K. & Cookson, M.R. (2009). The Parkinson's disease kinase LRRK2 autophosphorylates its GTPase domain at multiple sites. *Biochemical and biophysical research communications*. 389 (3). p.pp. 449–54.

Grienberger, C. & Konnerth, A. (2012). Imaging calcium in neurons. *Neuron*. 73 (5). p.pp. 862–85.

Grimm, C., Holdt, L.M., Chen, C.-C., Hassan, S., Müller, C., Jörs, S., Cuny, H., Kissing, S., Schröder, B., Butz, E., Northoff, B., Castonguay, J., Lubber, C. a, Moser, M., Spahn, S., Lüllmann-Rauch, R., Fendel, C., Klugbauer, N., Griesbeck, O., Haas, A., Mann, M., Bracher, F., Teupser, D., Saftig, P., Biel, M. & Wahl-Schott, C. (2014). High susceptibility to fatty liver disease in two-pore channel 2-deficient mice. *Nature communications*. 5. p.p. 4699.

Guicciardi, M.E., Deussing, J., Miyoshi, H., Bronk, S.F., Svingen, P.A., Peters, C., Kaufmann, S.H. & Gores, G.J. (2000). Cathepsin B contributes to TNF-alpha-mediated hepatocyte apoptosis by promoting mitochondrial release of cytochrome c. *The Journal of clinical investigation*. 106 (9). p.pp. 1127–37.



- Guzman, J.N., Sanchez-Padilla, J., Wokosin, D., Kondapalli, J., Ilijic, E., Schumacker, P.T. & Surmeier, D.J. (2010). Oxidant stress evoked by pacemaking in dopaminergic neurons is attenuated by DJ-1. *Nature*. 468 (7324). p.pp. 696–700.
- Hall, J.M. (1992). Bradykinin receptors: pharmacological properties and biological roles. *Pharmacology & therapeutics*. 56 (2). p.pp. 131–90.
- Haller, T., Dietl, P., Deetjen, P. & Völkl, H. (1996). The lysosomal compartment as intracellular calcium store in MDCK cells: a possible involvement in InsP3-mediated Ca<sup>2+</sup> release. *Cell Calcium*. 19 (2). p.pp. 157–165.
- Hardy, J. (2003). Impact of genetic analysis on Parkinson's disease research. *Movement disorders : official journal of the Movement Disorder Society*. 18 Suppl 6. p.pp. S96–8.
- Hayashi, T., Rizzuto, R., Hajnoczky, G. & Su, T.-P. (2009). MAM: more than just a housekeeper. *Trends in cell biology*. 19 (2). p.pp. 81–8.
- Heeman, B., Van den Haute, C., Aelvoet, S.-A., Valsecchi, F., Rodenburg, R.J., Reumers, V., Debyser, Z., Callewaert, G., Koopman, W.J.H., Willems, P.H.G.M. & Baekelandt, V. (2011). Depletion of PINK1 affects mitochondrial metabolism, calcium homeostasis and energy maintenance. *Journal of cell science*. 124 (Pt 7). p.pp. 1115–25.
- Heidemann, A.C., Schipke, C.G. & Kettenmann, H. (2005). Extracellular application of nicotinic acid adenine dinucleotide phosphate induces Ca<sup>2+</sup> signaling in astrocytes in situ. *The Journal of biological chemistry*. 280 (42). p.pp. 35630–40.
- Hertzman, C., Wiens, M., Snow, B., Kelly, S. & Calne, D. (1994). A case-control study of Parkinson's disease in a horticultural region of British Columbia. *Movement disorders : official journal of the Movement Disorder Society*. 9 (1). p.pp. 69–75.
- Higashi, S., Moore, D.J., Yamamoto, R., Minegishi, M., Sato, K., Togo, T., Katsuse, O., Uchikado, H., Furukawa, Y., Hino, H., Kosaka, K., Emson, P.C., Wada, K., Dawson, V.L., Dawson, T.M., Arai, H. & Iseki, E. (2009). Abnormal localization of leucine-rich repeat kinase 2 to the endosomal-lysosomal compartment in lewy body disease. *Journal of neuropathology and experimental neurology*. 68 (9). p.pp. 994–1005.
- Hohenegger, M., Suko, J., Gscheidlinger, R., Drobny, H. & Zidar, A. (2002). Nicotinic acid-adenine dinucleotide phosphate activates the skeletal muscle ryanodine receptor. *The Biochemical journal*. 367 (Pt 2). p.pp. 423–31.
- Horowitz, M., Wilder, S., Horowitz, Z., Reiner, O., Gelbart, T. & Beutler, E. (1989). The human glucocerebrosidase gene and pseudogene: structure and evolution. *Genomics*. 4 (1). p.pp. 87–96.
- Hruska, K.S., LaMarca, M.E., Scott, C.R. & Sidransky, E. (2008). Gaucher disease: mutation and polymorphism spectrum in the glucocerebrosidase gene (GBA). *Human mutation*. 29 (5). p.pp. 567–83.
- Hu, F.-Y., Xi, J., Guo, J., Yu, L.-H., Liu, L., He, X.-H., Liu, Z.-L., Zou, X.-Y. & Xu, Y.-M. (2010). Association of the glucocerebrosidase N370S allele with Parkinson's disease in two separate Chinese Han populations of mainland China. *European journal of neurology* :

*the official journal of the European Federation of Neurological Societies*. 17 (12). p.pp. 1476–8.

- Huang, H., Tan, B.Z., Shen, Y., Tao, J., Jiang, F., Sung, Y.Y., Ng, C.K., Raida, M., Köhr, G., Higuchi, M., Fatemi-Shariatpanahi, H., Harden, B., Yue, D.T. & Soong, T.W. (2012). RNA editing of the IQ domain in Ca(v)1.3 channels modulates their Ca<sup>2+</sup>-dependent inactivation. *Neuron*. 73 (2). p.pp. 304–16.
- Hurley, M.J., Brandon, B., Gentleman, S.M. & Dexter, D.T. (2013). Parkinson's disease is associated with altered expression of CaV1 channels and calcium-binding proteins. *Brain : a journal of neurology*. 136 (Pt 7). p.pp. 2077–97.
- Ilijic, E., Guzman, J.N. & Surmeier, D.J. (2011). The L-type channel antagonist isradipine is neuroprotective in a mouse model of Parkinson's disease. *Neurobiology of disease*. 43 (2). p.pp. 364–71.
- Ishibashi, K., Suzuki, M. & Imai, M. (2000). Molecular cloning of a novel form (two-repeat) protein related to voltage-gated sodium and calcium channels. *Biochemical and biophysical research communications*. 270 (2). p.pp. 370–6.
- Jadot, M., Colmant, C., Wattiaux-De Coninck, S. & Wattiaux, R. (1984). Intralysosomal hydrolysis of glycyl-L-phenylalanine 2-naphthylamide. *The Biochemical journal*. 219 (3). p.pp. 965–70.
- James, P., Maeda, M., Fischer, R., Verma, a K., Krebs, J., Penniston, J.T. & Carafoli, E. (1988). Identification and primary structure of a calmodulin binding domain of the Ca<sup>2+</sup> pump of human erythrocytes. *The Journal of biological chemistry*. 263 (6). p.pp. 2905–10.
- Jefferies, H.B.J., Cooke, F.T., Jat, P., Boucheron, C., Koizumi, T., Hayakawa, M., Kaizawa, H., Ohishi, T., Workman, P., Waterfield, M.D. & Parker, P.J. (2008). A selective PIKfyve inhibitor blocks PtdIns(3,5)P<sub>2</sub> production and disrupts endomembrane transport and retroviral budding. *EMBO reports*. 9 (2). p.pp. 164–70.
- Jennings, J.J., Zhu, J.-H., Rbaibi, Y., Luo, X., Chu, C.T. & Kiselyov, K. (2006). Mitochondrial aberrations in mucopolipidosis Type IV. *The Journal of biological chemistry*. 281 (51). p.pp. 39041–50.
- Jha, A., Ahuja, M., Patel, S., Brailoiu, E. & Muallem, S. (2014). Convergent regulation of the lysosomal two-pore channel-2 by Mg<sup>2+</sup>, NAADP, PI(3,5)P<sub>2</sub> and multiple protein kinases. *The EMBO journal*. 33 (5). p.pp. 501–11.
- Jiang, D., Zhao, L. & Clapham, D.E. (2009). Genome-wide RNAi screen identifies Letm1 as a mitochondrial Ca<sup>2+</sup>/H<sup>+</sup> antiporter. *Science (New York, N.Y.)*. 326 (5949). p.pp. 144–7.
- Jiang, D., Zhao, L., Clish, C.B. & Clapham, D.E. (2013). Letm1, the mitochondrial Ca<sup>2+</sup>/H<sup>+</sup> antiporter, is essential for normal glucose metabolism and alters brain function in Wolf-Hirschhorn syndrome. *Proceedings of the National Academy of Sciences of the United States of America*. 110 (24). p.pp. E2249–54.
- Johansson, M., Rocha, N., Zwart, W., Jordens, I., Janssen, L., Kuijl, C., Olkkonen, V.M. & Neefjes, J. (2007). Activation of endosomal dynein motors by stepwise assembly of

- Rab7-RILP-p150Glued, ORP1L, and the receptor betalll spectrin. *The Journal of cell biology*. 176 (4). p.pp. 459–71.
- Josephs, K. a., Matsumoto, J.Y. & Lindor, N.M. (2004). Heterozygous Niemann-Pick disease type C presenting with tremor. *Neurology*. 63 (11). p.pp. 2189–2190.
- Kamel, F., Tanner, C., Umbach, D., Hoppin, J., Alavanja, M., Blair, a, Comyns, K., Goldman, S., Korell, M., Langston, J., Ross, G. & Sandler, D. (2007). Pesticide exposure and self-reported Parkinson's disease in the agricultural health study. *American journal of epidemiology*. 165 (4). p.pp. 364–74.
- Karacsonyi, C., Miguel, A.S. & Puertollano, R. (2007). Mucolipin-2 Localizes to the Arf6-Associated Pathway and Regulates Recycling of GPI-APs. *Traffic*. 8 (10). p.pp. 1404–1414.
- Kaufman, R.J. & Malhotra, J.D. (2014). Calcium trafficking integrates endoplasmic reticulum function with mitochondrial bioenergetics. *Biochimica et biophysica acta*. 1843 (10). p.pp. 2233–9.
- Kaufmann, A.M. & Krise, J.P. (2007). Lysosomal sequestration of amine-containing drugs: analysis and therapeutic implications. *Journal of pharmaceutical sciences*. 96 (4). p.pp. 729–46.
- Khaliq, Z.M. & Bean, B.P. (2010). Pacemaking in dopaminergic ventral tegmental area neurons: depolarizing drive from background and voltage-dependent sodium conductances. *The Journal of neuroscience : the official journal of the Society for Neuroscience*. 30 (21). p.pp. 7401–13.
- Kiffin, R., Bandyopadhyay, U. & Cuervo, A.M. (2006). Oxidative stress and autophagy. *Antioxidants & redox signaling*. 8 (1-2). p.pp. 152–62.
- Kiffin, R., Christian, C., Knecht, E. & Cuervo, A.M. (2004). Activation of chaperone-mediated autophagy during oxidative stress. *Molecular biology of the cell*. 15 (11). p.pp. 4829–40.
- Kilpatrick, B.S., Eden, E.R., Schapira, A.H., Futter, C.E. & Patel, S. (2013). Direct mobilisation of lysosomal Ca<sup>2+</sup> triggers complex Ca<sup>2+</sup> signals. *Journal of cell science*. 126 (Pt 1). p.pp. 60–6.
- Kim, H.J., Li, Q., Tjon-Kon-Sang, S., So, I., Kiselyov, K. & Muallem, S. (2007). Gain-of-function mutation in TRPML3 causes the mouse Varitint-Waddler phenotype. *The Journal of biological chemistry*. 282 (50). p.pp. 36138–42.
- Kim, H.J., Soyombo, A. a, Tjon-Kon-Sang, S., So, I. & Muallem, S. (2009). The Ca<sup>2+</sup> channel TRPML3 regulates membrane trafficking and autophagy. *Traffic (Copenhagen, Denmark)*. 10 (8). p.pp. 1157–67.
- Kinncar, N.P., Boittin, F.-X., Thomas, J.M., Galione, A. & Evans, a M. (2004). Lysosome-sarcoplasmic reticulum junctions. A trigger zone for calcium signaling by nicotinic acid adenine dinucleotide phosphate and endothelin-1. *The Journal of biological chemistry*. 279 (52). p.pp. 54319–26.

- Kiselyov, K., Chen, J., Rbaibi, Y., Oberdick, D., Tjon-Kon-Sang, S., Shcheynikov, N., Muallem, S. & Soyombo, A. (2005). TRP-ML1 is a lysosomal monovalent cation channel that undergoes proteolytic cleavage. *The Journal of biological chemistry*. 280 (52). p.pp. 43218–23.
- Kiviluoto, S., Vervliet, T., Ivanova, H., Decuypere, J.-P., De Smedt, H., Missiaen, L., Bultynck, G. & Parys, J.B. (2013). Regulation of inositol 1,4,5-trisphosphate receptors during endoplasmic reticulum stress. *Biochimica et biophysica acta*. 1833 (7). p.pp. 1612–24.
- Kluenemann, H.H., Nutt, J.G., Davis, M.Y. & Bird, T.D. (2013). Parkinsonism syndrome in heterozygotes for Niemann-Pick C1. *Journal of the neurological sciences*. 335 (1-2). p.pp. 219–20.
- Kolter, T. & Sandhoff, K. (2005). Principles of lysosomal membrane digestion: stimulation of sphingolipid degradation by sphingolipid activator proteins and anionic lysosomal lipids. *Annual review of cell and developmental biology*. 21. p.pp. 81–103.
- Korkotian, E., Schwarz, a, Pelled, D., Schwarzmann, G., Segal, M. & Futerman, a H. (1999). Elevation of intracellular glucosylceramide levels results in an increase in endoplasmic reticulum density and in functional calcium stores in cultured neurons. *The Journal of biological chemistry*. 274 (31). p.pp. 21673–8.
- Kornmann, B., Currie, E., Collins, S.R., Schuldiner, M., Nunnari, J., Weissman, J.S. & Walter, P. (2009). An ER-mitochondria tethering complex revealed by a synthetic biology screen. *Science (New York, N.Y.)*. 325 (5939). p.pp. 477–81.
- Korolchuk, V.I., Saiki, S., Lichtenberg, M., Siddiqi, F.H., Roberts, E. a, Imarisio, S., Jahreiss, L., Sarkar, S., Futter, M., Menzies, F.M., O’Kane, C.J., Deretic, V. & Rubinsztein, D.C. (2011). Lysosomal positioning coordinates cellular nutrient responses. *Nature cell biology*. 13 (4). p.pp. 453–60.
- Kvam, E. & Goldfarb, D.S. (2006). Nucleus-vacuole junctions in yeast: anatomy of a membrane contact site. *Biochemical Society transactions*. 34 (Pt 3). p.pp. 340–2.
- Langston, J.W., Ballard, P., Tetrud, J.W. & Irwin, I. (1983). Chronic Parkinsonism in humans due to a product of meperidine-analog synthesis. *Science (New York, N.Y.)*. 219 (4587). p.pp. 979–80.
- Lashuel, H. a., Petre, B.M., Wall, J., Simon, M., Nowak, R.J., Walz, T. & Lansbury, P.T. (2002).  $\alpha$ -Synuclein, Especially the Parkinson’s Disease-associated Mutants, Forms Pore-like Annular and Tubular Protofibrils. *Journal of Molecular Biology*. 322 (5). p.pp. 1089–1102.
- Lee, B.D., Shin, J.-H., VanKampen, J., Petrucelli, L., West, A.B., Ko, H.S., Lee, Y.-I., Maguire-Zeiss, K. a, Bowers, W.J., Federoff, H.J., Dawson, V.L. & Dawson, T.M. (2010a). Inhibitors of leucine-rich repeat kinase-2 protect against models of Parkinson’s disease. *Nature medicine*. 16 (9). p.pp. 998–1000.
- Lee, H., Lee, J.K., Min, W.-K., Bae, J.-H., He, X., Schuchman, E.H., Bae, J.-S. & Jin, H.K. (2010b). Bone marrow-derived mesenchymal stem cells prevent the loss of Niemann-

- Pick type C mouse Purkinje neurons by correcting sphingolipid metabolism and increasing sphingosine-1-phosphate. *Stem cells (Dayton, Ohio)*. 28 (4). p.pp. 821–31.
- Lee, H.C. (1993). Potentiation of calcium- and caffeine-induced calcium release by cyclic ADP-ribose. *The Journal of biological chemistry*. 268 (1). p.pp. 293–9.
- Lee, H.C. & Aarhus, R. (1995). A Derivative of NADP Mobilizes Calcium Stores Insensitive to Inositol Trisphosphate and Cyclic ADP-ribose. *Journal of Biological Chemistry*. 270 (5). p.pp. 2152–2157.
- Lee, H.C. & Aarhus, R. (1991). ADP-ribosyl cyclase: an enzyme that cyclizes NAD<sup>+</sup> into a calcium-mobilizing metabolite. *Cell regulation*. 2 (3). p.pp. 203–9.
- Lee, H.C., Aarhus, R., Graeff, R., Gurnack, M.E. & Walseth, T.F. (1994). Cyclic ADP ribose activation of the ryanodine receptor is mediated by calmodulin. *Nature*. 370 (6487). p.pp. 307–9.
- Lee, J.-H., Yu, W.H., Kumar, A., Lee, S., Mohan, P.S., Peterhoff, C.M., Wolfe, D.M., Martinez-Vicente, M., Massey, A.C., Sovak, G., Uchiyama, Y., Westaway, D., Cuervo, A.M. & Nixon, R. a (2010c). Lysosomal proteolysis and autophagy require presenilin 1 and are disrupted by Alzheimer-related PS1 mutations. *Cell*. 141 (7). p.pp. 1146–58.
- Lehto, M., Hynynen, R., Karjalainen, K., Kuismanen, E., Hyvärinen, K. & Olkkonen, V.M. (2005). Targeting of OSBP-related protein 3 (ORP3) to endoplasmic reticulum and plasma membrane is controlled by multiple determinants. *Experimental cell research*. 310 (2). p.pp. 445–62.
- Liao, J., Li, H., Zeng, W., Sauer, D.B., Belmares, R. & Jiang, Y. (2012). Structural insight into the ion-exchange mechanism of the sodium/calcium exchanger. *Science (New York, N.Y.)*. 335 (6069). p.pp. 686–90.
- Lieberman, R.L., D'aquino, J.A., Ringe, D. & Petsko, G. a (2009). Effects of pH and iminosugar pharmacological chaperones on lysosomal glycosidase structure and stability. *Biochemistry*. 48 (22). p.pp. 4816–27.
- Lin-Moshier, Y., Keebler, M. V, Hooper, R., Boulware, M.J., Liu, X., Churamani, D., Abood, M.E., Walseth, T.F., Brailoiu, E., Patel, S. & Marchant, J.S. (2014). The Two-pore channel (TPC) interactome unmasks isoform-specific roles for TPCs in endolysosomal morphology and cell pigmentation. *Proceedings of the National Academy of Sciences of the United States of America*. p.pp. 1–6.
- Lin-Moshier, Y., Walseth, T.F., Churamani, D., Davidson, S.M., Slama, J.T., Hooper, R., Brailoiu, E., Patel, S. & Marchant, J.S. (2012). Photoaffinity labeling of nicotinic acid adenine dinucleotide phosphate (NAADP) targets in mammalian cells. *The Journal of biological chemistry*. 287 (4). p.pp. 2296–307.
- Liou, H.H., Tsai, M.C., Chen, C.J., Jeng, J.S., Chang, Y.C., Chen, S.Y. & Chen, R.C. (1997). Environmental risk factors and Parkinson's disease: A case-control study in Taiwan. *Neurology*. 48 (6). p.pp. 1583–1588.

- Lloyd-Evans, E., Morgan, A.J., He, X., Smith, D. a, Elliot-Smith, E., Sillence, D.J., Churchill, G.C., Schuchman, E.H., Galione, A. & Platt, F.M. (2008). Niemann-Pick disease type C1 is a sphingosine storage disease that causes deregulation of lysosomal calcium. *Nature medicine*. 14 (11). p.pp. 1247–55.
- Lloyd-Evans, E., Pelled, D., Riebeling, C., Bodennec, J., de-Morgan, A., Waller, H., Schiffmann, R. & Futerman, A.H. (2003). Glucosylceramide and glucosylsphingosine modulate calcium mobilization from brain microsomes via different mechanisms. *The Journal of biological chemistry*. 278 (26). p.pp. 23594–9.
- Lloyd-Evans, E. & Platt, F.M. (2011). Lysosomal Ca(2+) homeostasis: role in pathogenesis of lysosomal storage diseases. *Cell calcium*. 50 (2). p.pp. 200–5.
- López, J.J., Camello-Almaraz, C., Pariente, J. a, Salido, G.M. & Rosado, J. a (2005). Ca<sup>2+</sup> accumulation into acidic organelles mediated by Ca<sup>2+</sup>- and vacuolar H<sup>+</sup>-ATPases in human platelets. *The Biochemical journal*. 390 (Pt 1). p.pp. 243–52.
- López-Sanjurjo, C.I., Tovey, S.C., Prole, D.L. & Taylor, C.W. (2013). Lysosomes shape Ins(1,4,5)P<sub>3</sub>-evoked Ca<sup>2+</sup> signals by selectively sequestering Ca<sup>2+</sup> released from the endoplasmic reticulum. *Journal of cell science*. 126 (Pt 1). p.pp. 289–300.
- Lüllmann-rauch, R. (2005). *Lysosomes*. Boston, MA: Springer US.
- Macaskill, A.F., Rinholm, J.E., Twelvetrees, A.E., Arancibia-Carcamo, I.L., Muir, J., Fransson, A., Aspenstrom, P., Attwell, D. & Kittler, J.T. (2009). Miro1 is a calcium sensor for glutamate receptor-dependent localization of mitochondria at synapses. *Neuron*. 61 (4). p.pp. 541–55.
- Mackrill, J.J., Challiss, R. a, O’connell, D. a, Lai, F. a & Nahorski, S.R. (1997a). Differential expression and regulation of ryanodine receptor and myo-inositol 1,4,5-trisphosphate receptor Ca<sup>2+</sup> release channels in mammalian tissues and cell lines. *The Biochemical journal*. 327 ( Pt 1). p.pp. 251–8.
- Mackrill, J.J., Challiss, R.A., O’connell, D.A., Lai, F.A. & Nahorski, S.R. (1997b). Differential expression and regulation of ryanodine receptor and myo-inositol 1,4,5-trisphosphate receptor Ca<sup>2+</sup> release channels in mammalian tissues and cell lines. *The Biochemical journal*. 327 ( Pt 1 (11)). p.pp. 251–8.
- MacLeod, D. a, Rhinn, H., Kuwahara, T., Zolin, A., Di Paolo, G., McCabe, B.D., MacCabe, B.D., Marder, K.S., Honig, L.S., Clark, L.N., Small, S. a & Abeliovich, A. (2013). RAB7L1 interacts with LRRK2 to modify intraneuronal protein sorting and Parkinson’s disease risk. *Neuron*. 77 (3). p.pp. 425–39.
- MacLeod, D., Dowman, J., Hammond, R., Leete, T., Inoue, K. & Abeliovich, A. (2006). The familial Parkinsonism gene LRRK2 regulates neurite process morphology. *Neuron*. 52 (4). p.pp. 587–93.
- Mahdiyoun, S., Deshmukh, G.D., Abe, a, Radin, N.S. & Shayman, J. a (1992). Decreased formation of inositol trisphosphate in Madin-Darby canine kidney cells under conditions of beta-glucosidase inhibition. *Archives of biochemistry and biophysics*. 292 (2). p.pp. 506–11.

- Mak, S.K., McCormack, A.L., Manning-Bog, A.B., Cuervo, A.M. & Di Monte, D. a (2010). Lysosomal degradation of alpha-synuclein in vivo. *The Journal of biological chemistry*. 285 (18). p.pp. 13621–9.
- Mallilankaraman, K., Doonan, P., Cárdenas, C., Chandramoorthy, H.C., Müller, M., Miller, R., Hoffman, N.E., Gandhirajan, R.K., Molgó, J., Birnbaum, M.J., Rothberg, B.S., Mak, D.-O.D., Foskett, J.K. & Madesh, M. (2012). MICU1 is an essential gatekeeper for MCU-mediated mitochondrial Ca(2+) uptake that regulates cell survival. *Cell*. 151 (3). p.pp. 630–44.
- Manjarrés, I.M., Rodríguez-García, A., Alonso, M.T. & García-Sancho, J. (2010). The sarco/endoplasmic reticulum Ca(2+) ATPase (SERCA) is the third element in capacitative calcium entry. *Cell calcium*. 47 (5). p.pp. 412–8.
- Manning-Bog, A.B., McCormack, A.L., Li, J., Uversky, V.N., Fink, A.L. & Di Monte, D. a (2002). The herbicide paraquat causes up-regulation and aggregation of alpha-synuclein in mice: paraquat and alpha-synuclein. *The Journal of biological chemistry*. 277 (3). p.pp. 1641–4.
- Manning-Boğ, A.B., Schüle, B. & Langston, J.W. (2009). Alpha-synuclein-glucocerebrosidase interactions in pharmacological Gaucher models: a biological link between Gaucher disease and parkinsonism. *Neurotoxicology*. 30 (6). p.pp. 1127–32.
- Manzoni, C., Mamais, A., Dihanich, S., Abeti, R., Soutar, M.P.M., Plun-Favreau, H., Giunti, P., Tooze, S. a, Bandopadhyay, R. & Lewis, P. a (2013a). Inhibition of LRRK2 kinase activity stimulates macroautophagy. *Biochimica et biophysica acta*. 1833 (12). p.pp. 2900–10.
- Manzoni, C., Mamais, A., Dihanich, S., McGoldrick, P., Devine, M.J., Zerle, J., Kara, E., Taanman, J.-W., Healy, D.G., Marti-Masso, J.-F., Schapira, A.H., Plun-Favreau, H., Tooze, S., Hardy, J., Bandopadhyay, R. & Lewis, P. a (2013b). Pathogenic Parkinson's disease mutations across the functional domains of LRRK2 alter the autophagic/lysosomal response to starvation. *Biochemical and biophysical research communications*. 441 (4). p.pp. 862–6.
- Maor, G., Rencus-Lazar, S., Filocamo, M., Steller, H., Segal, D. & Horowitz, M. (2013). Unfolded protein response in Gaucher disease: from human to Drosophila. *Orphanet journal of rare diseases*. 8 (1). p.p. 140.
- Marchant, J.S., Lin-Moshier, Y., Walseth, T.F. & Patel, S. (2012). The Molecular Basis for Ca(2+) Signalling by NAADP: Two-Pore Channels in a Complex? *Messenger (Los Angeles, Calif. : Print)*. 1 (1). p.pp. 63–76.
- Van der Mark, M., Brouwer, M., Kromhout, H., Nijssen, P., Huss, A. & Vermeulen, R. (2012). Is pesticide use related to Parkinson disease? Some clues to heterogeneity in study results. *Environmental health perspectives*. 120 (3). p.pp. 340–7.
- Martin, O.C. & Pagano, R.E. (1994). Internalization and sorting of a fluorescent analogue of glucosylceramide to the Golgi apparatus of human skin fibroblasts: utilization of endocytic and nonendocytic transport mechanisms. *The Journal of cell biology*. 125 (4). p.pp. 769–81.

- Mattson, M.P. (2007). Calcium and neurodegeneration. *Aging cell*. 6 (3). p.pp. 337–50.
- Mattson, M.P., LaFerla, F.M., Chan, S.L., Leissring, M. a, Shepel, P.N. & Geiger, J.D. (2000). Calcium signaling in the ER: its role in neuronal plasticity and neurodegenerative disorders. *Trends in neurosciences*. 23 (5). p.pp. 222–9.
- Mazzulli, J.R., Xu, Y.-H., Sun, Y., Knight, A.L., McLean, P.J., Caldwell, G.A., Sidransky, E., Grabowski, G.A. & Krainc, D. (2011). Gaucher disease glucocerebrosidase and  $\alpha$ -synuclein form a bidirectional pathogenic loop in synucleinopathies. *Cell*. 146 (1). p.pp. 37–52.
- McNeill, A., Duran, R., Hughes, D. a, Mehta, A. & Schapira, A.H. V (2012). A clinical and family history study of Parkinson’s disease in heterozygous glucocerebrosidase mutation carriers. *Journal of neurology, neurosurgery, and psychiatry*. 83 (8). p.pp. 853–4.
- McNeill, A., Magalhaes, J., Shen, C., Chau, K.-Y., Hughes, D., Mehta, A., Foltynie, T., Cooper, J.M., Abramov, A.Y., Gegg, M. & Schapira, A.H. V (2014). Ambroxol improves lysosomal biochemistry in glucocerebrosidase mutation-linked Parkinson disease cells. *Brain : a journal of neurology*. 137 (Pt 5). p.pp. 1481–95.
- Meikle, P.J., Brooks, D. a, Ravenscroft, E.M., Yan, M., Williams, R.E., Jaunzems, a E., Chataway, T.K., Karageorgos, L.E., Davey, R.C., Boulter, C.D., Carlsson, S.R. & Hopwood, J.J. (1997). Diagnosis of lysosomal storage disorders: evaluation of lysosome-associated membrane protein LAMP-1 as a diagnostic marker. *Clinical chemistry*. 43 (8 Pt 1). p.pp. 1325–35.
- Meikle, P.J., Hopwood, J.J., Clague, A.E. & Carey, W.F. (1999). Prevalence of lysosomal storage disorders. *JAMA*. 281 (3). p.pp. 249–54.
- Mekahli, D., Bultynck, G., Parys, J.B., De Smedt, H. & Missiaen, L. (2011). Endoplasmic-reticulum calcium depletion and disease. *Cold Spring Harbor perspectives in biology*. 3 (6).
- Menteyne, A., Burdakov, A., Charpentier, G., Petersen, O.H. & Cancela, J.-M. (2006). Generation of specific Ca(2+) signals from Ca(2+) stores and endocytosis by differential coupling to messengers. *Current biology : CB*. 16 (19). p.pp. 1931–7.
- Michalak, M., Groenendyk, J., Szabo, E., Gold, L.I. & Opas, M. (2009). Calreticulin, a multi-process calcium-buffering chaperone of the endoplasmic reticulum. *The Biochemical journal*. 417 (3). p.pp. 651–66.
- Michelangeli, F. & East, J.M. (2011). A diversity of SERCA Ca<sup>2+</sup> pump inhibitors. *Biochemical Society transactions*. 39 (3). p.pp. 789–97.
- Milman, B.L. (2003). Cluster ions of diquat and paraquat in electrospray ionization mass spectra and their collision-induced dissociation spectra. *Rapid communications in mass spectrometry : RCM*. 17 (12). p.pp. 1344–9.
- Mizuta, I., Tsunoda, T., Satake, W., Nakabayashi, Y., Watanabe, M., Takeda, A., Hasegawa, K., Nakashima, K., Yamamoto, M., Hattori, N., Murata, M. & Toda, T. (2008). Calbindin



- 1, fibroblast growth factor 20, and alpha-synuclein in sporadic Parkinson's disease. *Human genetics*. 124 (1). p.pp. 89–94.
- Monaco, G., Decrock, E., Nuyts, K., Wagner, L.E., Luyten, T., Strelkov, S. V, Missiaen, L., De Borggraeve, W.M., Leybaert, L., Yule, D.I., De Smedt, H., Parys, J.B. & Bultynck, G. (2013). Alpha-helical destabilization of the Bcl-2-BH4-domain peptide abolishes its ability to inhibit the IP3 receptor. *PLoS one*. 8 (8). p.p. e73386.
- Montell, C. (2005). The TRP superfamily of cation channels. *Science's STKE : signal transduction knowledge environment*. 2005 (272). p.p. re3.
- Moran, M.M., Xu, H. & Clapham, D.E. (2004). TRP ion channels in the nervous system. *Current opinion in neurobiology*. 14 (3). p.pp. 362–9.
- Moreno-Sanchez, D., Hernandez-Ruiz, L., Ruiz, F. a & Docampo, R. (2012). Polyphosphate is a novel pro-inflammatory regulator of mast cells and is located in acidocalcisomes. *The Journal of biological chemistry*. 287 (34). p.pp. 28435–44.
- Morgan, A.J., Churchill, G.C., Ruas, M., Davis, L.C., Billington, R.A., Patel, S., Thomas, J.M., Genazzani, A. & Galione, A. (2005). *Methods in Cyclic ADP-Ribose and NAADP Research*. p.pp. 265–334.
- Morgan, A.J., Davis, L.C., Wagner, S.K.T.Y., Lewis, A.M., Parrington, J., Churchill, G.C. & Galione, A. (2013). Bidirectional Ca<sup>2+</sup> signaling occurs between the endoplasmic reticulum and acidic organelles. *The Journal of cell biology*. 200 (6). p.pp. 789–805.
- Morgan, A.J. & Galione, A. (2007). Fertilization and nicotinic acid adenine dinucleotide phosphate induce pH changes in acidic Ca(2+) stores in sea urchin eggs. *The Journal of biological chemistry*. 282 (52). p.pp. 37730–7.
- Morgan, A.J., Platt, F.M., Lloyd-Evans, E. & Galione, A. (2011). Molecular mechanisms of endolysosomal Ca<sup>2+</sup> signalling in health and disease. *The Biochemical journal*. 439 (3). p.pp. 349–74.
- Mu, T.-W., Fowler, D.M. & Kelly, J.W. (2008). Partial restoration of mutant enzyme homeostasis in three distinct lysosomal storage disease cell lines by altering calcium homeostasis. *PLoS biology*. 6 (2). p.p. e26.
- Muik, M., Fahrner, M., Schindl, R., Stathopoulos, P., Frischauf, I., Derler, I., Plenk, P., Lackner, B., Groschner, K., Ikura, M. & Romanin, C. (2011). STIM1 couples to ORAI1 via an intramolecular transition into an extended conformation. *The EMBO journal*. 30 (9). p.pp. 1678–89.
- Nalls, M. a, Plagnol, V., Hernandez, D.G., Sharma, M., Sheerin, U.-M., Saad, M., Simón-Sánchez, J., Schulte, C., Lesage, S., Sveinbjörnsdóttir, S., Stefánsson, K., Martínez, M., Hardy, J., Heutink, P., Brice, A., Gasser, T., Singleton, A.B. & Wood, N.W. (2011). Imputation of sequence variants for identification of genetic risks for Parkinson's disease: a meta-analysis of genome-wide association studies. *Lancet*. 377 (9766). p.pp. 641–9.

- Narendra, D.P., Jin, S.M., Tanaka, A., Suen, D.-F., Gautier, C. a, Shen, J., Cookson, M.R. & Youle, R.J. (2010). PINK1 is selectively stabilized on impaired mitochondria to activate Parkin. *PLoS biology*. 8 (1). p.p. e1000298.
- Naylor, E., Arredouani, A., Vasudevan, S.R., Lewis, A.M., Parkesh, R., Mizote, A., Rosen, D., Thomas, J.M., Izumi, M., Ganesan, a, Galione, A. & Churchill, G.C. (2009). Identification of a chemical probe for NAADP by virtual screening. *Nature chemical biology*. 5 (4). p.pp. 220–6.
- Neumann, J., Bras, J., Deas, E., O’Sullivan, S.S., Parkkinen, L., Lachmann, R.H., Li, A., Holton, J., Guerreiro, R., Paudel, R., Segarane, B., Singleton, A., Lees, A., Hardy, J., Houlden, H., Revesz, T. & Wood, N.W. (2009). Glucocerebrosidase mutations in clinical and pathologically proven Parkinson’s disease. *Brain : a journal of neurology*. 132 (Pt 7). p.pp. 1783–94.
- Nguyen, H.N., Byers, B., Cord, B., Shcheglovitov, A., Byrne, J., Gujar, P., Kee, K., Schüle, B., Dolmetsch, R.E., Langston, W., Palmer, T.D. & Pera, R.R. (2011). LRRK2 mutant iPSC-derived DA neurons demonstrate increased susceptibility to oxidative stress. *Cell stem cell*. 8 (3). p.pp. 267–80.
- Nishimura, A.L., Mitne-Neto, M., Silva, H.C. a, Richieri-Costa, A., Middleton, S., Cascio, D., Kok, F., Oliveira, J.R.M., Gillingwater, T., Webb, J., Skehel, P. & Zatz, M. (2004). A mutation in the vesicle-trafficking protein VAPB causes late-onset spinal muscular atrophy and amyotrophic lateral sclerosis. *American journal of human genetics*. 75 (5). p.pp. 822–31.
- Obeso, J. a, Rodriguez-Oroz, M.C., Goetz, C.G., Marin, C., Kordower, J.H., Rodriguez, M., Hirsch, E.C., Farrer, M., Schapira, A.H. V & Halliday, G. (2010). Missing pieces in the Parkinson’s disease puzzle. *Nature medicine*. 16 (6). p.pp. 653–61.
- Ong, D.S.T., Mu, T.-W., Palmer, A.E. & Kelly, J.W. (2010). Endoplasmic reticulum Ca<sup>2+</sup> increases enhance mutant glucocerebrosidase proteostasis. *Nature chemical biology*. 6 (6). p.pp. 424–32.
- Orci, L., Ravazzola, M., Le Coadic, M., Shen, W.-W., Demaurex, N. & Cosson, P. (2009). From the Cover: STIM1-induced precortical and cortical subdomains of the endoplasmic reticulum. *Proceedings of the National Academy of Sciences of the United States of America*. 106 (46). p.pp. 19358–62.
- Osellame, L.D., Rahim, A. a, Hargreaves, I.P., Gegg, M.E., Richard-Londt, A., Brandner, S., Waddington, S.N., Schapira, A.H. V & Duhen, M.R. (2013). Mitochondria and quality control defects in a mouse model of Gaucher disease--links to Parkinson’s disease. *Cell metabolism*. 17 (6). p.pp. 941–53.
- Osman, C., Voelker, D.R. & Langer, T. (2011). Making heads or tails of phospholipids in mitochondria. *The Journal of cell biology*. 192 (1). p.pp. 7–16.
- Paisan-Ruiz, C., Bhatia, K.P., Li, A., Hernandez, D., Davis, M., Wood, N.W., Hardy, J., Houlden, H., Singleton, A. & Schneider, S. a (2009). Characterization of PLA2G6 as a locus for dystonia-parkinsonism. *Annals of neurology*. 65 (1). p.pp. 19–23.

- Paisán-Ruíz, C., Jain, S., Evans, E.W., Gilks, W.P., Simón, J., van der Brug, M., López de Munain, A., Aparicio, S., Gil, A.M., Khan, N., Johnson, J., Martinez, J.R., Nicholl, D., Carrera, I.M., Pena, A.S., de Silva, R., Lees, A., Martí-Massó, J.F., Pérez-Tur, J., Wood, N.W. & Singleton, A.B. (2004). Cloning of the gene containing mutations that cause PARK8-linked Parkinson's disease. *Neuron*. 44 (4). p.pp. 595–600.
- Paisán-Ruíz, C., Nath, P., Washecka, N., Gibbs, J.R. & Singleton, A.B. (2008). Comprehensive analysis of LRRK2 in publicly available Parkinson's disease cases and neurologically normal controls. *Human mutation*. 29 (4). p.pp. 485–90.
- Di Palma, F., Belyantseva, I. a, Kim, H.J., Vogt, T.F., Kachar, B. & Noben-Trauth, K. (2002). Mutations in Mcoln3 associated with deafness and pigmentation defects in varitint-waddler (Va) mice. *Proceedings of the National Academy of Sciences of the United States of America*. 99 (23). p.pp. 14994–9.
- Palmer, A.E., Jin, C., Reed, J.C. & Tsien, R.Y. (2004). Bcl-2-mediated alterations in endoplasmic reticulum Ca<sup>2+</sup> analyzed with an improved genetically encoded fluorescent sensor. *Proceedings of the National Academy of Sciences of the United States of America*. 101 (50). p.pp. 17404–9.
- Palty, R., Silverman, W.F., Hershinkel, M., Caporale, T., Sensi, S.L., Parnis, J., Nolte, C., Fishman, D., Shoshan-Barmatz, V., Herrmann, S., Khananshvil, D. & Sekler, I. (2010). NCLX is an essential component of mitochondrial Na<sup>+</sup>/Ca<sup>2+</sup> exchange. *Proceedings of the National Academy of Sciences of the United States of America*. 107 (1). p.pp. 436–41.
- Pan, X., Roberts, P., Chen, Y., Kvam, E., Shulga, N., Huang, K., Lemmon, S. & Goldfarb, D.S. (2000). Nucleus-vacuole junctions in *Saccharomyces cerevisiae* are formed through the direct interaction of Vac8p with Nvj1p. *Molecular biology of the cell*. 11 (7). p.pp. 2445–57.
- Pandey, V., Chuang, C.-C., Lewis, A.M., Aley, P.K., Brailoiu, E., Dun, N.J., Churchill, G.C. & Patel, S. (2009). Recruitment of NAADP-sensitive acidic Ca<sup>2+</sup> stores by glutamate. *The Biochemical journal*. 422 (3). p.pp. 503–12.
- Panicker, L.M., Miller, D., Park, T.S., Patel, B., Azevedo, J.L., Awad, O., Masood, M.A., Veenstra, T.D., Goldin, E., Stubblefield, B.K., Tayebi, N., Polumuri, S.K., Vogel, S.N., Sidransky, E., Zambidis, E.T. & Feldman, R. a (2012). Induced pluripotent stem cell model recapitulates pathologic hallmarks of Gaucher disease. *Proceedings of the National Academy of Sciences of the United States of America*. p.pp. 1–6.
- Papkovskaia, T.D., Chau, K.-Y., Inesta-Vaquera, F., Papkovsky, D.B., Healy, D.G., Nishio, K., Staddon, J., Duchon, M.R., Hardy, J., Schapira, A.H. V & Cooper, J.M. (2012). G2019S leucine-rich repeat kinase 2 causes uncoupling protein-mediated mitochondrial depolarization. *Human molecular genetics*. 21 (19). p.pp. 4201–13.
- Parekh, A.B. (2011). Decoding cytosolic Ca<sup>2+</sup> oscillations. *Trends in biochemical sciences*. 36 (2). p.pp. 78–87.

- Park, M.K., Petersen, O.H. & Tepikin, a V (2000). The endoplasmic reticulum as one continuous Ca<sup>2+</sup> pool: visualization of rapid Ca<sup>2+</sup> movements and equilibration. *The EMBO journal*. 19 (21). p.pp. 5729–39.
- Parkesh, R., Lewis, A.M., Aley, P.K., Arredouani, A., Rossi, S., Tavares, R., Vasudevan, S.R., Rosen, D., Galione, A., Dowden, J. & Churchill, G.C. (2008). Cell-permeant NAADP: a novel chemical tool enabling the study of Ca<sup>2+</sup> signalling in intact cells. *Cell calcium*. 43 (6). p.pp. 531–8.
- Paschen, W. & Mengesdorf, T. (2005). Endoplasmic reticulum stress response and neurodegeneration. *Cell calcium*. 38 (3-4). p.pp. 409–15.
- Pasternak, B., Svanström, H., Nielsen, N.M., Fugger, L., Melbye, M. & Hviid, A. (2012). Use of calcium channel blockers and Parkinson's disease. *American journal of epidemiology*. 175 (7). p.pp. 627–35.
- Patel, S. & Brailoiu, E. (2012). Triggering of Ca<sup>2+</sup> signals by NAADP-gated two-pore channels: a role for membrane contact sites? *Biochemical Society transactions*. 40 (1). p.pp. 153–7.
- Patel, S. & Docampo, R. (2010). Acidic calcium stores open for business : expanding the potential for intracellular Ca<sup>2+</sup> signaling. *Trends in Cell Biology*. 20 (5). p.pp. 277–286.
- Pelled, D., Trajkovic-Bodenec, S., Lloyd-Evans, E., Sidransky, E., Schiffmann, R. & Futerman, A.H. (2005). Enhanced calcium release in the acute neuronopathic form of Gaucher disease. *Neurobiology of disease*. 18 (1). p.pp. 83–8.
- Penna, A., Demuro, A., Yeromin, A. V, Zhang, S.L., Safrina, O., Parker, I. & Cahalan, M.D. (2008). The CRAC channel consists of a tetramer formed by Stim-induced dimerization of Orai dimers. *Nature*. 456 (7218). p.pp. 116–20.
- Penny, C.J., Kilpatrick, B.S., Han, J.M., Sneyd, J. & Patel, S. (2014). A computational model of lysosome-ER Ca<sup>2+</sup> microdomains. *Journal of cell science*. 127 (Pt 13). p.pp. 2934–43.
- Pereira, G.J.S., Hirata, H., Fimia, G.M., do Carmo, L.G., Bincoletto, C., Han, S.W., Stilhano, R.S., Ureshino, R.P., Bloor-Young, D., Churchill, G., Piacentini, M., Patel, S. & Smaili, S.S. (2011). Nicotinic acid adenine dinucleotide phosphate (NAADP) regulates autophagy in cultured astrocytes. *The Journal of biological chemistry*. 286 (32). p.pp. 27875–81.
- Peretti, D., Dahan, N., Shimoni, E., Hirschberg, K. & Lev, S. (2008). Coordinated lipid transfer between the endoplasmic reticulum and the Golgi complex requires the VAP proteins and is essential for Golgi-mediated transport. *Molecular biology of the cell*. 19 (9). p.pp. 3871–84.
- Pfisterer, U., Kirkeby, A., Torper, O., Wood, J., Nelander, J., Dufour, A., Björklund, A., Lindvall, O., Jakobsson, J. & Parmar, M. (2011). Direct conversion of human fibroblasts to dopaminergic neurons. *Proceedings of the National Academy of Sciences of the United States of America*. 108 (25). p.pp. 10343–8.
- Piccoli, G., Condliffe, S.B., Bauer, M., Giesert, F., Boldt, K., De Astis, S., Meixner, A., Sarioglu, H., Vogt-Weisenhorn, D.M., Wurst, W., Gloeckner, C.J., Matteoli, M., Sala, C. &

- Ueffing, M. (2011). LRRK2 controls synaptic vesicle storage and mobilization within the recycling pool. *The Journal of neuroscience : the official journal of the Society for Neuroscience*. 31 (6). p.pp. 2225–37.
- Pinto, F. de T., Corradi, G.R., Hera, D.P. de la & Adamo, H.P. (2012). CHO cells expressing the human P<sub>5</sub>-ATPase ATP13A2 are more sensitive to the toxic effects of herbicide paraquat. *Neurochemistry international*. 60 (3). p.pp. 243–8.
- Pinton, P., Giorgi, C., Siviero, R., Zecchini, E. & Rizzuto, R. (2008). Calcium and apoptosis: ER-mitochondria Ca<sup>2+</sup> transfer in the control of apoptosis. *Oncogene*. 27 (50). p.pp. 6407–18.
- Pinton, P., Pozzan, T. & Rizzuto, R. (1998). The Golgi apparatus is an inositol 1,4,5-trisphosphate-sensitive Ca<sup>2+</sup> store, with functional properties distinct from those of the endoplasmic reticulum. *The EMBO journal*. 17 (18). p.pp. 5298–308.
- Piper, R.C. & Luzio, J.P. (2004). CUPpling calcium to lysosomal biogenesis. *Trends in cell biology*. 14 (9). p.pp. 471–3.
- Pitt, S.J., Funnell, T.M., Sitsapesan, M., Venturi, E., Rietdorf, K., Ruas, M., Ganesan, a, Gosain, R., Churchill, G.C., Zhu, M.X., Parrington, J., Galione, A. & Sitsapesan, R. (2010). TPC2 is a novel NAADP-sensitive Ca<sup>2+</sup> release channel, operating as a dual sensor of luminal pH and Ca<sup>2+</sup>. *The Journal of biological chemistry*. 285 (45). p.pp. 35039–46.
- Platt, F.M. (2014). Sphingolipid lysosomal storage disorders. *Nature*. 510 (7503). p.pp. 68–75.
- Plowey, E.D., Cherra, S.J., Liu, Y.-J. & Chu, C.T. (2008). Role of autophagy in G2019S-LRRK2-associated neurite shortening in differentiated SH-SY5Y cells. *Journal of neurochemistry*. 105 (3). p.pp. 1048–56.
- Polymeropoulos, M.H., Lavedan, C., Leroy, E., Ide, S.E., Dehejia, A., Dutra, A., Pike, B., Root, H., Rubenstein, J., Boyer, R., Stenroos, E.S., Chandrasekharappa, S., Athanassiadou, A., Papapetropoulos, T., Johnson, W.G., Lazzarini, A.M., Duvoisin, R.C., Di Iorio, G., Golbe, L.I. & Nussbaum, R.L. (1997). Mutation in the alpha-synuclein gene identified in families with Parkinson's disease. *Science (New York, N.Y.)*. 276 (5321). p.pp. 2045–7.
- Prinz, W. a (2014). Bridging the gap: Membrane contact sites in signaling, metabolism, and organelle dynamics. *The Journal of cell biology*. 205 (6). p.pp. 759–769.
- Prinz, W. a (2010). Lipid trafficking sans vesicles: where, why, how? *Cell*. 143 (6). p.pp. 870–4.
- Pryor, P.R., Mullock, B.M., Bright, N. a, Gray, S.R. & Luzio, J.P. (2000). The role of intraorganellar Ca<sup>2+</sup> in late endosome-lysosome heterotypic fusion and in the reformation of lysosomes from hybrid organelles. *The Journal of cell biology*. 149 (5). p.pp. 1053–62.
- Puzianowska-Kuznicka, M. & Kuznicki, J. (2009). The ER and ageing II: calcium homeostasis. *Ageing research reviews*. 8 (3). p.pp. 160–72.

- Rahman, T. & Taylor, C.W. (2009). Dynamic regulation of IP<sub>3</sub> receptor clustering and activity by IP<sub>3</sub>. *Channels (Austin, Tex.)*. 3 (4). p.pp. 226–32.
- Ramirez, A., Heimbach, A., Gründemann, J., Stiller, B., Hampshire, D., Cid, L.P., Goebel, I., Mubaidin, A.F., Wriekat, A.-L., Roeper, J., Al-Din, A., Hillmer, A.M., Karsak, M., Liss, B., Woods, C.G., Behrens, M.I. & Kubisch, C. (2006). Hereditary parkinsonism with dementia is caused by mutations in ATP13A2, encoding a lysosomal type 5 P-type ATPase. *Nature genetics*. 38 (10). p.pp. 1184–91.
- Ramsden, N., Perrin, J., Ren, Z., Lee, B.D., Zinn, N., Dawson, V.L., Tam, D., Bova, M., Lang, M., Drewes, G., Bantsche, M., Bard, F., Dawson, T.M. & Hopf, C. (2011). *Chemoproteomics-Based Design of Potent LRRK2-Selective Lead Compounds That Attenuate Parkinson's Disease-Related Toxicity in Human Neurons*. p.pp. 1021–1028.
- Rana, H.Q., Balwani, M., Bier, L. & Alcalay, R.N. (2013). Age-specific Parkinson disease risk in GBA mutation carriers: information for genetic counseling. *Genetics in medicine : official journal of the American College of Medical Genetics*. 15 (2). p.pp. 146–9.
- Reczek, D., Schwake, M., Schröder, J., Hughes, H., Blanz, J., Jin, X., Brondyk, W., Van Patten, S., Edmunds, T. & Saftig, P. (2007). LIMP-2 is a receptor for lysosomal mannose-6-phosphate-independent targeting of beta-glucocerebrosidase. *Cell*. 131 (4). p.pp. 770–83.
- Reeves, D.C., Liebelt, D. a, Lakshmanan, V., Roepe, P.D., Fidock, D. a & Akabas, M.H. (2006). Chloroquine-resistant isoforms of the Plasmodium falciparum chloroquine resistance transporter acidify lysosomal pH in HEK293 cells more than chloroquine-sensitive isoforms. *Molecular and biochemical parasitology*. 150 (2). p.pp. 288–99.
- Rigat, B. & Mahuran, D. (2009). Diltiazem, a L-type Ca<sup>2+</sup> channel blocker, also acts as a pharmacological chaperone in Gaucher patient cells. *Molecular genetics and metabolism*. 96 (4). p.pp. 225–32.
- Ritz, B., Rhodes, S.L., Qian, L., Schernhammer, E., Olsen, J.H. & Friis, S. (2010). L-type calcium channel blockers and Parkinson disease in Denmark. *Annals of neurology*. 67 (5). p.pp. 600–6.
- Rizzuto, R., Brini, M., Murgia, M. & Pozzan, T. (1993). Microdomains with high Ca<sup>2+</sup> close to IP<sub>3</sub>-sensitive channels that are sensed by neighboring mitochondria. *Science (New York, N.Y.)*. 262 (5134). p.pp. 744–7.
- Rizzuto, R., Pinton, P., Carrington, W., Fay, F.S., Fogarty, K.E., Lifshitz, L.M., Tuft, R.A. & Pozzan, T. (1998). Close contacts with the endoplasmic reticulum as determinants of mitochondrial Ca<sup>2+</sup> responses. *Science (New York, N.Y.)*. 280 (5370). p.pp. 1763–6.
- Rizzuto, R., De Stefani, D., Raffaello, A. & Mammucari, C. (2012). Mitochondria as sensors and regulators of calcium signalling. *Nature reviews. Molecular cell biology*. 13 (9). p.pp. 566–78.
- Rocha, N., Kuijl, C., van der Kant, R., Janssen, L., Houben, D., Janssen, H., Zwart, W. & Neefjes, J. (2009). Cholesterol sensor ORP1L contacts the ER protein VAP to control

- Rab7-RILP-p150 Glued and late endosome positioning. *The Journal of cell biology*. 185 (7). p.pp. 1209–25.
- Ron, I. & Horowitz, M. (2005). ER retention and degradation as the molecular basis underlying Gaucher disease heterogeneity. *Human molecular genetics*. 14 (16). p.pp. 2387–98.
- Rosen, D., Bloor-Young, D., Squires, J., Parkesh, R., Waters, G., Vasudevan, S.R., Lewis, A.M. & Churchill, G.C. (2012). Synthesis and use of cell-permeant cyclic ADP-ribose. *Biochemical and biophysical research communications*. 418 (2). p.pp. 353–8.
- Rosenbloom, B., Balwani, M., Bronstein, J.M., Kolodny, E., Sathe, S., Gwosdow, A.R., Taylor, J.S., Cole, J.A., Zimran, A. & Weinreb, N.J. (2011). The incidence of Parkinsonism in patients with type 1 Gaucher disease: data from the ICGG Gaucher Registry. *Blood cells, molecules & diseases*. 46 (1). p.pp. 95–102.
- Rothaug, M., Zunke, F., Mazzulli, J.R., Schweizer, M., Altmeyen, H., Lüllmann-Rauch, R., Kallemeijn, W.W., Gaspar, P., Aerts, J.M., Glatzel, M., Saftig, P., Krainc, D., Schwake, M. & Blanz, J. (2014). LIMP-2 expression is critical for  $\beta$ -glucocerebrosidase activity and  $\alpha$ -synuclein clearance. *Proceedings of the National Academy of Sciences of the United States of America*. p.pp. 1–6.
- Ruas, M., Chuang, K.-T., Davis, L.C., Al-Douri, A., Tynan, P.W., Tunn, R., Teboul, L., Galione, A. & Parrington, J. (2014). TPC1 Has Two Variant Isoforms, and Their Removal Has Different Effects on Endo-Lysosomal Functions Compared to Loss of TPC2. *Molecular and cellular biology*. 34 (21). p.pp. 3981–92.
- Saito, Y., Suzuki, K., Hulette, C.M. & Murayama, S. (2004). Aberrant phosphorylation of alpha-synuclein in human Niemann-Pick type C1 disease. *Journal of neuropathology and experimental neurology*. 63 (4). p.pp. 323–8.
- Sardiello, M., Palmieri, M., di Ronza, A., Medina, D.L., Valenza, M., Gennarino, V.A., Di Malta, C., Donaudy, F., Embrione, V., Polishchuk, R.S., Banfi, S., Parenti, G., Cattaneo, E. & Ballabio, A. (2009). A gene network regulating lysosomal biogenesis and function. *Science (New York, N.Y.)*. 325 (5939). p.pp. 473–7.
- SCHAPIRA, A. (1989). MITOCHONDRIAL COMPLEX I DEFICIENCY IN PARKINSON'S DISEASE. *The Lancet*. 333 (8649). p.p. 1269.
- Schapira, A.H. V (2012). Mitochondrial diseases. *Lancet*. 379 (9828). p.pp. 1825–34.
- Schapira, A.H. V (2009). Neurobiology and treatment of Parkinson's disease. *Trends in pharmacological sciences*. 30 (1). p.pp. 41–7.
- Schieder, M., Rötzer, K., Brüggemann, A., Biel, M. & Wahl-Schott, C. a (2010). Characterization of two-pore channel 2 (TPCN2)-mediated Ca<sup>2+</sup> currents in isolated lysosomes. *The Journal of biological chemistry*. 285 (28). p.pp. 21219–22.
- Schmidt, K., Wolfe, D.M., Stiller, B. & Pearce, D. a (2009). Cd<sup>2+</sup>, Mn<sup>2+</sup>, Ni<sup>2+</sup> and Se<sup>2+</sup> toxicity to *Saccharomyces cerevisiae* lacking YPK9p the orthologue of human

ATP13A2. *Biochemical and biophysical research communications*. 383 (2). p.pp. 198–202.

Schnaar, R.L., Suzuki, A. & Stanley, P. (2009). *Glycosphingolipids - Essentials of Glycobiology*. 2nd Editio. and M. E. E. Varki, Ajit, Richard D. Cummings, Jeffrey D. Esko, Hudson H. Freeze, Pamela Stanley, Carolyn R. Bertozzi, Gerald W. Hart (ed.). New York: Cold Spring Harbor (NY).

Schöndorf, D.C., Aureli, M., McAllister, F.E., Hindley, C.J., Mayer, F., Schmid, B., Sardi, S.P., Valsecchi, M., Hoffmann, S., Schwarz, L.K., Hedrich, U., Berg, D., Shihabuddin, L.S., Hu, J., Pruszek, J., Gygi, S.P., Sonnino, S., Gasser, T. & Deleidi, M. (2014). iPSC-derived neurons from GBA1-associated Parkinson's disease patients show autophagic defects and impaired calcium homeostasis. *Nature communications*. 5 (May). p.p. 4028.

Schulz, T. a, Choi, M.-G., Raychaudhuri, S., Mears, J. a, Ghirlando, R., Hinshaw, J.E. & Prinz, W. a (2009). Lipid-regulated sterol transfer between closely apposed membranes by oxysterol-binding protein homologues. *The Journal of cell biology*. 187 (6). p.pp. 889–903.

Selvaraj, S., Sun, Y., Watt, J.A., Wang, S. & Lei, S. (2012). Neurotoxin-induced ER stress in mouse dopaminergic neurons involves downregulation of TRPC1 and inhibition of AKT / mTOR signaling. 122 (4).

Seo, M.-D., Velamakanni, S., Ishiyama, N., Stathopoulos, P.B., Rossi, A.M., Khan, S. a, Dale, P., Li, C., Ames, J.B., Ikura, M. & Taylor, C.W. (2012). Structural and functional conservation of key domains in InsP3 and ryanodine receptors. *Nature*. 483 (7387). p.pp. 108–12.

Settembre, C., Zoncu, R., Medina, D.L., Vetrini, F., Erdin, S., Erdin, S., Huynh, T., Ferron, M., Karsenty, G., Vellard, M.C., Facchinetti, V., Sabatini, D.M. & Ballabio, A. (2012). A lysosome-to-nucleus signalling mechanism senses and regulates the lysosome via mTOR and TFEB. *The EMBO journal*. 31 (5). p.pp. 1095–108.

Sheehan, J.P., Swerdlow, R.H., Parker, W.D., Miller, S.W., Davis, R.E. & Tuttle, J.B. (1997). Altered calcium homeostasis in cells transformed by mitochondria from individuals with Parkinson's disease. *Journal of neurochemistry*. 68 (3). p.pp. 1221–33.

Shen, D., Wang, X., Li, X., Zhang, X., Yao, Z., Dibble, S., Dong, X., Yu, T., Lieberman, A.P., Showalter, H.D. & Xu, H. (2012). Lipid storage disorders block lysosomal trafficking by inhibiting a TRP channel and lysosomal calcium release. *Nature communications*. 3. p.p. 731.

Sherwood, M.W., Prior, I. a, Voronina, S.G., Barrow, S.L., Woodsmith, J.D., Gerasimenko, O. V, Petersen, O.H. & Tepikin, A. V (2007). Activation of trypsinogen in large endocytic vacuoles of pancreatic acinar cells. *Proceedings of the National Academy of Sciences of the United States of America*. 104 (13). p.pp. 5674–9.

Shin, N., Jeong, H., Kwon, J., Heo, H.Y., Kwon, J.J., Yun, H.J., Kim, C.-H., Han, B.S., Tong, Y., Shen, J., Hatano, T., Hattori, N., Kim, K.-S., Chang, S. & Seol, W. (2008). LRRK2 regulates synaptic vesicle endocytosis. *Experimental cell research*. 314 (10). p.pp. 2055–65.



- Shulman, J.M., De Jager, P.L. & Feany, M.B. (2011). Parkinson's disease: genetics and pathogenesis. *Annual review of pathology*. 6. p.pp. 193–222.
- Sidransky, E. (2004). Gaucher disease: complexity in a “simple” disorder. *Molecular genetics and metabolism*. 83 (1-2). p.pp. 6–15.
- Sidransky, E. & Lopez, G. (2012). The link between the GBA gene and parkinsonism. *Lancet neurology*. 11 (11). p.pp. 986–98.
- Sidransky, E., Nalls, M. a, Aasly, J.O., Aharon-Peretz, J., Annesi, G., Barbosa, E.R., Bar-Shira, a, Berg, D., Bras, J., Brice, a, Chen, C.-M., Clark, L.N., Condroyer, C., De Marco, E. V, Dürr, a, Eblan, M.J., Fahn, S., Farrer, M.J., Fung, H.-C., Gan-Or, Z., Gasser, T., Gershoni-Baruch, R., Giladi, N., Griffith, a, Gurevich, T., Januario, C., Kropp, P., Lang, a E., Lee-Chen, G.-J., Lesage, S., Marder, K., Mata, I.F., Mirelman, a, Mitsui, J., Mizuta, I., Nicoletti, G., Oliveira, C., Ottman, R., Orr-Urtreger, a, Pereira, L. V, Quattrone, a, Rogaeva, E., Rolfs, a, Rosenbaum, H., Rozenberg, R., Samii, a, Samaddar, T., Schulte, C., Sharma, M., Singleton, a, Spitz, M., Tan, E.-K., Tayebi, N., Toda, T., Troiano, a R., Tsuji, S., Wittstock, M., Wolfsberg, T.G., Wu, Y.-R., Zabetian, C.P., Zhao, Y. & Ziegler, S.G. (2009). Multicenter analysis of glucocerebrosidase mutations in Parkinson's disease. *The New England journal of medicine*. 361 (17). p.pp. 1651–61.
- Siebert, M., Sidransky, E. & Westbroek, W. (2014). Glucocerebrosidase is shaking up the synucleinopathies. *Brain : a journal of neurology*. 137 (Pt 5). p.pp. 1304–22.
- Singleton, A.B., Farrer, M., Johnson, J., Singleton, A., Hague, S., Kachergus, J., Hulihan, M., Peuralinna, T., Dutra, A., Nussbaum, R., Lincoln, S., Crawley, A., Hanson, M., Maraganore, D., Adler, C., Cookson, M.R., Muentner, M., Baptista, M., Miller, D., Blancato, J., Hardy, J. & Gwinn-Hardy, K. (2003). alpha-Synuclein locus triplication causes Parkinson's disease. *Science (New York, N.Y.)*. 302 (5646). p.p. 841.
- Sivaramakrishnan, V., Bidula, S., Campwala, H., Katikaneni, D. & Fountain, S.J. (2012). Constitutive lysosome exocytosis releases ATP and engages P2Y receptors in human monocytes. *Journal of cell science*. 125 (Pt 19). p.pp. 4567–75.
- Smith, W.W., Pei, Z., Jiang, H., Moore, D.J., Liang, Y., West, A.B., Dawson, V.L., Dawson, T.M. & Ross, C.A. (2005). Leucine-rich repeat kinase 2 (LRRK2) interacts with parkin, and mutant LRRK2 induces neuronal degeneration. *Proceedings of the National Academy of Sciences of the United States of America*. 102 (51). p.pp. 18676–81.
- Soares, S., Thompson, M., White, T., Isbell, A., Yamasaki, M., Prakash, Y., Lund, F.E., Galione, A., Chini, E.N. & Is-, A. (2007). NAADP as a second messenger : neither CD38 nor base-exchange reaction are necessary for in vivo generation of NAADP in myometrial cells. 55905. p.pp. 227–239.
- Steen, M., Kirchberger, T. & Guse, A.H. (2007). NAADP mobilizes calcium from the endoplasmic reticular Ca(2+) store in T-lymphocytes. *The Journal of biological chemistry*. 282 (26). p.pp. 18864–71.
- Stefan, C.J., Manford, A.G., Baird, D., Yamada-Hanff, J., Mao, Y. & Emr, S.D. (2011). Osh proteins regulate phosphoinositide metabolism at ER-plasma membrane contact sites. *Cell*. 144 (3). p.pp. 389–401.

- Stefan, C.J., Manford, A.G. & Emr, S.D. (2013). ER-PM connections: sites of information transfer and inter-organelle communication. *Current opinion in cell biology*. 25 (4). p.pp. 434–42.
- De Stefani, D., Raffaello, A., Teardo, E., Szabò, I. & Rizzuto, R. (2011). A forty-kilodalton protein of the inner membrane is the mitochondrial calcium uniporter. *Nature*. 476 (7360). p.pp. 336–40.
- Steinberg, B.E., Huynh, K.K., Brodovitch, A., Jabs, S., Stauber, T., Jentsch, T.J. & Grinstein, S. (2010). A cation counterflux supports lysosomal acidification. *The Journal of cell biology*. 189 (7). p.pp. 1171–86.
- Striessnig, J., Bolz, H.J. & Koschak, A. (2010). Channelopathies in Cav1.1, Cav1.3, and Cav1.4 voltage-gated L-type Ca<sup>2+</sup> channels. *Pflügers Archiv : European journal of physiology*. 460 (2). p.pp. 361–74.
- Stutzmann, G.E. & Mattson, M.P. (2011). *Endoplasmic Reticulum Ca<sup>2+</sup> Handling in Excitable Cells in Health and Disease*. 63 (3). p.pp. 700–727.
- Sun, Y., Liou, B., Quinn, B., Ran, H., Xu, Y.-H. & Grabowski, G. a (2009). In vivo and ex vivo evaluation of L-type calcium channel blockers on acid beta-glucosidase in Gaucher disease mouse models. *PloS one*. 4 (10). p.p. e7320.
- Surmeier, D.J. & Schumacker, P.T. (2013). Calcium, bioenergetics, and neuronal vulnerability in Parkinson's disease. *The Journal of biological chemistry*. 288 (15). p.pp. 10736–41.
- Szabadkai, G., Bianchi, K., Várnai, P., De Stefani, D., Wieckowski, M.R., Cavagna, D., Nagy, A.I., Balla, T. & Rizzuto, R. (2006). Chaperone-mediated coupling of endoplasmic reticulum and mitochondrial Ca<sup>2+</sup> channels. *The Journal of cell biology*. 175 (6). p.pp. 901–11.
- Taira, T., Saito, Y., Niki, T., Iguchi-Ariga, S.M.M., Takahashi, K. & Ariga, H. (2004). DJ-1 has a role in antioxidative stress to prevent cell death. *EMBO reports*. 5 (2). p.pp. 213–8.
- Takeshima, H., Komazaki, S., Nishi, M., Iino, M. & Kangawa, K. (2000). Junctophilins: a novel family of junctional membrane complex proteins. *Molecular cell*. 6 (1). p.pp. 11–22.
- Tanner, C.M., Kamel, F., Ross, G.W., Hoppin, J. a, Goldman, S.M., Korell, M., Marras, C., Bhudhikanok, G.S., Kasten, M., Chade, A.R., Comyns, K., Richards, M.B., Meng, C., Priestley, B., Fernandez, H.H., Cambi, F., Umbach, D.M., Blair, A., Sandler, D.P. & Langston, J.W. (2011). Rotenone, paraquat, and Parkinson's disease. *Environmental health perspectives*. 119 (6). p.pp. 866–72.
- Tao, F., Okano, Y. & Nozawa, Y. (1988). Bradykinin-induced generation of inositol 1,4,5-trisphosphate in fibroblasts and neuroblastoma cells: Effect of pertussis toxin, extracellular calcium, and down-regulation of protein kinase C. *Biochemical and Biophysical Research Communications*. 157 (3). p.pp. 1429–1435.
- Tarasov, A.I., Griffiths, E.J. & Rutter, G. a (2012). Regulation of ATP production by mitochondrial Ca(2+). *Cell calcium*. 52 (1). p.pp. 28–35.

- Tayebi, N., Callahan, M., Madike, V., Stubblefield, B.K., Orvisky, E., Krasnewich, D., Fillano, J.J. & Sidransky, E. (2001). Gaucher disease and parkinsonism: a phenotypic and genotypic characterization. *Molecular genetics and metabolism*. 73 (4). p.pp. 313–21.
- Tekoah, Y., Tzaban, S., Kizhner, T., Hainrichson, M., Gantman, A., Golembo, M., Aviezer, D. & Shaaltiel, Y. (2013). Glycosylation and functionality of recombinant  $\beta$ -glucocerebrosidase from various production systems. *Bioscience reports*. 33 (5).
- Thayanidhi, N., Helm, J.R., Nycz, D.C., Bentley, M., Liang, Y. & Hay, J.C. (2010a).  $\alpha$ -Synuclein Delays Endoplasmic Reticulum (ER) -to-Golgi Transport in Mammalian Cells by Antagonizing ER / Golgi SNAREs. 21. p.pp. 1850–1863.
- Thayanidhi, N., Helm, J.R., Nycz, D.C., Bentley, M., Liang, Y. & Hay, J.C. (2010b). Alpha-synuclein delays endoplasmic reticulum (ER)-to-Golgi transport in mammalian cells by antagonizing ER/Golgi SNAREs. *Molecular biology of the cell*. 21 (11). p.pp. 1850–63.
- Tong, Y., Giaime, E., Yamaguchi, H., Ichimura, T., Liu, Y., Si, H., Cai, H., Bonventre, J. V & Shen, J. (2012). Loss of leucine-rich repeat kinase 2 causes age-dependent bi-phasic alterations of the autophagy pathway. *Molecular neurodegeneration*. 7 (1). p.p. 2.
- Tong, Y., Yamaguchi, H., Giaime, E., Boyle, S., Kopan, R., Kelleher, R.J. & Shen, J. (2010). Loss of leucine-rich repeat kinase 2 causes impairment of protein degradation pathways, accumulation of alpha-synuclein, and apoptotic cell death in aged mice. *Proceedings of the National Academy of Sciences of the United States of America*. 107 (21). p.pp. 9879–84.
- Trinh, J. & Farrer, M. (2013). Advances in the genetics of Parkinson disease. *Nature reviews. Neurology*. 9 (8). p.pp. 445–54.
- Tu, H., Nelson, O., Bezprozvanny, A., Wang, Z., Lee, S.-F., Hao, Y.-H., Serneels, L., De Strooper, B., Yu, G. & Bezprozvanny, I. (2006). Presenilins form ER Ca<sup>2+</sup> leak channels, a function disrupted by familial Alzheimer's disease-linked mutations. *Cell*. 126 (5). p.pp. 981–93.
- Tu, P., Gibon, J. & Bouron, A. (2010). The TRPC6 channel activator hyperforin induces the release of zinc and calcium from mitochondria. *Journal of neurochemistry*. 112 (1). p.pp. 204–13.
- Tucci, A., Nalls, M. a, Houlden, H., Revesz, T., Singleton, A.B., Wood, N.W., Hardy, J. & Paisán-Ruiz, C. (2010). Genetic variability at the PARK16 locus. *European journal of human genetics : EJHG*. 18 (12). p.pp. 1356–9.
- Verity, C., Winstone, A.M., Stelitano, L., Will, R. & Nicoll, A. (2010). The epidemiology of progressive intellectual and neurological deterioration in childhood. *Archives of disease in childhood*. 95 (5). p.pp. 361–4.
- Vilariño-Güell, C., Wider, C., Ross, O. a, Dachsel, J.C., Kachergus, J.M., Lincoln, S.J., Soto-Ortolaza, A.I., Cobb, S. a, Wilhoite, G.J., Bacon, J. a, Behrouz, B., Melrose, H.L., Hentati, E., Puschmann, A., Evans, D.M., Conibear, E., Wasserman, W.W., Aasly, J.O., Burkhard, P.R., Djaldetti, R., Ghika, J., Hentati, F., Krygowska-Wajs, A., Lynch, T., Melamed, E., Rajput, A., Rajput, A.H., Solida, A., Wu, R.-M., Uitti, R.J., Wszolek, Z.K., Vingerhoets, F.

- & Farrer, M.J. (2011). VPS35 mutations in Parkinson disease. *American journal of human genetics*. 89 (1). p.pp. 162–7.
- Visentin, S., De Nuccio, C., Bernardo, A., Peponi, R., Ferrante, A., Minghetti, L. & Popoli, P. (2013). The stimulation of adenosine A2A receptors ameliorates the pathological phenotype of fibroblasts from Niemann-Pick type C patients. *The Journal of neuroscience : the official journal of the Society for Neuroscience*. 33 (39). p.pp. 15388–93.
- Vitner, E.B., Platt, F.M. & Futerman, A.H. (2010). Common and uncommon pathogenic cascades in lysosomal storage diseases. *The Journal of biological chemistry*. 285 (27). p.pp. 20423–7.
- De Vos, K.J., Mórotz, G.M., Stoica, R., Tudor, E.L., Lau, K.-F., Ackerley, S., Warley, A., Shaw, C.E. & Miller, C.C.J. (2012). VAPB interacts with the mitochondrial protein PTPIP51 to regulate calcium homeostasis. *Human molecular genetics*. 21 (6). p.pp. 1299–311.
- Te Vrugte, D., Speak, A.O., Wallom, K.L., Al Eisa, N., Smith, D.A., Hendriksz, C.J., Simmons, L., Lachmann, R.H., Cousins, A., Hartung, R., Mengel, E., Runz, H., Beck, M., Amraoui, Y., Imrie, J., Jacklin, E., Riddick, K., Yanjanin, N.M., Wassif, C.A., Rolfs, A., Rimmele, F., Wright, N., Taylor, C., Ramaswami, U., Cox, T.M., Hastings, C., Jiang, X., Sidhu, R., Ory, D.S., Arias, B., Jeyakumar, M., Sillence, D.J., Wraith, J.E., Porter, F.D., Cortina-Borja, M. & Platt, F.M. (2014). Relative acidic compartment volume as a lysosomal storage disorder-associated biomarker. *The Journal of clinical investigation*. 124 (3). p.pp. 1320–8.
- Walker, D.S., Ly, S., Lockwood, K.C. & Baylis, H. a (2002). A direct interaction between IP(3) receptors and myosin II regulates IP(3) signaling in *C. elegans*. *Current biology : CB*. 12 (11). p.pp. 951–6.
- Wang, F., Agnello, G., Sotolongo, N. & Segatori, L. (2011a). Ca<sup>2+</sup> homeostasis modulation enhances the amenability of L444P glucosylcerebrosidase to proteostasis regulation in patient-derived fibroblasts. *ACS chemical biology*. 6 (2). p.pp. 158–68.
- Wang, F., Chou, A. & Segatori, L. (2011b). Lacidipine remodels protein folding and Ca<sup>2+</sup> homeostasis in Gaucher's disease fibroblasts: a mechanism to rescue mutant glucocerebrosidase. *Chemistry & biology*. 18 (6). p.pp. 766–76.
- Wang, X., Zhang, X., Dong, X.-P., Samie, M., Li, X., Cheng, X., Goschka, A., Shen, D., Zhou, Y., Harlow, J., Zhu, M.X., Clapham, D.E., Ren, D. & Xu, H. (2012). TPC proteins are phosphoinositide- activated sodium-selective ion channels in endosomes and lysosomes. *Cell*. 151 (2). p.pp. 372–83.
- Wei, H., Kim, S.-J., Zhang, Z., Tsai, P.-C., Wisniewski, K.E. & Mukherjee, A.B. (2008). ER and oxidative stresses are common mediators of apoptosis in both neurodegenerative and non-neurodegenerative lysosomal storage disorders and are alleviated by chemical chaperones. *Human molecular genetics*. 17 (4). p.pp. 469–77.
- West, A.B., Moore, D.J., Biskup, S., Bugayenko, A., Smith, W.W., Ross, C. a, Dawson, V.L. & Dawson, T.M. (2005). Parkinson's disease-associated mutations in leucine-rich repeat

kinase 2 augment kinase activity. *Proceedings of the National Academy of Sciences of the United States of America*. 102 (46). p.pp. 16842–7.

- Wheeler, D.G., Groth, R.D., Ma, H., Barrett, C.F., Owen, S.F., Safa, P. & Tsien, R.W. (2012). Ca(V)1 and Ca(V)2 channels engage distinct modes of Ca(2+) signaling to control CREB-dependent gene expression. *Cell*. 149 (5). p.pp. 1112–24.
- Whitfield, P.D., Nelson, P., Sharp, P.C., Bindloss, C. a, Dean, C., Ravenscroft, E.M., Fong, B. a, Fietz, M.J., Hopwood, J.J. & Meikle, P.J. (2002). Correlation among genotype, phenotype, and biochemical markers in Gaucher disease: implications for the prediction of disease severity. *Molecular genetics and metabolism*. 75 (1). p.pp. 46–55.
- Wu, M.M., Buchanan, J., Luik, R.M. & Lewis, R.S. (2006). Ca<sup>2+</sup> store depletion causes STIM1 to accumulate in ER regions closely associated with the plasma membrane. *The Journal of cell biology*. 174 (6). p.pp. 803–13.
- Yamada, T., McGeer, P.L., Baimbridge, K.G. & McGeer, E.G. (1990). Relative sparing in Parkinson's disease of substantia nigra dopamine neurons containing calbindin-D28K. *Brain research*. 526 (2). p.pp. 303–7.
- Yamaguchi, S., Jha, A., Li, Q., Soyombo, A. a, Dickinson, G.D., Churamani, D., Brailoiu, E., Patel, S. & Muallem, S. (2011). Transient receptor potential mucolipin 1 (TRPML1) and two-pore channels are functionally independent organellar ion channels. *The Journal of biological chemistry*. 286 (26). p.pp. 22934–42.
- Yamasaki, M., Masgrau, R., Morgan, A.J., Churchill, G.C., Patel, S., Ashcroft, S.J.H. & Galione, A. (2004). Organelle selection determines agonist-specific Ca<sup>2+</sup> signals in pancreatic acinar and beta cells. *The Journal of biological chemistry*. 279 (8). p.pp. 7234–40.
- Yang, W. & Tiffany-Castiglioni, E. (2008). Paraquat-induced apoptosis in human neuroblastoma SH-SY5Y cells: involvement of p53 and mitochondria. *Journal of toxicology and environmental health. Part A*. 71 (4). p.pp. 289–99.
- Yi, M., Weaver, D. & Hajnóczky, G. (2004). Control of mitochondrial motility and distribution by the calcium signal: a homeostatic circuit. *The Journal of cell biology*. 167 (4). p.pp. 661–72.
- Zamponi, G.W., Lory, P. & Perez-Reyes, E. (2010). Role of voltage-gated calcium channels in epilepsy. *Pflügers Archiv : European journal of physiology*. 460 (2). p.pp. 395–403.
- Zech, M., Nübling, G., Castrop, F., Jochim, A., Schulte, E.C., Mollenhauer, B., Lichtner, P., Peters, A., Gieger, C., Marquardt, T., Vanier, M.T., Latour, P., Klünemann, H., Trenkwalder, C., Diehl-Schmid, J., Pernecky, R., Meitinger, T., Oexle, K., Haslinger, B., Lorenzl, S. & Winkelmann, J. (2013). Niemann-Pick C disease gene mutations and age-related neurodegenerative disorders. *PLoS one*. 8 (12). p.p. e82879.
- Zeng, Y., Lv, X., Zeng, S., Tian, S., Li, M. & Shi, J. (2008). Sustained depolarization-induced propagation of [Ca<sup>2+</sup>]<sub>i</sub> oscillations in cultured DRG neurons: the involvement of extracellular ATP and P2Y receptor activation. *Brain research*. 1239. p.pp. 12–23.

- Zhang, F., Xu, M., Han, W.-Q. & Li, P.-L. (2011). Reconstitution of lysosomal NAADP-TRP-ML1 signaling pathway and its function in TRP-ML1(-/-) cells. *American journal of physiology. Cell physiology*. 301 (2). p.pp. C421–30.
- Zhang, L., Sheng, R. & Qin, Z. (2009). *The lysosome and neurodegenerative diseases Structure and Function of Lysosomes*. p.pp. 437–445.
- Zhang, S., Malmersjö, S., Li, J., Ando, H., Aizman, O., Uhlén, P., Mikoshiba, K. & Aperia, A. (2006). Distinct role of the N-terminal tail of the Na,K-ATPase catalytic subunit as a signal transducer. *The Journal of biological chemistry*. 281 (31). p.pp. 21954–62.
- Zheng, J., Yan, T., Feng, Y. & Zhai, Q. (2010). Involvement of lysosomes in the early stages of axon degeneration. *Neurochemistry international*. 56 (3). p.pp. 516–21.
- Zimmer, K.P., le Coutre, P., Aerts, H.M., Harzer, K., Fukuda, M., O'Brien, J.S. & Naim, H.Y. (1999). Intracellular transport of acid beta-glucosidase and lysosome-associated membrane proteins is affected in Gaucher's disease (G202R mutation). *The Journal of pathology*. 188 (4). p.pp. 407–14.
- Zong, X., Schieder, M., Cuny, H., Fenske, S., Gruner, C., Rötzer, K., Griesbeck, O., Harz, H., Biel, M. & Wahl-Schott, C. (2009). The two-pore channel TPCN2 mediates NAADP-dependent Ca<sup>2+</sup>-release from lysosomal stores. *Pflügers Archiv : European journal of physiology*. 458 (5). p.pp. 891–9.